ESTIMATING ABUNDANCE OF AFRICAN GREAT APES

Eric John Howe

A Thesis Submitted for the Degree of PhD
at the
University of St Andrews

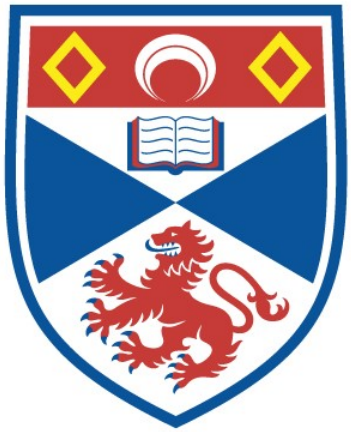

2019

ESTIMATING ABUNDANCE OF AFRICAN GREAT APES

Eric John Howe

A Thesis Submitted for the Degree of PhD
at the
University of St Andrews

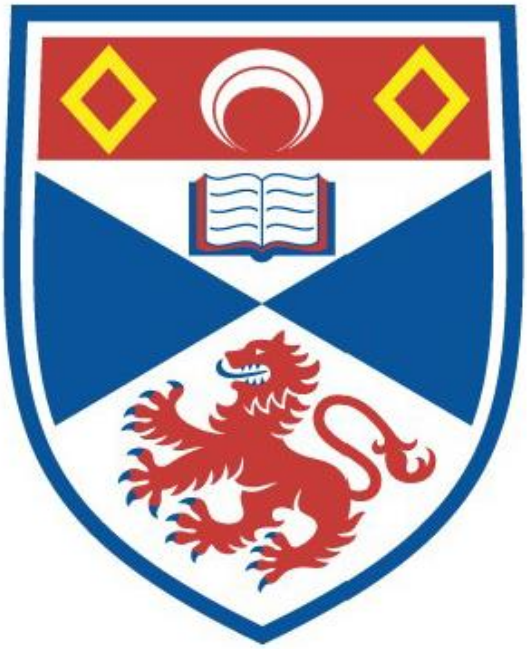

2019

Estimating Abundance of African Great Apes

Eric John Howe

University of
St Andrews

This thesis is submitted in partial fulfilment for the degree of

Doctor of Philosophy (PhD)

at the University of St Andrews

March 2019

Candidate's declaration
I, Eric John Howe, do hereby certify that this thesis, submitted for the degree of PhD, which is approximately 69,000 words in length, has been written by me, and that it is the record of work carried out by me, or principally by myself in collaboration with others as acknowledged, and that it has not been submitted in any previous application for any degree.
I was admitted as a research student at the University of St Andrews in September 2014.
I received funding from an organisation or institution and have acknowledged the funder(s) in the full text of my thesis.

Date Signature of candidate

Supervisor's declaration
I hereby certify that the candidate has fulfilled the conditions of the Resolution and Regulations appropriate for the degree of PhD in the University of St Andrews and that the candidate is qualified to submit this thesis in application for that degree.

Date Signature of supervisor

Permission for publication
In submitting this thesis to the University of St Andrews we understand that we are giving permission for it to be made available for use in accordance with the regulations of the University Library for the time being in force, subject to any copyright vested in the work not being affected thereby. We also understand, unless exempt by an award of an embargo as requested below, that the title and the abstract will be published, and that a copy of the work may be made and supplied to any bona fide library or research worker, that this thesis will be electronically accessible for personal or research use and that the library has the right to migrate this thesis into new electronic forms as required to ensure continued access to the thesis.
I, Eric John Howe, confirm that my thesis does not contain any third-party material that requires copyright clearance.
The following is an agreed request by candidate and supervisor regarding the publication of this thesis:

Printed copy
No embargo on print copy.

Electronic copy
No embargo on electronic copy.

Date Signature of candidate

Date Signature of supervisor

Underpinning Research Data or Digital Outputs

Candidate's declaration

I, Eric John Howe, hereby certify that no requirements to deposit original research data or digital outputs apply to this thesis and that, where appropriate, secondary data used have been referenced in the full text of my thesis.

Date Signature of candidate

Estimating Abundance of African Great Apes

Eric Howe

Abstract

All species and subspecies of African great apes are listed by the International Union for the Conservation of Nature as endangered or critically endangered, and populations continue to decline. As human populations and industry expand into great ape habitat, efficient, reliable estimators of great ape abundance are needed to inform conservation status and land-use planning, to assess adverse and beneficial effects of human activities, and to help funding agencies and donors make informed and efficient contributions. Fortunately, technological advances have improved our ability to sample great apes remotely, and new statistical methods for estimating abundance are constantly in development. Following a brief general introduction, this thesis reviews established and emerging approaches to estimating great ape abundance, then describes new methods for estimating animal density from photographic data by distance sampling with camera traps, and for selecting among models of the distance sampling detection function when distance data are overdispersed. Subsequent chapters quantifiy the effect of violating the assumption of demographic closure when estimating abundance using spatially explicit capture–recapture models for closed populations, and describe the design and implementation of a camera trapping survey of chimpanzees at the landscape scale in Kibale National Park, Uganda. The new methods developed have generated considerable interest, and allow abundances of multiple species, including great apes, to be estimated from data collected during a single photographic survey. Spatially explicit capture–recapture analyses of photographic data from small study

areas yielded accurate and precise estimates of chimpanzee abundance, and this combination of methods could be used to enumerate great apes over large areas and in dense forests more reliably and efficiently than previously possible.

Publications associated with this thesis

McCarthy MS, Lester JD, Howe EJ, Arandjelovic M, Stanford CB, Vigilant L. 2015. Genetic censusing identifies an unexpectedly sizeable population of an endangered large mammal in a fragmented forest landscape. BMC Evolutionary Biology 15:21

Després-Einspenner M-L, Howe EJ, Drapeau P, Kühl HS. 2017. An empirical evaluation of camera trapping and spatially explicit capture-recapture models for estimating chimpanzee density. American Journal of Primatology 79:e22647

Howe EJ, Buckland ST, Després-Einspenner ML, Kühl HS. 2017. Distance sampling with camera traps. Methods in Ecology and Evolution 8:1558–1565

Howe EJ, Buckland ST, Després-Einspenner ML, Kühl HS. 2019. Model selection with overdispersed distance sampling data. Methods in Ecology and Evolution 10:38–47

Cappelle N, Després-Einspenner ML, Howe EJ, Boesch C, Kühl HS. 2019. Validating camera trap distance sampling for chimpanzees. American Journal of Primatology 81:e22962

Acknowledgements

Sincere thanks to my supervisory committee Steve Buckland, David Borchers, and Hjalmar Kühl for this opportunity, and for patient and thoughtful guidance throughout, and to my committee, Rhona Rodger, Letizia Vettor, Len Thomas, James Mitchell, and Thomas Neukirch for making studying at St Andrews remotely possible and convenient.

Josephine Head provided provided data files and analytical results from the spatially explicit capture–recapture analysis of chimpanzees described in Head et al. (2013). Thanks to Marie-Lyne Després-Einspenner for conducting the survey of Maxwell's duikers in Tai National Park, Côte d'Ivoire, and estimating distances to duikers from videos. Thanks to the Ministère de l'Enseignement Supérieur et de la Recherche Scientifique and the Ministère de l'Environnement et des Eaux et Forêts in Côte d'Ivoire for permission to conduct field research in Taï National Park, and Dr. Roman Wittig for permitting data collection in the area of the Taï Chimpanzee Project. I collaborated with Samual Angedakin to design and implement the camera-trapping survey of chimpanzees in the northern portion of Kibale National Park. Thanks to the Uganda Wildlife Authority and the Uganda National council for Science and Technology for permission to conduct research in Uganda.

Versions of Chapter 3 (Distance Sampling with Camera Traps) and Chapter 4 (Model Selection with Overdispersed Distance Sampling Data) were published as articles in Methods in Ecology and Evolution (Howe et al. 2017a, and Howe et al. 2019). Since I wrote the original versions of these chapters, they were revised in response to comments from co-authors and anonymous reviewers of those manuscrpts. Thesis examiners Eric Rexstad and Marcus Rowcliffe also made substantive comments which contributed to the final versions of these chapters. Data from Maxwell's duikers in Taï National Park and songbirds from Montrave estate were archived at the Dryad data repository (Howe et al. 2017b, Howe et al. 2018).

Thanks to Richard Glennie, Ben Augustine, and Murray Efford for answering questions regarding software implementations of spatial capture–recapture models for open populations.

I'd like to personally thank Samuel Angedakin, Noémie Cappelle, Peter Carter, J. Chris Davies, Marie-Lyne Després-Einspenner, Greg Distiller, Murray Efford, Richard Glennie, Maureen McCarthy, Kevin Middel, Joe Nocera, Joseph Northrup, Martyn Obbard, Derek Potter, Eric Rexstad, Carolyn Rowney, and Ben Stevenson.

This thesis is dedicated to my wife, Alison Clark, and could not have been undertaken without the love and support of my family, especially Alder, Severn, and Valerie Howe, and Bruce Stirling.

Funding

This work was supported by a St Leonard's College Scholarship from the University of St Andrews, and the Max Planck Institute for Evolutionary Anthropology.

Contents

List of Figures

Figure 6.4. Maps of Kibale National Park (KNP), Uganda (boundary as heavy black lines, axes show Universal Transverse Mercators for longitude zone 36), showing (a) potential centroids of clusters of detectors as black dots at 4 km spacing, research stations or camps at which researchers could begin and end fieldwork when visiting different detectors (red triangles), and the road we used to divide the park into northern and southern portions, which would be sampled in sequence, and (b) rivers as light blue lines, and habitat types as described by Drichi (2003). High tropical forests appear in dark green, planted and degraded or encroached high tropical forests in light green, sparsely-treed woodland and bushland in orange, grasslands in yellow, open (sedge-dominated) wetlands in light blue, and open water in dark blue. Some of the degraded forest and open bushland and grassland habitat depicted here have been restored to more closely resemble native forests since these data were collected (Omeja et al. 2011).

Figure 6.5. Photographs of bushland and grassland habitat in Kibale National Park, Uganda (2016), where we were not able to sample chimpanzees using camera traps.

Figure 6.7. Location of the territory of the Ngogo community within Kibale National Park, Uganda (black lines), CTs deployed to sample Ngogo chimpanzees (2016; black dots), and forested (grey) vs. non-forested (grassland or bushland; white) habitats. Axis labels show UTM coordinates. Right: grey dots depict the habitat mask used when fitting SECR models and estimating population sizes.

Figure 6.8. Distances moved between spatial recaptures in simulated SECR surveys of eastern chimpanzee mothers employing clusters of detectors of different shapes (crosses and lines). The top row shows results with centroids $\geq$ 2 km apart, the bottom row results with centroids $\geq$ 4 km apart. Histograms show all movements from 100 replicates with each cluster shape and distance between centroids. A single spatial recapture at a distance of 3310 m between crosses 4 km apart occurred but is not apparent on the plot.

Figure 6.9. Estimates of the scale parameter of the encounter rate function (σ, meters) from SECR models fit to simulated data from eastern chimpanzee mothers from simulated surveys employing clusters of detectors of different shapes (crosses [left] and lines [right]). The top row shows results with centroids $\geq$ 2 km apart, the bottom row results with centroids $\geq$ 4 km apart. Histograms show 100 estimates from 100 replicates with each cluster shape and distance between cluster centroids. True values are shown as heavy black lines, means across replicates as solid red lines, and medians across replicates as dashed red lines.

Figure 6.10. Estimates of density (animals / km^2) from SECR models fit to simulated data from eastern chimpanzee mothers from simulated surveys employing clusters of detectors of different shapes (crosses [left] and lines [right]). The top row shows results with centroids $\geq$ 2 km apart, the bottom row results with centroids $\geq$ 4 km apart. Histograms show 100 estimates from 100 replicates with each cluster shape and distance between cluster centroids. True values are shown as heavy black lines, means across replicates as solid red lines, and medians across replicates as dashed red lines.

List of Tables

Table 4.4 Mean (SD) sample sizes (n) of distance observations and numbers of observations per independent encounter ($\hat{c}_2$) from simulated data from each habitat type, and from data pooled across habitat types, and mean values of the χ^2 GOF statistic divided by its degrees of freedom ($\hat{c}_1$) from the most highly parameterized half-normal and hazard rate models fit to the recently-logged and pooled data sets, across 500 iterations.

Table 4.5. Number of times each detection function model fit to simulated data from the recently logged study area was selected by AIC, and by each of $QAIC_1$ and $QAIC_2$ following the two-step procedure described in the methods section, of 500 replicate iterations.

Table 4.6. Medians of density estimates, and of coefficients of variation (CV) of those estimates, from models fit to simulated data from recently logged forests selected by AIC, and by $QAIC_1$ and $QAIC_2$ following the two-step procedure, across 500 iterations. True density was 15.0.

Table 4.7. The number of times, out of 500 iterations, that each of the 20 candidate models was selected by each model selection criterion, and below this, the number of times each of four forms of the detection function, and each of three covariate effects, was included in the selected models. Key refers to the key function, either half-normal (hn) or hazard rate (hr); covariates were: Logging (2), with differences in detectability between logged and old growth forests, Logging (3), with differences among all habitat types, and camera trap model (CT), which did not affect detectability; Adj. refers to the number of cosine adjustment terms included in the model (either 0 or 1).

Table 4.8. Medians of estimated densities ($\widehat{D}$) and their coefficients of variation (CV), by model selection criterion and habitat type. In parentheses under AIC, medians across the 439 data sets where density was estimable and total $\widehat{D}$ was within an order of magnitude of the true value (median CVs from AIC-selected models, and median densities from $QAIC_1$- and $QAIC_2$-selected models were similar when extreme values were excluded).

Table 4.9. Model selection by AIC, and step one of the two-step model selection procedure (see Table 4.11 for the 2nd step), for the seven detection function models successfully fitted to the "daytime" data from Maxwell's duikers in Taï National Park, Côte d'Ivoire (2014), and considered for density estimation (see Chapter 3 and Howe et al. 2017a). Values of $\hat{c}_1$ and $\hat{c}_2$ are those used to calculate $QAIC_1$ and $QAIC_2$, respectively, as opposed to model-specific values. The top AIC-ranked model, and the top $QAIC_1$- and $QAIC_2$-ranked models within each key function are marked with asterisks. Under "Model", Hr = hazard rate, Un = uniform, Hn = half-normal, cos = cosine adjustment, Hp = Hermite polynomial adjustment, and numbers following cos or Hp indicate the number of adjustment terms. "npar" is number of parameters in the model. We included c as one of the K parameters when calculating QAIC.

Table 4.10. Model selection by AIC, and step one of the two-step model selection procedure (see Table 4.12 for the 2nd step), for the eight detection function models fit to the "peak activity" data from Maxwell's duikers in Taï National Park, Côte d'Ivoire (2014; see Chapter 3 and Howe et al. 2017a). Values of $\hat{c}_1$ and $\hat{c}_2$ are those used to calculate $QAIC_1$ and $QAIC_2$, respectively, as opposed to model-specific values. The top AIC-ranked model, and the top $QAIC_1$- and $QAIC_2$-ranked models within each key function are marked with asterisks. Under "Model", Hr = hazard rate, Un = uniform, Hn = half-normal, cos = cosine adjustment, Hp = Hermite polynomial adjustment, and numbers following cos or Hp indicate the number of adjustment terms. "npar" is number of parameters in the model. We included *c* as one of the *K* parameters when calculating QAIC.

Table 4.11. Step two of the two-step model selection procedure applied to the models from Table 4.9, showing the top $QAIC_1$- and $QAIC_2$-ranked models within each key function, and corresponding values of the χ^2 GOF statistic divided by its degrees of freedom (*df*). For each of $QAIC_1$ and $QAIC_2$, the model with the lowest χ^2 / *df* value is marked with an asterisk, and was selected for estimation.

Table 4.12. Step two of the two-step model selection procedure applied to the models from Table 4.10, showing the top $QAIC_1$- and $QAIC_2$-ranked models within each key function, and corresponding values of the χ^2 GOF statistic divided by its degrees of freedom (*df*). For each of $QAIC_1$ and $QAIC_2$, the model with the lowest χ^2 / *df* value is marked with an asterisk, and was selected for estimation.

Table 4.13. Model selection results and density estimates ($\widehat{D}$) and coefficients of variation (CV) of $\widehat{D}$ for European robins at Montrave Estate. "Adj". denotes the number of cosine adjustment terms included in the model. The hazard rate model with two adjustment terms was not considered because the fit was not monotonically nonincreasing. The minimum AIC value, χ^2 / *df* values used to calculate QAIC within key functions, minimum QAIC values within key functions, and the density estimate from the model selected by the two-step $QAIC_1$ procedure are marked with asterisks. The density estimate from the model selected by Buckland (2006) is marked with a †. The territory mapping estimate was 0.84 territories per hectare.

Table 4.14. Model selection results and density estimates ($\widehat{D}$) and coefficients of variation (CV) of $\widehat{D}$ for winter wrens at Montrave Estate. "Adj." denotes the number of cosine adjustment terms included in the model. The minimum AIC value, χ^2 / *df* values used to calculate QAIC within key functions, minimum QAIC values within key functions, and the density estimate from the model selected by the two-step QAIC procedure are marked with asterisks. The density estimate from the model selected by Buckland (2006) is marked with a †. The territory mapping estimate was 1.30 territories per hectare.

Table 6.8. Age and sex class-specific abundance estimates with associated standard errors (SE) and 95% confidence intervals (CI) from the top AIC_c-ranked SECR model, and known or approximately known abundances from daily direct observations (provided by Samuel Angedakin).

Chapter 1: Introduction

All African great apes are either endangered or critically endangered and continue to decline (Table 1; Walsh et al. 2003, Campbell et al. 2008, IUCN 2014). The principal causes of decline are habitat loss and degradation, hunting, and outbreaks of disease (Boesch and Boesch-Achermann 2000, Huijbregts et al. 2003, Walsh et al. 2003, Bednar-Friedl et al. 2012, Junker et al. 2012, Arcus Foundation 2014). Clear cutting forests for timber or agriculture renders an area unsuitable for occupation by great apes (Arcus Foundation 2014), and unfortunately, 3.4 million hectares of Africa's forests were removed annually from 2000–2010 (FAO 2010). Within remaining forests, chimpanzee densities tend to be higher in unlogged, mature forest far from human disturbance (Matthews and Matthews 2004, Stokes et al. 2010), but there is also evidence to indicate that chimpanzees can occur at high densities in selectively logged and otherwise fragmented habitat (Plumptre and Reynolds 1994, Hashimoto 1995, Matthews and Matthews 2004, Chancellor et al. 2012, Moore and Vigilant 2014, McCarthy et al. 2015). In contrast, gorillas benefit from abundant successional herbaceous vegetation in recently logged-areas, exhibiting higher densities than in mature forest (Matthews and Matthews 2004, Stokes et al. 2010, but see Poulsen et al. 2011). The current rapid expansion of mechanized logging also impacts great apes directly, because new transportation infrastructure facilitates access by humans (Laporte et al. 2007). Reductions in density and local extirpations of African wildlife are often attributable to hunting, and are more severe for populations in proximity to large or growing human populations (Harcourt and Parks 2003, Walsh et al. 2003, Campbell et al. 2008, N'Goran Kouamé et al. 2012), so the adverse effects of logging and hunting often act in combination to cause declines (Poulsen et al. 2011). Great ape populations

may also decline more rapidly during times of civil unrest (Dudley et al. 2002, Campbell et al. 2008).

Table 1.1 Conservation status of African great apes (IUCN 2014). "EN" = Endangered, "CR" = Critically endangered.

Common name		Scientific Name			IUCN
Species	Subspecies	Genus	Species	Subspecies	Status
Bonobo	Bonobo	*Pan*	*paniscus*		EN
Chimpanzee	Eastern chimpanzee	*Pan*	*troglodytes*	*schweinfurthii*	EN
Chimpanzee	Central chimpanzee	*Pan*	*troglodytes*	*troglodytes*	EN
Chimpanzee	Nigeria-Cameroon chimpanzee	*Pan*	*troglodytes*	*ellioti*	EN
Chimpanzee	Western chimpanzee	*Pan*	*troglodytes*	*verus*	EN
Western Gorilla	Cross river gorilla	*Gorilla*	*gorilla*	*diehli*	CR
Western Gorilla	Western lowland gorilla	*Gorilla*	*gorilla*	*gorilla*	CR
Eastern Gorilla	Grauer's gorilla	*Gorilla*	*beringei*	*graueri*	EN
Eastern Gorilla	Mountain gorilla	*Gorilla*	*beringei*	*beringei*	CR

Reliable and precise estimates of great ape abundance, and of trends in abundance, are urgently needed to inform conservation status and land-use planning, to assess adverse and beneficial effects of human activities such as hunting, logging, and conservation actions, to identify correlates of abundance, and to help funding agencies and donors make efficient contributions (Ferraro and Pattanayak 2006, Hockings et al. 2006, Kühl et al. 2008, Yanggen et al. 2010, Plumptre et al. 2010, Morgan et al. 2011). However, up-to-date and reliable estimates of population size and trend are currently lacking for most populations of African great apes (Campbell et al. 2008, Walsh et al. 2008, Plumptre et al. 2010, Morgan et al. 2011, Arcus Foundation 2014, Humle et al. 2016). Effective management for conservation also requires that information about

great ape abundance is available at multiple spatial scales, and is updated frequently (Devos et al. 2008a, Stokes et al 2010, Hoppe-Dominik et al. 2011).

Large-bodied, forest-dwelling mammals are particularly difficult to enumerate because they typically occupy remote areas with limited access, are elusive, range widely, exist at low and variable densities, and exhibit low and heterogeneous probabilities of detection (Karanth and Nichols 1998, Kouakou et al. 2009, Obbard et al. 2010, Arandjelovic and Vigilant 2018), so field surveys designed to estimate their abundance are both labour-intensive and costly (Caughlan and Oakley 2001). Low densities and detection probabilities require intensive field sampling at a given location to yield adequate samples (Kouakou et al. 2009, Head et al. 2013, Wilton et al. 2014). Hence, field studies of unhabituated great apes are often limited in spatial scale and duration (Kühl et al. 2008), and densities estimated on small study areas have been extrapolated over much larger areas of potentially occupied habitat to estimate regional population sizes (Plumptre et al. 2010, Humle et al. 2016). Such extrapolations are unreliable because great ape density varies in space in response to many factors, including the spatial distribution of above-mentioned causes of decline, habitat productivity, and temporal variability in habitat productivity (Boesch and Boesch-Achermann 2000, Matthews and Matthews 2004, Morgan et al. 2006, Potts et al. 2009, Stokes et al. 2010). Spatial variation in density requires that sampling takes place over relatively large spatial scales to quantify this variation, and hence to obtain reliable estimates of regional abundance when extrapolating to areas not sampled. An additional challenge unique to studies of great apes is that it is considered both logistically infeasible and unethical to physically capture, trap, or chemically immobilize great apes for research purposes.

Technological advancements that allow animals to be observed remotely are changing the ways we monitor wildlife (Woodruff 1993, Karanth and Nichols 1998, Burton et al. 2015). Spatially explicit capture–recapture modelling of data obtained via genetic and photographic sampling can provide improved information about great ape abundance (Head et al. 2003, McCarthy et al. 2015, Després-Einspenner et al. 2017, Arandjelovic and Vigilant 2018). When I began my studies, there was no established framework for estimating densities of animals that cannot be individually identified from camera trapping data (Burton et al. 2015), but this was an open area of research.

I pursued this PhD seeking to improve methods for monitoring great apes to help address the aforementioned conservation concerns. During the course of my studies, my research became more focused on chimpanzees than gorillas, and followed two distinct avenues: (1) extending distance sampling analytical methods to accommodate data from camera traps, and (2) designing, implementing, and evaluating spatially explicit capture–recapture (SECR) surveys of chimpanzees, primarily from camera trapping data. In Chapter two, I review established and emerging methods for estimating great ape abundance, devoting considerable attention to the sources and implications of misidentification errors in capture–recapture data to address the specific questions of one of my committee members. In Chapter three, I develop, and test using simulated and real data, a novel method for estimating animal abundance by distance sampling with camera traps. Chapter four presents novel model selection criteria adjusted for use with overdispersed distance sampling data. It was motivated by the fact that distance sampling with camera traps yields overdispersed data, but is also applicable in other contexts. Chapter five explores the consequences of violating the assumption of demographic closure in closed-population SECR analyses of

chimpanzees. Chapter six describes the design and implementation of a photographic SECR survey of chimpanzees in Kibale National Park, Uganda, and Chapter seven presents conclusions and directions for future research.

Chapter 2: Literature Review: Estimating Abundance of African Great Apes

Here I review established and emerging field sampling and statistical methods for estimating great ape abundance, emphasizing estimation of population density as opposed to population size, to place the primary research described in subsequent chapters in context. In section one I review established methods, such as line transect surveys of nests. Section two begins with a description of genetic and photographic sampling methods as applied or applicable to great apes. Subsequently, I review novel statistical estimators of animal density from genetic and photographic data, including spatially explicit capture–recapture, the random encounter model, and newer methods. Section three presents brief conclusions.

2.1 Established Methods

2.1.1 Habituation

Chimpanzees are born into stable social groups (termed "communities") of about 20 to 200 individuals. Male chimpanzees usually remain part of the same community for life, whereas females typically transfer to new communities as adolescents (Mitani et al. 2012). Since the famous pioneering work by Louis Leakey's "three primates" (Jane Goodall, Diane Fossey, and Birute Galdikas; Montgomery 2009), several communities of African great apes have been habituated to human presence to facilitate research (Boesch and Boesch-Achermann 2000, Gruen et al. 2013). Habituation of an entire chimpanzee community allows both the number of individuals present and the size of their territory, and hence population density, to be quantified with minimal error or uncertainty (Boesch and Boesch-Achermann 2000). Intensive study of habituated

great apes is crucial to behavioural research (Boesch and Boesch-Achermann 2000), and provides populations of known size and composition which can be sampled to assess the accuracy of methods for estimating abundance (Kouakou et al. 2009, Head et al. 2013, Després-Einspenner et al. 2017, Cappelle et al. 2019). Furthermore, the long-term presence of researchers on a study area, and the associated use of habituated groups for ecotourism, in itself provides a measure of protection in the immediate vicinity of study areas (Campbell et al. 2011, N'Goran Kouamé et al. 2012). However, as a means of estimating abundance, habituation is far too labour-intensive and logistically challenging to apply over the large spatial scales at which abundance information is required, and too time-consuming to inform the urgent management decisions required to conserve great apes.

2.1.2 Strip transect surveys of nests

Great apes are elusive, and difficult to observe directly, especially in dense forests (Plumptre 2000). However, weaned chimpanzees and gorillas build nests, typically daily, in which they sleep at night and sometimes rest during the day (Boesch and Boesch-Achernann 2000, Mehlman and Doran 2002). Therefore, until very recently, great ape abundance has almost universally been estimated via indirect sampling methods, where the density of signs left by the animals (dung piles or nests) is estimated from field data, and subsequently converted to an estimate of animal density (Kühl et al. 2008, Devos et al. 2008a, b, Stokes et al. 2010, Nakashima et al. 2013).

Estimates of abundance derived from surveys of nests exclude infants, which share their mothers' nests until they are weaned. Such estimates are generally adequate for management purposes. However, changes in population size detected via nest count

surveys lag behind the actual numeric change if the mechanism of change involves reproduction or infant survival. Information about the proportion of nest-builders or infants in a population could be used to estimate the number of infants and hence the total density and population size, however, as these are likely to vary in time and space with stochastic demography (Boesch and Boesch Achermann, 2000, Thompson and Wrangham 2008, Mitani et al. 2010), local, concurrent information would be needed.

In strip transect surveys, a set of linear transects is distributed randomly with respect to the distribution of nests throughout the region of interest. Randomized designs allow nest density in the vicinity of transects to be extrapolated to estimate population size over the larger region of interest (Burnham et al. 1980, Buckland et al. 2001). Transects should not overlap, and should be far enough apart that they can be treated as independent samples. Otherwise, line placement may be purely random, but systematic designs with random origin are more common, and study areas may also be stratified, with random or systematic sampling within strata (Burnham et al. 1980, Plumptre 2000, Buckland et al. 2001, 2010, Stokes et al. 2010, Nakashima et al. 2013, Tweh et al. 2018). If the study area includes habitat types or treatments among which density is expected to vary, transects can be allocated to spatial subsets of the study area, either at a sufficient intensity to estimate density from different subsets separately, or with transect lengths proportional to the area of each subset if data are to be pooled to estimate average density across the region of interest (Burnham et al. 1980, Buckland et al. 2001, 2015).

To conduct the surveys, researchers walk along transects, counting all the nests or groups of nests within a fixed width (w) of the line. All nests or nest groups within w of the line are assumed to be detected with certainty, so nest or group density can be

estimated as the number of nests or nest groups divided by the known area of the strip surveyed. The high probability that not all nests within *w* of the line will be detected makes this method almost guaranteed to underestimate density, but by an unknown magnitude. Other aspects of nest surveys along transects will therefore be addressed in the context of methods that allow for imperfect detection.

2.1.3 Line transect (distance sampling) surveys of nests

Until recently the only well-established, scientifically defensible method for enumerating unhabituated chimpanzees and gorillas combined line transect surveys of nests with distance sampling (DS) methods that account for imperfect detection by modelling detectability as a decreasing function of the distance from the line (Plumptre 2000, Kühl et al. 2008, Stokes et al. 2010, Nakashima et al. 2013, Piel et al. 2015, Tweh et al. 2015, 2018, Kamgang et al. 2018). Randomized designs are again required (Buckland et al. 2001, 2010). Researchers walk along transects and measure the perpendicular distance from the transect line to either each nest, or the center of each group of nests, that they detect. Additional information is required to convert nest density to animal density, as described below. These methods were thoroughly reviewed by Kühl et al. (2008).

The combination of line transect nest count surveys and DS methods provides several advantages. Observing nests as opposed to live animals avoids any effect of avoidance or animal movement on encounter rates or the distribution of observed distances (Glennie et al. 2015), and makes it easier to record distances accurately. Furthermore, nests persist for weeks or months (Tutin et al. 1995, Plumptre and Reynolds 1997, Walsh and White 2005, Kouakou et al. 2009), so nest density far

exceeds animal density, and we obtain larger samples than we could by surveying animals directly. The DS framework provides an accessible suite of methods for estimating density and population size in the absence of individual identification (Buckland et al. 2001, 2004, 2015). Provided that all nests at distance zero from the line are detected, the pooling robustness property ensures that estimates are not biased when detectability varies among nests, and variation in detectability can also be modelled using covariates (Marques and Buckland 2003, Burnham et al. 2004). If differences in density within the greater study area are of interest, density can be estimated separately for different spatial subsets of the study area (while potentially sharing information about detectability across subsets), or spatial covariates can be combined with DS data to fit density surface models, which can enhance the reliability of extrapolations to estimate population size, and facilitates the depiction of results and predictions as maps (Miller et al. 2013). Modifications and extensions relax assumptions, allow for greater design flexibility, or improve precision (Buckland et al. 2006, Fewster et al. 2009, Marques et al. 2013, Buckland et al. 2015). DS studies can be designed and the data analyzed using free software (Thomas et al. 2010, Fisk and Chandler 2011, Miller 2017, Laake et al. 2018), and online courses and advice from experts are also available at no cost to researchers via the Distance project website.

Shortcomings of this combination of methods for estimating great ape abundance include: (1) problems with how surveys are designed and carried out, leading to violations of assumptions, (2) difficulties in the obtaining the information needed to convert nest densities to animal densities, (3) lack of precision, and (4) concerns about accuracy. These are discussed in more detail below.

Line transect DS methods assume (1) lines are placed randomly with respect to the distribution of objects being sampled, (2) objects on or directly above the line are always detected, (3) objects are detected at their original location (always met in the case of nest surveys), and (4) distances are measured accurately, or are counted in the correct distance interval for grouped data, and (5) detections are independent events. Violations of any of assumptions 1, 2 or 4 can cause bias and render the associated estimates of density unreliable (Buckland et al. 2001). Non-independent detections do not bias point estimates, but require that sampling variances be estimated empirically from the variation in encounter rate across independent lines (Buckland 1984, Fewster et al. 2009). In addition to these assumptions, it is important that the position, number, and length of lines be adequate to provide a representative sample of the region of interest, and to achieve reasonable precision (Buckland et al. 2001, 2010).

Use of established roads or trails, or transects set along habitat features such as ridgelines or watercourses, is likely to violate assumption one and yield samples that are not representative of the region of interest (Plumptre 2000, Buckland et al. 2001, 2010, Harmsen et al. 2010). This is particularly problematic in studies of great apes, because their distribution is affected by human use of trails, and even by trails themselves via effects on light penetration and understory vegetation (Kühl et al. 2008). Because using trails as line transects is not recommended, it is often necessary to clear vegetation along randomly or systematically located transects to enable researchers to travel along straight lines. However, clearing vegetation along the line creates a trade-off between assumptions one and two, making it difficult to ensure both are met. If enough vegetation is cut to ensure that observers can travel in straight lines and see far enough above themselves to detect nests directly above the line with certainty, transects become

trails. Cut transects can affect great ape behaviour and distribution on or close to the line, leading to a non-random, non-representative sample, and improve access for illegal extraction activity including poaching, which not only poses a conservation concern, but can also lead to a non-representative sample if the presence of humans affects animal behaviour and distribution (Plumptre and Reynolds 1997, Tagg and Willie 2013, Tweh et al. 2018). If researchers minimize cutting along transects (Matthews and Matthews 2004, Kouakou et al. 2009, Stokes et al. 2010), observers may fail to detect nests directly above the line (Van Schaik et al. 2005), particularly if they are inexperienced, fatigued, or distracted (Kühl et al. 2008). This would violate assumption two above and cause potentially severe underestimation of density (Buckland et al. 2001, Van Schaik et al. 2005). When distances are estimated by eye, field researchers tend to underestimate distances, violating assumption four and causing density estimates to be positively biased; laser rangefinders improve the accuracy of distance measurements (Buckland et al. 2010).

The assumption that detections are independent events is usually violated because chimpanzees and gorillas live in social groups (Mitani et al. 2012), but this is not particularly problematic (Buckland et al. 2010). Point estimates of abundance are not affected, variance estimators that avoid this assumption or are robust to violations are available (Buckland 1984, Fewster et al. 2009), and model selection criteria adjusted for the overdispersion induced by the inclusion of non-independent observations were developed recently (Chapter 4, Howe et al. 2019). Researchers can also treat a group of nests as the unit of observation to be more consistent with the independence assumption. In this case, distances are measured to the center of each group of nests, the density of groups of nests is estimated from the data, and multiplied by group size to obtain an

estimate of nest density (Buckland et al. 2001, Kühl et al. 2008, Buckland et al. 2010). Larger groups may be more likely to be detected, but regressing the log of group size on the estimated detection probability reduces associated bias in the estimated group size (Buckland et al. 2001, 2010).

Obtaining an adequate, representative sample is a non-trivial concern in the case of surveys of great apes. Buckland et al. (2010) recommend that at least 10 but preferably closer to 20 lines should be sampled, more if density varies across the study area. Chimpanzees occur at low densities, so even encounter rates with nests may be too low to yield adequate samples without revisiting the same transects (Matthews and Matthews 2004, Devos et al. 2008a, b). Repeat visits to the same transect are modelled as increased effort rather than as additional replicates and do not improve representativity (Buckland et al. 2001, 2010). Researchers must frequently walk over 100 km along transects to obtain adequate and representative samples from even small study areas (Devos et al. 2008b, Kouakou et al. 2009, Carvalho et al. 2013, Tagg and Willie 2013). This can increase to 100's or 1000's of km for surveys at the landscape scale (Matthews and Matthews 2004, Plumptre and Cox 2006, Clark et al. 2009, Stokes et al. 2010). The time-consuming, labour-intensive, and costly nature of the surveys, as well as limited funding and periods of civil unrest, have led to large temporal gaps in monitoring (Hoppe-Dominik et al. 2011), yet the immediate conservation concern necessitates continuous or frequent monitoring to detect declines and facilitate rapid management in response to new threats (Campbell et al. 2008, Devos et al. 2008a, Hoppe-Dominik et al. 2011).

The conversion from nest density to animal density is frequently more problematic than meeting assumptions and achieving adequate sample sizes during the

survey (Laing et al. 2003, Walsh and White 2005, Kühl et al. 2008, Walsh et al. 2008, Kamgang et al. 2018). Depending on the type of survey conducted, either nest production rates, or both nest production and nest decay rates, are required. When distances are measured to all nests, or to the centre of all groups of nests, encountered during a survey, this is referred to as the "standing crop" (SC) nest count method, and estimates of both nest production and decay rates are required to convert associated estimates of nest density to estimates of animal density (Plumptre and Reynolds 1996).

Local nest decay rates can be estimated by marking all nests encountered during initial surveys, then recording the approximate date of construction of new, unmarked nests encountered during subsequent surveys, and observing these nests until they decay completely. The estimated decay rate is then specific to the nests that are surveyed (Laing et al. 2003). However, nest duration is affected by many factors, and so it varies considerably in space and time (Kühl et al. 2008, Kouakou et al. 2009). Therefore, animal density cannot be assumed to be a constant function of nest density, so field studies to estimate local nest decay rates should be conducted prior to and concurrently with the line transect survey (Plumptre and Reynolds 1997, Walsh and White 2005, Kouakou et al. 2009). Ideally, nest decay rate would be estimated from multiple visits to many nests before and during the survey, but because nests usually take several months to decay, such studies can take months or years to complete (Laing et al. 2003, Matthews and Matthews 2004, Kühl et al. 2008, Kouakou et al. 2009). Kühl et al. (2008) noted that a larger sample of nests is required to estimate decay rate accurately than might suffice for the DS survey.

Alternative methods for estimating nest decay rates have been proposed, but considerable time and effort must still be expended in the field to implement them.

Laing et al. (2003) proposed a method for estimating decay rate from only two visits to each nest. This approach still required researchers to search for freshly constructed nests at least six times at regular intervals prior to the survey, with the date of the first visit selected such that 90% of fresh signs would be expected to decay by the beginning of the survey. It was recommended that 50 to 100 fresh signs be located to ensure that variation in nest decay rate contributed a small fraction of the total variance in animal density (Laing et al. 2003). All nests are revisited only once (unless the distance sampling survey was conducted over a long time period including more than one season, in which case more revisits would be needed), just prior to the line transect survey to determine if they have decayed, and decay rate is estimated as a function of time, and potentially also environmental or nest-specific covariates, by logistic regression. This approach should yield reliable estimates of local decay rates over the appropriate time interval, but applying it is still labour intensive, with much time devoted to traveling between transects and searching for fresh nests along them, and it may be impractical where densities are low (Laing et al. 2003, Kühl et al. 2008, Piel et al. 2015). Decay rates of orangutan nests have been estimated modelling transitions between well-defined states of decay using matrix mathematics and MCMC estimation methods (Van Schaik et al. 1995, Matthewson et al. 2008). This method allows nests that are partially-decayed when first located to contribute information, providing larger samples from less extensive searches than Laing et al.'s (2003) approach. However, because the lifetime of nests varies, there is a tendency for more longer-lasting nests to be monitored, leading to positive bias in nest lifetime in the absence of site-specific correction factors (Kühl et al. 2008). Furthermore, Mathewson et al. (2008) demonstrated that applying these methods to data collected during short-term studies

resulted in severe underestimation of nest lifetime and overestimation of density. They argued that these methods require either further development, or studies of similar duration as are required by other methods for estimating nest decay rate. To my knowledge, these methods have not been applied to African great apes.

An alternative to standing crop nest counts that avoids the need to estimate the nest decay rate is the "marked nest count" (MN) method (Hashimoto 1995, Plumptre and Reynolds 1996). Prior to a marked nest count survey, all existing nests along transects are located and marked. During the DS survey, distances are measured only to unmarked nests, i.e., those built during the survey. Nest densities can then be converted to animal densities by dividing by the expected number of nests produced by each weaned individual over the course of the survey (the daily nest production rate × the length of the survey in days). This has the major advantage of eliminating nest decay rate from the conversion to animal density. However, marked nest surveys yield much smaller samples, such that substantially more effort must be expended to estimate nest density with similar precision, and attaining adequate sample sizes may not be possible where animal and nest densities are low (Hashimoto 1995, Plumptre & Reynolds 1996, Plumptre 2000, Laing et al. 2003, Matthews and Matthews 2004, Devos et al. 2008a, b, Kouakou et al. 2009, Carvalho et al. 2013). Replicate surveys of the same line must be frequent enough that no new nests completely decay between visits (Hashimoto 1995, Plumptre and Reynolds 1996). Consequently, marked nest count surveys can be as or more time-consuming and labour-intensive than standing crop surveys (Plumptre and Cox 2006, Kühl et al. 2008).

Although great apes typically build nests daily, such that some researchers assumed an average nest production rate of 1.0 for weaned individuals (Plumptre and

Reynolds 1997, Plumptre 2000, Matthews and Matthews 2004), daily nest production rates typically exceed 1 due to occasional construction of day nests by chimpanzees (Plumptre and Reynolds 1996, 1997, Kouakou et al. 2009), and of day nests or multiple night nests by gorillas (Tutin et al. 1995, Bradley et al. 2008, Sunderland-Groves et al. 2009). Gorillas may also sleep on bare ground, leaving no discernible nest (Tutin et al. 1995, Bradley et al. 2008, Sunderland-Groves et al. 2009), and both species sometimes reuse nests (Plumptre and Reynolds 1997, Iwata and Ando 2007). If estimated or assumed nest production rates are inaccurate, density estimates will be as well. Nest construction rate can only be determined for habituated communities, so few estimates are available (Plumptre and Cox 2006, Kühl et al. 2008). Abundance estimates for most populations must rely on estimates of nest production rate from data collected elsewhere. Fortunately, situations that deviate from a daily nest production rate of 1 (construction of day nests, and nest reuse) are relatively infrequent, and have opposite effects on the mean production rate, such that the magnitude of bias in nest production rate is likely to be slight if values between 1.0 and 1.2 are assumed (Plumptre and Reynolds 1997, Kouakou et al 2009). Therefore, the marked nest count method reduces uncertainty associated with the conversion of nest density to animal density. Nevertheless, because studies that rely on information about nest production and decay rates from the literature, from different study areas, or even different seasons on the same study area are likely to yield biased estimates of ape density, they are often mistrusted (Plumptre 2000, Walsh and White 2005, Kühl et al. 2008, Walsh et al. 2008).

Even where nest count DS surveys are appropriately designed and carried out, abundance estimates are frequently imprecise, limiting their utility for management, and making it difficult to detect temporal trends or differences among study areas or

treatments. Coefficients of variation are usually > 25%, and approach 50% when most or all sources of uncertainty are included in the variance of the density estimate (Plumptre and Cox 2006, Devos et al. 2008a, b, Kouakou et al. 2009, Stokes et al. 2010, Carvalho et al. 2013, Kamgang et al. 2018, Tweh et al. 2018). In some studies including many earlier ones, uncertainty in conversion factors or group size was often ignored, making it difficult to assess the actual degree of uncertainty in density estimates, yet confidence limits were still wide (Plumptre 2000, Matthews and Matthews 2004, Clark et al. 2009). Plumptre (2000) showed that changes in population size of 30 to 50% were unlikely to be detected by two replicate surveys and suggested that a combination of survey methods would be required to detect trends. Devos et al. (2008a) were able to detect a dramatic decline in chimpanzee abundance near the end of a marked nest count survey.

Wide confidence intervals from nest count DS surveys may include the true abundance, but point estimates may be inaccurate. Because nests must be marked during initial walks to estimate decay rate for the standing crop method, researchers frequently apply both SC and MN methods during the same survey. Where this was the case, results often differed between estimation methods (Plumptre and Reynolds 1997, Matthews and Matthews 2004, Devos et al. 2008b, Kouakou et al. 2009). Genetic data indicated that nest count methods (Ogawa et al. 2007) underestimated chimpanzee density in the Ugalla region of Tanzania, possibly due to problems with the study design, and estimation of conversion factors (Moore and Vigilant 2014). Kouakou et al. (2009) sampled an habituated population of known size using SC and MN methods. A local, concurrent estimate of nest production rate was available, and an extensive nest decay rate study was conducted. Point estimates of abundance were similar to, but

usually slightly lower than, the true abundance, and coefficients of variation were > 25%. This survey may be indicative of the accuracy and precision achievable with these methods.

Line transect surveys of nests have, and still are, contributing a great deal to our understanding of the status of great apes, and sources of variation in great ape abundance (Plumptre and Cox 2006, Devos et al 2008a, b, Clark et al. 2009, Stokes et al. 2010, Carvalho et al. 2013, Tweh et al. 2018). However, the problems and difficulties described above make it clear that new, more efficient methods for monitoring great apes are needed.

2.2 Emerging sampling methods

Technological advancements that allow animals to be observed remotely are changing the ways we monitor wildlife, including great apes (Karanth and Nichols 1998, Woods et al. 1999, Waits and Paetkau 2005, Head et al. 2013, Burton et al. 2015, Rovero and Zimmermann 2016, Arandjelovic and Vigilant 2018). Statistical ecologists are responding by developing or extending statistical models to take advantage of the novel types of data being collected. For example, in traditional capture–recapture surveys, animals were individually identified by physically capturing and uniquely marking them. The resulting data were modelled as binary events within temporally discrete sampling occasions (Otis et al. 1978, Borchers and Efford 2008) because animals could only be captured in one trap until released. Remote sampling methods do not involve confining animals, so individuals may be detected more than once between trap checks, or over the duration of a continuous sampling effort. Capture-with-replacement estimators of population size and spatially explicit capture–recapture

(SECR) models that model detections as counts and in continuous time were developed to take advantage of information from these additional recaptures (Miller et al. 2005, Petit and Valiere 2006, Efford et al. 2009a, Borchers et al. 2014).

Emerging statistical methods potentially useful for estimating great ape abundance from data collected using new technologies can be categorized according to the extent to which they require that individuals are identifiable or recognizable ("marked" animals). Most capture–recapture and spatially explicit capture–recapture models assume that detected individuals can be identified without error (Otis et al. 1978, Borchers and Efford 2008), while other statistical estimators do not require that animals are identifiable at all (Rowcliffe et al. 2008, Howe et al. 2017a, Nakashima et al. 2018, Moeller et al. 2019). Below, I describe genetic and photographic methods for sampling wildlife. I then review recently developed statistical methods for analyzing genetic and photographic data to estimate density.

2.2.1 Remote genetic sampling

The potential to identify individual animals from their DNA gave rise to a proliferation of genetic capture–recapture surveys that do not require researchers to physically capture, come into contact with, or even see the target animals (Woodruff 1993, Woods et al. 1999; Taberlet et al. 1999, Waits and Paetkau 2005, Schwartz et al. 2007, Arandjelovic and Vigilant 2018). The probability of two individuals having the same multilocus genotype is estimable, and becomes very low as the number of loci and the allelic diversity at those loci increase, such that DNA profiles can be interpreted as unique individual identifiers, often termed "genetic tags" or "DNA fingerprints" (Palsbøll et al. 1997, Woods et al. 1999, Morin et al. 2001, Banks et al. 2002). The sex

of sampled animals, which is often a useful covariate in analyses, can usually be determined as well (Ennis and Gallagher 1994, Bradley et al. 2001).

Such remote or "noninvasive" sampling is most appropriate where physical capture is difficult, intrusive, or likely to disturb the population (Forcada and Aguilar 2000) all of which apply to great apes (Morin et al. 2001), so it is not surprising that primatologists were among the first wildlife researchers to evaluate remote genetic sampling methods, extracting DNA from shed and plucked hairs, food wadges, and epithelial cells from faeces (Woodruff 1993, Morin et al. 1994*a*, *b*, 2001, Gerloff et al. 1995, Garner and Ryder 1996, Gagneux et al. 1997). Attempts to extract DNA from shed hairs were usually unsuccessful, or yielded much lower quantities of DNA than faeces (Morin et al. 2001 [Appendix 1]). Plucked hair samples yield more DNA than shed hairs (Goossens et al. 1998, Morin et al. 2001) but methods for snagging hairs from free-ranging great apes have not been developed (Arandjelovic and Vigilant 2018), and might not be deemed safe or ethical. Improved methods for storing, extracting, quantifying, amplifying, and genotyping fecal DNA (Flagstad et al. 1999, Frantzen et al. 1998, Morin et al. 2001, Nsubuga et al. 2004, Arandjelovic et al. 2009) make it the most reliable source of genetic material from great apes (Kühl et al. 2008).

Genetic sampling is appealing for several reasons. Genetic CR studies have been shown to yield more accurate and precise abundance estimates from shorter field studies relative to nest count surveys (Guschanski et al. 2009, Arandjelovic et al. 2010, 2011, Roy et al. 2014, Granjon et al. 2017). Also, because individuals' genotypes are stable over time, they can be matched in samples collected and analyzed several years apart, facilitating the estimation of demographic rates and abundance in open populations (Gardner et al. 2010, Glennie et al. 2019). Furthermore, once collected,

fecal and DNA samples can be used to address a range of questions via studies of molecular epidemiology, genetic diversity and gene flow, mating systems and social structure, and diet (Woodruff 1993, Morin et al. 1994a, DeYoung and Honeycut 2005, Boesch et al. 2006, Schwartz et al. 2007, Arandjelovic and Vigilant 2018).

Disadvantages of genetic surveys are the time and funding required to collect and analyze the samples, respectively. Considerable field effort is required to search for and collect fecal samples (Roy et al. 2014, Basabose et al. 2015, McCarthy et al. 2015, Granjon et al. 2017, Arandjelovic and Vigilant 2018). Samples must be fresh when collected (e.g. 1 – 3 days old [Vigilant 2002, Roy et al. 2014]) to yield sufficient DNA, so field sampling often involves first locating and following groups of animals, or locating their trails and following them to nest sites (Moore and Vigilant 2014, Roy et al. 2014, McCarthy et al. 2015), although samples are sometimes collected opportunistically during the course of other field work (Arandjelovic et al. 2010, 2011, Granjon et al 2017). Locating groups of chimpanzees or gorillas (or their nest sites) is both labour-intensive and time consuming (Roy et al. 2014), and it can take years to collect sufficient samples to estimate abundance by sampling opportunistically (Arandjelovic et al. 2010, Granjon et al. 2017). Trained detection dogs improved the efficiency and representativeness of fecal sampling of Cross River gorillas, but are currently cost-effective only on small study areas (Arandjelovic et al. 2015).

The sophisticated equipment and expertise required to analyze genetic samples comes at a considerable cost to researchers (Paetkau 2004, Tredick et al. 2007, Guschanski et al. 2009), and large-scale surveys can quickly exhaust available funding (Tredick et al. 2007, Howe et al. 2013). Furthermore, noninvasively-collected samples may yield only small quantities of potentially degraded or contaminated DNA, and

extracts from fecal samples may contain PCR inhibitors, making genotyping error-prone and reliable individual identification difficult and even more expensive (Monteiro et al. 1997, Taberlet et al. 1999, Morin et al. 2001). Misidentification errors violate the capture–recapture assumption that marks are not lost or misread, and can severely bias abundance estimates from models that rely on this assumption (Mills et al. 2000, Creel et al. 2003, Link et al. 2010). Misidentification error in genetic CR studies is addressed in detail subsequently.

Genetic surveys designed for abundance estimation should aim to collect 2.5 – 3.0 times as many usable samples as the expected number of individuals detected (Miller et al. 2005, Petit and Valière 2006) while allowing for the fact that some samples will not yield reliable genotypes (Lucaks and Burnham 2005). Abundance was estimated precisely in several studies in which these targets were achieved (Arandjelovic et al. 2010, Chancellor et al. 2012, McCarthy et al. 2015) but precision was lower (CV = 0.38), where individuals were detected only 1.6 times on average (Arandjelovic et al. 2011). Samples should be representative of the entire area of interest, and of the age and social classes of individuals in the population (Arandjelovic et al. 2010, 2015). Opportunistic sampling may not yield representative samples, and complicates (but does not preclude) accurate quantification of sampling effort in statistical models (Moore and Vigilant 2014, Roy et al. 2014, Arandjelovic et al. 2015, McCarthy et al. 2015).

2.2.2 Remote photographic sampling (camera-trapping)

Wildlife sampling via remote, motion-sensitive photography, termed "camera-trapping", is achieved by deploying cameras triggered by passive infra-red (PIR) motion

sensors in wildlife habitats (Griffiths and Van Schaik 1993). Camera traps (CTs) are particularly useful for sampling medium- to large-bodied, rare, cryptic, and elusive animals in habitats where dense vegetation, rugged terrain, limited access, or the potential for researchers to affect the distribution and abundance of animals in their vicinity limit the effectiveness of other sampling methods (Griffiths and Van Schaik 1993, Karanth 1995, Ahumada et al. 2011, Sollmann et al. 2013a, Pebsworth and LaFleur 2014), so seem ideally suited for monitoring great apes. Once deployed, CTs operate continuously, automatically recording time- and location-specific images or videos of multiple species for weeks to months at a time, providing data that are otherwise either expensive and difficult or impossible to obtain, at a relatively low cost (Burton et al. 2015, Rovero and Zimmermann 2016, Apps and McNutt 2018, Glover-Kapfer et al. 2019). The advantages of camera traps are perhaps most apparent in their rapid adoption by wildlife researchers including primatologists. Over the past decade, there has been a rapid increase in both the number of wildlife and biodiversity monitoring programs employing CTs and the number of publications presenting CT data (Karanth et al. 2006, Ahumada et al. 2011, 2013, Pebsworth and LaFleur 2014, Burton et al. 2015, Rovero and Zimmermann 2016, Wearn and Glover-Kapfer 2017). The International Journal of Primatology recently published a special issue devoted to camera trapping (Pebsworth and LaFleur 2014). CTs have been used to assess site occupancy and distribution of single species (Linkie et al. 2007, Thorn et al. 2009), sympatric great apes (Nakashima et al. 2013), and of multiple species simultaneously, in which case the data also informed studies of species richness and community structure (Pettorelli et al. 2010, Treves et al. 2010, Ahumada et al. 2011), and have also been used in studies of spatial and temporal interactions between species (Foster et al. 2013,

Klailova et al. 2013, Kukielka et al. 2013, Keim et al. 2019), and activity patterns (Leuchtenberger et al. 2014), among other topics (Meek et al. 2014, Burton et al. 2015).

Felid researchers were quick to implement camera-trapping surveys because individuals could be identified from their unique pelage patterns, allowing CR or SECR data to be collected (Karanth and Nichols 1998, Silver et al. 2004, Foster and Harmsen 2012). Similar methods have more recently been applied to great apes, which can be individually recognized in images from facial characteristics and other distinguishing features (Head et al. 2013, Després-Einspenner et al. 2017). However, identifying and matching individual chimpanzees from large photographic data sets is time-consuming and potentially error-prone (Head et al. 2013, Kühl and Burghardt 2013, Després-Einspenner et al. 2017), and individuals of many species are not individually recognizable in images. Most existing methods for estimating animal density from CT data without identifying individuals assume certain or near-certain detection of animals of a certain size range when they pass close to the CT (Rowcliffe et al. 2008, Howe et al. 2017a, Nakashima et al. 2018, Moeller et al. 2019), which raises questions about whether CTs perform well enough under field conditions to meet such assumptions (Apps and McNutt 2018, Jacobs and Ausband 2018). PIR sensors sometimes fail to trigger the camera, and the probability of triggering is influenced by many factors, including the manufacturer and model, the height and angle at which the camera is deployed, background temperature, vegetation density, weather conditions, and the animal's size, speed, distance and angle of approach relative to the camera, and sociality or gregariousness (Treves et al. 2010, Rowcliffe et al. 2011, Wellington et al. 2014, Burton et al. 2015, Meek et al. 2015, Newey et al. 2015, Howe et al. 2017a, Apps and McNutt 2018, Jacobs and Ausband 2018), although Keim et al (2019) achieved near

perfect detection rates of humans and large mammals (evaluated using the presence of tracks in snow) using Reconyx Professional series cameras. There are also slight delays which may be unavoidable (1) between detection and image capture, referred to as the "trigger speed" (cameras with slow trigger speeds may fail to detect fast-moving animals), and (2) between the time when cameras stop recording images, and when they can be triggered again. Both delays tend to be longer when cameras are programmed to record video (Apps and McNutt 2018). Performance characteristics such as trigger speed and delay time, sensor coverage and sensitivity, image quality, robustness to field conditions, power consumption, and researcher satisfaction vary among CT models, and different models may be more appropriate for different types of surveys (Trolliet et al. 2014, Newey et al. 2015, Meek et al. 2015, Apps and McNutt 2018, Glover-Kapfer et al. 2019). Cost is not necessarily the best predictor of performance (Driessen et al. 2017, Apps and McNutt 2018). Fortunately, CTs' popularity, and the ongoing development of methods for evaluating CT performance and taking advantage of CT data (Rowcliffe et al. 2008, Howe et al. 2017a, Apps and McNutt 2018, Schneider et al. 2019, Tabak et al. 2019) are driving the development of superior products (Glover-Kapfer et al. 2019).

As well as failing to detect animals in front of the camera ("false negatives"), CTs can be triggered by changing light conditions or swaying vegetation, so they frequently record images with no animals ("false positives"; Newey et al. 2015, Jacobs and Ausband 2018). False positives increase the already considerable time required to process the large numbers of images recorded during CT surveys. CTs deployed worldwide are currently collecting more images than can be feasibly processed manually, but automated animal biometric systems for recognizing whether animals are

present in images, classifying those animals by taxon, and recognizing individuals are also rapidly improving (Kühl and Burghardt 2013, Kumar and Singh 2016, Schneider et al. 2019, Taback et al. 2018).

There can be little doubt that CTs will remain an important wildlife sampling tool, and that CT technology and animal biometric systems will continue to improve. Our current challenge is to develop and test statistical methods for taking advantage of resulting data to provide reliable estimates of abundance (Nakashima et al. 2013). Frequencies of detection at camera traps have been used as indices of relative abundance (Rovero and Marshall 2009, Treves et al. 2010), however, comparisons of relative abundance across species, time periods or study sites rely on the unrealistic assumption of common detection probabilities (Rovero and Marshall 2009, Harmsen et al. 2010, Sollmann et al. 2013b, Burton et al. 2015). Abundance estimation is frequently the main objective of CT surveys, but camera trapping survey designs are often poorly-linked to survey objectives (Kelly 2008, Foster and Harmsen 2012, Meek et al., 2014, Trolliet et al. 2014, Burton et al. 2015), possibly because researchers are tempted to address multiple questions from data collected during surveys designed to meet one key objective. For example, surveys designed to maximize detections of a particular species for the purposes of collecting CR data usually sample intensively and target specific habitat features including trails (Karanth and Nichols 1998, Head et al. 2013, Després-Einspenner et al. 2017), but randomized designs with wider trap spacing are more appropriate, and may be required, for studies of occupancy, community structure, or when estimating abundance of species that cannot be individually recognized (MacKenzie et al. 2002, Rowcliffe et al. 2008, 2013, Wearn et al. 2013, Burton et al. 2015, Howe et al. 2017a), particularly over larger spatial scales.

2.3 Emerging statistical methods for estimating abundance

2.3.1 Spatially explicit capture–recapture

The technological advancements described above facilitated estimation of great ape abundance via capture–recapture (CR) analytical methods, which require that individuals can be uniquely identified (Darroch 1958, Seber 1965, Otis et al. 1978, Efford 2004). CR has a long history and was described in reviews by Schwarz and Seber (1999) and Buckland et al. (2000). Statistical foundations of modern, non-spatial CR methods were described in Otis et al. (1978), Pollock et al. (1990), and Lebreton et al. (1992). Non-spatial CR methods require that all members of the sampled population are exposed to a non-negligible risk of detection, and yield estimates of the number of individuals at risk of detection by a fixed array of traps or detectors (*N*; Otis et al. 1978, Lebreton et al. 1992). However, *N* is only biologically relevant if the sampled population occupies a known, discrete area (Dice 1938). Animal density (*D*) is of greater interest and relevance because it is comparable among surveys, and can be extrapolated to estimate abundance across larger areas. However, if occupied habitat extends beyond the area surveyed (i.e., if the population is not geographically closed), *N* cannot be reliably converted to the more biologically relevant *D* without collecting additional data because many of the animals detected spend much of their time off the study area, and so the area sampled is larger than the area of the array, but unknown (Dice 1938, Boulanger and McLellan 2001, White and Schenk 2001, Efford 2004, Dillon and Kelly 2008). Methods for estimating the "effective trapping area" from information about location of capture relative to the grid edge, or distances between recapture locations, have been proposed, but these either lack statistical validity, or require large samples of recaptures at different traps or that data from peripheral traps

are discarded (Otis et al. 1978, Wilson and Anderson 1985, Karanth and Nichols 1998, Boulanger and McLellan 2001), and they have proven unreliable when applied to wide-ranging animals or sparse data sets (Soisalo and Cavalcanti 2006, Dillon and Kelly 2008, Obbard et al. 2010).

More recently-developed spatially explicit capture–recapture (SECR) models (Efford 2004, Borchers and Efford 2008, Royle and Young 2008, Royle et al. 2009a, b) treat detectability as a function of the distance between traps or detectors and animals' spatial center of activity, taking advantage of the fact that animals that spend more time close to detectors are more likely to be detected. The locations of centers of activity are not observed, so are treated as latent variables, and need not have biological significance (Borchers and Efford 2008, Borchers 2012). SECR models represent a major advancement. Modelling the spatial components of the encounter process freed researchers from the need to expose all animals to a risk of detection, providing much greater design flexibility (Efford 2004). By assuming that activity centers are distributed across the landscape according to a (usually Poisson or binomial) spatial point process, animal density can be estimated directly from spatially-referenced detections of individuals (Efford 2004). Furthermore, by accounting for differences in detectability attributable to differential exposure to traps explicitly, SECR models account for an important source of individual heterogeneity in capture probabilities (Efford 2004, Borchers and Efford 2008), reducing the need to rely on statistical approaches for modelling heterogeneity due to unobserved factors, which have been criticized (Dorazio and Royle 2003, Link 2004). Models can be fitted using maximum likelihood or Bayesian methods (Borchers and Efford 2008, Royle and Young 2008, Royle et al. 2009a, b). CR and SECR models may yield biased estimates when

detection probabilities vary in space, time, or among individuals, if this variation is not modelled (Otis et al. 1978, Pledger 2000), but SECR models allow detection parameters to be modelled as functions of temporal, spatial, or individual covariates; individual heterogeneity due to unobserved factors can also be modelled using mixture distributions (Borchers and Efford 2008). Density can also be modelled as a function of spatial or temporal covariates (Borchers and Efford 2008).

There have been several extensions of the general SECR framework. For example, models specific to different types of traps and detectors have been developed to account for cases where animals compete for traps, or vice versa (i.e., depending on whether 1 or >1 individual can be detected at a location during a sampling occasion, and whether detectors confine animals until they are released; Borchers and Efford 2008, Efford et al. 2009). See Efford et al. 2009a for a method for count data within a single sampling interval, Gardner et al. (2010) and Glennie et al. (2019) for demographically open populations, Royle and Young (2008) and Efford (2011) for area searches, Efford et al. (2013) for temporally variable sampling effort, Royle et al. 2013a for estimating abundance and landscape connectivity, Royle et al. 2013b and Efford (2014) regarding integrating resource selection information, Borchers et al. (2014) for continuous-time models, and Sutherland et al. (2015) for modelling non-Euclidean movement and landscape connectivity. Reich and Gardner (2014) presented a model for territorial species, which, although not appropriate to group-living territorial species such as great apes, demonstrates the potential to include repulsive activity centers in an SECR model.

Most genetic surveys of great apes used CR or capture-with-replacement (Miller et al. 2005, Petit and Valiere 2006) models to estimate *N* instead of using SECR to estimate *D* (Arandjelovic et al. 2010, 2011, Roy et al. 2014, Arandjelovic and Vigilant

2018). Head et al. (2013) and Moore and Vigilant (2014) were the first to use SECR to estimate densities of African great apes from photographic and genetic data, respectively. Head et al. (2013) estimated densities of chimpanzees, gorillas, and forest elephants in Loango National Park, Gabon, from CT data collected at 45 locations over a 20-month period; chimpanzees were habituated and their approximate density known within a subset of the area surveyed. Estimates for all three species were plausible, reasonably precise, and consistent with results from capture-with-replacement models, and estimates for habituated chimpanzees were accurate. Moore and Vigilant (2014) collected chimpanzee fecal samples over a 624 km^2 study area in the Ugalla region of Tanzania, and also estimated *N* using capture-with-replacement methods and *D* using SECR. Data were sparse; only 28 of the 113 individuals identified were captured more than once, but density estimates were nevertheless within the range expected based on prior information about chimpanzees in the Ugalla region and similar habitat elsewhere. SECR estimates of density were lower than those obtained by dividing the estimated population size by the nominal size of the study area, consistent with underestimation of the area surveyed and overestimation of *D* in this survey of a geographically open population (Dice et al. 1938, Efford et al. 2004, Obbard et al. 2010), as noted by the authors.

Reading Head et al. (2013) inspired me to pursue this PhD, and evaluating and effectively implementing SECR to estimate chimpanzee densities remained an important focus of my research (McCarthy et al. 2015, Després-Einspenner et al. 2017, Chapter 5, Chapter 6). McCarthy et al. (2015) provided the first reliable estimate of chimpanzee density in a densely-inhabited (by humans) forest-agricultural mosaic between two forest reserves in Uganda, from fecal DNA sampling over two years and

both capture-with-replacement and SECR methods. SECR methods accommodate spatially explicit definitions of the possible locations of animals' activity centers (Borchers and Efford 2008), which allowed us to estimate *D* both within forested fragments (spatial data describing habitat types were available), and across the fragmented mosaic. Densities within forest fragments were as high, or higher, than in nearby contiguous forests (McCarthy et al. 2015). This study demonstrated that in the absence of unsustainable, direct anthropogenic mortality, chimpanzees and humans can coexist in multiple-use landscapes provided that riparian forest fragments are preserved, and provides a useful reference for future surveys of chimpanzees occupying fragmented landscapes, and potentially also savannah and woodland habitats.

Després-Einspenner et al. (2017) intensively sampled an habituated chimpanzee community of known size and approximately known density in Taï National Park, Ivory Coast, for ten months, using an array of CTs deployed at randomized locations (a grid of 23 cameras with random origin), and another array with CTs distributed throughout the same area but with specific CT locations selected to maximize detections by targeting locations frequently visited by chimpanzees, and by moving cameras that did not detect chimpanzees over a one-month period. Density was estimated separately from each type of array by SECR, and replicate analyses of spatiotemporal subsets of the data were also analyzed to facilitate an evaluation of the effects of survey design and sampling effort on estimator performance. Most individuals were detected multiple times by both arrays, and density and abundance estimates from complete data sets were accurate. Detection probabilities at CTs that targeted preferred habitat features were more than double those at randomly-located CTs. Analyses of subsets of the data showed that estimates remained accurate when as few as ten CTs were deployed at

random locations, and as few as five CTs were deployed at targeted locations. An array of 24 targeted CTs yielded accurate estimates from a 20-week survey, but 30 weeks were required when 25 CTs were deployed at random locations. Density estimates from complete data and large subsets were highly precise, but this was partially attributable to the fact that variances were estimated under the assumption that activity centers were binomially distributed (Borchers and Efford 2008, Després-Einspenner et al. 2017). When we subsequently assumed an underlying Poisson distribution and estimated spatially unconditional variances, precision was comparable, though still slightly superior, to that achievable using other methods that require randomized designs (Cappelle et al. 2019). These and other results presented in Després-Einspenner et al. (2017) could help researchers to effectively design surveys and analyze data to obtain reliable estimates of chimpanzee densities (also see Chapter 6). For example, we evaluated more forms of heterogeneity in detection probabilities were evaluated than in prior SECR studies of great apes. Responses to initial detection, individual heterogeneity, and differences between seasons and sexes were supported, so we recommended that plausible forms of detection heterogeneity should be considered in candidate sets of SECR models of chimpanzee detectability, and where feasible, movements. That most individuals in the community were detected at as few as five CTs deployed within their territory highlighted the potential of this combination of methods to estimate chimpanzee density over large spatial scales (Després-Einspenner et al. 2017).

Density estimates were negatively biased when the region of integration extended beyond the known territory of the sampled community, so in our discussion (Després-Einspenner et al. 2017, pp. 7–10), we described how territoriality affected the

data collected and violated model assumptions, as follows: "when the region of integration extends beyond the trap array, animals with activity centers outside the array are expected to be detected at peripheral traps at a probability that depends on the distance between their activity centers and the traps (Borchers & Efford, 2008). However, because chimpanzees recognize territory boundaries and rarely cross them, members of neighboring communities will be detected less frequently than would be expected based on distance alone. We suspect similar effects contributed to the underestimation of chimpanzee density and population size reported by Granjon et al. (2016 [*sic*]), who also collected (genetic) SECR data within the known territory of a single community of known size". We further recommended "that future camera trapping studies of chimpanzees employ a trapping array at least as large as an average territory and located independently of territory boundaries, as this would allow density as well as population size to be estimated accurately in the absence of independent information about territory size (Borchers & Efford, 2008). We further suggest that the total extent of the array should ideally span the territories of several communities because in this case animals would have negligible detection probabilities at traps far from their activity center, providing more information to estimate σ, and the spatial distribution of activity centers would more closely resemble the Poisson point process underlying SECR models (Borchers & Efford, 2008)."

Granjon et al. (2017) used SECR methods to estimate the density of another chimpanzee community of known size from genetic samples collected during 3 months of intensive searching and 3 years of opportunistic data collection, and estimated abundance by SECR and other methods. Authors concluded that SECR models that tended to underestimate, but I suspect the underestimation they observed was

attributable to the fact that their integration mesh extended well beyond the territory of the sampled community, as described above. This highlights the importance of adapting statistical models or analyses to account for unique characteristics of the species under investigation, and therefore of collaboration between statisticians and ecologists.

Most of the surveys described above were of relatively long duration (many months to 3 years). Therefore, authors of all of the above-described SECR surveys of great apes, and Arandjelovic and Vigilant (2018) in their review of genetic surveys of primates, expressed concerns about violation of the assumption of demographic closure estimating models relied on. Granjon et al. (2017) described their sampled community as "effectively closed" over the duration of their three-year survey, but other authors suggested that chimpanzees' long lifespans and low reproductive rates should minimize violations, but acknowledged that violations likely occurred. Arandjelovic and Vigilant (2018) argued that improvements in precision achieved by increasing survey duration outweighed biases arising from closure violation. However, the potential for bias remains, so I investigated the consequences of demographic closure violation via simulation (Chapter 5).

2.3.1.1 Misidentification error in remote CR and SECR data

Both genetic and photographic data are potentially prone to various types of misidentification error. Coping with misidentification errors in genetic and photographic CR data became an active area of research concurrently with widespread implementation of these methods (Taberlet et al. 1999, Mills et al. 2000, Stevick et al. 2001, Lukacs and Burnham 2005). This issue deserves close attention here because genetic and photographic SCR could provide reliable estimates of great ape abundance

from relatively short field studies if misidentification error can be minimized or avoided. Here, I describe types of misidentification errors, their implications for CR estimation of abundance, their sources and efforts to minimize them, and models that allow for misidentification error in CR data.

Types of errors potentially resulting from misidentification include (1) false individuals, where multiple detections of one individual are attributed to more than one individual (also termed "false negatives" or "false rejections"), (2) missed individuals, where a newly detected individual is incorrectly considered a recapture of one previously identified (termed "false positives" or "false acceptances"), and (3) incorrect recaptures, where a detection of one previously identified individual is attributed to a different, previously identified individual.

The original formulations of both CR and SCR methods assume that detected individuals are always correctly identified (Darroch 1958, Otis et al. 1978, Pollock et al. 1990, Efford 2004). Violations cause bias (Arnason and Mills 1981), the direction and magnitude of which depends on the type of error. False individuals simultaneously cause negative bias in probabilities of detection, and positive bias in the number of individuals detected, leading to severe positive bias in population estimates even with relatively low (< 5%) error rates (Mills et al. 2000, Waits and Leberg 2000, Stevick et al. 2001, Creel et al. 2003, Lukacs and Burnham 2005, Roon et al. 2005, Yoshizaki et al. 2011, Vale et al. 2014). The potential conservation consequences of overestimating the abundance of populations of endangered species make this type of error the most important one to minimize. Missed individuals simultaneously induce positive bias in detection probabilities and negative bias to the number of individuals detected, leading to negatively biased population estimates, but the magnitude of bias to population

estimates is usually less severe (Schwartz and Stobo 1999, Mills et al. 2000, Waits and Leberg 2000). Incorrect recaptures would not affect the average probability of detection or the number of individuals detected, but could affect estimates of activity center locations and movement rates, and therefore density, from SECR models. Any type of misidentification error could induce, exaggerate, or mask, individual heterogeneity in probabilities of detection (Waits and Leberg 2000, Roon et al. 2005).

Human errors in data collection and management (e.g. transcription errors, mislabelling, pipetting errors) are rarely addressed and may be underestimated as a source of misidentification error (Stevick et al. 2001, Bonin et al. 2004). Clear protocols for data collection and management should be established and followed, and automation (e.g. Niedballa et al. 2016) could further reduce human errors. Sources of different types of errors differ between genetic and photographic surveys, so I describe them in turn.

When small quantities of potentially degraded or contaminated DNA are analyzed, laboratory errors can cause misidentification errors in genetic CR data (Taberlet et al. 1999, Morin et al. 2001, Paetkau 2003). If multiple individuals have the same genotype at the loci examined ("shadow effects"), individuals will be missed (Mills et al. 2000, Paetkau 2003). Shadow effects are avoidable provided the number and allelic diversity of the loci examined are sufficient to ensure that the probability of two individuals having the same genotype (P_{ID}) is negligible (Mills et al. 2000, Waits et al. 2001, Woods et al. 1999, Paetkau 2003). If individuals are closely related, for example due to philopatry, reproductive isolation, founder effects in colonizing or recovering populations, or genetic bottlenecks, more loci may be needed to ensure shadow effects do not occur (Woodruff 1993, Woods et al. 1999, Paetkau 2003).

If only one of two alleles at a heterozygous locus amplifies during PCR, the individual appears homozygous at that locus (referred to as "allelic dropout" Taberlet et al. 1996, 1999). False alleles, i.e. alleles apparent in the results of molecular analyses but not carried by the individual sampled, are less common than allelic dropout (Paetkau 2003, Arandjelovich et al. 2009, Guschanski et al. 2009), but can arise in several ways: (1) polymerase slippage during early cycles of the PCR reaction (Taberlet et al. 1996), (2) amplification of foreign DNA, whether from researchers (Woodruff 1993, Taberlet et al. 1999), or, in the case of fecal samples, microbial DNA (Montiero et al. 1997, Vigilant 2002), or (3) by errors in the measurement of allele lengths (bandreading or scoring errors; Paetkau 2003). If a false allele is generated at a locus for which the individual is heterozygous, it is likely to be detected because there will apparently be three alleles at that locus, but homozygotes will appear heterozygous (Taberlet et al. 1999). Allelic dropout and false alleles can theoretically generate all three types of misidentification errors, but false individuals are the most likely, and the other types become less probable as P_{ID} decreases (Taberlet et al. 1999, Paetkau 2004). The expected number of errors due to allelic dropout and false alleles increases with the numbers of samples and loci analyzed; the number of loci analyzed should therefore be no more than the number required to ensure P_{ID} is small enough to avoid shadow effects (McKelvey and Schwartz 2004).

Amplifying and genotyping DNA from each sample multiple times ("multi-tubing") and comparing the resulting genotypes can allow researchers to resolve results to a single, reliable genotype, or to identify and reject low-quality or error-prone samples that yield ambiguous results; it also facilitates quantification of genotyping error rates (Navidi et al. 1992, Taberlet et al. 1996, 1999, Bonin et al. 2004, McKelvey

and Schwartz 2004). Multi-tubing is likely the best way to detect and remove errors caused by allelic dropout and false alleles but it significantly increases the costs of genetic analyses, and the number of replicates is sometimes limited by the quantity of DNA initially collected (Taberlet et al. 1996, 1999, Morin et al. 2001, Paetkau 2003, 2004, Roon et al. 2005). Vigilant (2002) further recommended examining the specific sequences of anomalous alleles after multi-tubing to increase the chance of detecting false alleles. Paetkau (2003, 2004) argued that in many situations multi-tubing was unnecessarily costly because genotyping errors could be minimized by good laboratory practices. He recommended discarding low quality samples that yield incomplete genotypes, selectively reanalyzing only those pairs of genotypes that differed at only one to three loci, and having more than one experienced technician scrutinize the results of automated scoring procedures (also see Bonin et al. 2004 and Waits and Paetkau 2005). With DNA from plucked hairs, culling low quality samples and selective reanalysis can effectively remove errors, but with more error-prone samples (such as shed hair or faeces) selective reanalysis might not be sufficient (Paetkau 2004, Roon et al. 2005). For example, Navidi et al. (1992) recommended ten replicate amplifications to avoid genotyping error where small quantities of DNA are available, and Taberlet et al. (1996) recommended two replicates at each allele for heterozygous loci and seven for homozygous loci. However, by recognizing that the probability of obtaining an incorrect genotype is a function of sample quality, including the quantity of template DNA initially extracted, a large portion of errors can be removed by discarding low-quality samples (Woods et al. 1999, Morin et al. 2001, Creel et al. 2003). This strategy could reduce the cost of genetic analyses, but could also result in the loss of useful data. Morin et al. (2001) found a strong relationship between the frequency of allelic dropout

and the initial quantity of template DNA. They argued that the more extensive multi-tubing recommended by Navidi et al. (1992) and Taberlet et al. (1996) was unnecessary if the amount of DNA in extracts was quantified, and samples with low amounts of template discarded.

The past fifteen years have seen many improvements to methods for storing, extracting, amplifying, and genotyping DNA (reviewed by Beja-Pereira et al. 2009). For example, multiplexing, in which several loci are amplified in a single reaction, makes more efficient use of low quantities of template DNA. Two-step multiplexing, whereby an initial PCR is used to amplify DNA at all loci under consideration, and a second PCR uses the products of the first as template for genotyping individual loci, requires even less original template, increases amplification success, and reduces the frequency of allelic dropout and false alleles (Hedmark and Ellegren 2006, Arandjelovic et al. 2009, Beja-Pereira et al. 2009). Arandjelovic et al. (2009) presented and evaluated a two-step multiplex procedure for genotyping DNA from western chimpanzee, western gorilla, and mountain gorilla fecal samples to up to 19 loci. Average rates of allelic dropout and false alleles varied from 4–9%, and from 0.3–1.7%, respectively, for the different species. However quantification of the amount of DNA initially extracted demonstrated that the majority of errors occurred in samples with low initial template. They calculated that up to five replicate amplifications would be required to ensure 99% genotyping accuracy where very small amounts of template were available, but only two or three would be required for the majority of samples. Quantifying DNA template and excluding low-template samples is becoming common practice during analyses of fecal DNA from great apes (Guschanski et al. 2009, Arandjelovic et al. 2010, 2011, Moore and Vigilant 2014, Arandjelovic and Vigilant 2018).

Recent genetic CR studies of great apes exemplify thoroughness to avoid genotyping errors, typically employing the extraction and amplification methods recommended by Arandjelovic et al. (2009), as well as strict laboratory protocols, matching criteria, and selective reanalysis. P_{ID} is consistently low enough to minimize shadow effects even where closely-related individuals are sampled; multi-tubing is commonly applied, including both multiple (frequently three to five) initial replicates from each sample, and additional replicates where required to resolve ambiguous genotypes; allele lengths are scored using a combination of automatic processes and human screening of results, and pairs of similar genotypes are carefully scrutinized and ancillary data checked to confirm or exclude the possibility that the mismatches resulted from allelic dropout or scoring errors (Arandjelovic et al. 2010, 2015, Chancellor et al. 2012, Moore and Vigilant 2014, Roy et al. 2014, McCarthy et al. 2005). Thus, current protocols for identifying and removing genotyping errors, and for matching similar genotypes, should effectively minimize misidentification errors in genetic CR studies of great apes.

Misidentification errors can also arise where naturally-occurring phenotypic marks or features are used to identify individuals (e.g. from direct observations or photographs; Bateson 1977, Stevick et al. 2001). Distinguishing features that are similar across individuals could lead to errors of any type, and markings that change over time could generate false individuals (Bretagnolle et al. 1994, Friday et al. 2000, Stevic et al. 2001, Yoshizaki et al. 2009). Failure to recognize multiple images of the same individual as such (i.e. attributing the images to >1 individual) would also generate false individuals. Some authors have argued or shown that with sufficiently variable markings that are stable over time, trained observers matching photographs,

and stringent matching protocols, missed individuals should be rare in photographic data (Stevick et al. 2001, Vincent et al. 2001, Morrison et al. 2011). However, for CR or SCR estimates of great ape abundance to be reliable, the rate of misidentification error should be demonstrably low.

One approach to reducing errors is to have multiple observers familiar with the target species independently identify individuals from the same set of images, and to include only identifications upon which all observers agree in the data (Stevic et al. 2001, Vale et al. 2014). In the absence of independent information about identities, error rates cannot be estimated directly, but agreement among observers and hence observer "reliability" can (Landis and Koch 1977). Head et al. (2013) assumed error-free identification of individual chimpanzees, gorillas, and forest elephants by the principal investigator, but also assessed the ability of other observers to identify individuals accurately. Another photographic SECR survey of an habituated chimpanzee community relied on identifications from either of two highly experienced observers, but both observers independently identified individuals in 25% of the videos (Despres-Enspenner et al. 2017). Both authors measured agreement using Cohen's Kappa coefficient (K), where a value of 1 indicates perfect agreement, and values > 0.81 indicate almost perfect agreement (Cohen 1960, Landis and Koch 1977). K was > 0.5 across all observers and species in Head et al.'s (2013) survey, and the most experienced category of observers had $K \geq 0.8$ for all species except gorillas; elephants were apparently easier to identify than great apes. Despres-Enspenner et al. (2017) also showed that agreement between observers was high but imperfect ($K = 0.814$), and further noted that misidentification errors did not appear to bias their estimates, which were highly accurate.

Like genetic samples, the quality of images for the purposes of identifying individuals varies, for example with lighting, resolution, and the animal's distance, angle, and aspect relative to the camera (Bateson 1977, Friday et al. 2000, Loos and Ernst 2013). Stevic et al. (2001) ranked images of humpback whales in terms of image clarity and the distinctiveness of markings, and estimated error rates in photographic CR data using high-quality genetic data as a reference. Across 2326 genetic and 4207 photographic detections, there were 14 errors that created false individuals and no errors that resulted in missed individuals; the probability of error was strongly related to image quality and weakly related to the distinctiveness of markings (Stevic et al. 2001). When images with quality rankings in only the highest two categories were included, photographic data were error-free and CR estimates of *N* were unbiased, but as more lower-quality images were included, (uncorrected) estimates were increasingly positively biased (Stevick et al. 2001). Forcada and Aguilar (2000) similarly found that the use of low quality images resulted in errors that created false individuals. Therefore, errors can be reduced while simultaneously reducing the time required to identify individuals by culling low-quality samples at an early stage, as in genetic analyses, and having multiple, highly experienced observers independently identify chimpanzees from the same images, and including only agreed-upon identifications in SECR data.

Manually matching images to build encounter histories would still be laborious and time-consuming (Crunchant et al. 2017). Fortunately, automated computer vision methods for recognizing the presence of animals, and identifying their species, sex, age class, and even individual identity have improved dramatically since CTs gained widespread use (Ardovini et al. 2007, Kühl and Burghardt 2013, Schneider et al. 2019, Tabak et al. 2019). Methods for great apes in particular were able to build upon prior

efforts to identify human faces, and are now sufficiently well-developed for supervised use with real field data (Kühl and Burghardt 2013, Loos and Ernst 2013, Freytag et al. 2016, Brust et al. 2017, Crunchant et al. 2017). Computer vision methods also improve as libraries or galleries of annotated images of identified individuals get larger; currently performance, and evaluations of performance, are hindered by the relatively small amount of this "training data" available (Freytag et al. 2016). It may always be necessary to exclude low-quality samples, so this should be recognized when designing field surveys to collect sufficient data to achieve a desired level of precision (Lukacs and Burnham 2005); this is equally true for photographic and genetic surveys.

2.3.1.2 Models that allow for misidentification errors

Concerns about bias in estimates of abundance from CR data that include misidentification errors motivated the development of CR models that allow for such errors (Stevic et al. 2001, Lukacs and Burnham 2005, Link et al. 2010, Wright et al. 2009, Yoshizaki et al. 2009, 2011, Vale et al. 2014).

Wright et al.'s (2009) model estimated rates of allelic dropout directly from genetic results from multiple genotyping attempts (multi-tubing), and treated capture histories as latent variables to be sampled by a MCMC algorithm. Modelling allelic dropout improved the accuracy of abundance estimates for European badgers estimated from a fecal DNA data set.

Most other CR models that allow for misidentification error were intended to account for the presence of false individuals and assumed that all errors generated a false individual detected only once, and all have a similar form, where a classical CR model that allows for occasion-specific probability of detection (model M_t; Otis et al.

1978) is extended to include an additional parameter (α) for the probability that the individual was correctly identified (model $M_{t,\alpha}$; Lukacs and Burnham 2005, Link et al. 2010, Yoshizaki et al. 2011, Bonner and Holmberg 2013, Vale et al. 2014). The frequency of encounter histories with only one detection ("unit histories"), or more specifically a surplus of unit histories, informs α, because errors that generate false individuals will usually generate unit histories unless the same error appears twice in the same data set. Performance of model $M_{t,\alpha}$ therefore decreases as conditions that make real unit histories more likely (fewer sampling occasions, or lower detection probabilities; Vale et al. 2014). Lukacs and Burnham (2005) developed the first such model, but the likelihood was often difficult or impossible to compute, and mis-specified with respect to misidentifications on first capture (Link et al. 2010, Yoshizaki et al. 2011). Yoshizaki et al. (2009, 2011) developed a least-squares method for fitting the model and Link et al. (2010) developed a Bayesian approach with model fitting via MCMC. Both of these formulations avoided the problem of misidentifications upon first capture and improved accuracy in the presence of misidentification error relative to the original, but the least-squares method lacked a variance estimator, and the Bayesian implementation was computationally expensive.

Yoshizaki et al. (2009) proposed a model to account for misidentification errors in photographic CR data caused by changes in natural markings over time. It assumed that misidentification leads to the creation of a false individual, and that once such an individual is generated, the original, real individual is never subsequently recaptured, but the false individual may be. An explicit likelihood could not be derived; estimation was achieved via unweighted least squares and minimum χ^2, using formulations that removed *N* from the estimating function; *N* was estimated as a derived parameter after

fitting the model. The authors demonstrated the efficacy of their model at removing severe positive bias in abundance estimates from M_t for salamander larvae with misidentification rates of 0.06 – 0.29. In simulations model M_t overestimated *N*, though only slightly at error rates ≤ 0.05. Modelling misidentification errors removed the bias, but caused negative bias at low *p* and *N*, and reduced precision. With $p = 0.2$ and error rates ≤ 0.05, models that ignored errors produced estimates with similar accuracy and lower root mean squared error. The authors described their model as a basis for developing more realistic models and did not recommend its general use without further development.

All of the above-mentioned studies demonstrated by simulation that if ≥ 2.5% of samples generate a false individual, M_t underestimated *p* and overestimated abundance, but modelling the errors using $M_{t,\alpha}$ removed the bias and, where variances were estimable, improved confidence interval coverage. Vale et al. (2014) developed an efficient maximum likelihood estimator following Link et al.'s (2010) formulation, and conducted more extensive simulations employing wider ranges of survey durations, detection probabilities, and error rates to evaluate its performance. These simulations confirmed previous results in that with 8 sampling occasions, $p = 0.4$, and a misidentification rate of only 3%, model M_t underestimated *p* and yielded population estimates that were positively biased by 10% with 0% CI coverage, whereas $M_{t,\alpha}$ yielded accurate estimates with nominal coverage. However, when *p* was < 0.2, both models yielded estimates with some bias and less than nominal confidence interval coverage, but estimates from model M_t were more accurate and consistent across replicates, such that better estimates were obtained by ignoring errors than by modelling them; furthermore, at higher error rates (>5%) estimates from $M_{t,\alpha}$, though unbiased,

were so imprecise that little could be inferred about abundance (Vale et al. 2014, also see Lukacs and Burnham 2005). Authors concluded that (1) ensuring a low error rate was likely to be less costly than ignoring errors and obtaining enough data to achieve the same level of precision by fitting model $M_{t\alpha}$, (2) that where correcting errors was not feasible, better results would be obtained by ignoring errors rather than trying to model them in many realistic scenarios, and (3) no satisfactory method is available for analyzing real data sets that include misidentification error (Vale et al. 2014).

Morrison et al. (2011) extended the Cormack-Jolly-Seber model (Cormack 1964) to account for misidentification error when estimating survival from photographic data. Again, the method accounted only for unique errors that generated unit encounter histories of false individuals. However, their approach was to censor first observation of all individuals, thereby conditioning on releases, and removing all unit histories (an approach also used to remove transients from CR data sets [Pradel et al. 1997]). Recapture probabilities were modelled as the true probability of recapture times the probability of correct identification (α). Analysis of simulated sets drawn from large populations with relatively high (≥ 0.3) occasion-specific probabilities of detection and a wide range of error rates showed that survival was underestimated when errors were ignored, particularly at higher sampling intensities and error rates, but estimates generated using the conditional approach were unbiased, but considerably less precise. However, when applied to a real data set (2571 photographs of 1539 male wildebeest), survival estimates were similar regardless of whether errors were modelled or ignored, but modelling them reduced precision considerably. Authors concluded that at misidentification rates of 0.01 to 0.05, ignoring errors would provide better estimates.

Models that allow for misidentification error do little to improve estimates of abundance from real CR data, which tend to be sparse and include true unit encounter histories, and include few errors. They might be useful for informing abundance in situations where data are likely to include errors but there is no means to identify and exclude error-prone samples, but avoiding or minimizing errors when processing genetic or photographic data, and ignoring errors at the abundance estimation stage is preferable.

To my knowledge, this issue has not been addressed in the SECR context specifically.

2.3.2 Emerging methods that do not require individual identification

Here I describe recently-developed statistical methods for estimating animal density from CT data when few or no individuals are individually identifiable. Animal density is a more ecologically relevant and comparable parameter than occupancy or population size (*N*), so methods for estimating those quantities from CT data will not be described here, but see Denes et al. (2015) for a recent review.

The random encounter model

Rowcliffe et al. (2008) developed the first method for estimating animal density from CT data in the absence of individual identification: the random encounter model (REM). I describe it in some detail because it addresses the same problem, and has similar design requirements and assumptions, as distance sampling with camera traps, described in Chapter 3 of this thesis and by Howe et al. (2017a). The REM adapted a two-dimensional mechanistic model of rates of collision between gas molecules

(Hutchinson and Waser 2007) to situations where contact occurs within a segment-shaped area. The expected number of contacts (y; where each contact is the initial detection of a moving animal at a CT, yielding one image) was expressed as a function of animal speed (v), animal density (D), time (t), and the width of the profile of the detection zone averaged across all possible angles of approach, which is a function of the radius (r) and central horizontal angle (θ) of the detection zone of the CTs. Rearranging this expression yielded a model for estimating density as a function of camera trapping rate, given unbiased independent estimates of v, r, and θ. For animals that travel in groups, density of groups is estimated from the model, and an estimate of mean group size (g) is required to obtain animal density.

Rowcliffe et al. (2008) estimated r and θ using trials with humans moving past a CT perpendicular and parallel to the direction it was aimed. Later, Rowcliffe et al. (2011) developed maximum likelihood methods for estimating the dimensions (r and θ) of the area effectively monitored by CTs directly from field data. Their approach borrowed from DS theory to estimate detectability as a function of the distances and angles at which animals were first detected, and environmental, camera-specific, and animal-specific covariates. Furthermore, authors were rightfully concerned that smaller animals could pass beneath the field of view of the camera at shorter distances, which would cause overestimation of detectability at short distances and hence underestimation of density, if a conventional monotonically nonincreasing detection function model was fitted to the data. They therefore developed logistic mixture models of the relationship between detectability and distance that combined a standard, decreasing detection function with a sigmoid increasing function at very short distances. The performance of the models was evaluated by simulation and with real data. In one

set of simulations, authors parameterized the REM with model-derived estimates of *r* and θ from simulated data where detectability decreased monotonically with distance; resulting density estimates had low (< 5%) bias, except where θ was < 15° such that the detection zone was nearly as well described by a line as a sector, and radial (point transect) detection function models did not fit the data well. We therefore expect these methods to perform better when the horizontal range of the sensor is similar to or greater than the horizontal field of view (FOV) of the camera. Estimates of *r* from logistic mixture models were also evaluated by simulation, and were most accurate when the true detection function included a broad plateau of certain detectability. Where detection was certain only at a point or narrow range of distances, average bias remained relatively low, but the distribution of outcomes was skewed and included severe underestimates, especially at smaller sample sizes. Estimates were completely unreliable where detection was not certain at any distance. Multiple detection function models including logistic mixture models were also fitted to real data from nine mammals of different sizes. Detectability was strongly affected by both distance and angle, and logistic mixture models of detectability as a function of distance were supported for the 5 smaller species more likely to pass beneath the FOV at short distances. Furthermore, relationships between detectability and each of distance and angle varied among species and between seasons. Authors concluded that these methods could provide reliable estimates of *r* and θ for use with the REM. Hofmeester et al. (2017) described methods for estimating *r* while reducing field effort, by placing distance markers along the midline of the field of view and assigning animals to distance intervals rather than measuring continuous distances.

Rowcliffe et al. (2008) suspected that unbiased estimates of *g* and *v* would be more difficult to obtain. Both are likely to vary in space and time, so estimates should be derived from data collected at the same time and location as the CT survey. For their original field test, Rowcliffe et al. (2008) were able to estimate day range and therefore *v* from direct observations because the animals they sampled were habituated to the presence of humans. Rowcliffe et al. (2011) programmed cameras to record 10 images at 1 second intervals when triggered, with the potential to be triggered again immediately (no programmed delay) and calculated *v* as the geometric mean of measured distances animals moved between photographs. Since then, however, the same authors formalized statistical methods for estimating both the proportion of time animals are active (activity level) and the speed of movement while active (travel speed), at the population level, directly from CT data (Rowcliffe et al. 2014, 2016). The product of daily activity level and travel speed is referred to as day range, and is a suitable estimate of *v* for use with the REM. Activity level is only estimable if it is reasonable to assume that 100% of the population are active and available for detection by CTs simultaneously at some time during each day, which is likely reasonable for many species, but complicates applications to e.g., semi-arboreal or semi-fossorial species, and large predators (Rowcliffe et al. 2014, Howe et al. 2017a, but see Capelle et al. 2019). One hundred observations were sufficient for accurate and reasonably precise (CV about 10%) estimation of daily activity curves, with diminishing returns at larger sample sizes (Rowcliffe et al. 2014, Lashey et al. 2018). Field estimates of travel speed seemed reliable, in that they co-varied as expected with body mass and diet, and were similar to independent estimates from telemetry data (after telemetry estimates were

corrected for negative bias induced by low sampling frequency; Rowcliffe et al. 2012, 2016).

The REM, and methods for estimating travel speed, require a randomized design, or, more specifically, that habitats and habitat features that are either preferred or avoided by animals are sampled in proportion to their occurrence on the study area (Rowcliffe et al. 2013, 2016). The REM further relies on the following assumptions. Firstly, to derive the model it was necessary to assume that animals move randomly and independently of each other, but violations are not expected to cause bias (Hutchison and Waser 2007, Rowcliffe et al. 2008, 2013). Second, it assumes that "animals conform adequately to the model used to describe the detection process" (Rowcliffe et al. 2008, pp 1233). This assumption implies at least two, more specific assumptions: (1) certain detection of animals within the sector described by r and θ (because the model does not allow for missed detections within this sector), and (2) animals are neither attracted to nor repelled by the cameras. Other key assumptions are independence of observations and demographic closure of the sampled population (Rowcliffe et al. 2008). The independence assumption requires that correlated detections (e.g. the same animal triggering the camera more than once without leaving the detection zone) can be recognized as such and excluded. Rowcliffe et al. (2008) programmed their cameras to delay at least 2 minutes between successive photographs to avoid correlated detections, but acknowledged that animals might remain in the detection zone longer than this, and that the delay could also result in missed independent detections. Shorter surveys reduce violations of the closure assumption, but where the assumption is violated, the REM should still yield an estimate of average density during the entire survey.

Variances around densities estimated from the REM are obtained by a nonparametric bootstrap across camera locations (with replacement), and the variances of r, θ, v, and g can be incorporated via the delta method (Rowcliffe 2008), the variances of the two components of v having first been combined as a variance of products (Rowcliffe et al. 2016). Stratification, for example by habitat type, when designing surveys and analyzing data allows densities within different strata to be estimated, and can improve efficiency and precision (Rowcliffe et al. 2008, 2013, Buckland et al. 2015).

There have been several evaluations and applications of the REM with simulated and real data. Rowcliffe et al.'s (2008) estimates for three of four species were within 22% of the true value, inaccuracy in the fourth case was attributed to biased camera placement with respect to habitat preferences. Measures of uncertainty were presented only as figures, but estimates from real data appeared imprecise, and CVs from simulated data declined to 0.20 when at least 40 locations were monitored. Lucas et al. (2015) developed a generalized REM to accommodate data from different types of detectors. Their simulations indicated that all derivations of the REM yielded estimates with low bias, that original REM yielded the most precise estimates, and that estimates remained accurate when different models of animal movement were used to generate the simulated data (beyond any effect on sample size). CVs approached 0.10 when the sample size of detections approached 100 in simulations with constant density and random movement, but authors acknowledged that precision would be reduced in real situations with locally variable density and non-random movement (Lucas et al. 2015).

Rovero and Marshall (2009) estimated densities of Harvey's duikers (*Cephalophus harveyi*) on multiple study sites using both human observers and line

transect methods, and the REM. Line transect surveys were expected to underestimate because duikers may avoid observers, and densities estimated using the REM were double to nearly four times those from line transects (Rovero and Marshall 2009). Unfortunately, camera placement targeted trails and dung piles (Rovero and Marshall 2009), violating the assumption that areas preferred by animals were sampled in proportion to their availability on the study area and preventing a meaningful assessment of the REM. The REM was used to generate the first estimate of pine marten density in Italy and the estimate of density was within the range previously reported for the same species elsewhere (Manzo et al. 2012). However, in a subsequent study where a local concurrent, genetic CR estimate of abundance was available for comparison, the REM was found to underestimate pine marten density by at least 60% (Balestrieri et al. 2016). Authors suggested this was largely due to difficulties estimating *v* for elusive species, but it also seems likely that failure to account for the fact that semi-arboreal martens spend part of their active time above the vertical range of CTs was a contributing factor (Howe et al. 2017a, Cappelle et al. 2019). In a study of endangered Grevy's Zebra (*Equus grevyi*), REM, line transect DS, and photographic CR yielded comparable density estimates (range 0.93 to 1.82, in different years; Zero et al. 2013). Again, however, cameras were placed at "optimal" locations, usually along roads or trails used by animals – a situation in which the REM should overestimate. Day range and group size were estimated independently of the CT survey, and authors noted that estimating these directly from CT data might not have been feasible. Precision of the REM, where uncertainty in *v* and *g*, but not *r* and θ, contributed to the overall variance of density, was inferior to CR but superior to DS. European wildcat densities were estimated from genetic and photographic SECR, and the REM, on the

same study area in Italy (Anile et al. 2014). Photographic SECR detected most or all of the individuals on the study area and yielded a precise estimate; the REM estimate was comparable but higher (Anile et al. 2014), likely because cameras were again set on trails to maximize SECR sample sizes. Cusack et al. (2015a) used the REM to estimate densities of female lions in an area where independent estimates from telemetry-assisted direct observations were available. Cameras were placed non-randomly targeting resting sites under shade trees to maximize detections, and the REM, not surprisingly, overestimated abundance. However when only night-time observations were included in the data, such that animal movement during sampling may have been approximately random with respect to trap placement, bias was substantially reduced and CIs of REM estimates overlapped those of independent estimates (Cusack et al. 2015a). Caravaggi et al. (2016) used the REM and line transect DS to demonstrate that densities of the native Irish hare were lower where invasive European hares were established. DS and the REM detected similar spatial patterns between natives and invasives, but total population estimates from the REM were considerably higher (1.4 times higher on average) than those from DS; differences may have been attributable to differences in the spatial scale of sampling, or non-independent redetections of the same hares (Caravaggi et al. 2016).

The REM and associated methods constitute a complete framework for estimating densities of unmarked animals from CT data exclusively (Rowcliffe et al. 2008, 2011, 2014, 2016). To date, targeted as opposed to randomized trap placement and unreliable estimates of *v* have hindered their effective application (Rovero et al. 2009, Zero et al. 2013, Anile et al. 2014, Balestrieri et al. 2016), but clarifications of

assumptions (Rowcliffe et al. 2013), and recently-developed methods for estimating *v* from CT data (Rowcliffe et al. 2016) could improve this situation.

Spatial count models

Chandler et al. (2011) and Chandler and Royle (2013) developed SECR-like models for unmarked animals, where the spatial autocorrelation of detections alone informs the number and locations of individual activity centers. Closely-spaced detectors are required, and estimates are too imprecise to be useful unless a subset of the population can be reliably identified (Chandler and Royle 2013, Le Saout et al. 2014). Furthermore, I expect these methods to perform best with solitary animals that maintain exclusive use of much of their home range. It is not recommended for social animals like great apes that travel in groups, because of the high spatial autocorrelation among locations of different individuals.

Distance sampling with camera traps

Chapter 3 and Howe et al. (2017a) extended point transect DS methods to accommodate data from camera traps. Similarly to the REM, camera trap distance sampling (CTDS) provides a complete framework for estimating animal density directly from data collected at CTs deployed independently of the density and distribution of animals (Howe et al. 2017a). However, rather than relying on the assumption of independence and including only initial detections in the data, we recommend predetermining (*a priori*) a set of closely-spaced (< 1 to 3 seconds apart) snapshot moments at which to measure distances to animals, and that CTs are programmed to record video. Then, measured distances are independent of the location of the animal

when first detected, and approximates animals' continuous path in front of a CT, hence avoiding any positive bias in observed distances associated with animals approaching through the arc of the sector (Howe et al. 2017a). Violation of the independence assumption does not bias point estimates of abundance from DS models, we can avoid this assumption when estimating variances (by bootstrapping), and adjusted methods for selecting among models of the detection function when the data include non-independent observations were recently developed (Chapter 4 and Howe et al. 2019). Recording video (or long, rapid bursts of still images) ensures that some animals will be filmed at the edges of the field of view, and the pooling robustness property of DS models ensures that heterogeneity in detectability with increasing angle from centre does not cause bias (Burnham et al. 2004), so it is not necessary to estimate the effective detection angle. However, survey duration is a parameter in the model, so estimates of the proportion of this time that animals are active within the vertical range of CTs are required to avoid overestimating sampling effort and underestimating density (Howe et al. 2017a). For animals that are always within the vertical range of CTs when active, it will frequently be reasonable to assume that 100% of the population is available for detection at the peak of activity, and use Rowcliffe et al.'s (2014) methods to estimate this proportion and associated uncertainty.

CTDS and the REM can be used to address the same questions from the same data, so I will briefly highlight their similarities and differences. The small area monitored by CTs combined with random trap placement could yield insufficient data to estimate densities of rare animals with reasonable precision using either method. Both methods are subject to negative bias if suboptimal camera performance causes missed detections very close to the camera (CTDS) or at short-to-moderate distances and small

angles (REM). Either attraction or avoidance of the cameras is expected to cause bias if it affects the encounter rate. CTDS data include fine-scale measures of instantaneous animal locations, and temporal sampling effort, and in future the REM may often rely on CT-derived estimates of *v*, so even slight behavioural responses, such as a change in speed of movement, could cause bias even if they did not affect the number of independent encounters. Rowcliffe et al. (2016) recommended excluding observations of animals responding to cameras when estimating *v*.

Although applying the REM in its original form would place less demand on CT power and memory usage, estimating *v* requires video or near-video rapid-fire settings (Rowcliffe et al. 2016), so in practice demands would likely be similar. CTDS accounts for imperfect detection by estimating effective detection distance from radial distance observations, and uncertainty in both detectability and encounter rate are included in bootstrap estimates of variance (Buckland et al. 2001), whereas the REM requires both the effective detection radius and angle to be estimated, and that uncertainty in these parameters is combined with other sources of uncertainty using the delta method (Rowcliffe et al. 2008, 2011). The REM requires estimates of the proportion of time active and the speed of animal movement while active, whereas CTDS requires only the former. When animals travel in groups, CTDS treats the individual as the unit of observation since the independence assumption is already severely violated, but the REM currently relies on an estimate of mean group size (Rowcliffe et al. 2008). Unless groups are typically small (1 to 3 animals), animals travel very close together relative to the area monitored by a CT, or CTs are deployed along narrow trails in dense habitat (which would be inappropriate if data contributed to abundance estimation by either method), it seems likely that group size will be underestimated from CT data because

some members of the group could easily pass behind or beside the camera without being detected. CTDS therefore seems more appropriate for social species, unless individuals as opposed to groups of animals were treated as the unit of observation when applying the REM. Another advantage of CTDS is that it is an extension of a well-described existing framework for estimating animal abundance (Buckland et al. 2001, 2004, 2015) that is familiar to many ecologists and supported by free software (Thomas et al. 2010, Laake et al. 2018), training materials, and advice from experts (http://distancesampling.org/).

The random encounter and staying time (REST) model

Nakashima et al. (2018) reparameterized the REM to estimate density as a function of camera trapping rate and "staying time" defined as the amount of time animals spend within a specific area (the "focal area") within the field of view of a CT (the random encounter and staying time or REST model). Estimating staying time requires that CTs be programmed to record video with the potential to trigger again immediately. Assumptions were similar to those for the REM and CTDS (sampling locations independent of animal density and movements, certain detection of animals within the focal area), with the additional assumption that staying time follows a specific parametric distribution, and that this distribution is representative of animal movements. To better meet this assumption, authors recommended estimating staying time when active and correcting estimates using an estimate of the proportion of time active (similar to CTDS). Densities estimated from simulated data were unbiased, provided any unusually long staying times were identified as outliers and censored. Density was underestimated when simulated animal activity was asynchronous, but we

would also expect the REM and CTDS to underestimate in this situation because if less than 100% of the population were active at the daily peak, activity level would be overestimated and density underestimated (Rowcliffe et al. 2011, Howe et al. 2017a). Densities estimated from real data were slightly higher than those from line transect DS surveys, and followed a similar pattern of variation among habitat types. Authors concluded that the REST model was more efficient and easier to implement than the REM. This model seems worthy of consideration in situations where the REM or CTDS might alternatively be applied. CTs deployed according to a randomized design and programmed to record video could provide the data necessary to fit the REM, the REST model, and CTDS models. Field trials applying all of these methods simultaneously, especially to a population of known or approximately known size, would be informative about the relative performance of these three methods.

Time to event, space to event, and instantaneous sampling estimators

Moeller et al. (2019) presented three new estimators of the density of unmarked animals from CT data, all of which require randomized designs. The time to event model (TTE) resembles the REM and has similar requirements (including an estimate of movement rate) and assumptions, but is parameterized like other time-to-event (or survival) models, where the response variable is the time elapsed prior to detection, and taking advantage of the relationship between Poisson-distributed events and exponentially-distributed intervals between events to develop the model. Only the first detection of an animal (of a particular species) within each (daily) sampling occasion contributes information, so the TTE could reduce time spent processing images. Authors initially assumed certain detection within the field of view of the camera out to

the “trigger distance”, proposing, but not evaluating, a possible extension to account for imperfect detection at the camera level (i.e., irrespective of location within the zone of potential detection). The other two estimators use time-lapse as opposed to motion-sensitive remote photography to eliminate uncertainty associated with the performance of the sensor. In time-lapse photography, cameras record images at specified times, usually at regular intervals, regardless of whether or not an animal triggers the sensor. The space-to-event (STE) model treats the number of animals detected by a camera as a Poisson-distributed random variable, and since events are again Poisson-distributed, the space between animals is expected to be exponentially distributed (Moeller et al. 2019). Survey duration is subdivided into smaller (e.g. hourly) periods within occasions, and the area sampled is calculated as the area monitored by the camera multiplied by the number of periods before an animal is first observed. The instantaneous sampling (IS) estimator is similar to a point count survey. The data consist of counts within replicate fixed-area plots, replicated in time, density is estimated as the number of animals observed (maximum one per period of a given species) divided by the total area sampled and number of sampling periods, and variance estimation follows Fewster et al (2009), or by bootstrapping across locations. Authors acknowledged that the TTE, which ignores imperfect detection by motion-sensitive photography, requires further development, but argued that this assumption may be reasonable with time-lapse photography. In my opinion, the most important aspect of this research is not the novel model formulations, but rather this recognition that time-lapse photography avoids many of the problems that reduce the defensibility and reliability of densities estimated from CT data, allowing similar data to be collected in a more rigorous though less efficient manner (Hamel et al. 2013; also see Chapter 7).

2.4 Conclusions

There is clearly the potential to combine genetic or photographic sampling with SECR methods to estimate great ape density reliably and precisely. SECR methods offer greater design flexibility than methods for estimating abundance of unmarked animals, allowing researchers to target habitat features such as trails to maximize sample sizes of detections. Genetic surveys are effective, but collecting samples is labour-intensive, and analyzing them to identify individuals is costly. Photographic sampling could reduce field time and avoid costs of molecular analyses, and is expected to become increasingly practical as CT technology and automated methods for identifying individuals improve. Minimizing misidentification error is critical to accurate estimation, and should be achievable.

Methods for estimating animal density from CT data that do not require individuals to be identified, and are appropriate to social species, generally require randomized designs. Real animals are not uniformly distributed in space, nor do they move randomly, so encounter rates at randomly-located CTs are expected to be lower and highly variable among sampling locations, such that even ambitious surveys could yield imprecise estimates, especially for rare species. However, unlike in SECR surveys, it is not necessary to detect the same individuals at more than one location, so traps can be spaced further apart. Methods like CTDS, the REM, or the REST model could therefore be used to estimate density over larger spatial scales.

Chapter 3: Distance Sampling with Camera Traps

3.1 Introduction

Remote motion-sensitive photography, or camera trapping, is increasingly used in wildlife research, and allows multiple research objectives to be addressed (Sollmann et al. 2013*a*, Burton et al. 2015, Rovero and Zimmermann 2016). Estimation of population density (D) is a key objective of many ecological studies and assessments of conservation status employing camera traps (Burton et al. 2015, Rovero and Zimmermann 2016). If individuals are recognizable, density can be estimated using spatially explicit capture–recapture (SECR) models (Efford et al. 2009a, b), but methods for estimating D from camera trapping data in the absence of individual identification are still in development (Sollmann et al. 2013b, Burton et al. 2015, Dénes et al. 2015, Rovero and Zimmermann 2016). Detection rates at camera traps have been used to index abundance, however, due to spatiotemporal variation in detection rates indices can rarely be converted to estimates of absolute density, nor provide reliable evidence of differences or trends in abundance (Sollmann et al. 2013a, Burton et al. 2015). The random encounter model (REM) estimates absolute density as a function of the detection rate, the dimensions of a sector within which detection is certain, and the speed of animal movement; methods for quantifying the latter two parameters from camera trapping data have been described (Rowcliffe et al. 2008, 2011, 2016). The REM has been recognized as a potentially useful model, but its accuracy and reliability remains to be demonstrated (Rovero and Marshall 2009, Sollmann et al. 2013b, Zero et al. 2013, Cusack et al. 2015a, Balestrieri et al. 2016, Caravaggi et al. 2016). SECR estimators for unmarked populations estimate the number and location of animals'

activity centers from the spatial correlation of counts at different sampling locations; sampling must be sufficiently intensive to detect the same animals at multiple locations, and estimates lack precision (Chandler and Royle 2013).

Here we describe how densities of unmarked animal populations can be estimated by distance sampling (DS) with camera traps, allowing researchers to take advantage of a well-described theoretical framework complete with software and advice for designing studies and analyzing data (Buckland et al. 2001, 2004, 2015, Thomas et al. 2010, Miller 2015, distancesampling.org). Below, we formulate a point transect distance sampling model specific to camera traps and describe its assumptions and the estimation of variances. We test for bias in estimated density ($\widehat{D}$) and its variance by simulation, and apply the method to estimate the density of Maxwell's duikers (*Philantomba maxwellii*) in Taï National Park, Côte d'Ivoire.

3.2 Methods

3.2.1 Formulation of the model

A camera trap (CT) is deployed at a point k that is independent of animal density for a period of time T_k and set to record images for as long as an animal is present to trigger it. We predetermine a finite set of snapshot moments within T_k, t units of time apart, at which an image of an animal could be obtained. Temporal effort at the point is then T_k / t. When images of animals are obtained, we estimate the horizontal radial distance r_i between the midpoint of each animal and the camera, at each snapshot moment, for as long as it remains in view. If the camera covers an angle θ radians, then $\frac{\theta}{2\pi}$ describes the fraction of a circle covered by the camera, so we define overall

sampling effort at point k as $\frac{\theta T_k}{2\pi t}$. We regard the data as a series of snapshots, and density estimation follows by standard point transect methods (Buckland et al. 2001). We estimate D as

$$\widehat{D} = \frac{\sum_{k=1}^{K} n_k}{\pi w^2 \sum_{k=1}^{K} e_k \hat{P}_k} \quad (1)$$

where $e_k = \frac{\theta T_k}{2\pi t}$ is the effort expended at point k, K is the set of points, θ is the horizontal angle of view (AOV) of the camera, w is the truncation distance beyond which any recorded distances are discarded, n_k is the number of observations of animals in the population of interest at point k, and $\hat{P}_k$ is the estimated probability of obtaining an image of an animal that is within θ and w in front of the camera at a snapshot moment. Substituting e_k in (1), we have

$$\widehat{D} = \frac{2t \sum_{k=1}^{K} n_k}{\theta w^2 \sum_{k=1}^{K} T_k \hat{P}_k} \quad (2)$$

We use the distances r_i to model the detection function and hence to estimate P_k.

3.2.2 Assumptions and Practical Considerations

The usual DS assumptions apply (see Chapter 2 of Buckland et al. 2001). We record distances at instantaneous snapshot moments to ensure that animal movement does not bias the distribution of detection distances. Below, we describe an approach for accurately assigning animals to distance intervals; Rowcliffe et al. (2011) and Caravaggi et al. (2016) describe methods for measuring continuous distances between CTs and detected animals.

Random designs or systematic designs with random origin are consistent with the assumption that points are placed independently of animal locations. Selecting camera orientations as part of the design is also advisable. Orientations could be

selected randomly, or the same orientation could be used for all cameras. Deviating slightly from the location and orientation selected by design (e.g., to attach the camera to a nearby tree or to avoid an obscured field of view) would not bias estimates provided field staff do not intentionally target habitat features known to be either preferred or avoided by the animals.

Empirical, design-based estimators of the encounter rate variance are robust to violation of the assumption that detections are independent events (Fewster et al. 2009, Buckland et al. 2015). However, in CT surveys we expect violations to be severe because we include multiple detections of the same animal during a single pass through the detection zone. We can avoid this assumption by estimating variances using a nonparametric bootstrap, resampling points with replacement (Buckland 1984, Buckland et al. 2001). Another consequence of lack of independence is that the usual goodness-of-fit tests and model selection criteria are invalid (Buckland et al. 2001). Methods for selecting among DS models when observations are not independent were recently developed (see Chapter 4 and Howe et al. 2019).

The assumption that detection is certain at zero distance could be violated by (1) animals passing beneath the field of view (FOV) of the camera, (2) failure to identify the species because only part of the animal is visible, and possibly (3) the delay between the time the sensor is activated and the time the first image is recorded (the "trigger speed"), if animals directly in front of the camera at a snapshot moment do not yield images. Such violations may be detectable during exploratory analysis in the form of fewer than expected detections near the point, and bias can be avoided via left-truncation (Buckland et al. 2001, Marques et al. 2007, e.g. Obbard et al. 2015). To minimize violations and ensure that detection probability is certain or high at some

distance near the point, cameras should be set at a height appropriate to the species of main interest (Rovero and Zimmermann 2016). Lower heights would reduce the chance of small animals passing beneath the camera at short distances, but would also reduce the range of distances over which animals could be detected and therefore sample size and flexibility when modelling the detection function. Pairs of cameras mounted facing each other could reveal violations caused by any of the three sources mentioned above. Paired cameras mounted some distance apart targeting the same location (but not necessarily facing each other) would also provide the data needed to apply mark–recapture distance sampling methods, which avoid this assumption (Buckland et al. 2004, Laake et al. 2011).

In traditional point transect surveys, human observers measure distances to each detected animal only once during each visit to a point, and effort at each point is the number of times it was visited. CTs remain at the point, but the snapshot approach discretizes the number of times we could potentially detect each animal (as T_k / t as described above). However, CTs detect only moving animals within the range of the sensor and the FOV of the camera, and can be programmed to record multiple still images, or video footage, each time the sensor is triggered (Rovero and Zimmermann 2016). These characteristics of CTs as observers must be taken into consideration. Observed distances upon first detection are expected to be positively biased because distances observed upon initial detection at CTs is a function of both distance and angle of approach (Rowcliffe et al. 2008), so animals entering the zone of potential detection while approaching the front of the CT contribute a disproportionate number of observations at far distances (Fig. 3.1).

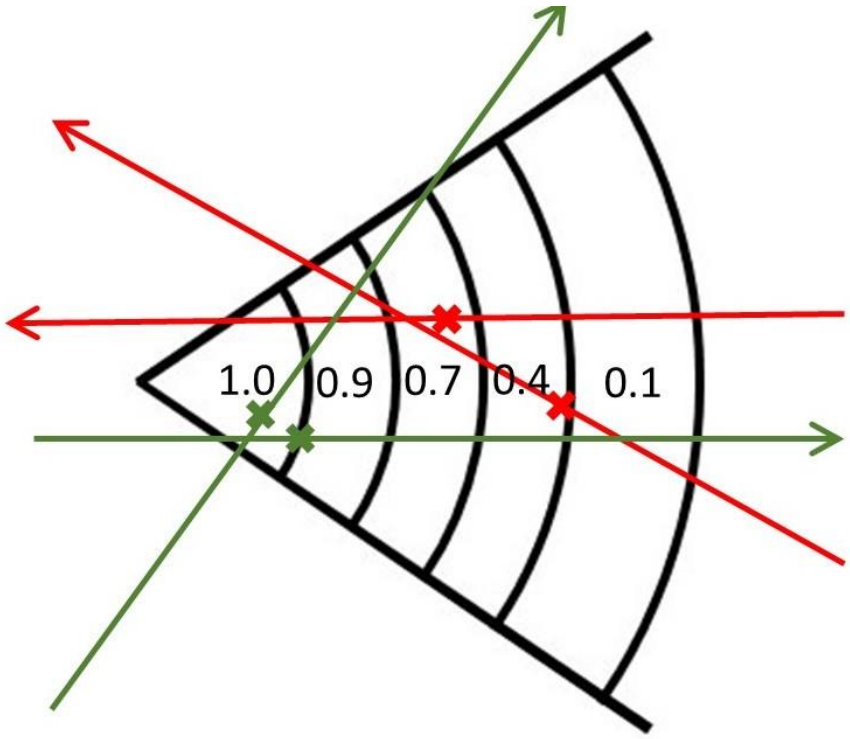

Figure 3.1. An illustration of the effects of distance and angle of approach on the observed distance upon initial detection at a camera trap. Black sectors show zones of potential detection by a camera trap, numbers are hypothetical probabilities of detection (*P*) at different distances. Arrows and crosses depict animals' direction of travel through the zone of potential detection, and examples of their locations upon initial detection, respectively. When animals approach from behind the camera (dark green) they will be initially detected at short distances where *P* is high, but not subsequently as they move away from the camera if only initial detections are recorded. When they approach from in front of the camera (red), they will be detected at a distance dependent on the sensitivity of the sensor, but again, not subsequently. Differences in the number of these potential subsequent observations of distance that are not recorded cause the bias, because recording only initial detections will result in more missed observations at shorter distances where *P* is high; missed observations of animals moving away from the camera when first detected will be fewer, because *P* is lower there.

Bias would be slight if the time between snapshot moments (*t*) was small enough to ensure that the animals did not move far relative to the range of the sensor between snapshots, as then the observations would be representative of animals' continuous paths past the CTs. However, we prefer to avoid the potential for bias by assuming that the snapshot moments are selected independently of animal locations, and predetermining them as specific times of day to ensure that the assumption is met.

Practical considerations constrain *t*. If *t* is large, animals that trigger the sensor might leave the detection zone before a snapshot moment arises, which would not cause bias but wastes data. As *t* is reduced, there would be fewer missed detections and larger samples as we record distance to each animal multiple times during a single pass in front of the CT. Eventually, improvements in the precision of $\widehat{D}$ with larger samples would become negligible because variation in the encounter rate among points would contribute most of the variation in estimated density. Reducing *t* further might only increase the time required to process and analyze the data. We suggest that values from 0.25 to 3 seconds are likely to be useful, with values at the lower end of the range being more appropriate for faster-moving or rarer animals, and CTs with faster trigger speeds.

Programming cameras to record time-stamped video would make it straightforward to record distances at the predetermined snapshot moments. If still images are preferred, cameras should be programmed to record an image at the next several snapshot moments when triggered, or, if this is not feasible, to record a rapid series or "burst" of still images to ensure that images are recorded at times that align with snapshot moments. There should always be the potential for the camera to be triggered again immediately or after a minimal delay. Note that depending how cameras are programmed, the sample of distances observed in CT data may or may not comprise a realization from the detection function described by the probability that an animal at distance *r* triggers the sensor. If cameras record a single image at the subsequent snapshot moment, or a rapid series of images for < *t* seconds, when the sensor is triggered, then each detection of an animal that triggers the sensor several times during a pass in front of a CT is a function of the sensitivity of the sensor. If cameras are set to record video, or a series of still images for > 2*t* seconds, then all but

the first detection is certain for as long as the animal remains in the FOV and the camera continues to record images. Furthermore, regardless of how the camera is programmed, any other animals in the FOV while the camera is recording images would contribute observations that do not depend on the sensitivity of the sensor. These differences do not invalidate the method provided we define the detection function as representing the proportion of locations at different distances which are recorded, regardless of whether an animal triggered the sensor at that distance.

Obviously, we can only estimate the density of populations that are available for detection by CTs. Similarly, because the sampling duration at each location (T_k) is part of the model definition, we expect densities of animals that spend part of their time outside the vertical range of camera traps to be underestimated, and for the bias to be proportional to time animals are not available for detection. For example, with T_k set to the study duration, we expect $\widehat{D}$ of a species that spends all its time in the canopy to be zero, and of a species that spends half its time underground and the rest at ground level to be half of the true density. Negative bias would also result if animals went undetected only because movement was insufficient to trigger the sensor. To avoid this bias, either T_k should be defined as the amount of time that the entire population was available for detection while cameras were operating, or, equivalently, the proportion of time when animals were available for detection should be included as a parameter in the model. Animals are unavailable for detection when outside the vertical range of CTs, and may not be available when within this range depending on their level of activity. We explore this issue further in subsequent sections.

3.2.3 Simulations

We tested the method using simulations employing simple and complex models of animal movement and different sampling scenarios. The simple model allowed us to demonstrate that the method can yield accurate results under an idealized scenario; the complex model was intended to be more realistic, mimicking animals' varied daily schedule of behaviours, such as foraging, resting, and travelling. We simulated movements of 40 animals, over 12 days, within a 2 km by 2 km square study area (true density = 10 animals / km^2), simulating distance sampling of these populations using camera traps, and estimated density from the resulting data using point transect models. Simulations were performed in R software (version 3.2.1; R Core Team 2015). Density was estimated using models implemented in the "Distance" and "mrds" R packages (versions 0.9.4 and 2.1.5, respectively; Miller 2015, Laake et al. 2016).

In both movement models, animals started with a random initial location and heading, after which new locations were generated every two seconds. When an animal left the study area, it reappeared on the opposite side at the same heading to ensure that density was constant and that animal locations were uniformly distributed. In the simple model, animals moved continuously and tended to maintain their initial heading (Fig. 3.2). Movements in meters were drawn from a lognormal distribution with mean -1.3 and SD 0.5, such that animals moved 0.28 m / second on average, and travelled ≈12 km over the course of a day. Turn angles in degrees were drawn from a normal distribution with mean 0 and SD 0.5. In the more complex model, animals moved rapidly for 144 minutes, then moved slowly and more tortuously for 216 minutes, and repeated this pattern once for a total of 12 hours of activity before stopping to rest for 12 hours (Fig. 3.2). When moving rapidly, movements were lognormally distributed with

mean 0.0 and SD 0.3, and turn angles in degrees were normally distributed with mean 0 and SD 4. When moving slowly, movements and turn angles followed the same distributions but with means +/- SDs of -1.61 +/- 0.3, and 0 +/- 8, respectively. These values yielded average speeds of 1 m per second or 3.6 km per hour when moving quickly, and 0.2 m per second or 0.72 km per hour when moving slowly, such that animals travelled ≈11.5 km per day on average.

Our initial sampling design was 25 locations in a square grid at 300 m spacing, positioned randomly within the study area (Fig. 3.2). Two alternative designs doubled the spatial sampling effort, once by doubling the number of sampling locations (by replicating and shifting the original grid 283 m to the northeast), and once by doubling θ at each location (as though 2 cameras were mounted on the same tree with non-overlapping detection zones).

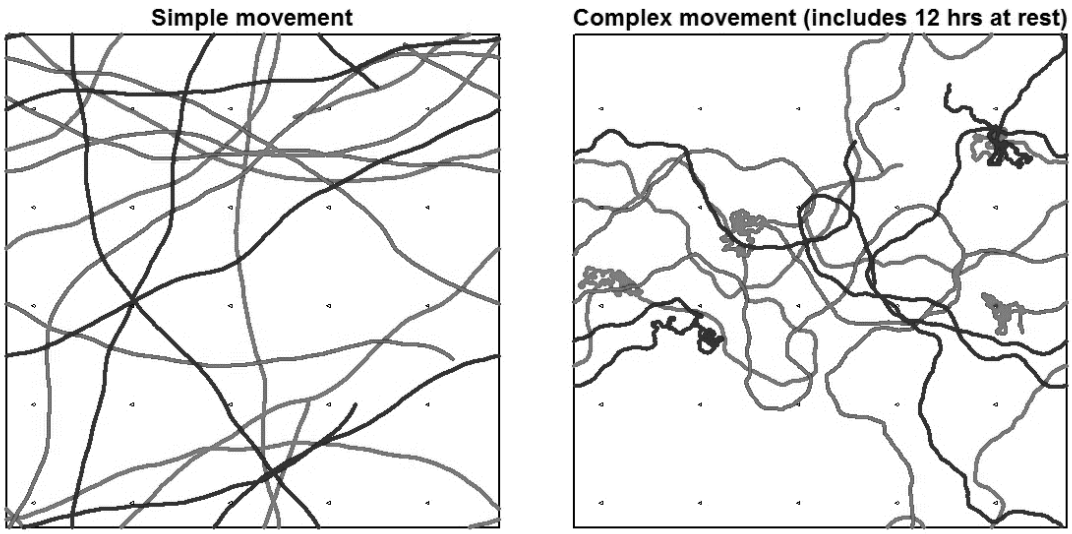

Figure 3.2. Simulated movement paths of 3 animals (in different shades of grey) over one day within a 2 km by 2 km study area. A grid of 25 east-facing camera traps appears as sectors with radius 16 m and central angle 42˚ (to scale).

We defined the zone of potential detection by a camera trap as a sector with a radius of 16 m and a central angle (θ) of 42 degrees (0.733 radians; Rovero et al. 2013, Meek et al. 2012, Trailcampro.com 2015). Where the simple model of animal movement was used, we recorded the distance between animals within detection zones and cameras at each two second time step, 24 hours per day. Where the complex model was used, we recorded distances as above, but we also collected data only when animals were moving. We simulated imperfect detection by randomly removing distance observations according to a half-normal function with SD 10, which yielded detection probabilities of 0.96, 0.78, 0.61, and 0.32 at 3, 7, 10, and 15 m, respectively.

We left-truncated the data at 1 m to and binned it into four distance categories, with cutpoints at 1, 4, 7, 10, and 15 m (beyond which data were right-truncated) to mimic a situation where some animals within 1 m passed beneath the detection zone, and estimating distances precisely was difficult. We estimated density by fitting a point transect model with a half-normal detection function and no adjustment terms to each data set. Sampling effort at each location was defined as $\frac{\theta T_k}{2\pi t}$, where T_k was the total sampling time in seconds, t was 2 seconds, and θ was 0.733 radians.

We performed 1000 iterations of each of the six scenarios, and report mean sample size of distance observations, mean and median $\hat{D}$, and mean percent relative bias (%RB) across iterations. From the design-based variances, we present the mean coefficient of variation (CV), root mean squared error (RMSE), and confidence interval (CI) coverage (as the proportion confidence intervals that included the true density). We present the CV derived from the sampling variance of $\hat{D}$ across iterations for comparison. For one scenario (complex movement, data collected only when animals were active, and the initial sampling design), we resampled the distance data across

camera locations (with replacement) 999 times from each of the 1000 simulated data sets and calculated CVs and percentile CIs across resamples, and CI coverage across iterations. We only calculated variances by bootstrapping for one of the six scenarios because it was computationally intensive, requiring models be fitted to one million data sets per scenario.

3.2.4 Example: Maxwell's duikers in Taï National Park

We used point transect DS methods to estimate the density of Maxwell's duikers within the territory of the "east group" habituated chimpanzee community in Taï National Park, Côte d'Ivoire (Després-Einspenner et al. 2017; Fig. 3.3a). Maxwell's duikers were sampled from 28-June through 21-Sept, 2014 at 23 camera traps (Bushnell Trophy Cam™; Model 119576C) mounted at a height of 0.7 – 1.0 m and set to high sensitivity. Cameras were deployed with a fixed orientation of 0˚ at the intersections of a grid with 1 km spacing and a random origin superimposed over the study area (Fig. 3.3b). Realized sampling locations and orientations deviated from the design by as much as 30 m, and 40˚, respectively, to mount cameras on trees and to ensure there was some chance of detecting animals. During installation of each camera, we measured horizontal radial distances from the camera, and recorded videos of researchers holding distance markers, at 1 m intervals out to 15 m, in the center and along both sides of the FOV. We estimated distances to filmed duikers by comparing their locations to those of researchers in the reference videos. We set t = 2 seconds, and recorded the distance interval within which the midpoint of each animal fell at 0, 2, 4, … , 58 seconds after the minute. Larger distances were more difficult to measure precisely, so we assigned

animals to 1-m intervals out to 8 m, but binned observations between 8 and 10 m, 10 and 12 m, 12 and 15 m, and beyond 15 m.

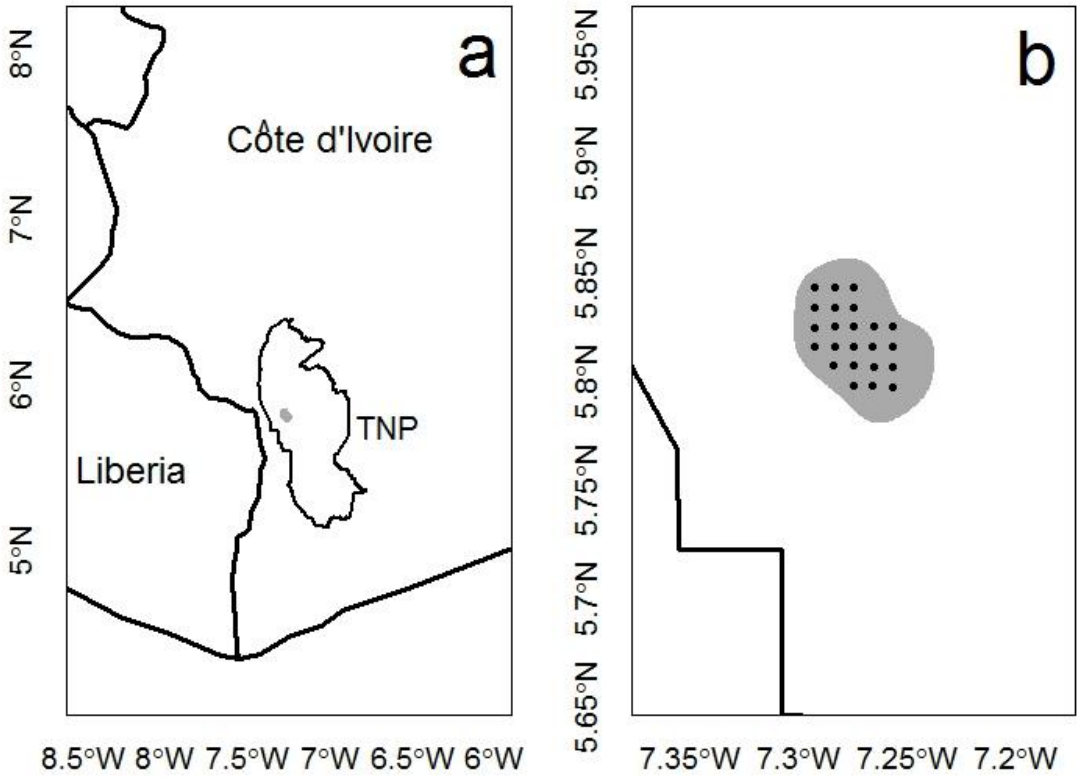

Figure 3.3. Location of the study area (grey polygon) in Taï National Park (TNP), Côte d'Ivoire, 2014 (a), and (b) locations of 23 camera traps deployed in a grid with 1 km spacing within the study area.

We excluded data from one camera because the FOV was largely obscured by vegetation, and another which was placed on a slope and failed to detect any animals, but we included data from a third camera that functioned normally but did not detect any duikers. Maxwell's duikers sleep or rest for most of each night and for shorter periods during the day (Newing 1994, 2001). We assumed they would not be available for detection overnight and excluded the hours of darkness (19:00 – 6:00) from T_k *a-priori*. We accounted for limited availability during the daytime three different ways.

First we naively assumed that all duikers were active by 6:30:00 and remained so through 17:59:59, included distances observed during this interval in a "daytime" data set, and defined temporal effort at each location (T_k / t) as the number of 2-second time steps during that time interval (20699), multiplied by the number of sampling days. Second, we assumed that all animals were available only during apparent times of peak activity (6:30:00 – 8:59:59 and 16:00:00 – 17:59:59) and recalculated temporal effort and censored distance observations accordingly (T_k / t per day = 8098). Third, we defined T_k and included observations as above for the daytime data set, and included an independent estimate of the proportion of time captive Maxwell's duikers were active during the same time interval in the denominator of Eq. 2. We included only data from complete days when cameras were operating and not visited by researchers.

We fit point transect models in program Distance (version 7.0; Thomas et al. 2010), defining survey effort at each location as $\frac{\theta T_k}{2\pi t}$. The cameras had an AOV of 42˚, and a wider effective angle of the sensor (Trailcampro.com 2015), so we set $\theta = 42^{\circ}$ or 0.733 radians. We considered models of the detection function with the half-normal key function with 0, 1 or 2 Hermite polynomial adjustment terms, the hazard rate key function with 0, 1, or 2 cosine adjustments , and the uniform key function with 1 or 2 cosine adjustments. Adjustment terms were constrained, where necessary, to ensure the detection function was monotonically decreasing. We selected among candidate models of the detection function by comparing AIC values, acknowledging the potential for overfitting because many observations were not independent. We present measures of uncertainty derived from design-based variances ("P2" of Fewster et al. 2009, Web Appendix B), and from 999 bootstrap resamples, with replacement, across camera locations.

3.3 Results

3.3.1 Simulations

Where we used the simple model of animal movement, and where we used the complex model of animal movement and collected data only when animals were active, $\hat{D}$ was unbiased (Table 3.1), but results were biased and erratic when we collected data when animals were at rest. For example, of 1000 density estimates from our initial sampling design, seven hundred and eighty-five were tightly distributed about a mean of 5.0 / km^2 (Fig. 3.4) but there were few estimates close to the true value of 10, $\hat{D}$ was > 20 in 101 cases, > 100 in 38 cases, and in 50 cases models could not be fit to the data. Where $\hat{D}$ was < 9, sample size averaged 3172, but higher estimates were derived from sample sizes > 10 000 (mean 18806), indicating that estimates ≥ 9 were obtained where data were collected while an animal rested in a detection zone. In the cases where decreasing functions could not be fitted an animal had rested within the detection zone between 10 and 15 m away from the camera.

In scenarios where estimates were unbiased, they were also precise, with mean CV < 0.10 (Table 3.1). Doubling sampling effort improved precision, slightly more so where we doubled the number of locations as opposed to θ. However, design-based analytic variances underestimated the actual uncertainty in $\hat{D}$, and associated confidence interval coverage was < 90% (Table 3.1). Where we estimated variance by bootstrapping, the CV was 0.119, similar to the sampling variance of $\hat{D}$, and CI coverage was 93.6% across 1000 iterations.

Table 3.1. Summary of simulated point transect distance sampling of 40 moving animals within a 4 km^2 study area (D = 10/km^2), over 12 days, using camera traps. Specifications are the animal movement model, simple or complex, as described above; the number of sampling locations (k); the central angle of the detection sector (θ) in degrees; and the number of potential visits by an animal to a sampling location (T_k / t) in one day (=21600 where we did not record distances to resting animals). Results are the mean sample size of radial distance observations (r_i), the number of successful fits of point transect models (N), the mean, median, and mean percent relative bias (%RB) of estimated densities ($\hat{D}$), the mean coefficient of variation (CV), root mean squared error (RMSE) of density estimates, and confidence interval (CI) coverage of $\hat{D}$ derived from design-based variances, and the CV derived from the sampling variance of $\hat{D}$ across iterations.

Specifications				Sample size (r_i)	Successful model fits	Density estimates			Design-based variances			Sampling variance of $\hat{D}$
Animal movement	k	θ	Daily T_k / t	Mean	N	Mean	Median	Mean %RB	Mean CV	RMSE	CI cov	CV
Simple	25	42	43200	6413	1000	10.05	10.05	0.52	0.058	0.86	0.82	0.085
Simple	50	42	43200	12823	1000	10.05	10.06	0.48	0.041	0.61	0.82	0.060
Simple	25	84	43200	12807	1000	10.03	10.04	0.34	0.044	0.64	0.82	0.064
Complex	25	42	43200	6310	950	15.42	6.13	54.29	0.207	42.46	0.11	2.731
Complex	50	42	43200	11920	887	14.07	5.25	40.69	0.240	25.91	0.21	1.820
Complex	25	84	43200	12030	895	13.98	5.29	39.82	0.251	25.00	0.22	1.766
Complex	25	42	21600	3210	1000	10.08	10.08	0.81	0.090	1.20	0.86	0.118
Complex	50	42	21600	6423	1000	10.07	9.97	0.60	0.064	0.78	0.89	0.077
Complex	25	84	21600	6418	1000	10.11	10.07	1.12	0.073	1.00	0.85	0.098

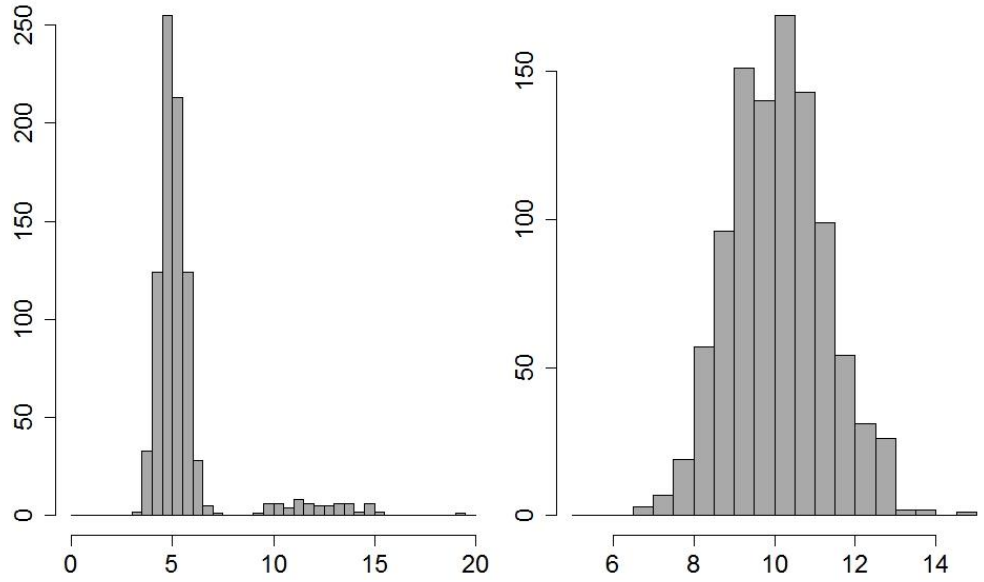

Figure 3.4. Histograms of animal densities (animals / km^2) estimated from simulated distance sampling data from camera traps, where observations of distance were recorded while animals were at rest (left; n = 849 estimates < 20 from the 950 models successfully fitted to the data) and where they were only recorded while animals were moving (right, n = 1000). Simulations used the complex model of animal movement and the minimum sampling effort (25 locations, θ = 0.733 radians). The true density was 10 animals / km^2.

3.3.2 Example: Maxwell's duikers in Taï National Park

We obtained 11324 observations of the distance between Maxwell's duikers and cameras in 806 different videos. Duikers were rarely filmed during hours of darkness, and none were filmed between midnight and 6:00. The frequency of detection increased steadily after 6:00 to a maximum between 6:30 and 7:00 and remained relatively high until 9:30, after which it decreased slightly and remained relatively low until 16:30, then increased again and remained high until 18:00, then declined gradually until 19:00 (Fig. 3.5). Duikers were always active when detected; CTs did not record any duikers that were asleep or stationary for an entire minute. We recorded 11180 distances from 6:30:00 through 17:59:59, and 6274 during times of peak activity (6:30:00 – 8:59:59 and 16:00:00 – 17:59:59).

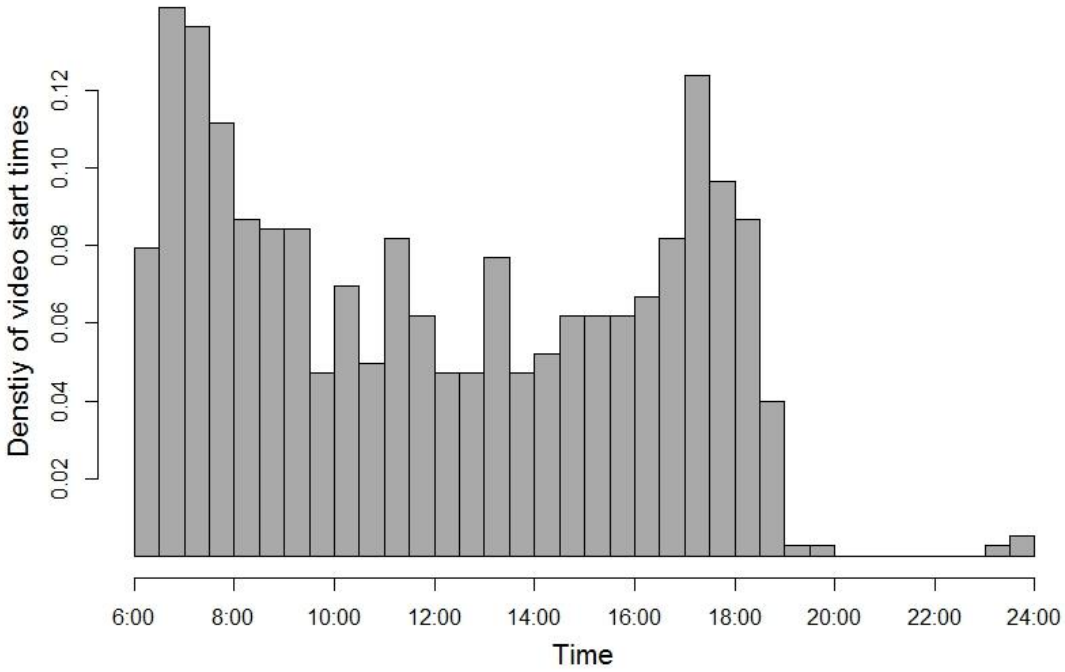

Figure 3.5. Histogram of start times of videos of Maxwell's duikers in Taï National Park, Côte d'Ivoire, 2014.

Exploratory analyses revealed no evidence of data collection errors, and a paucity of observations between 1 and 2 m but not between 2 and 3 m, so we left-truncated at 2 m. Fitted detection functions and probability density functions were heavy-tailed when distances > 15 m were included, so we right-truncated at 15 m. Truncating removed 8% of observations from the daytime data set, leaving $n = 10284$, and 6.5% of observations from the peak activity data set, leaving $n = 5865$. Mean encounter rates (mean numbers of duikers observed per 2-second time interval) across all points were 3.27×10^{-4} during the daytime and 4.76×10^{-4} during times of peak activity. Encounter rates were highly variable among locations but did not exhibit an obvious spatial pattern across the study area, and there was no evidence of spatial autocorrelation (Moran's I $P = 0.47$; Fig. 3.6).

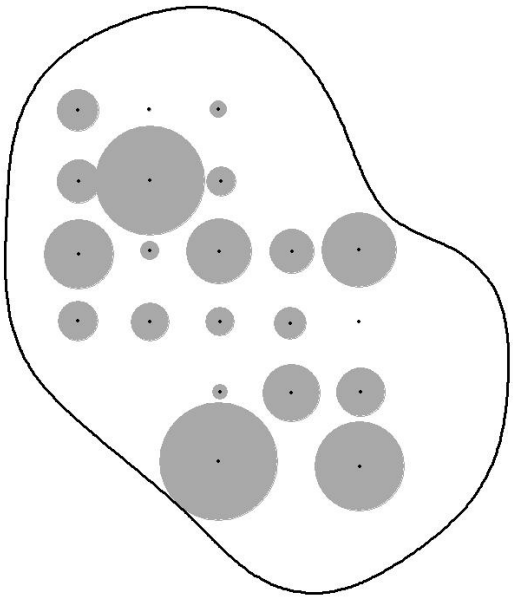

Figure 3.6. Variation in encounter rates of Maxwell's duikers among 21 camera trap locations in Taï National Park, Côte d'Ivoire, 2014 (range 0.00 – 1.45 × 10^{-3}). The areas of the grey circles are proportional to the encounter rates.

When we fit the hazard rate model with two adjustment terms to the daytime data set, the detection function was not monotonically decreasing, so this model was not considered for estimation. All models were fitted successfully to the peak activity data set. The hazard rate model with no adjustments minimized AIC and was used to estimate density in both cases. Probability density functions of observed distances and relationships between detection probability and distance were similar between data sets (Fig. 3.7). Detection probability was ~1.0 within 5 m and 0.05 at 15 m; effective detection radii were 9.1 and 9.4 m from the daytime and peak activity data sets, respectively.

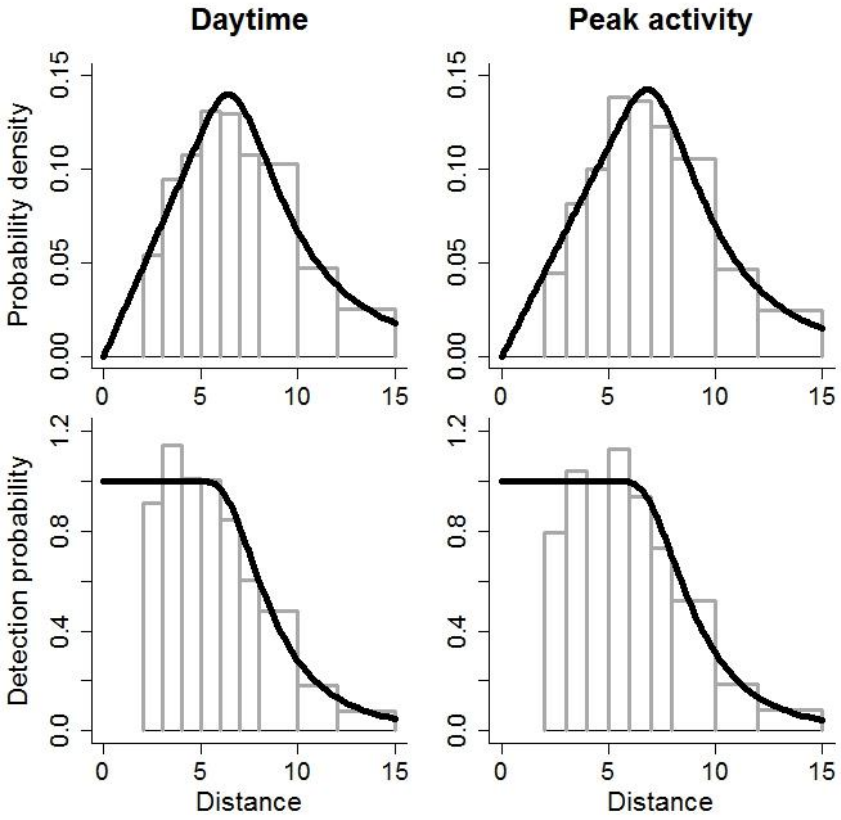

Figure 3.7. Probability density functions of observed distances (top) and detection probability as a function of distance (bottom) from hazard-rate point transect models fit to data from Maxwell's duikers in Taï National Park, 2014, collected during the daytime (left) and during times of peak activity (right).

We expected to underestimate density where we assumed duikers were active all day; $\widehat{D}$ was 37% higher when we included only data from times of peak activity (Table 3.2). Including an independent estimate of the proportion of time active during the daytime (0.64; Newing 2001) as a parameter in the model fit to the daytime data set yielded a still higher estimate ("Active daytime" in Table 3.2). Measures of uncertainty in the proportion of time active were not available (Newing 2001) so did not contribute to the variance of $\widehat{D}$. Bootstrap variances were larger than design-based analytic variances (Table 3.2). The vast majority (99.8%) of the design-based variance of $\widehat{D}$ was

attributable to the variation in encounter rate between locations, and only 0.2% to detection probability.

Table 3.2. Densities of Maxwell's duikers in Taï National Park, 2014, estimated using different methods to account for limited availability for detection ("Daytime" assumes all animals available all day, "Peak activity" assumes all animals were available during daily peaks of activity, and "Active daytime" corrects for limited availability during the day using an independent estimate of the proportion of time active during the day). Bootstrap confidence intervals were calculated using the percentile method.

		Design-based		Bootstrap	
Availability	$\hat{D}$	CV	95% CI	CV	95% CI
Daytime	10.6	0.27	6.1–18.3	0.40	5.0–21.8
Peak activity	14.5	0.30	7.8–26.9	0.36	6.1–26.9
Active daytime	16.5	0.27	9.5–28.6	0.40	7.7–34.1

3.4 Discussion

Simulations demonstrated the potential for the method to yield unbiased density estimates, but also that animals' activity patterns must be accounted for. Where simulated animals rested for half of each day and we set T_k equal to the survey duration, the most common scenario was that animals did not rest in front of CTs and negative bias in $\widehat{D}$ was proportional to the time spent resting. When we recorded distance at each snapshot moment while animals rested in front of CTs, the encounter rate and therefore $\widehat{D}$ was higher on average, but the shape of the detection function was strongly affected, leading to erratic estimates and cases where models could not be fitted to the data. In practice, it is unlikely that we would detect animals while they sleep or rest because movement will be insufficient to trigger the sensor. Therefore, estimates of the proportion of time animals are active within the vertical range of CTs will be required to avoid negatively biased $\widehat{D}$. Ideally, this proportion would be estimated from data collected concurrently with the distance data to ensure it is representative. Fortunately,

the temporal distribution of camera trap detections is informative regarding animal activity patterns (Lynam et al. 2013, Cruz et al. 2014, Rowcliffe et al. 2014). If it is reasonable to assume that the entire population is available for detection for any part of each day, additional data would not be required to estimate $\widehat{D}$ accurately, because we could either (1) analyze only the data collected at that time, censoring effort and distance data from other times, or (2) estimate the overall proportion of time active directly from the CT data (e.g. Rowcliffe et al. 2014). Newing's (1994) data from Taï indicated that there was no time at which all wild duikers could be assumed to be active. If this was true during our survey, we may have underestimated density where we did not correct for limited availability within the time included in T_k, because even at times of peak activity some animals may have been resting and unavailable for detection. Activity data from wild duikers were presented only as figures and could not be converted into estimates of the overall proportion of time active (Newing 1994). We therefore relied on the assumption that activity data from captive duikers (Newing 1994, Newing 2001) were representative of activity patterns during our survey. If this assumption held, then the density estimate calculated using their estimate of the proportion of time active during the day should not be biased as a result of limited availability. We suggest that the need to account for availability should not pose a serious obstacle to reliable estimation of the density of many species, but for others, notably ectotherms, and semi-arboreal and fossorial species, it will require careful consideration, and possibly additional data. We further suggest that combining Rowcliffe et al.'s (2014) or similar methods for estimating the proportion of time active from detection times at CTs with the point transect method described here could yield accurate density estimates for many species from CT data alone.

Avoidance of, or attraction to, CTs would bias encounter rates and therefore density estimates. Some species exhibit complex responses to CTs or are particularly wary of humans (Séquin et al. 2003). If behavioural responses are expected or apparent in images of detected animals, CTs could be deployed prior to the start of the actual survey to allow animals to become accustomed to them and for signs of human presence to dissipate. Similarly, effort and distance data from times when animals may have been displaced from the trap sites by humans visiting them to download data, replace batteries, etc., should be censored.

The probability of detection at PIR CTs is lower at greater angles from the center of the FOV, due to a combination of the trigger speed, the effective horizontal angle of the sensor relative to the AOV of the camera (which varies among CT models) and possibly reduced sensitivity of the sensor at the periphery of its horizontal range (Rowcliffe et al. 2011, Rovero et al. 2013, Rovero and Zimmermann 2016). This introduces heterogeneity in the detection function. Fortunately, provided that detection is certain at zero distance, the pooling robustness property ensures that estimation is unbiased in the presence of heterogeneity in detectability among individuals (Burnham et al. 2004), and this also applies to heterogeneity caused by differences in angle at different snapshot moments. However, if detection probability at high θ is much lower than in the centre, fitted models of the detection function might show a rapid drop in detection probability near the point, whereas detection functions with a gradual decrease near the point are preferred for stable density estimation (Buckland et al. 2001). The expected distribution of angles within a sector within which the sensor is fully effective is uniform. We recommend that researchers measure angles as well as distances to detected animals (e.g. Carravaggi et al. 2016), and test for departures from the

uniformity assumption at increasing angles as part of their exploratory analysis. If departures are apparent, the data could be truncated to exclude observations beyond an angle within which the distribution is approximately uniform, in which case θ should be set to two times the truncation angle rather than the AOV of the camera in the definition of effort. An alternative approach that would allow us to retain all of the data would be to develop a two dimensional detection function where detection probability depends on both radial distance and angle from center, using methods similar to those developed by Marques et al. (2010). We expect heterogeneity with angle to be more severe with CT models with narrow horizontal ranges of the sensor relative to the AOV of the camera, or slow trigger speeds, and where faster-moving animals are sampled. CTs with fast trigger speeds, short recovery times, and curved array Fresnel lenses (which provide a wide effective angle of detection such that the camera begins recording images as or even before the animal enters the FOV; Rovero and Zimmermann 2016) could reduce or eliminate differences in detection probability at different angles in future studies.

The encounter rate variance accounted for the vast majority of the design-based variance in duiker density, and variances around $\widehat{D}$ were larger than for simulated data despite similar sample sizes. Real populations exhibit clumped or patchy distributions and non-random movement, leading to variable encounter rates among sampling locations and hence greater uncertainty in $\widehat{D}$ (Buckland et al 2001, Fewster et al. 2009); the small area sampled at each location exacerbates this problem. Increasing the area sampled will therefore enhance precision, more so than would increasing temporal effort at a point. Theory predicts that increasing the number of points will yield the largest improvements to precision (Buckland 1984, Fewster et al. 2009). That the improvement in precision in simulations was only slightly greater where we doubled the

number of sampling locations than where we doubled θ is not representative of real studies because the expected spatial distribution of animal locations was uniform, and movement was random. Coefficients of variation around $\widehat{D}$ for duikers were >35% despite large samples of distance observations, so we recommend that future studies employ more points to improve precision.

The average density of Maxwell's duikers throughout Taï National Park was recently estimated as 1.6 / km^2 from line transect DS surveys (N'Goran 2006). However, line transect sampling by human observers is believed to severely underestimate densities of forest-dwelling animals in general, and forest antelopes in particular, due to effects of evasive movement and behaviour in response to observers on both the encounter rate and the distribution of observed distances (Koster and Hart 1988, Jathanna et al. 2003, Rovero and Marshall 2004, 2009, N'Goran 2006, Marshall et al. 2008, Marini et al. 2009). For this reason, line transect surveys of sign are frequently performed, and sign densities converted to animal densities. This approach is expected to yield biased estimates in the absence of local and concurrent estimates of sign production and decay rates, which are time-consuming to estimate (Plumptre 2000, Kuehl et al. 2007, Todd et al. 2008). Dung surveys may further require genetic analysis to identify the species (Bowkett et al. 2009). Distance sampling with CTs apparently avoided the underestimation characteristic of line transect surveys of live animals, in less time than would be required to obtain reliable estimates from sign surveys.

The recent proliferation of CT studies is providing new information about wildlife in diverse habitats (Burton et al. 2015, Rovero and Zimmermann 2016). Where estimating the density of a rare but individually identifiable species is the primary research objective, it may be preferable to deploy CTs non-randomly to obtain sufficient

detections of individuals to estimate density by SECR (Wearn et al. 2013, Cusack et al. 2015*b*, Després-Einspenner et al. 2017). However, multiple research objectives can be addressed, and useful data for multiple species obtained, if CTs are deployed according to a randomized design (MacKenzie and Royle 2005, Wearn et al. 2013, Burton et al. 2015, Dénes et al. 2015). The size of unmarked populations can then be estimated from CT data using Poisson and negative binomial GLMs or hierarchical N-mixture models (Dénes et al. 2015), but population density is of greater interest because it is more biologically relevant and comparable across studies. Densities of unmarked animal populations can only be estimated from CT data using SECR models for unmarked populations, the REM, or DS methods; the latter two require randomized designs (Rowcliffe et al. 2008, Buckland et al. 2001). SECR methods for unmarked populations require intensive designs, and even then estimates will often be too imprecise to be useful unless a subset of the population can be reliably identified (Chandler and Royle 2013, Le Saout et al. 2014). The REM requires an estimate of the average speed of animal movement, assumes that detection is certain within an estimable area in front of the camera, and makes use of only one observation from each detected animal (Rowcliffe et al. 2008). Our point transect approach requires an estimate of the proportion of time animals are available for detection, assumes that detection is certain only at zero distance, and each detected animal contributes multiple observations of distance. We expect the extension of point transect DS methods to provide an effective and efficient tool for estimating animal density and to enhance the information derived from CT surveys.

Chapter 4: Model Selection with Overdispersed Distance Sampling Data

4.1 Introduction

Distance sampling (DS) is an established framework for estimating animal abundance (Buckland et al. 2001, 2004, 2015, Borchers et al. 2002). It allows for imperfect detection by assuming detection probability is a function of the distance between objects (e.g., animals or their sign), and specified locations (lines or points) from which objects may be observed. Careful modelling of this function is required to obtain accurate abundance estimates (Buckland et al. 2001, 2004, 2015). Exploratory analyses, goodness-of-fit (GOF) testing, and model selection are therefore critical components of DS analyses (Buckland et al. 2001, 2004, 2015, Marques et al. 2007, Thomas et al. 2010). GOF tests evaluate the null hypothesis that a model adequately fits the data; GOF tests for continuous and binned DS data were described by Buckland et al. (2001, 2015) and are implemented in DS software (Thomas et al. 2010, Laake et al. 2017). Rejection may indicate problems in the data or the structure of the model being tested, or violations of model assumptions. The purpose of model selection is the identification of a model or models that optimize the trade-off between bias and precision of the parameters estimated from a given data set (Burnham and Anderson 2002, Johnson and Omland 2004).

DS methods assume that observations are independent (Buckland et al. 2001), but some DS surveys violate this assumption. For example, some animals travel in groups. Violation of the independence assumption can be avoided by treating the group as the unit of observation, measuring or estimating distances to the centre of detected

groups, and estimating animal density as the product of group density and mean group size (Buckland et al., 2001). However, this is only effective if the size and central location of the group are measured accurately (Buckland et al. 2001, 2010). When they cannot be, for example, because groups are widely spread or in motion, the recourse is to treat the individual as the unit of observation, and to record distances to all group members detected, in which case the data include non-independent observations. Furthermore, some animals, such as cetaceans that are often submerged, or songbirds that perch concealed in trees, are only available to be observed intermittently. However, if they give discrete cues of their presence and location, such as whale blows or bursts of birdsong, density of cues can be estimated using DS methods, and converted to estimates of animal density by dividing by the cue production rate (Buckland 2006, Buckland et al. 2001). During cue counting surveys, distances to all cues are recorded, so the data may include observations of distances to multiple cues given by the same animal(s), which again violates the independence assumption (Buckland 2006). Finally, Chapter 3 and Howe et al. (2017a) extended DS methods to accommodate data from camera traps (CTs). Distances to animals when first detected by CTs are expected to be positively biased, so authors recommended programming cameras to record video, or multiple still images, each time the sensor is triggered, and measuring distances to each detected animal multiple times at predetermined "snapshot moments" during an independent encounter with a CT. Authors acknowledged that these observations would not be independent of each other.

Violations of the independence assumption do not bias point estimates of model parameters, but introduce overdispersion (Buckland et al. 2001) – a situation where the data are more variable than are expected under a given statistical model. When distance

data are overdispersed: (1) GOF tests, and likelihood ratio tests to compare the fit of nested models, are invalid and prone to type I error; (2) analytic variance estimators underestimate the actual uncertainty associated with the estimates, though modern empirical design-based estimators are robust to some violations (Fewster et al. 2009); (3) model selection criteria that have not been adjusted for overdispersion favour overly complex models with more than the optimal number of parameters (Cox and Snell 1989, McCullagh and Nelder 1989, Anderson et al. 1994, Burnham and Anderson 2002, Buckland 1984, Buckland et al. 2001, 2010, 2015, Richards 2008, Fewster et al. 2009). Akaike's Information Criterion (AIC; Akaike 1973) is usually recommended for selecting among candidate models of the detection function (Buckland et al. 2001, 2004, 2015, Marques and Buckland 2003, Marques et al. 2007, Thomas et al. 2010), however if the data are overdispersed, AIC is likely to favour unnecessarily complex models (Buckland 2006, Buckland et al. 2001, 2010). This additional complexity reduces precision, and can cause bias if it affects the slope of the detection function near the line or the point. Criteria adjusted to account for overdispersion in observed distances have not been developed previously.

Detectability may vary in response to multiple factors other than distance. DS methods are pooling robust, so the total or average density estimated from the entire data set will generally be unbiased even when variation in detectability is ignored (in the case of differences between distinct spatial subsets of the greater study area, sampling effort should be proportional to the areas of the subsets; Burnham et al. 2004). However, density estimates specific to different population strata among which detectability varies, which might be different species, treatments, habitat types, time periods, etc., are expected to be biased if estimated from a common detection function

(Marques and Buckland 2003, Marques et al. 2007, Buckland et al. 2004, 2015). Observations within different strata can be analyzed separately to avoid this bias, but this can reduce sample sizes to the point where densities of some strata may not be estimable, or estimates may be too imprecise to be useful. The multiple covariate approach to DS analysis (MCDS) allows variation in detectability to be modelled using covariates, and support for differences among strata to be evaluated using model selection criteria (Marques and Buckland 2003, Buckland et al. 2004, Marques et al. 2007); if models with constant detectability are supported over those with differences among strata, data can pooled across levels of those covariates when estimating detectability. MCDS can therefore improve precision and allow density to be estimated for strata with few detections without relying on an assumption of constant detectabity across strata. It also casts decisions about how much stratification is necessary as a model selection problem, but in this case the quality of inferences about strata-specific densities is affected by the reliability of the model selection criterion. When the independence assumption is suspected or known to have been violated, it has been recommended that analysts constrain the complexity of the detection function and the number of covariates to avoid overfitting (Buckland et al. 2004, 2010, 2015, Marques et al. 2007). However, limiting the candidate set to simple models may not be desirable if there are multiple potential covariates of the detection function. Model selection criteria unadjusted for overdispersion will tend to select models that subdivide the data more than necessary, with adverse effects on precision. Conversely, "underfitting", that is, failure to include significant sources of variation in the estimating model, would cause stratum-specific densities to be underestimated if true detection probabilities in that stratum tend to be lower than the average across strata, and vice versa. Adjusted criteria

could underfit if they overcompensated for overdispersion (e.g., if the magnitude of overdispersion was overestimated).

Although explicitly modeling the sources of overdispersion would be ideal, this is not always possible or practical (Cox and Snell 1989, McCullagh and Nelder 1989, Lebreton et al. 1992, Anderson et al. 1994, Burnham and Anderson 2002, Richards 2008). In practice in other contexts, the total overdispersion (c) was estimated from a χ^2 GOF test of the global model (i.e., the most highly parameterized or most general model) divided by its degrees of freedom (df); the result was denoted $\hat{c}$, and included in the calculation of information criteria adjusted for overdispersion for all models in the candidate set, and this was sufficient to avoid overfitting (Cox and Snell 1989, Lebreton et al. 1992, Liang and McCullagh 1993, Anderson et al. 1994, Burnham and Anderson 2001, 2002). The adjusted version of AIC (QAIC) is calculated as

$$QAIC = -2\left\{\frac{\log L\left(\hat{\theta}\right)}{\hat{c}}\right\} + 2K$$

where $\hat{\theta}$ is a vector of maximum likelihood parameter estimates, and K is the number of parameters in the current model (Lebreton et al. 1992). Burnham and Anderson (2001, 2002) clarified that the parameter $\hat{c}$ should be included as one of the K parameters to estimate. Technically, "QAIC" is a misnomer because no quasilikelihood theory is involved; I used this term to refer to an information criteria adjusted for overdispersion because it may be familiar to ecologists from other contexts, such as capture–recapture (Lebreton et al. 1992).

Given an estimator of c ($\hat{c}$), the same approach could be used to calculate QAIC for models of the DS detection function. However, candidate sets usually include models with different general forms (termed "key functions"; e.g., half-normal, hazard rate, and uniform; Buckland et al. 2001) and numbers of adjustment terms, as well as

different covariate combinations (Buckland et al. 2004, 2015, Marques et al. 2007). Models with different key functions are not nested (not all models can be defined as simplifications of the most highly-parameterized model) within any one model, hence it may not always be straightforward to identify a single "global" model from which to estimate $\hat{c}$. For example, Buckland (2006) considered an unadjusted hazard rate model, a half-normal model with a maximum of one adjustment term, and a uniform model with a maximum of two adjustment terms in his analysis of cue counting data from 4 songbird species. Thus three different models included two parameters, and no single model was the most general or most highly-parameterized. Below we propose and evaluate two estimators of $\hat{c}$, and a two-step model selection procedure that does not require that a single global model is identifiable, for use with overdispersed DS data.

4.2 Methods

4.2.1 Model selection criteria and procedures

We suggest the χ^2 GOF statistic for binned distance data (Buckland et al. 2001, p. 71, eqn. 3.57) divided by its degrees of freedom as one estimator of c ($\hat{c}_1$). Johnson et al. (2010) proposed a one-stage, model-based approach for simultaneously estimating detectability and spatially variable abundance from DS data, and also evaluated the effectiveness of an overdispersion factor calculated from a χ^2 test performed on transect-specific counts for inflating model-based variances around abundance estimates to account for overdispersion introduced by fine-scale variation in local abundance. They found that variances were still underestimated except where there were many transects, and suggested the χ^2 GOF test for binned distance data divided by its degrees of

freedom as an alternative estimator. However, it is not clear to us how a statistic derived from the observed distances would quantify overdispersion induced by variation in local abundance, so we use this statistic to adjust for overdispersion only when modeling the detection function.

To allow for the possibility that multiple models may include the maximum number of parameters, and the fact that DS models have different general forms, we propose the following "two-step" model selection procedure. In step one we use QAIC to identify the best-supported model within each key function, and in step two we compare the relative goodness-of-fit of the best-supported models with different key functions. More specifically, in step one, we obtain $\hat{c}_1$ from the most highly-parameterized model within each key function (rather than from the most highly-parameterized model overall), use those values of $\hat{c}_1$ to calculate QAIC for all models with the same key function, and identify the QAIC-minimizing model within each key function. In this step, the same value of $\hat{c}_1$ is used to calculate QAIC for all models with the same key function, but different values of $\hat{c}_1$ are used to calculate QAIC for different key functions. In step two, we compare values of the χ^2 GOF statistic divided by its *df* across QAIC-minimizing models (one from each key function), and select the model with the smallest value for estimation, hence, the final decision is based on the values of $\hat{c}_1$, not QAIC (a different metric is used for decision making the two steps). If continuous distances are recorded in the field, distance observations will first need to be grouped into categories so that the GOF test for binned distance data can be performed. See Buckland et al. (2001) for advice regarding binning continuous observations.

In CT surveys or surveys of groups of animals, the number of distance observations per independent encounter (which might be a single triggering event at a

CT, or a sinlge observation of a group of animals) between an animal and an observer describes the frequency of violations directly, and so provides an alternative measure of the magnitude of overdispersion ($\hat{c}_2$). $\hat{c}_2$ can be calculated from the raw data, and will be the same for all models in the candidate set. In CT surveys of solitary animals, $\hat{c}_2$ would be the mean number of distance observations recorded during a single pass by an animal in front of a CT. In surveys of social animals employing human observers, $\hat{c}_2$ would be the mean number of detected animals per detected group, and in CT surveys of social animals $\hat{c}_2$ would be the mean number of distance observations recorded per triggering event. In cue counting surveys, $\hat{c}_2$ would be unknown because multiple cues from the same animal cannot be identified as such. Where calculable, $\hat{c}_2$ could be used instead of multiple values of $\hat{c}_1$ to calculate QAIC values as in step one above. QAIC values would still be compared only within key functions, and the χ^2 GOF statistic divided by its *df* would still be used in step two to select among QAIC-minimizing models with different key functions, i.e., the two step procedure would remain the same, but the definition of $\hat{c}$ and therefore the values of QAIC used in step one would differ. Hereafter, we will refer to QAIC calculated from $\hat{c}_1$ as $QAIC_1$, and from $\hat{c}_2$ as $QAIC_2$.

4.2.2 Simulations

We conducted simulations where non-independent observations were all at the same distance so that we could evaluate performance where the true magnitude of overdispersion (*c*), and the true underlying model were known, but we would not expect this scenario to arise in practice. When non-independent observations during a single independent encounter are at different distances (e.g. to different members of a group, different cues from a moving animal, or as an animal moves past a CT), true *c* is

unknown because the different distance observations contribute information about the shape of the detection function. We therefore also simulated camera-trapping (CT) surveys of moving animals where cameras recorded video and distance was recorded every 2 seconds as animals moved through the field of view. These simulations mimic real surveys where animals move and *c* is unknown. Furthermore, the distribution of observed distances differed from the expected distribution of independent detections (see Results), so the true underlying model was also unknown.

For the simulations with known *c*, we sampled distance to animals within a circular point transect with radius 20 m, where the trude density was 2.00 per m^2. To generate independent DS data, we simulated detections via random trials where detection probability declined according to a half-normal function with scale parameter (σ) of 7. Each observation was arbitrarily assigned one of three levels of a categorical covariate that had no effect on detectability, which we will refer to as "observer". We then replicated each observation five times to generate overdispersed data with $c = 6$. We fitted eight point transect DS models to each dataset, including the half normal model used to generate the data, and overparameterised models.

For the CT surveys, we simulated sampling of ungulates inhabiting old growth forests, recently logged forests, and previously logged but regrowing forests. Simulation parameters were based on the survey of Maxwell's duikers described in Chapter 3 and by Howe et al. (2017a), but were also selected to ensure that data were overdispersed, not sparse, and included multiple potential covariates of detectability. We assumed that the density of understorey vegetation increased immediately after logging and decreased gradually as forests regrew, such that food supply and therefore animal density was highest, but detection probability as a function of distance was

lowest, in recently logged forests; we further assumed a larger difference in detection probability between old growth and logged forests than between recently logged and regrowing forests (Table 4.1).

Table 4.1. Animal densities (*D*) and scale parameters (σ) of a half normal detection probability function in different habitat types used to generate simulated distance sampling data.

Forest type	*D*	σ
Old growth	10	7.0
Regrowing	12	5.5
Recently logged	15	5.0
Mean	12.33	

We simulated movements of 10, 12, and 15 animals within 1 km by 1 km square study areas in old growth, regrowing, and recently logged habitats, respectively. Each animal started with a random initial location and heading, after which new locations were generated every two seconds for 12 hours. Step lengths were drawn from an exponential distribution with a rate parameter of 2 m, and turn angles were drawn from a normal distribution with mean of 0 and standard deviation of 0.05 radians (we used the exponential distribution rather than the lognormal distribution used in Chapter 3 to ensure there would be many small steps lengths and therefore many observations at the same distance so that data would be severely overdispersed). Animals that moved beyond the boundaries of the study areas reappeared immediately on the opposite side of the same study area at the same heading. We simulated sampling at a grid of 36 CTs at 150 m spacing within each study area. We defined the zone of potential detection by a CT as a sector with a central angle of 0.733 radians and a radius of 25 m, and recorded distances between CTs and animal locations that fell within these sectors. We initially conducted random trials assuming detection probability declined according to a half-normal function with scale parameters as in Table 4.1 to determine whether animals

were detected at each time step. However, we assumed that cameras were programmed to record video when triggered, so once an animal was randomly detected once within a sector we set the probability of subsequent detection to 1.0 for as long as the animal remained within the sector. Therefore, the observed distances were those recorded within the sector defined by the location and angle of view of the CT, at predetermined snapshot moments after initial detection, following Howe et al. (2017a). With this movement model and sampling scenario, each animal was expeted to travel 10.8 km per day. Most step lengths were between 0 and 0.5 m, which ensured that animals would be observed multiple times, including at similar distances, during a single independent encounter with a CT, and hence distance data would be severely overdispersed. Density remained constant, and the expected distribution of animal locations was uniform within the study areas.

We conducted conventional distance sampling (CDS) analyses of data from recently logged forests, where only the key function and number of adjustment terms varied among 6 candidate models.

We also analysed data from all three habitat types simultaneously using multiple covariate distance sampling. Different habitat types were treated as different strata, with the potential to estimate a common detection function across all strata, or to model differences in detectability among strata using categorical covariates affecting the scale parameter of the detection function. We considered a habitat type covariate with two levels (old growth or logged), and one with three levels (old growth, regrowing, and recently logged). The 36 cameras in each study area were arbitrarily assigned to one of three different CT models (12 of each type). Detectability therefore varied among habitat types (Table 4.1) but not among camera trap models. Both habitat type and

camera trap model were considered as potential covariates of the detection function; only one habitat type covariate was included in any model. We fitted 20 models with either the half-normal or the hazard rate key function, 0 or 1 cosine adjustment terms, and different covariate combinations to each dataset. These simulations were designed to be challenging from a model selection perspective, in that we sought criteria and procedures that would support small but real differences in detectability while avoiding overfitting the detection function model.

During all simulations, distance data were binned into intervals prior to analysis. Howe et al. (2017a), were confident of their assignments of duikers into 1 m intervals out to 8 m, but found it more difficult to estimate distances to this level of precision beyond 8 m. We similarly binned data into one-meter intervals out to 8 m, and at 10, 12, 15 and 20 m. In the case of the CT surveys of moving animals, distance observations <1 m and >20 m were also truncated because we expected that the limitations of CTs would require similar truncation in real applications. At short distances, it might not be possible to identify species, and small animals may not trigger CTs set e.g. 0.5 to 1.0 m from ground-level. We conducted 500 replicate iterations, recording the number of estimated parameters, the log-likelihood value, the estimated density ($\widehat{D}$) and associated empirical, design-based variances (Fewster et al. 2009), and the χ^2 GOF statistic and its *df* and *p*-value, from all models fit to each dataset. We selected among candidate models by comparing AIC values across all models fitted to the same dataset, and using both $QAIC_1$ and $QAIC_2$ following the two-step procedure described in the methods section. Simulations were performed using R software, version 3.3.2 (R Core Team, 2016).

4.2.3 Applications with real data

We applied the same model selection criteria and procedures used in the simulations to real data from Maxwell's duikers sampled in Taï National Park, Côte d'Ivoire, originally presented in Chapter 3 and Howe et al. (2017a, b). We also reanalyzed cue count data from singing males of four species of songbirds sampled at Montrave Estate in Fife, Scotland, originally presented in Buckland (2006) and used as an example data set by Buckland et al. (2015). The Montrave study area was small enough that densities of singing males were estimable by mapping their territories; these estimates served as benchmarks by which the accuracy of DS estimates were assessed (Buckland 2006). Aware of the potential for overdispersion and therefore overfitting with cue count data, Buckland (2006) did not consider models with > 2 parameters, and used a combination of AIC and plots of fitted probability density functions and detection functions to select among six models with different key functions and numbers of adjustment terms. We fit a total of 9 models to each data set (uniform with 1, 2, or 3 cosine adjustment terms, half-normal with 0, 1, or 2 Hermite polynomial adjustment terms, and hazard rate with 0, 1, or 2 cosine adjustment terms) and used the two-step procedure with $QAIC_1$ to select among them. Truncation distances and cutpoints for the χ^2 GOF test followed Buckland (2006). $\hat{c}_2$ and therefore $QAIC_2$ could not be calculated from cue count data as described above. We used diagnostic plots only to identify and exclude implausible models, such as cases where estimated detection probabilities exceeded 1.0, or fitted detection functions that were not monotonically nonincreasing. When fitting models with adjustment terms, we used the parameter estimate(s) from the model with the same key function and one fewer

adjustment term as starting value(s). Analyses of real data sets were conducted using program Distance version 7.0 (Thomas et al. 2010).

4.3 Results

4.3.1 Simulations

Where the correct underlying model and the true magnitude of overdispersion were known, $\hat{c}_1$ varied considerably among iterations, but on average it was a reasonably accurate estimator (mean and median $\hat{c}_1$ from the data generating model were 6.16 and 5.73, respectively; c was 6.0). AIC selected the most highly parameterised model most frequently, selected models with the spurious observer covariate for 71.4% of datasets, and selected the correct model for only 2.8% of datasets (Table 4.2). QAIC selected the correct model most frequently, followed by the hazard rate model with one adjustment and no covariates. $QAIC_1$ and $QAIC_2$ selected models with the spurious covariate for 14% and 13% of datasets respectively (Table 4.2). $\widehat{D}$ from QAIC-selected models was both more accurate and more precise than $\widehat{D}$ from AIC-selected models (Table 4.3). The χ^2 GOF test rejected the null hypothesis of adequate fit of the correct model for 492 of 500 datasets. Mean sample size of distance observations was 3,630.

Table 4.2. Number of times each detection function model fitted to simulated, overdispersed data from stationary animals (where the correct underlying model and true *c* were known) was selected by AIC, and by each of $QAIC_1$ and $QAIC_2$ following the two-step procedure described in the methods section, of 500 replicate iterations. "Key" denotes the key function, either half-normal (hn) or hazard rate (hr); "Adj." denotes the number of adjustment terms. The underlying true (data-generating) model was the undjusted half-normal model.

Models				Model selection criteria		
Key	Covariates	Adj.	Parameters	AIC	$QAIC_1$	$QAIC_2$
hn	None	0	1	14	248	238
hn	Observer	0	3	54	21	29
hn	None	1	2	9	32	39
hn	Observer	1	4	92	9	4
hr	None	0	2	1	30	29
hr	Observer	0	4	8	1	2
hr	None	1	3	57	120	127
hr	Observer	1	5	265	39	32

Table 4.3. Medians of density estimates ($\widehat{D}$) and of coefficients of variation (CV) of those estimates, from models fitted to simulated overdispersed data from stationary animals, selected by AIC, and by $QAIC_1$ and $QAIC_2$ following the two-step procedure, across 500 iterations. True *D* was 2.00.

	AIC	$QAIC_1$	$QAIC_2$
Median $\widehat{D}$	1.89	2.00	2.00
Median CV($\widehat{D}$)	0.054	0.029	0.028

In our simulated CT surveys of moving animals, where we assumed that, after initial detection, detection probability was 1.0 for as long as the animal remained in the field of view of the CT (as though CTs were programmed to record long bursts of still images or videos) observed distances included more observations at longer distances than where animals were detected via random trials at each time step (as though CTs were programmed to record a single image when triggered). The mode of the distribution was shifted right, and the number of observations at longer distances declined more slowly than under the data generating model (Fig. 4.1). These differences arose because detected animals moving away from the CT continued to

contribute observations at longer distances where detection probability would otherwise be low. As a result, hazard rate models frequently provided a better fit than the half-normal model from which the random detections were simulated (Fig. 4.1).

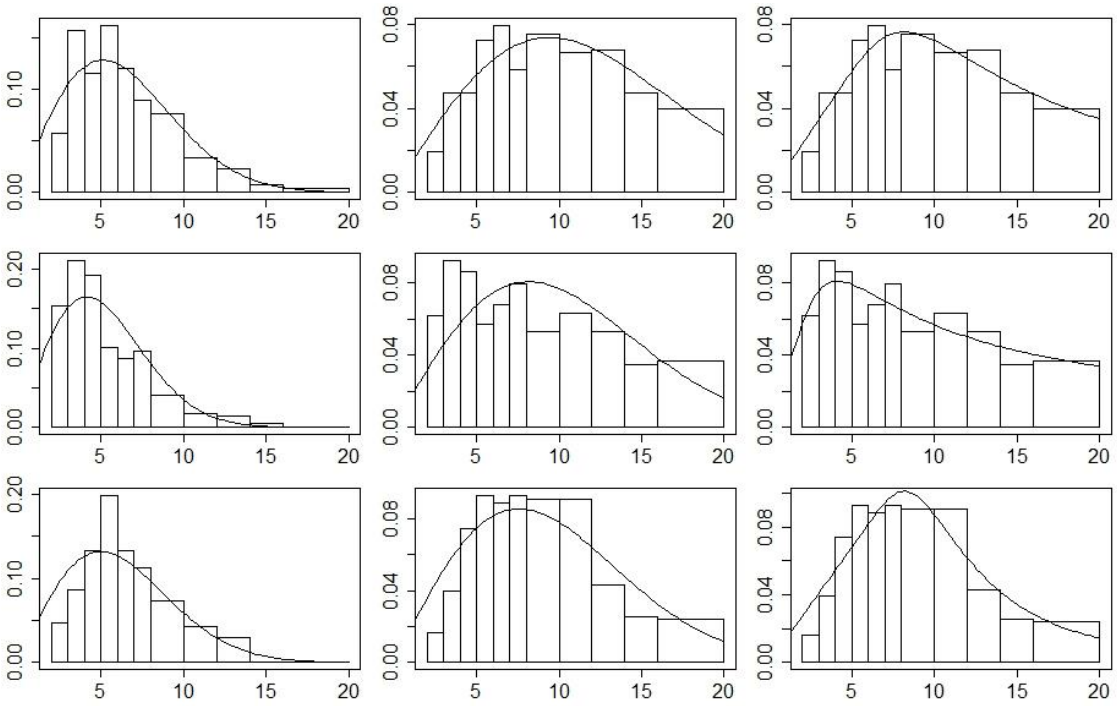

Figure 4.1. Histograms of observed distances to detected animals from simulations where detection occurred via random trials at each time step (left column), and where detection was certain for as long as animals remained in the field of view of the camera after initial detection (right 2 columns), for each of 3 randomly-selected data sets from recently logged forests. Distance data were left-truncated at 1 m, and right-truncated at 20 m. Lines show fitted probability density functions of the probability of detection under the half-normal (left 2 columns) and hazard rate detection functions with no adjustments.

The χ^2 GOF test for binned distance data tended to reject the null hypothesis of adequate fit. *P* was < 0.05 for 77% of the 3000 CDS models fitted to data from recently logged forests, and 89% of the 10000 MCDS models fitted to pooled data.

Sample sizes of distance observations, and of the number of observations per independent encounter ($\hat{c}_2$) were slightly higher in old growth forests where detection

probability as a function of distance was highest, even though densities there were lowest (Table 4.2). $\hat{c}_1$ was generally lower, indicating less overdispersion, than $\hat{c}_2$ from a given data set and model. $\hat{c}_1$ was also more variable among iterations than $\hat{c}_2$ (Table 4.4).

Table 4.4 Mean (SD) sample sizes (n) of distance observations and numbers of observations per independent encounter ($\hat{c}_2$) from simulated data from each habitat type, and from data pooled across habitat types, and mean values of the χ^2 GOF statistic divided by its degrees of freedom ($\hat{c}_1$) from the most highly parameterized half-normal and hazard rate models fit to the recently-logged and pooled data sets, across 500 iterations.

	Old growth	Regrowing	Recently logged	Pooled data
n	919 (149)	730 (134)	787 (130)	2437 (246)
$\hat{c}_1$ half-normal	--	--	3.50 (1.89)	6.70 (3.61)
$\hat{c}_1$ hazard rate	--	--	3.48 (2.02)	8.57 (7.74)
$\hat{c}_2$	16.8 (1.66)	14.8 (1.78)	14.2 (1.65)	15.3 (0.99)

In the CDS analysis of data from recently-logged forests, all model selection criteria selected a hazard rate model with no adjustments for the majority of the data sets (Table 4.5). AIC selected models with adjustments more often than $QAIC_1$, and $QAIC_1$ selected models with adjustments more frequently than $QAIC_2$ (Table 4.5). Both the accuracy and precision of $\widehat{D}$ were slightly improved by the use of our two-step procedure and QAIC, particularly $QAIC_2$ (Table 4.6).

Table 4.5. Number of times each detection function model fit to simulated data from the recently logged study area was selected by AIC, and by each of $QAIC_1$ and $QAIC_2$ following the two-step procedure described in the methods section, of 500 replicate iterations.

Model			Model selection criteria		
Key function	Adjustments	Parameters	AIC	$QAIC_1$	$QAIC_2$
Half-normal	0	1	69	103	137
Half-normal	1	2	34	19	0
Half-normal	2	3	16	14	0
Hazard rate	0	2	299	330	362
Hazard rate	1	3	50	22	1
Hazard rate	2	4	32	12	0

Table 4.6. Medians of density estimates, and of coefficients of variation (CV) of those estimates, from models fit to simulated data from recently logged forests selected by AIC, and by $QAIC_1$ and $QAIC_2$ following the two-step procedure, across 500 iterations. True density was 15.0.

	AIC	$QAIC_1$	$QAIC_2$
Median $\widehat{D}$	15.5	15.3	15.0
Median CV ($\widehat{D}$)	0.185	0.180	0.176

In the MCDS analysis of data pooled across habitat types, AIC again tended to select highly-parameterized models. Density was not estimable from the AIC-minimizing model in 9 cases, and in 53 other cases, estimates were unrealistically high (>10 times the true density). $QAIC_1$ and $QAIC_2$ each selected models from which density was not estimable twice, and from which density was severely overestimated 4 times; these problematic estimates were associated with the same six data sets. AIC favoured detection function models with more complex forms, selecting adjusted hazard rate models for 49% of data sets, and either unadjusted hazard rate or adjusted half normal models for another 45% (Table 4.7). $QAIC_1$ and $QAIC_2$ selected unadjusted hazard rate models most frequently, followed by unadjusted half normal models (Table 4.7).

Table 4.7. The number of times, out of 500 iterations, that each of the 20 candidate models was selected by each model selection criterion, and below this, the number of times each of four forms of the detection function, and each of three covariate effects, was included in the selected models. Key refers to the key function, either half-normal (hn) or hazard rate (hr); covariates were: Logging (2), with differences in detectability between logged and old growth forests, Logging (3), with differences among all habitat types, and camera trap model (CT), which did not affect detectability; Adj. refers to the number of cosine adjustment terms included in the model (either 0 or 1).

Models				Model selection criteria		
Key	Covariates	Adj.	parameters	AIC	$QAIC_1$	$QAIC_2$
hn	None	0	1	0	8	26
hn	Logging (2)	0	2	0	52	104
hn	Logging (3)	0	3	3	34	19
hn	Logging (2) + CT	0	4	9	32	7
hn	Logging (3) + CT	0	5	20	14	3
hn	None	1	2	0	0	0
hn	Logging (2)	1	3	3	37	28
hn	Logging (3)	1	4	6	22	5
hn	Logging (2) + CT	1	5	16	18	0
hn	Logging (3) + CT	1	6	71	13	0
hr	None	0	2	0	45	70
hr	Logging (2)	0	3	2	106	182
hr	Logging (3)	0	4	15	48	35
hr	Logging (2) + CT	0	5	31	31	12
hr	Logging (3) + CT	0	6	79	18	1
hr	None	1	3	0	0	0
hr	Logging (2)	1	4	4	11	8
hr	Logging (3)	1	5	28	2	0
hr	Logging (2) + CT	1	6	50	7	0
hr	Logging (3) + CT	1	7	163	2	0
Forms				AIC	$QAIC_1$	$QAIC_2$
hn (0 adjustment terms)				32	140	159
hn (1 adjustment term)				96	90	33
hr (0 adjustment terms)				127	248	300
hr (1 adjustment term)				245	22	8
Covariate effects				AIC	$QAIC_1$	$QAIC_2$
Logging (2-level)				115	294	341
Logging (3-level)				385	153	63
CT model				439	135	23

AIC always supported an effect of habitat type on detection probability, and supported the 3-level habitat covariate for 77% of data sets (Table 4.7). $QAIC_1$ and

$QAIC_2$ selected models with habitat type covariates for 89% and 81% of data sets, respectively, but tended to favour the 2-level covariate (selected for 59% and 68% of data sets, respectively) over the 3-level covariate (Table 4.7). Most (88% of) AIC-selected models, 27% of $QAIC_1$-selected models, and 5% of $QAIC_2$-selected models included the spurious CT model covariate (Table 4.7).

$QAIC_2$ and our two-step model selection procedure maximized both the accuracy and precision of $\widehat{D}$ (Table 4.8). AIC-selected models yielded negatively biased $\widehat{D}$ on average (Table 4.6). Differences in $\widehat{D}$ among habitat types were greatest, and slightly exaggerated, where AIC was used for model selection; AIC-selected models yielded the most accurate $\widehat{D}$ only in recently-logged forests (Table 4.8). QAIC-selected models rarely included the 3-level habitat covariate, and as a result, $\widehat{D}$ in recently-logged forests, and differences in $\widehat{D}$ among habitat types, were underestimated. However, QAIC-selected models yielded more accurate estimates of total density, and of density in regrowing and old growth forests (Table 4.8). $QAIC_2$-selected models yielded the most precise density estimates, followed closely by $QAIC_1$-selected models (Table 4.8).

Table 4.8. Medians of estimated densities ($\widehat{D}$) and their coefficients of variation (CV), by model selection criterion and habitat type. In parentheses under AIC, medians across the 439 data sets where density was estimable and total $\widehat{D}$ was within an order of magnitude of the true value (median CVs from AIC-selected models, and median densities from $QAIC_1$- and $QAIC_2$-selected models were similar when extreme values were excluded).

	Regrowing (D = 12)		Recently-logged (D = 15)		Old growth (D = 10)		Total (D = 12.33)	
	$\widehat{D}$	CV	$\widehat{D}$	CV	$\widehat{D}$	CV	$\widehat{D}$	CV
AIC	11.5 (11.1)	0.21	15.1 (14.4)	0.19	8.9 (9.0)	0.19	12.1 (11.7)	0.13
$QAIC_1$	11.8	0.19	14.2	0.18	9.7	0.18	12.0	0.11
$QAIC_2$	12.0	0.18	14.1	0.17	10.1	0.17	12.2	0.11

4.3.2 Applications with real data

In the data from Maxwell's duikers, the number of observations per independent encounter ($\hat{c}_2$) was 15.35 during the daytime, and 16.98 during times of peak activity. The χ^2 GOF statistic divided by its *df* ($\hat{c}_1$) from different models fit to the daytime data set ranged between 20 and 25, and from models fit to the peak activity data set ranged between 12 and 35 (Tables 4.9 and 4.10). Model selection criteria and procedures adjusted for overdispersion selected the same models as AIC for estimation from each data set (the unadjusted hazard rate model, see Howe et al. 2017a and Tables 4.11 and 4.12), so $\widehat{D}$ was unaffected.

Table 4.9. Model selection by AIC, and step one of the two-step model selection procedure (see Table 4.11 for the 2nd step), for the seven detection function models successfully fitted to the "daytime" data from Maxwell's duikers in Taï National Park, Côte d'Ivoire (2014), and considered for density estimation (see Chapter 3 and Howe et al. 2017a). Values of $\hat{c}_1$ and $\hat{c}_2$ are those used to calculate $QAIC_1$ and $QAIC_2$, respectively, as opposed to model-specific values. The top AIC-ranked model, and the top $QAIC_1$- and $QAIC_2$-ranked models within each key function are marked with asterisks. Under "Model", Hr = hazard rate, Un = uniform, Hn = half-normal, cos = cosine adjustment, Hp = Hermite polynomial adjustment, and numbers following cos or Hp indicate the number of adjustment terms. "npar" is number of parameters in the model. We included *c* as one of the *K* parameters when calculating QAIC.

Model	npar	Log Ω	AIC	$\hat{c}_2$	$\hat{c}_1$	$QAIC_1$	$QAIC_2$
Hr	2	-22014.4	44032.73*	15.35	20.42	2162.16*	2874.32*
Hr cos 1	3	-22014.2	44034.40	15.35	20.42	2164.14	2876.30
Un cos 2	2	-22041.4	44086.82	15.35	24.91	1775.68	2877.85
Un cos 1	1	-22045.3	44092.54	15.35	24.91	1773.99*	2876.35*
Hn Hp 1	2	-22052.6	44109.17	15.35	22.22	1991.021	2879.30
Hn	1	-22071.6	44145.18	15.35	22.22	1990.731	2879.78
Hn Hp 2	3	-22020.5	44047.02	15.35	22.22	1990.133*	2877.12*

Table 4.10. Model selection by AIC, and step one of the two-step model selection procedure (see Table 4.12 for the 2nd step), for the eight detection function models fit to the "peak activity" data from Maxwell's duikers in Taï National Park, Côte d'Ivoire (2014; see Chapter 3 and Howe et al. 2017a). Values of $\hat{c}_1$ and $\hat{c}_2$ are those used to calculate $QAIC_1$ and $QAIC_2$, respectively, as opposed to model-specific values. The top AIC-ranked model, and the top $QAIC_1$- and $QAIC_2$-ranked models within each key function are marked with asterisks. Under "Model", Hr = hazard rate, Un = uniform, Hn = half-normal, cos = cosine adjustment, Hp = Hermite polynomial adjustment, and numbers following cos or Hp indicate the number of adjustment terms. "npar" is number of parameters in the model. We included *c* as one of the *K* parameters when calculating QAIC.

Model	npar	Log Ω	AIC	$\hat{c}_2$	$\hat{c}_1$	$QAIC_1$	$QAIC_2$
Hr (0)	2	-12436.8	24877.61*	16.98	12.39	2013.55*	1470.62*
Hr cos 1	3	-12436.8	24879.61	16.98	12.39	2015.55	1472.62
Hr cos 2	4	-12436.8	24881.60	16.98	12.39	2017.55	1474.62
Un cos 2	2	-12495.9	24995.81	16.98	26.58	946.25	1477.58
Un cos 1	1	-12497.7	24997.46	16.98	26.58	944.39*	1475.80*
Hn Hp 2	3	-12504.1	25014.18	16.98	34.90	724.57	1480.55
Hn Hp 1	2	-12511.0	25025.90	16.98	34.90	722.96	1479.35*
Hn	1	-12539.8	25081.60	16.98	34.90	722.61*	1480.75

Table 4.11. Step two of the two-step model selection procedure applied to the models from Table 4.9, showing the top $QAIC_1$- and $QAIC_2$-ranked models within each key function, and corresponding values of the χ^2 GOF statistic divided by its degrees of freedom (*df*). For each of $QAIC_1$ and $QAIC_2$, the model with the lowest χ^2 / *df* value is marked with an asterisk, and was selected for estimation.

	$QAIC_1$		$QAIC_2$	
Key function	Top model	χ^2 / *df*	Top model	χ^2 / *df*
Hazard rate	Unadjusted	17.21*	Unadjusted	17.21*
Uniform	cos 1	22.34	cos 1	22.34
Half-normal	Hp 2	22.22	Hp 2	22.22

Table 4.12. Step two of the two-step model selection procedure applied to the models from Table 4.10, showing the top $QAIC_1$- and $QAIC_2$-ranked models within each key function, and corresponding values of the χ^2 GOF statistic divided by its degrees of freedom (*df*). For each of $QAIC_1$ and $QAIC_2$, the model with the lowest χ^2 / *df* value is marked with an asterisk, and was selected for estimation.

	$QAIC_1$		$QAIC_2$	
Key function	Top model	χ^2 / *df*	Top model	χ^2 / *df*
Hazard rate	Unadjusted	8.26*	Unadjusted	8.26*
Uniform	cos 1	23.22	cos 1	23.22
Half-normal	Unadjusted	34.84	Hp 1	31.17

In the original analysis of the European robin data from Montrave Estate, the half-normal model with one adjustment term minimized AIC and was selected for estimation (Buckland 2006). In our reanalysis, the fitted detection function from the hazard rate model with two adjustments was not monotonically nonincreasing so was not considered further, and the uniform model with three cosine adjustment terms minimized AIC (Table 4.13). $QAIC_1$ selected the uniform model with 1 adjustment term, which yielded $\widehat{D}$ that was more similar to the territory mapping estimate, and more precise, than estimates from either the model selected by Buckland (2006) or the model that minimized AIC in our reanalysis (Table 4.13).

In the original analyses of data from winter wrens, the unadjusted hazard rate model minimized AIC and was selected by Buckland (2006) for estimation. The same

model minimized AIC across our larger candidate set, and was also selected by $QAIC_1$ (Table 4.14). The associated density estimate represents a reasonable trade-off between bias and precision, though estimates from three other models were slightly closer to the territory mapping estimate (Table 4.14).

The unadjusted hazard rate model also minimized AIC and was selected by Buckland (2006) to estimate chaffinch densities. In our reanalysis, the hazard rate model with one cosine adjustment and the half-normal model with two Hermite polynomial adjustments had lower AIC values and yielded slightly lower and less accurate density estimates (Table 4.15). The unadjusted half normal model was selected by $QAIC_1$ and also yielded a less accurate estimate than the unadjusted hazard rate model (Table 4.15), though the territory mapping estimate was still well within the 95% confidence interval.

In our reanalysis of data from great tits, hazard rate models minimized AIC (Table 4.16), but estimates of the shape parameter were at the upper bound, and the estimated detection probability was still 1.0 beyond 70 m. The fitted half normal model with two adjustment terms had a bimodal probability density function, and the fitted uniform model with three adjustment terms was not monotonically nonincreasing. These models yielded inaccurate density estimates, but were not considered for estimation for the above reasons. Buckland (2006) did not comment on the fit of hazard rate models to these data, but selected the unadjusted half normal model for estimation. $QAIC_1$ selected this model without reference to diagnostic plots or estimates of effective detection radii (Table 4.16).

Table 4.13. Model selection results and density estimates ($\widehat{D}$) and coefficients of variation (CV) of $\widehat{D}$ for European robins at Montrave Estate. "Adj." denotes the number of cosine adjustment terms included in the model. The hazard rate model with two adjustment terms was not considered because the fit was not monotonically nonincreasing. The minimum AIC value, χ^2 / *df* values used to calculate QAIC within key functions, minimum QAIC values within key functions, and the density estimate from the model selected by the two-step $QAIC_1$ procedure are marked with asterisks. The density estimate from the model selected by Buckland (2006) is marked with a †. The territory mapping estimate was 0.84 territories per hectare.

Key function	Adj.	Parameters	Log Ω	AIC	χ^2 / *df*	$QAIC_1$	$\widehat{D}$	CV
Half-normal	2	3	-3372.63	6751.25	29.76*	234.64	0.812	0.238
Half-normal	1	2	-3373.13	6750.25	23.82	232.67	0.823†	0.239
Half-normal	0	1	-3382.59	6767.18	19.93	231.31*	1.059	0.220
Hazard rate	1	3	-3380.07	6766.15	37.78*	186.95	0.720	0.243
Hazard rate	0	2	-3380.07	6764.15	30.19	184.95*	0.721	0.219
Uniform	3	3	-3371.71	6749.42*	30.15*	231.66	0.793	0.237
Uniform	2	2	-3374.03	6752.07	22.14	229.81	0.926	0.223
Uniform	1	1	-3375.45	6752.90	19.63	227.91*	0.842*	0.216

Table 4.14. Model selection results and density estimates ($\widehat{D}$) and coefficients of variation (CV) of $\widehat{D}$ for winter wrens at Montrave Estate. "Adj." denotes the number of cosine adjustment terms included in the model. The minimum AIC value, χ^2 / *df* values used to calculate QAIC within key functions, minimum QAIC values within key functions, and the density estimate from the model selected by the two-step QAIC procedure are marked with asterisks. The density estimate from the model selected by Buckland (2006) is marked with a †. The territory mapping estimate was 1.30 territories per hectare.

Key function	Adj.	Parameters	Log Ω	AIC	χ^2 / *df*	$QAIC_1$	$\widehat{D}$	CV
Half-normal	2	3	-3312.79	6631.57	31.02*	221.57	1.234	0.253
Half-normal	1	2	-3314.46	6632.92	24.38	219.68	1.269	0.244
Half-normal	0	1	-3328.00	6658.00	23.00	218.55*	1.504	0.200
Hazard rate	2	4	-3308.69	6625.38	35.58*	196.01	1.211	0.299
Hazard rate	1	3	-3308.75	6623.51	26.77	194.01	1.209	0.280
Hazard rate	0	2	-3308.76	6621.52*	21.35	192.01*	1.212*†	0.200
Uniform	3	3	-3315.46	6636.93	32.89*	209.62	1.130	0.277
Uniform	2	2	-3316.91	6637.82	24.34	207.71	1.245	0.226
Uniform	1	1	-3332.54	6667.07	22.28	206.66*	1.579	0.196

Table 4.15. Model selection results and density estimates ($\widehat{D}$) and coefficients of variation (CV) of $\widehat{D}$ for common chaffinches at Montrave Estate. "Adj." denotes the number of cosine adjustment terms included in the model. The minimum AIC value, χ^2 / *df* values used to calculate QAIC within key functions, minimum QAIC values within key functions, and the density estimate from the model selected by the two-step QAIC procedure are marked with asterisks. The density estimate from the model selected by Buckland (2006) is marked with a †. The territory mapping estimate was 0.75 territories per hectare.

Key function	Adj.	Parameters	Log Ω	AIC	χ^2 / *df*	$QAIC_1$	$\widehat{D}$	CV
Half-normal	2	3	-2757.45	5520.91	28.07*	204.47	0.681	0.240
Half-normal	1	2	-2760.43	5524.86	19.48	202.68	0.743	0.260
Half-normal	0	1	-2765.30	5532.61	16.37	201.03*	0.847*****	0.235
Hazard rate	2	4	-2757.02	5522.03	31.17*	186.91	0.699	0.309
Hazard rate	1	3	-2757.10	5520.21*	23.67	184.92	0.681	0.274
Hazard rate	0	2	-2759.06	5522.12	18.06	183.04*	0.712†	0.236
Uniform	3	3	-2759.48	5524.95	24.51*	233.20	0.686	0.280
Uniform	2	2	-2761.91	5527.82	18.33	231.40	0.702	0.261
Uniform	1	1	-2771.75	5545.49	16.57	230.20*	0.911	0.234

Table 4.16. Model selection results and density estimates ($\widehat{D}$) and coefficients of variation (CV) of $\widehat{D}$ for great tits at Montrave Estate. "Adj." denotes the number of cosine adjustment terms included in the model. Fits of several models were problematic and those models were not considered for estimation (see methods text). The minimum AIC value, χ^2 / *df* values used to calculate QAIC within key functions, minimum QAIC values within key functions, and the density estimate from the model selected by the two-step QAIC procedure are marked with asterisks. The density estimate from the model selected by Buckland (2006) is marked with a †. The territory mapping estimate was 0.21 territories per hectare.

Key function	Adj.	Parameters	Log Ω	AIC	χ^2 / *df*	$QAIC_1$	$\widehat{D}$	CV
Half-normal	2	3	-779.03	1564.06	23.57*	74.10	0.510	0.634
Half-normal	1	2	-786.03	1576.07	22.01	72.70	0.259	0.609
Half-normal	0	1	-786.03	1574.07	18.34	70.70*	0.259*†	0.592
Hazard rate	2	4	-774.25	1556.51	32.85*	57.14	0.163	0.653
Hazard rate	1	3	-774.25	1554.51	24.64	55.14	0.163	0.646
Hazard rate	0	2	-774.25	1552.51*	19.71	53.14*	0.163	0.585
Uniform	3	3	-781.20	1568.39	23.68*	73.98	0.587	0.613
Uniform	2	2	-785.66	1575.32	22.25	72.36	0.331	0.607
Uniform	1	1	-788.12	1578.25	18.91	70.57*	0.259	0.591

4.4 Discussion

In the simulations presented in Chapter 3 and Howe et al. (2017a), animals within zones of potential detection were randomly detected at each time step regardless of whether they had been previously detected during the same encounter with a CT, which is inconsistent with a recommendation to program cameras to record video or multiple still images each time the CT is triggered. The simulations presented here therefore provide more direct evidence that DS with CTs can yield unbiased density estimates. They also illustrate how certain detection within the field of view of a CT after initial detection (CTs programmed to record video or long, rapid bursts of still images), and redefining the detection function to represent the proportion of locations at different distances *which are recorded*, regardless of whether an animal triggered the sensor at that distance, causes the distribution of observed distances to include more observations at longer distances relative to expectations based on independent detections (CTs programmed to record single images). This effect will generalize to all CT studies where cameras are programmed to record video or multiple images while animals move through the area covered by the field of view.

In all of our simulations, AIC selected models that were more complex, including more parameters, than the optimal model. AIC consistently supported models with adjustment terms even though density was sometimes inestimable or drastically overestimated by these models, and a covariate that had no real effect on detectability. Associated inferences regarding sources of variation in detectability were flawed, and estimates of animal abundance were adversely affected. QAIC-selected models included fewer adjustment terms and rarely yielded implausible density estimates. QAIC was also much less likely to support the spurious CT model covariate. Models

selected via the two-step procedure and QAIC yielded slightly more accurate and more precise $\widehat{D}$ from simulated data.

Of the two proposed estimators of the magnitude of overdispersion, the mean number of observations per independent encounter ($\hat{c}_2$) was more stable than the χ^2 GOF statistic divided by its degrees of freedom ($\hat{c}_1$), which was highly variable across iterations of the same sampling scenario. $QAIC_2$-selected models yielded the most accurate and precise density estimates on average.

Relative to AIC, QAIC more frequently supported models where detectability differed between old growth and logged forests, but not between recently-logged and regrowing forests. This suggests that QAIC frequently selected a model with fewer than the optimal number of parameters, but it may not indicate that QAIC will generally underfit because there was little difference in detectability between recently-logged and regrowing forests, and the effect of certain detection after initial detection on the distribution of observed distances may have obscured this small difference. Sources of variation in detectability that have small effect sizes may frequently go undetected by any model selection criteria. Nevertheless, failure to detect and support this difference in our simulated data caused underestimation of density in recently-logged forests where detection probability was lowest. The difference in density between recently-logged and other forest types was therefore also underestimated, however, differences among all three habitat types were still apparent.

Although QAIC, particularly $QAIC_2$, consistently outperformed AIC in the simulation study, results of our reanalyses of previously-published overdispersed data sets were equivocal. All model selection criteria selected the same models for estimation from both data sets from Maxwell's duikers. With the Montrave songbird

data, $QAIC_1$ selected the same model as Buckland (2006) to estimate densities of wrens and tits, a model that yielded a more accurate and precise estimate of robin density than the one Buckland (2006) presented, and a model that yielded a less accurate estimate of chaffinch density. Accuracy was evaluated by comparison with territory mapping estimates, which we assume minimized bias. However, the accuracy of cue counting DS estimates of Montrave songbird densities were affected by uncertainty and possibly bias in estimates of cue production rate (Buckland 2006), and this prevents us from making strong inferences regarding which model selection criteria performed best with these data.

Our analyses of simulated and real data focused on overdispersed data from CT surveys and cue counting surveys, however, the independence assumption is also violated when animals travel in groups and more than one member of a group is detected during an encounter between the group of animals and an observer. Model selection criteria adjusted for overdispersion could therefore also be useful when social animals that travel in loosely-clumped or moving groups are surveyed. Buckland et al. (2010) simulated line transect sampling of primate groups and found that treating the individual as the unit of observation yielded more accurate and precise $\widehat{D}$ than approaches that treated the group as the unit of observation, despite overfitting.

When selecting among models fit to simulated data, we applied model selection criteria and procedures "blindly", in that we always estimated $\widehat{D}$ from the model that minimized AIC, or χ^2 / *df* from the QAIC-minimizing model within each key function. We also used the same distance bins and truncation distances with all of the simulated data sets. In thorough analyses of real data suspected or known to include non-independent distance observations, candidate model sets would emphasize simple

models, and model fitting and selection would be preceded by exploratory analysis to identify the most appropriate cutpoints and truncation distances, and to investigate relationships between distance observations and potential covariates (Buckland et al. 2004, Marques et al. 2007). Covariates with weak, imprecisely-estimated, or no apparent relationships with distance observations would be excluded from candidate model sets, reducing the potential for overfitting (Buckland et al. 2001, Marques et al. 2007). After model fitting, the estimated detection functions from high-ranking models, especially those with adjustment terms, would be scrutinized to ensure that they (1) are plausible based on knowledge of the species and sampling process, (2) have a slope near zero at distance zero, and (3) are monotonically nonincreasing. Models that do not meet these criteria would not be considered for estimation regardless of their rank. Estimated parameters would also be examined, and if the effect of a particular covariate was slight or imprecisely estimated (e.g., such that the 95% confidence interval of the estimate included zero), a model that excluded the covariate might be preferred for estimation, especially if it yielded a similar but more precise density estimate. Furthermore, ΔAIC values would be taken into consideration, where complex models might again be rejected in favour of a simpler model if the difference was small, especially if the simpler model is nested within the more complex one (Burnham and Anderson 2002, Richards 2008). AIC would likely have performed better with simulated data if we had followed these guidelines when analyzing each data set. Models that yielded extreme estimates would have been excluded post hoc, and we might have chosen to exclude the CT covariate from estimating models even if the AIC-minimizing model included it.

In our analyses of real data candidate model sets were not constrained, and we used diagnostic plots only to exclude models with obviously problematic fits, not to

select among models with plausible fits, and QAIC did not consistently outperform AIC.

Therefore our results, where the accuracy and precision of densities estimated from simulated data improved only slightly, and of densities estimated from real data improved in only one of six cases, when we used model selection criteria adjusted for overdispersion, as well as Buckland et al.'s (2010) simulation results, suggest that in many situations adverse effects of overfitting by AIC when distance observations lack independence may be minor.

The novel approaches to model selection described here are ad hoc, and we do not suggest that they are a final solution to the problem of lack of independence in DS data. Ideally, the different sources of overdispersion would be modelled explicitly; omnibus overdispersion factors like $\hat{c}$ estimate total overdispersion from all sources. We had considered a one-step approach to model selection using QAIC, where we used the value of $\hat{c}_1$ from the most highly parameterized model in each candidate set, and $\hat{c}_2$ calculated from the data, to calculate $QAIC_1$ and $QAIC_2$, respectively, for all other models, including those with different key functions, and used the QAIC-minimizing model for estimation. This approach underfit severely, favouring models with simple forms and few covariates that yielded biased but apparently precise density estimates. Retrospectively, this should not be surprising because if the most highly parameterized model fits the data poorly, $\hat{c}_1$ includes overdispersion attributable to model misspecification and $QAIC_1$ overcompensates for lack of independence. Similarly, we would expect $\hat{c}_2$ to accurately quantify overdispersion only if all non-independent observations were at the same distance and hence contributed no new information about the shape of the detection function. Non-independent observations at different distances

do contribute information, so when animals move between repeat observations recorded during an independent encounter, $\hat{c}_2$ also overestimates, and $QAIC_2$ overcompensates for, overdispersion due to lack of independence. We did not consider the smallest value of χ^2 / *df* across the candidate set as an estimator of *c*, however, this might minimize the contribution of model misspecification and more accurately quantify overdispersion attributable to lack of independence, potentially making a one-step approach to model selection using $QAIC_1$ effective.

We did not inflate variances or standard errors as a function of $\hat{c}$, as is common in other contexts (Lebreton et al. 1992, Liang and McCullagh 1993, Burnham and Anderson 2002). The design-based analytic variance of densities estimated by DS includes components for both detectability and the encounter rate (Fewster et al. 2009). Since we expected violation of the independence assumption to cause overdispersion in the observed distances, and only detectability is estimated from the distance observations, we would only inflate the detectability component of the variance. In most line transect surveys, the encounter rate variance contributes the majority of the total variance in $\widehat{D}$ (Fewster et al. 2009). Detectability typically contributes a larger fraction of of the total variance from point count surveys (Buckland et al. 2001, Fewster et al. 2009), but this was not the case in CT surveys (Howe et al. 2017a, Cappelle et al. 2019), and in cue counting surveys, uncertainty in the cue production rate may exceed the total uncertainty from the encounter rate and detectability (Buckland 2006, Marques et al. 2011, Warren et al. 2017), so inflating the detectability component might have only a small effect on the precision of $\widehat{D}$. Nevertheless, the potential to improve analytic estimates of the variance using the overdispersion factors described here warrants further research.

4.5 Synthesis and recommendations

We described novel approaches to estimating an overdispersion factor ($\hat{c}$), and criteria and procedures for selecting among models of the DS detection function when the assumption that distance observations are independent is violated. Simulations demonstrated the potential for these approaches to reduce overfitting and to improve inferences about animal abundance. However, where analysts are aware of the potential for overfitting, careful model evaluation and model selection informed by AIC may perform as well or better as criteria and procedures adjusted for overdispersion (Buckland 2006, Buckland et al. 2010, this study). We therefore recommend additional research, but also that these criteria and procedures be considered as alternatives to AIC when overfitting by AIC is apparent (e.g., if AIC favours models that include both adjustment terms and covariates, multiple adjustment terms, or weak or imprecisely-estimated covariate effects), or when researchers wish to avoid any subjectivity in the model selection process.

Chapter 5: Demographic Closure in Spatially Explicit Capture–Recapture Surveys of Chimpanzees

5.1 Introduction

Capture–recapture (CR) and spatially-explicit capture recapture (SECR) are widely-used analytical frameworks for estimating animal detectability and abundance from data describing captures or remote detections of uniquely marked or individually identifiable animals (Borchers et al. 2002, Royle et al. 2013c). CR models assume that all members of the sampled population have non-negligible risks of detection, and yield estimates of the size of the population at risk of detection by an array of traps or passive detectors (Otis et al. 1978). If occupied habitat extends beyond the area surveyed (i.e., if the population is not geographically closed), CR models estimate the "superpopulation" of animals present on the study area at any time, including animals with home ranges only partly within the area surveyed (Dice 1938, Schwarz and Seber 1999, Kendall 1999). Estimates of superpopulation size cannot be reliably converted to estimates of the more biologically relevant population density unless the effectively sampled area can be quantified (Otis et al. 1978, White et al. 1982), which is problematic unless functional islands are sampled. SECR models explicitly account for reduced detection probabilities of animals with home range center locations that are further from traps or detectors (Efford 2004). Therefore, not all members of the population must be exposed to a risk of detection, and population density of geographically open populations can be estimated directly from spatially referenced detections of individuals (Efford 2004, Borchers and Efford 2008). For this and other

reasons, SECR has become increasingly popular, replacing non-spatial CR analyses in many contexts (Obbard et al. 2010, Sollmann et al. 2011, Head et al. 2013).

CR and SECR models can be categorized into two types: those that do, and those that do not, rely on the assumption that the population is demographically closed for the duration of sampling (Otis et al. 1978, Lebreton et al. 1992, Schwarz and Seber 1999, Borchers and Efford 2008, Gardner et al. 2010, Glennie et al. 2019). Note that if animals with home ranges that partially overlap the area surveyed move onto and off of the area surveyed during the course of their normal movements, this violates the assumption of geographic, not demographic closure, whereas animals that permanently enter or leave the population at risk of detection by immigration or emigration violate the demographic closure assumption. A demographically closed population has fixed size and membership – no new animals are added via recruitment or immigration, and none are removed via death or emigration. CR and SECR models that rely on this assumption are termed "closed population" models; those that do not are termed "open population" models. Open population models estimate rates of additions and losses as well as population size or density (Lebreton et al. 1992, Gardner et al. 2010, Glennie et al. 2019). Closed population models require fewer parameters to be estimated, allowing abundance, which is usually the parameter of main interest, to be estimated more precisely. Open population SECR models were also developed more recently (Gardner et al. 2010, Glennie et al. 2019) and may not yet be familiar to many ecologists.

Closed-population CR or SECR models assume that all detected individuals were present for the duration of the survey, so detections of new permanent additions to the population increase the the total number detected, but when previously detected animals permanently emigrate or die they are still assumed to have been alive and

present but undetected for the remainder of the survey. Therefore, if animals permanently enter or leave the population during sampling, closed population models estimate the total number of individuals present over the duration of the survey, not the average number. Furthermore, individuals present for only part of the survey have lower net detection probabilies, causing the average probability of detection over the duration of the survey to be underestimated, and hence both the number undetected and total number present to be overestimated. This leads to the expectations that violations will positively bias estimates of abundance, and that bias relative to the true density at the end of the survey will be greater for declining than increasing populations.

The design of CR and SECR surveys involves trade-offs. Given a fixed number of traps or detectors, studies of longer duration yield larger samples, but also increase the risk of violating the assumption of demographic closure. Technological advancements including genetic and photographic CR have improved the potential to survey animals that are difficult or costly to physically capture in a relatively short time period (Karanth 1995, Woods et al. 1999). Shorter surveys and slow rates of population turnover make the assumption of demographic closure more reasonable, but do not validate it; additions and losses may still occur without investigators' knowledge, in which case the severity of violation of the closure assumption and any associated bias are unknown. Unlike hunting seasons and fruiting seasons in temperate habitats, temporal variation in factors influencing chimpanzee survival and recruitment are difficult to predict, so it may not be possible to avoid periods of elevated mortality or recruitment when designing a survey, as recommended by Dupont et al. (2019). Statistical tests for violations are of limited use because they are either insensitive to violations that occur during the middle of the survey, or are sensitive to individual

heterogeneity or trap responses even when populations are demographically closed (Otis et al. 1978, Stanley and Burnham 1999). Tests for demographic closure specific to SECR data have not been developed, and the robustness of closed population SECR models to violations of this assumption, of any magnitude, have not been evaluated. Therefore, researchers frequently assume demographic closure, and estimate abundance from closed-population SECR models, without being able to test this assumption (Royle et al. 2009a, b, Sollmann et al. 2011, McCarthy et al. 2015, Boulanger et al. 2018).

Closed population SCR models have recently been used to estimate chimpanzee densities from genetic and photographic (camera-trapping; "CT") surveys; low encounter rates of chimpanzees at CTs and of fresh great ape scats during searches necessitate long survey durations (e.g. 3 months to 3 years, Head et al. 2013, Després-Einspenner et al. 2017, Granjon et al. 2017, Arandjelovic and Vigilant 2018), so some violations of the closure assumption are inevitable. I sought to quantify the bias in chimpanzee densities estimated from closed-population SCR models when the assumption of demographic closure is violated. I simulated SCR surveys of demographically open and closed chimpanzee populations, and compared densities estimated from closed-population SCR models to true densities at the beginning and the end of the surveys. Dupont et al. (2019) recently presented generalized simulations exploring effects of closure violation on estimates of abundance from SCR models for closed populations, and the trade-off between bias and precision of estimates from surveys of different durations. Some of the scenarios I simulated were similar to some of theirs for long-lived species, and lead to similar conclusions, but I also identified situations in which the consequences of closure violation could be more severe and lead to inappropriate management decisions. I expect my simulation study to help

researchers minimize bias due to closure violation when estimating chimpanzee densities by SECR.

5.2 Methods

5.2.1 Chimpanzee demography informing simulations

Chimpanzees live in stable social groups of between 10 and 200 animals, termed communities (Mitani et al. 2012). Community members share a common territory, which is also relatively stable over time (Boesch and Boesch-Achermann 2000, Mitani et al. 2012, but see Mitani et al. 2010) Males remain in their natal community; females transfer communities, usually only once, as adolescents (around age 14 years; Mitani et al. 2012).

Chimpanzees breed continuously, though seasonal variation in food availability can lead to seasonality in reproduction (Boesch and Boesch-Achermann 2000, Thompson and Wrangham 2008). Females usually give birth to single infants; twins are rare (Ely et al. 2006). Chimpanzees are weaned at about 5 years of age, until which time they are considered infants, and remain close to their mothers (Boesch and Boesch-Achermann 2000). Interbirth intervals for females whose infants survive are generally about 6 years (Wallis 1995, Boesch and Boesch-Achermann 2000, Nishida et al. 2003, Thompson et al. 2007).

Chimpanzee densities estimated by line transect distance sampling to nests on eight study areas in Uganda ranged from about 1 to 2.5 per km^2 (Plumptre and Cox 2006). Recently-estimated or approximately known densities of forest-dwelling chimpanzees ranged from 0.7 to > 5 per km^2 (Mitani et al. 2010, Granjon et al. 2017, Després-Einspenner et al. 2017).

Annual mortality rates of chimpanzees are typically low, but epidemics, predation, hunting, poaching, or lethal aggression can temporarily increase them (Boesch and Boesch-Achermann 2000, Hill et al. 2001, Mitani et al. 2010, Williams et al. 2008, Muller and Wrangham 2014, Wood et al. 2017). Hill et al. (2001) combined data from five habituated communities to construct a life table for wild chimpanzees; their life table describes a slowly declining population. However, recent data from relatively undisturbed communities (the Kanyawara and Ngogo communities in Kibale National Park, Uganda; Muller and Wrangham 2014, Wood et al. 2017), showed that annual mortality rates can be considerably lower than those presented by Hill et al. (2001). Wood et al.'s (2017) life table derived from data from the Ngogo chimpanzees describes a slowly increasing population. Most studied chimpanzee populations are in fact declining, and some are declining rapidly as a result of anthropogenic impacts including disease transmission, hunting, and habitat destruction (Hill et al. 2001, Campbell et al. 2008, Köndgen et al. 2008, Muller and Wrangham 2014, Kühl et al. 2017).

5.2.2 Simulations

Infants' encounter histories are expected to be highly correlated with those of their mothers. Furthermore, relative to other age classes, infants are more difficult to individually identify in photographic data (Després-Einspenner et al. 2017), and their smaller scats are less likely to be detected during fecal DNA surveys (McCarthy et al. 2015, Granjon et al. 2017, Arandjelovic and Vigilant 2018). Historically, line transect surveys of the nests chimpanzees build have been used to estimate densities (Chapter 2); these estimates exclude infants, which do not build nests of their own (Plumptre 2000,

Kühl et al. 2008). I therefore assumed that infants will generally be excluded from SCR data to avoid uncertainty associated with lower detectability or misidentification of infants and violations of the assumption that detections of different individuals are independent, and excluded them from the simulations.

For the purposes of simulating mortality and recruitment during SCR sampling, I calculated mean annual mortality rates of chimpanzees aged ≥ 5 years, and approximated the expected number of 5 year-old recruits per individual aged ≥ 5 years (of both sexes), in slowly increasing and slowly declining populations from data presented in Wood et al. (2017) and Hill et al. (2001), respectively (Tables 5.1 and 5.2). I assumed that females of reproductive age (15 – 45 years) produce one infant every 6 years, but differences in survival rates in slowly declining vs. slowly increasing populations led to different expectations about rates of annual recruitment of 5 year-olds (Tables 5.1 and 5.2). I did not simulate additions and losses of adolescent females attributable to immigration or emigration.

I simulated SECR sampling of four different types of chimpanzee populations: demographically closed, slowly increasing, slowly declining, and more rapidly declining as a result of increased mortality (see Table 5.2). I assumed rapidly declining populations were subject to an annual mortality rate of 15% (affecting non-infants), and had recruitment rates similar to those in slowly declining populations.

Table 5.1. Approximate annual recruitment of 5-year-olds per non-infant member of standing chimpanzee populations, and the population characteristics used to calculate these recruitment rates, derived from life tables presented in Hill et al. (2001) and Wood et al. (2017).

Source	Reproductive (aged 15-45) females per individual aged ≥ 5 years	Births per reproductive female per year	Survival from birth to age 5 years	Age 5 recruits per individual aged ≥ 5 years per year
Hill et al. 2001	0.3176	0.1667	0.56	0.0296
Wood et al. 2017	0.3345	0.1667	0.79	0.0440

Table 5.2. Mortality and recruitment rates used in different simulation scenarios for chimpanzees, expressed as percentages of the standing population aged ≥ 5 years (of both sexes), derived either from life tables presented by Hill et al. (2001) and Wood et al. (2017), or, in the case of closed and rapidly declining populations, assumptions.

Type of population	Annual mortality	Annual recruitment
Demographically closed	0%	0%
Slowly increasing	2.3%	4.5%
Slowly declining	5.6%	3.0%
Rapidly declining	15%	3.0%

I generated simulated locations of activity centers of weaned chimpanzees as two-dimensional spatial Poisson point processes with intensity = 3.0 / km^2 (Fig. 5.1). The spatial extents of both the simulated populations, and the region of integration used when fitting SCR models (the "integration mesh", "mask" or "state space"), were defined as a buffer around the array of CTs, where the width of the buffer ensured all members of the population had an expected encounter rate ≥ 0.0001 on each occasion (Fig. 5.1). Specifically, I calculated buffer widths (W), in meters, as

$$W = \sqrt{\log\left(\frac{0.0001}{\lambda_0}\right) \times -2\sigma^2}$$

Animals with activity centers further than *W* from detectors would be unlikely to contribute data, so limiting the extent of the population to within *W* of detectors ensured that random removals affected individuals that might have been previously detected.

I simulated sampling at a six by ten grid of sixty CTs spaced 1.0 km apart (Fig. 5.1), over 12 monthly sampling occasions, where individuals could be detected multiple times at any trap on each occasion. I assumed encounter rate declined with increasing distance between animals' activity centers and traps according to a half normal function with scale parameter (σ) = 1300 m, which corresponds to a 95% circular home range size of 31.8 km^2. Josephine Head provided data files and analytical results from the only SCR surveys of chimpanzees that had been published at the time simulations were conducted (Head et al. 2013). There, the probability of detecting individual chimpanzees at a particular location during a 30-day sampling occasion was approximately 0.02 (though a small fraction had higher detectability as estimated from a model with individual heterogeneity modelled using a two-point finite mixture distribution). I simulated multiple scenarios in which the expected trap- and occasion-specific encounter rate of an individual with a trap placed at its activity center (λ_0) varied from 0.005 to 0.035 in increments of 0.010. There was the potential to recapture the same individuals at the same or different locations within as well as across sampling occasions. Buffer widths and therefore population extents and expected population sizes varied with λ_0 as described above (Table 5.3).

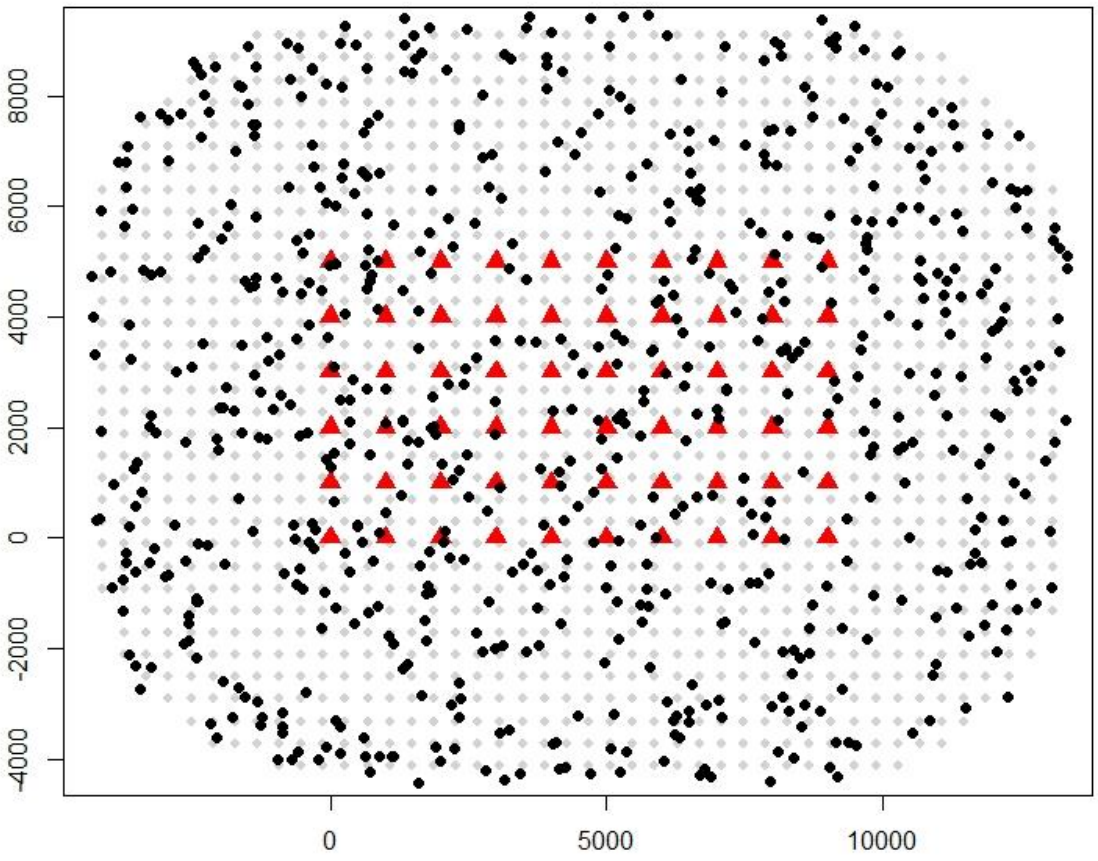

Figure 5.1. One realization of simulated activity center locations of individual chimpanzees (black dots) within the region of integration used when fitting SCR models (grey dots), aruond a 10 by 6 grid of 60 camera traps (red triangles) at 1 km spacing. Axes show distances in meters. The extents of this population and region of integration were defined as a buffer of width (W) 4320 m around the grid of traps, associated with a λ_0 value of 0.025.

Table 5.3. Buffer widths (W) associated with each value of λ_0 used to define extents of simulated populations and regions of integration, and the associated expected population size (N) at the beginning of surveys (prior to any mortality or reproduction).

λ_0	W (m)	Extent (km^2)	Expected N
0.005	3636	190.6	572
0.015	4115	213.3	640
0.025	4320	224.3	673
0.035	4450	233.6	701

I initially generated 4000 populations and sampled 1000 populations at each value of λ_0 to generate data from closed populations. Subsequently, to generate data

sets affected by mortality and recruitment during sampling, I (1) randomly selected 2.3%, 5.6% and 15% of the individuals in each population for removal, randomly assigned each of them a sampling occasion for removal, and censored their capture data from that and all subsequent occasions; (2) generated populations of recruits at 4.5% and 3.0% of the expected density of 3.0 animals per km^2, sampled them as I did the original population, censored capture data prior to a randomly-selected occasion of recruitment, and appended their encounter histories to the appropriate data sets for slowly increasing, slowly declining, or rapidly declining populations. Finally, I subset each data set to include only the first 6 sampling occasions to generate data sets from 6-month surveys. In total I generated 32 000 data sets (4 values of λ_0 × 4 types of populations [including closed] × 2 study durations × 1000 replicate iterations).

I fit one SECR model with a half-normal encounter rate function, such that $\lambda(d) = \lambda_0 \exp(-d^2 / 2\sigma^2)$, to each data set, and recorded estimates of λ_0 ($\hat{\lambda}_0$), σ ($\hat{\sigma}$), and density ($\widehat{D}$), and calculated percent relative bias (PRB) of each parameter, as PRB = (estimated value – true value) / true value × 100%. We present mean percent relative bias (MPRB) of $\hat{\lambda}_0$, $\hat{\sigma}$, and MPRB and confidence interval (CI) coverage (α = 0.05) of $\widehat{D}$ relative to true densities at both the beginning and the end of the surveys.

5.2.3 Tests of the closure assumption in CR data

For 100 of 1000 data sets for each species and scenario, we performed tests for violation of the assumption of demographic closure in non-spatial CR data described by Otis et al (1978, p. 66 and Appendix K p. 120) and Stanley and Burnham (1999), and recorded the number of times the null hypothesis of demographic closure was rejected at an alpha level of 0.05.

Analyses were performed in R version 3.4.2 (R Core Team 2017) using functions included with the 'secr' package (version 3.1.3; Efford 2017).

5.3 Results

5.3.1 Tests of the closure assumption in CR data

Tests for violations of the assumption of demographic closure in CR data were unreliable. Otis et al.'s (1978) test had low power to detect closure violation of the magnitudes we simulated (Table 5.4). Stanley and Burnham's (1999) test tended to fail to reject the null hypothesis with smaller data sets, and to reject it with larger ones, although it was also slightly more likely to reject where closure violation was more severe (Table 5.4).

Table 5.4. The number times tests rejected the null hypothesis of demographic closure ($P < 0.05$) in simulated data from chimpanzees at camera traps (of 100 tests at each value of λ_0 and type of population change).

	6-month surveys				12-month surveys			
λ_0	Closed	Slow increase	Slow decline	Rapid decline	Closed	Slow increase	Slow decline	Rapid decline
Test of Otis et al. (1978)								
0.005	6	6	6	5	8	9	7	8
0.015	7	8	7	7	3	3	1	3
0.025	7	7	7	7	3	7	6	11
0.035	6	6	7	6	8	8	9	12
Test of Stanley and Burnham (1999)								
0.005	5	5	5	4	7	7	7	5
0.015	5	4	4	6	7	10	9	11
0.025	5	5	5	5	18	18	23	36
0.035	5	4	6	9	47	59	61	69

5.3.2 Simulations

At the lowest value of λ_0 we simulated (0.005 monthly), I obtained small samples of recaptures (means of 5 and 20 total recaptures of 52 and 94 detected animals from 6- and 12-month surveys, respectively), so I suspected results might not be reliable even where the closure assumption was met. For example, λ_0 was overestimated and σ severely overestimated from 6-month surveys. Distributions of $\widehat{D}$ were skewed right, and MPRB was strongly affected by relatively rare cases where $\widehat{D}$ was much higher than true densities, so I present median PRB (instead of mean PRB [MPRB] as presented elsewhere) of $\widehat{D}$ from simulations with $\lambda_0 = 0.005$ here, separately from other results. Median $\widehat{D}$ from different types of populations and survey durations ranged from 3.0 – 3.2 animals / km^2, similar to true densities at the beginning of the surveys. However, where surveys were conducted over 6 months, $\widehat{D}$ was highly variable (median absolute PRB was 31% from all types of populations), and imprecisely estimated (median

coefficients of variation of $\widehat{D}$ were 0.46 or 0.47). Results improved where surveys were conducted over 12 months, but bias was still apparent and there was considerable variability among iterations even when populations were demographically closed (median absolute PRB was 2.7%, 5.6%, 2.6%, and 0.21% relative to true densities at the beginning of the surveys from closed, slowly increasing, slowly declining, and rapidly declining populations, respectively). I deemed these results potentially indicative of small sample size rather than violations of assumptions, so hereafter I present results only from simulations that assumed higher encounter rates (λ_0 = 0.015, 0.025, or 0.035 monthly).

At values of $\lambda_0 > 0.005$, MPRB of $\widehat{D}$ of closed populations was < 2%, and CI coverage was > 95% (Fig. 5.2, Table 5.5). In slowly increasing and slowly declining populations, $\widehat{D}$ overestimated *D* by 0.4 – 4.4%, and CI coverage remained ≥ 93%, regardless of whether we compared estimates to true densities at the beginning or the end of the surveys, or whether surveys were conducted over 6 or 12 months (Fig. 5.2, Table 5.5).

$\widehat{D}$ of rapidly declining populations underestimated true densities at the beginning of the surveys only slightly, and CI coverage was > 90% (Fig. 5.2, Table 5.5). However, $\widehat{D}$ more severely overestimated true densities of these populations at the end of the surveys. MPRB was 5.0 – 6.5% after 6-month surveys, and 10.5 – 12.5% after 12-month surveys (Fig. 5.2). CI coverage was less than nominal, lower when surveys spanned 12 rather than 6 months, and lowest, falling to 53%, where λ_0 was highest and hence densities were estimated with the greatest precision, though inaccurately (Table 5.5).

MPRB of $\hat{\lambda}_0$ from closed populations was consistently positive, < 2.5% at all values of λ_0 and both survey durations, and ≤ 1.0% from 12-month surveys (Table 5.6). Where the closure assumption was violated, we observed increasing negative bias at higher values of λ_0, and at greater magnitudes of closure violation, but absolute MPRB was always < 5% (Table 5.6). There was a slight tendency for $\hat{\sigma}$ to underestimate σ, likely because the extent of the region of integration was not large enough to allow for the presence of activity center locations of animals with expected encounter rates < 0.0001, except where negative bias in λ_0 was most severe, in which cases σ was slightly overestimated (Table 5.7).

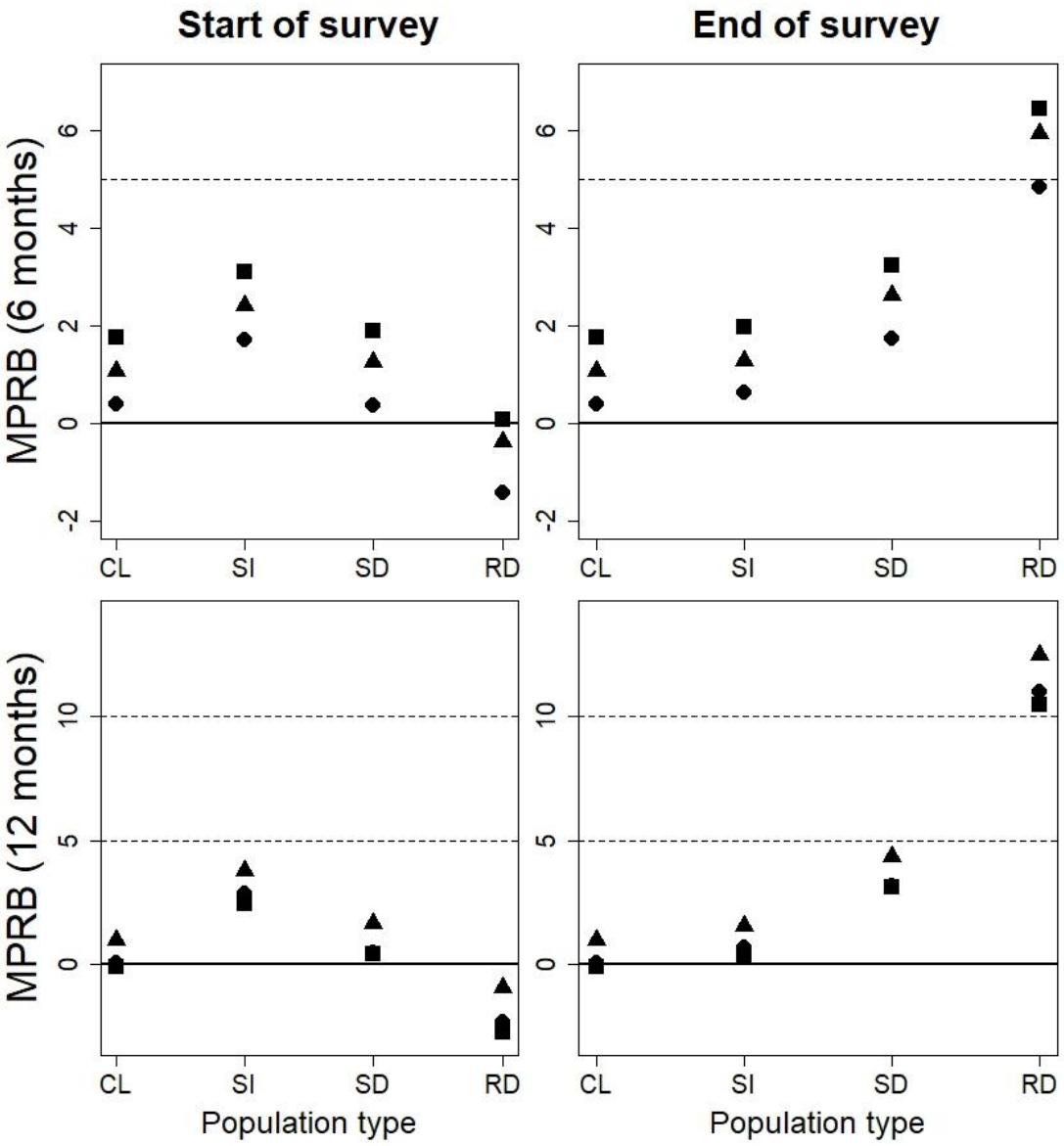

Figure 5.2. Mean percent relative bias (MPRB) of estimated chimpanzee densities relative to true densities at the beginning (left) and at the end (right) of simulated surveys conducted over 6 months (top) and 12 months (bottom). Population types are demographically closed (CL), slowly increasing (SI), slowly decreasing (SD), and rapidly decreasing (SD). Squares, circles, and triangles show results from simulations assuming monthly λ_0 of 0.015, 0.025, and 0.035, respectively. I added a heavy horizontal line where MPRB = 0, and dashed horizontal line at MPRB = 5% and 10%, for the sake of visualization.

Table 5.5. Confidence interval coverage of estimated densities relative to true densities at the beginning and end of the surveys, across 1000 iterations for each type of population, survey duration, and value of λ_0, from simulated photographic spatial capture–recapture surveys of chimpanzees.

Coverage of true densities at the beginning of the surveys								
	6-month surveys				12-month surveys			
λ_0	Closed	Slowly increasing	Slowly declining	Rapidly declining	Closed	Slowly increasing	Slowly declining	Rapidly declining
0.015	0.96	0.96	0.95	0.94	0.97	0.96	0.96	0.94
0.025	0.96	0.97	0.96	0.93	0.97	0.96	0.96	0.91
0.035	0.98	0.97	0.97	0.94	0.98	0.96	0.98	0.92
Coverage of true densities at the end of the surveys								
	6-month surveys				12-month surveys			
λ_0	Closed	Slowly increasing	Slowly declining	Rapidly declining	Closed	Slowly increasing	Slowly declining	Rapidly declining
0.015	0.96	0.96	0.95	0.94	0.97	0.97	0.96	0.81
0.025	0.96	0.97	0.96	0.92	0.97	0.97	0.96	0.66
0.035	0.98	0.97	0.96	0.88	0.98	0.98	0.93	0.53

Table 5.6. Mean percent relative bias in λ_0, across 1000 iterations for each type of population, survey duration, and value of λ_0, from simulated photographic spatial capture–recapture surveys of chimpanzees.

	6-month surveys				12-month surveys			
λ_0	Closed	Slowly increasing	Slowly declining	Rapidly declining	Closed	Slowly increasing	Slowly declining	Rapidly declining
0.015	2.45	1.73	1.69	0.75	1.01	-0.36	-0.86	-2.72
0.025	1.50	0.70	0.64	-0.26	0.96	-0.65	-1.01	-3.23
0.035	1.00	0.34	0.07	-0.87	0.36	-1.22	-1.67	-4.13

Table 5.7. Mean percent relative bias in σ, across 1000 iterations for each type of population, survey duration, and value of λ_0, from simulated photographic spatial capture–recapture surveys of chimpanzees.

	6-month surveys				12-month surveys			
λ_0	Closed	Slowly increasing	Slowly declining	Rapidly declining	Closed	Slowly increasing	Slowly declining	Rapidly declining
0.015	-0.099	-0.056	-0.113	-0.256	-0.021	0.012	-0.013	-0.060
0.025	-0.179	-0.161	-0.145	-0.173	-0.260	-0.225	-0.179	-0.192
0.035	-0.225	-0.229	-0.207	-0.236	-0.027	0.021	0.071	0.122

5.4 Discussion

Our ability to understand, conserve, and manage wildlife often relies on the reliability of information derived from statistical models for estimating population parameters from observational data. Violations of the assumptions these models rely on can lead to flawed information being provided to decision-makes or funding agencies. Results of the simulations presented here indicate that in approximately stable (slowly increasing or declining) chimpanzee populations, rates of mortality and recruitment are low enough that infrequent violation of the assumption of demographic closure induces only slight bias, and confidence interval coverage remains approximately nominal, even when sampling spans 12 months. This is reassuring because the assumption of demographic closure can rarely be validated and is likely often violated to some extent during field surveys. These results are consistent with real data from chimpanzee communities of known size and density presented by Head et al. (2013) and Després-Einspenner et al. (2017), where violations of the closure assumption were known to have occurred, but closed-population SECR models yielded accurate abundance estimates. They are also consistent with recommendations recently published in a review of genetic methods for monitoring primates (Arandjelovic and Vigilant 2018), and the only prior simulation study of effects of closure violation on SECR estimates of abundance (Dupont et al. 2019); both of these articles recommended increasing SECR survey durations for long-lived species because the benefits of improved precision were expected to exceeded adverse effects of bias arising from violation of the assumption of demographic closure.

However, I showed that where populations were declining more rapidly as a result of elevated mortality, density at the end of the surveys was overestimated,

sometimes severely, and true densities at the end of the surveys were often not within the 95% CI of the estimates. The conservation status of most chimpanzee populations is precarious (Walsh et al. 2003, Campbell et al. 2008, IUCN 2017), so the consequences of positive bias in estimated abundance are potentially severe. Consider a single survey of a small and declining population: inference would be that the population is larger and more viable than it is, potentially leading to the decision that conservation interventions were not immediately necessary. Similarly, consider a population for which an accurate, prior abundance estimate is available, but the mortality rate has recently increased, for example due to disease outbreaks, predation, or industrial expansion into previously inaccessible habitat (Boesch and Boesch-Achermann 2000, Laporte et al. 2007). Comparing an overestimate of density obtained while the population was declining to an accurate one obtained when the population was stable could lead to the incorrect inference that the new risk factor did not cause a population decline. Surveys are labour-intensive and time-consuming (Head et al. 2013, Després-Einspenner et al. 2017, Arandjelovic and Vigilant 2018), so it might not be practical to conduct them frequently. This exacerbates the potential negative impacts of flawed inference from a single survey during which the population was declining. Many chimpanzee populations are undergoing or have undergone rapid decline as a result of human activities (Huijbregts et al. 2003, Walsh et al. 2003, Campbell et al. 2008, Hicks et al. 2010, IUCN 2017, Kühl et al. 2017), so there is real potential for declining populations to be surveyed.

I suspect that these results are generalizable to SECR studies of other long-lived species with low detection probabilities or encounter rates and slow rates of population turnover. For example, surveys of felids frequently must be conducted over long time

intervals to yield sufficient data to estimate abundance (Trolle and Kéry 2003, Gardner et al. 2010, Negrões et al. 2010, Jedrzejewski et al. 2017). The results are not relevant to species with faster rates of population turnover, such as small mammals, where closure violation might be severe even from rapid surveys of stable populations. Furthermore, I did not investigate whether violation of the closure assumption could affect the data in ways that could be confounded with heterogeneity in encounter rates or probabilities of detection. If closure violation caused some individuals to have apparently lower encounter rates than others, individual heterogeneity might be supported by model selection criteria even if detection probabilities were actually similar across individuals. Including this effect in estimating SECR models would inflate density estimates futher.

I simulated data collection differently than Dupont et al. (2019). They simulated data collection in continuous time or during a single survey; we simulated surveys with temporally discrete sampling occasions. Both routines randomly determined whether and when animals survived or reproduced, but Dupont et al. (2019) then used the amount of time each animal was present in the population to calculate its total detection probability over the duration of the survey. I suggest that my simulation routine, where animals were added and removed via random trials and could only be detected if present, provided similar realism with respect to the effects of both population membership and detectability on the data collected. My simulations may lack the temporal resolution they were able to achieve, because I did not simulate additions or removals within occasions, rather, animals were instantaneously added or removed between occasions. The similarity between their results for "slow-living" species and mine indicates that differences in the ways simulated data were generated did not affect

inferences. Dupont et al. (2019) did not simulate surveys of populations that were systematically declining due to elevated mortality, or compare estimates to true abundances at the end of the surveys, so they could not have detected the potential for bias to mask declines.

There are several options available to researchers in situations where it is not feasible to increase sampling resources to obtain sufficient data from short term studies that minimize closure violations. One is to apply the robust design, where the same population is surveyed repeatedly over a long time period (e.g. years), but each survey is short enough that the assumption of demographic closure is reasonable within surveys (Kendall et al. 1995). This method allows the estimation of survey-specific (time-specific) abundance, as well as rates of additions and losses between surveys (provided that animals are recognizable across as well as within surveys). Alternatively, if populations are sampled continuously, the data can subsequently be separated into distinct temporal "sessions" (see Jedrzejewski et al. [2017] for an example). Different models can then be fitted to evaluate relative support for, e.g., session-specific abundance, constant abundance over the duration of the survey, or temporal covariates of abundance across sessions. With this approach, animals need not be recognizable across sessions, because data from each session are treated as independent. Strictly, sessions may not be independent because the same animals are likely to be detected during more than one session, but this may be of less concern population closure during sampling.

A third option is to avoid the assumption of demographic closure, and estimate abundance using open population models. Methods and software for estimating abundance of open populations by spatial capture–recapture are currently undergoing

rapid development (Gardner et al. 2010, 2018, Augustine 2019, Efford 2019, Glennie and Borchers 2019, Glennie et al. 2019). My results indicate that to avoid bias, it may be preferable to avoid the assumption of demographic closure where (1) violations are potentially severe, (2) populations could decline by up to 10% during sampling, or (3) rates of additions and losses, as well as abundance, are of interest.

Chapter 6: Photographic Spatially Explicit Capture–Recapture Surveys of Chimpanzees at the Landscape Scale

6.1 Introduction

Head et al. (2013) demonstrated that the combination of camera trapping, identification of individual chimpanzees by trained human observers, and spatially explicit capture–recapture (SECR) analysis could yield accurate and reasonably precise estimates of chimpanzee density. Sampling was spatially intensive, with up to 45 cameras deployed across a 60 km^2 study area (Head et al. 2013), such that most individuals present on the study area would have had opportunities to encounter many traps during the course of normal movements within their territories. Most individuals were detected multiple times, including at more than one location, providing abundant information to estimate the relatively small number of animals that went undetected (Head et al. 2013). Camera trapping is appealing to great ape researchers because it is less labour intensive than other sampling methods (Pebsworth and LaFleur 2014), and avoids the costs of molecular analyses to identify individuals from fecal DNA samples (Arandjelovic and Vigilant 2018). However, the question remains whether this combination of methods can be effectively applied over large areas, i.e., at the landscape scale as opposed to the scale of one or a few chimpanzee territories.

Uganda, East Africa, is home to several disjunct populations of eastern chimpanzees (*Pan troglodytes schweinfurthii*; Plumptre and Cox 2006), including some in fragmented habitat shared with dense human populations (McCarthy et al. 2015), but Uganda's National Parks and other protected areas represent strongholds for eastern

chimpanzee conservation and research (Plumptre and Cox 2006). Kibale National Park (KNP) in western Uganda protects nearly 800 km^2 of tropical forest, bushland, grassland, and wetland, much of which is occupied by eastern chimpanzees, but the current size of the population isolated within this park is unknown. Two communities (stable social groups) of chimpanzees in KNP have been habituated to the presence of humans to facilitate research (Potts et al. 2009), and more are habituated or undergoing habituation for research or tourism purposes. A fecal genetic survey of much of the park is ongoing, with results already published for the habituated Ngogo community (Granjon et al. 2017). KNP is therefore an ideal location to evaluate and compare methods for estimating chimpanzee abundance at large spatial scales.

SECR models take advantage of the fact that animals that spend more time near detectors are more likely to be detected, and estimate detection probabilities or encounter rates as a function of the distance between animals' activity centers and detectors (Efford 2004, Borchers and Efford 2008, Borchers 2012). A simple SECR model (one ignoring heterogeneity in detectability, movements, or density) has only three parameters: animal density, and the magnitude and scale of a half-normal detection probability or encounter rate function (Efford 2004, Borchers and Efford 2008, Efford et al. 2009a, b). Camera traps (CTs) can record multiple, identifiable, independent observations of the same individual at the same location between visits by researchers, so I focus on encounter rate functions rather than detection probability functions here. The magnitude or intercept of such a function is denoted λ_0, and describes the trap- and occasion-specific encounter rate of an animal with a detector located at its center of activity. The scale parameter, denoted σ, describes the rate at which detectability declines from λ_0 towards zero, and for a half normal encounter rate

function it can be converted to an estimate of the radius of a 95% circular bivariate normal home range (r) as $r = \sqrt{-2\log(1-p)} \times \sigma$, with $p = 0.95$. The expected radius of a circular 95% home range is therefore approximately 2.45σ, so it is often convenient to describe detector spacing in SECR surveys as a function of expected home range size or σ.

SECR offers considerable flexibility with respect to sampling design. Detectors need not be placed at randomly-selected locations, and can employ baits or lures and target habitat features known to be used by the animals to increase encounter rates. Furthermore, unlike nonspatial CR, it is not necessary to expose all members of the population of interest to a risk of detection (Efford 2004). Arrays of detectors can therefore be of almost any spatial configuration, and can include gaps larger than the home range size of the species under investigation. However, not all designs will yield the data required to fit SCR models, and some designs are more efficient than others (Sollmann et al. 2012, Sun et al. 2014, Wilton et al. 2014, Clark 2019). Minimally, field surveys must detect at least some of the same individuals more than once (recaptures) including at different locations (spatial recaptures). All detections inform λ_0 and activity center locations; spatial recaptures further inform σ. If most detected individuals are detected only once, estimated encounter rates will be low and imprecise, inference is that a large and uncertain number of animals went undetected, and so density estimates also will be imprecise. If most animals are detected at only one location there is little information to inform σ and therefore density. Therefore, SECR surveys should be designed to provide abundant opportunities to detect the same animals more than once, including at more than one location. Spatially intensive sampling (with closely-spaced detectors) increases sample sizes of recaptures and

spatial recaptures, and hence precision (Sollmann et al. 2012, Wilton et al. 2014, Després-Einspenner et al. 2017, Clark 2019, Efford and Boulanger 2019). However, the resulting estimates are specific to areas in the vicinity of detectors, so unless density can be assumed to be constant over the entire area of interest, it is also important to obtain a representative sample of that area (Wilton et al. 2014, Clark 2019). There is therefore a direct trade-off between spatial sampling intensity and the total extent of the array of detectors. With a fixed number of detectors, one can only be increased by reducing the other. Larger arrays with wide detector spacing expose more animals to a risk of detection, providing greater representativity. Close detector spacing provides more opportunities for spatial recaptures, but the number of animals detected will be a smaller sample of the population of interest. Fortunately, the expected home range size of the species under investigation imposes a lower limit on the total extent of the array, and an upper limit to the spacing between adjacent traps; these can form the starting point of the spatial design of an SECR survey.

The minimum extent of an area searched to collect SECR data was investigated by Efford (2011) and Marques et al. (2011). Both concluded that for SECR models to perform well, the area surveyed should be at least as large as one home range of the species under investigation. Noss et al. (2012) and Tobler and Powell (2013) similarly recommended that arrays of detectors should be at least as large as the area animals may cover during regular movements during the survey. Applying these recommendations to group-living, territorial chimpanzees would lead to a recommendation that the entire array be as large as, or larger than, the expected territory size (also see Després-Einspenner et al. 2017).

The trade-off between detector spacing and array extent was explored in detail in the context of hair-snagging surveys of American black bears (Sollmann et al. 2012, Sun et al. 2014, Wilton et al. 2014, Clark 2019). Analyses of simulated and real data sets yielded several generalizable conclusions. For example, when adjacent traps were spaced > 3.5σ apart, samples of spatial recaptures were small even where encounter rates were high; density was often inestimable, and where it was estimable, confidence interval coverage was less than nominal even though estimates were imprecise (Sollmann et al. 2012, Sun et al. 2014, Clark 2019). Designs with traps spaced 2.5σ to 3σ, or more than a home range radius, apart, were effective only when animal densities or encounter rates were relatively high; at lower densities or encounter rates, designs with traps spaced σ to 2σ, or approximately half a home range radius, apart, performed best (Sollmann et al. 2012, Sun et al. 2014, Wilton et al. 2014, Clark 2019).

If all detectors were spaced σ to 2σ, apart (e.g. in a continuous, regular grid), the number of detectors required to sample large areas could quickly become prohibitive. Fortunately, the developers of SECR models have long recognized the potential of clustered designs for obtaining representative samples over large study areas while keeping some detectors close enough together to provide spatial recaptures (Efford et al. 2005, Borchers and Efford 2008, Efford and Fewster 2013). Randomizing sampling locations, for example by taking a random sample (without replacement), or a spatially representative random sample, of locations across the area of interest, or by superimposing a systematic grid with random origin over it, provides a spatially representative sample of that area (Buckland et al. 2001, Stevens and Olsen 2004, Efford and Fewster 2013). For a clustered SECR design, locations of centroids can be distributed randomly throughout the region of interest to ensure representativity, but

individual detectors within clusters can be tightly spaced to provide opportunities for spatial recaptures and can use baits or lures and target habitat features known to be used by the animals to increase encounter rates. Clusters can, but need not be, spaced far enough apart to ensure that individuals would be detected at only one cluster, and hence that different clusters can be treated as independent samples (Efford and Fewster 2013).

Evaluations of SECR survey designs for black bears demonstrated that clustered designs, with detectors spaced optimally as described above within clusters, but much wider spacing between clusters, were the most efficient and effective approach to sampling over large areas (Sun et al. 2014, Wilton et al. 2014, Clark 2019). Where density varied in space beyond what would be expected if activity centers were homogeneously Poisson-distributed, designs with more, smaller clusters provided more representative samples and therefore a greater probability of obtaining an accurate estimate of mean density across the study area (Clark 2019). However, if individuals are expected to be detected at only one cluster, Sun et al. (2014) recommended a minimum of four detectors per cluster, and the above-cited recommendations that arrays be as large as home ranges would then apply to individual clusters. Combined, these recommendations imply that there should be many clusters distributed throughout the region of interest, but also that each cluster should include traps spaced σ to 2σ apart and have an extent larger than the expected home range size. Designs that follow all of these recommendations might be only slightly more efficient than more regular arrays with similar spacing between most detectors, and therefore difficult and costly to implement. I sought more efficient designs.

To evaluate the potential of photographic SECR for monitoring chimpanzees over large spatial scales, I simulated SECR surveys of eastern chimpanzees, designed

and helped to implement a camera trapping survey of eastern chimpanzees in KNP in collaboration with Samuel Angedakin (hereafter "SA", who at the time was a PhD candidate at Makerere University and manager of the Ngogo Chimpanzee Project, and lived and worked full-time in KNP). I also analyzed SECR data from a subset of CTs deployed within the territory of an habituated community of known size with approximately known territory boundaries.

6.2 Methods

6.2.1 Background information

Chimpanzees live in stable social groups of between 10 and 200 animals, termed communities (Mitani et al. 2012). Community members share a common territory, which is also relatively stable over time (Boesch and Boesch-Achermann 2000, Mitani et al. 2012, but see Mitani et al. 2010). I therefore expected that real chimpanzee activity centers would be clustered near territory centers, rather than Poisson-distributed. If all community members used the entire territory, the expected home range size of individuals would equal the expected territory size, which could then be used to inform the design. All members of some chimpanzee communities do use the entire territory (Boesch and Boesch-Achermann 2000, Mitani et al. 2012), however, reproductive females (pregnant females and those accompanied by offspring < 5 years of age, hereafter "mothers") of the eastern subspecies, including those in KNP, are less gregarious and usually remain within smaller home range core areas (Chapman and Wrangham 1993, Thompson et al. 2007, Kahlenberg et al. 2008, Mitani et al. 2010, Mitani et al. 2012). It was therefore necessary to design the survey with detector spacings appropriate to social classes with different home range sizes. Gregariousness

increases encounter rates at camera traps (Treves et al. 2010), and female central chimpanzees (*Pan troglodytes troglodytes*) in Gabon had lower detection probabilities than males (Head et al. 2013), so we expected that eastern chimpanzee mothers would have lower λ_0 and possibly much lower σ than other age-sex classes, and would therefore be the most problematic fraction of the population to sample.

I reviewed published estimates of home range and territory sizes of eastern chimpanzees of different social classes in forested habitats to identify potentially effective within- and between-cluster detector spacings. Prior research in KNP revealed that territory sizes range from about 10 km^2 to nearly 40 km^2, and mothers' home range core areas could be as large as 9 km^2 or as small as 1.3 km^2 (Chapman and Wrangham 1993, Thompson et al. 2007, Kahlenberg et al. 2008, Mitani et al. 2010). Assuming circular bivariate normal home ranges, expected σ for animals that use the entire territory ranged from about 725 m to 1500 m, but expected σ for reproductive females ranged from only 260 m to 700 m (Table 6.1).

Table 6.1: Sizes of eastern chimpanzee territories, and of eastern chimpanzee mothers' home range core areas, in forested habitats, and associated expected radii, half radii, and σ of a half-normal encounter rate function, assuming circular bivariate normal home ranges.

Territories shared by communities			
Size (km^2)	Expected radius (m)	Expected radius / 2 (m)	Expected σ (m)
40	3568	1784	1456
25	2820	1410	1151
10	1784	892	728
Home ranges of individual mothers			
Size (km^2)	Expected radius (m)	Expected radius / 2 (m)	Expected σ (m)
8	1596	798	651
4	1128	564	461
1.5	690	345	282

6.2.2 Simulations

Given the lack of similar prior surveys and considerable uncertainty regarding home range sizes, simulations were intended to address the question of whether photographic SECR could feasibly be used to monitor chimpanzees over large areas, rather than to identify an optimal design. When simulating SECR surveys, various characteristics of the survey design, the population, and the sampling process could vary or have associated uncertainty, and their effects on the data collected and the accuracy and precision of estimates of density interact, so the number of scenarios of interest can quickly become very large (Sollmann et al. 2012, Wilton et al. 2014, Sun et al. 2014, Clark 2019, Dupont et al. 2019). Furthermore, fitting SECR models is time-consuming, but the effectiveness of different design strategies in the presence of uncertainty can be evaluated relatively quickly by simulating only data collection and comparing sample sizes of animals, recaptures, and spatial recaptures (Efford and Boulanger 2019).

I simulated sampling of eastern chimpanzee mothers at CTs deployed according to clustered designs. I assumed one hundred CTs were available to sample a square

region of interest covering nearly 2000 km^2 for twelve months. The CTs were always deployed in twenty clusters of five CTs each (because more clusters improve representativeness but each cluster should include at least four traps, as described above), but distances between CTs within clusters and the minimum distance between cluster centroids varied. I emphasized close trap spacing within clusters to increase the probability of detecting mothers at more than one location. I expected that other age sex classes that use most or all of the territory would be detected more frequently than mothers, and would sometimes be detected at different clusters, and therefore that designs focussed on obtaining adequate data from mothers should also provide adequate data from other social classes. Simulation scenarios are described in more detail below.

Populations

Recently-estimated or approximately known densities of forest-dwelling chimpanzees ranged from 0.7 to > 5 per km^2 (Mitani et al. 2010, Granjon et al. 2017, Després-Einspenner et al. 2017). I assumed a density of 3.0 weaned animals / km^2, and calculated that adult females make up approximately one third of weaned individuals from published life tables (Hill et al. 2001, Wood et al. 2017); most adult females would be either pregnant or accompanied by infants at any given time (Wood et al. 2017), so I simulated populations of mothers at a density of 0.8 / km^2. I generated randomly-located activity centers of chimpanzee mothers at this density within a 44 × 44 km square region of interest (area = 1936 km^2, expected population size [N] = 1549). I initially considered two types of spatial distributions of activity center locations: (1) a homogeneous spatial Poisson point process, (2) an inhomogeneous Poisson point process where density varied from zero to double the expected mean density according

to a sine curve in the x- and y-directions, resulting in clusters of activity centers. I simulated three different cluster spacings corresponding to three assumptions regarding territory size (Table 6.1, Fig. 6.1).

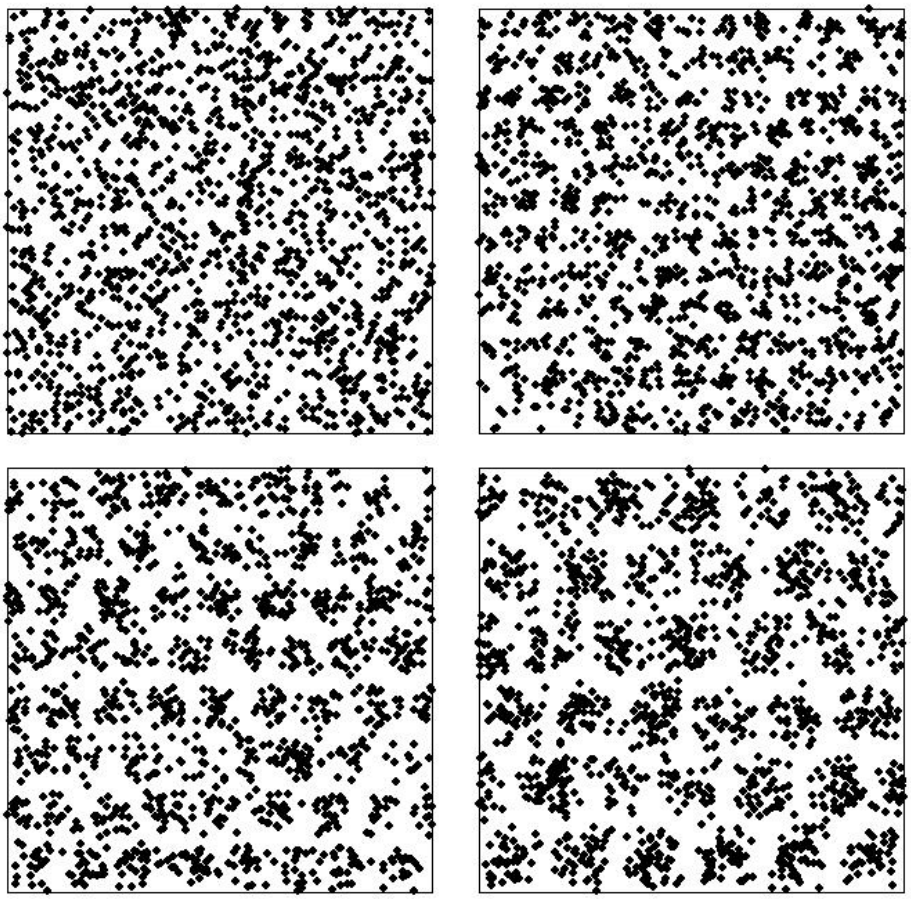

Figure 6.1. Examples of randomized activity center locations at an expected density of 0.8 per km^2. Top-left: Poisson-distributed; top-right assumes clustered activity centers within territories 10 km^2 in size, so we expect 12 territories in each of the x- and y-directions; bottom-left assumes territory size = 25 km^2 (expect 8 × 8 territories); bottom-right assumes territory size = 40 km^2 (6 × 6 territories). Bounding squares are 44 × 44 km regions of interest.

Detector layouts

I considered two cluster shapes and three within-cluster detector spacings for a total of six different cluster geometries. Shapes were crosses with a central CT and four peripheral CTs (one in each of the cardinal directions), and lines. Detector spacing within clusters was 345 m, 564 m, or 798 m, corresponding to half the expected radii of mothers' home range core areas (Table 6.1).

Locations of centroids of clusters of CTs were selected as random samples without replacement from grids of points distributed within a 40 km × 40 km square centered within the region of interest. Grids describing possible locations of cluster centroids were smaller than the region of interest to ensure that peripheral detectors fell within that region. I used two different grid point spacings for cluster centroids: 1 km, such that some clusters would be close together and could even overlap slightly (Fig. 6.2), and 4 km, which distributed clusters more evenly throughout the region of interest and ensured that they did not overlap (Fig. 6.3).

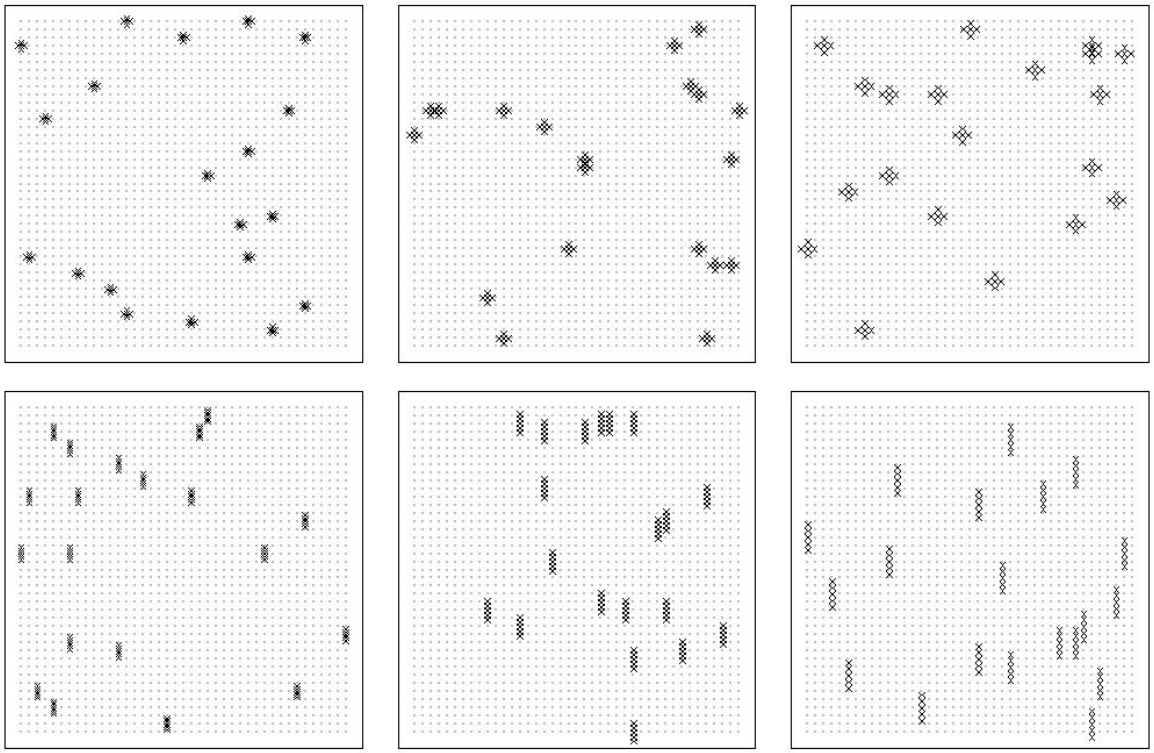

Figure 6.2. Examples of randomized detector layouts (each detector appears as a black "×"), where potential locations of cluster centroids (grey dots) were 1 km apart. Cross-shaped clusters are shown across the top, lines across the bottom, and within-cluster detector spacings increase from 282 m at left, to 564 m in the center and 798 m at right. Bounding squares are 44 × 44 km regions of interest.

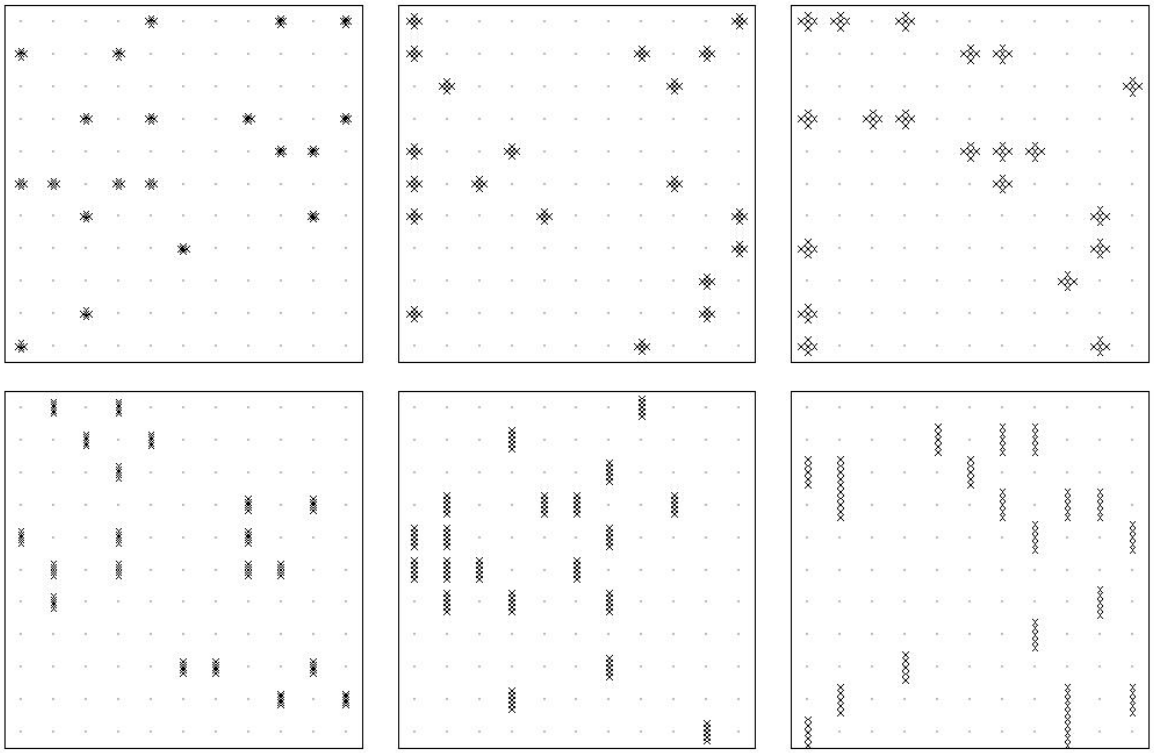

Figure 6.3. Examples of randomized detector layouts (each detector appears as a black "×"), where potential locations of cluster centroids (grey dots) were 4 km apart. Cross-shaped clusters are shown across the top, lines across the bottom, and within-cluster detector spacings increase from 282 m at left, to 564 m in the center and 798 m at right. Bounding squares are 44 × 44 km regions of interest.

Simulating detections

I simulated sampling assuming that the expected encounter rate decreased with increasing distance between activity centers and detectors, such that $\lambda(d) = \lambda_0 \exp(-d^2 / 2\sigma^2)$, where d is distance (in meters), λ_0 is the expected number of detections of animals at detectors placed at their activity center (at distance 0), and $\lambda(d)$ is the expected number of detections of animals at detectors d meters from their activity center. Individuals could be recaptured at the same location within as well as across sampling occasions. Josephine Head provided data files and analytical results from the only photographic SECR survey of chimpanzees published prior to implementation of the survey of KNP (Head et al. 2013). There, the probability of detecting most

individual female chimpanzees at a detector coincident with their activity center (g_0) during a 30-day sampling occasion was approximately 0.020, but approximately one third of females had detection probabilities closer to 0.080 (as estimated from an SECR model with individual heterogeneity modelled using a two-point finite mixture distribution). These detection probabilities can be converted (Efford and Boulanger 2019) to monthly encounter rates of 0.020 and 0.0833. In the absence of other information about encounter rates of chimpanzees at CTs I assumed an expected monthly encounter rate for animals with detectors placed at their activity centers (λ_0) of 0.05 in all simulations. I considered three different values for σ (282 m, 461 m, and 651 m) corresponding to expected σ of circular bivariate normal home ranges of eastern chimpanzee mothers (Table 6.1).

Scenarios

I simulated sampling over twelve monthly occasions using every combination of the three types of clustered populations, the six cluster geometries, the two minimum distances between cluster centroids, and the three values of σ (108 scenarios, 36 per population type). I simulated only twelve scenarios with homogeneously Poisson-distributed populations because although a comparison of results from these and clustered populations was of interest, detailed results for homogeneously Poisson-distributed populations were not. Simulations with homogeneously Poisson-distributed populations crossed all cluster geometries with both distances between centroids, but σ was fixed at 461 meters.

I conducted 1000 replicates of each scenario, generating a new set of activity center locations and selecting new centroids for clusters of CTs for each replicate. I

recorded the number of animals detected (*n*), numbers of recaptures and spatial recaptures, and calculated the mean number of detections per animal ("DPA", as detections / *n*), and the fraction of the total population detected (*n* / *N*), during each replicate.

Criteria for successful surveys

Prior evaluations of spatial SECR survey designs provided clear recommendations regarding maximum detector spacing and minimum cluster or array extent, and demonstrated that where trap spacing is appropriate to inform σ and the expected density does not vary in space, precision is largely a function of numbers of recaptures or detections per animal (Efford 2011, Marques et al. 2011, Sollmann et al. 2012, Sun et al. 2014, Wilton et al. 2014). However, they did not identify minimum numbers of recaptures, spatial recaptures, or DPA for reliable inference, or an optimal trade off between either *n* or the fraction of population sampled, which increase with detector spacing, and the number of movements or DPA, which vary inversely with detector spacing. To facilitate comparisons across a large number of scenarios, I developed criteria for minimum sample sizes of recaptures, movements, and DPA to meet different objectives (Table 6.2). These criteria were derived from the studies of SECR survey design cited above, simulation studies published after the survey of chimpanzees in KNP had been designed and implemented (Clark 2019, Efford and Boulanger 2019), analyses of subsets of a large photographic SECR data set from chimpanzees in Taï National Park, Ivory Coast (Després-Einspenner et al. 2017), reviews of published SECR analyses of data from long-lived species (Chapters 2 and 5), and my own experience fitting SECR models to simulated and real data sets, including

sparse data sets, and data from chimpanzees (e.g. Chapter 5, Obbard et al. 2010, Howe et al. 2013, McCarthy et al. 2015, Després-Einspenner et al. 2017).

Table 6.2. Minimum sample sizes of recaptures, spatial recaptures, and mean detections per animal (DPA) to meet different objectives by fitting spatially explicit capture–recapture (SECR) models.

	Recommended minima		
Objectives	Total recaptures	Spatial recaptures	DPA
Estimate density from a model with constant density, λ_0, and σ.	10	5	1.1
Estimate density with reasonable precision (e.g. coefficient of variation < 35%).	30	10	1.5
Detect and model heterogeneity in λ_0 and σ; estimate density with reasonable precision.	60	20	3.0

Detailed simulations with small clusters

Given low encounter rates or uncertainty regarding home range size, designs with closer trap spacing were predicted to yield more spatial recaptures and total recaptures, and therefore superior estimates from SECR models (Sollmann et al. 2012, Wilton et al. 2014, Sun et al. 2014). However, in clustered designs with few cameras per cluster, there is a risk that individual clusters will be too small to detect the actual scale of movements (e.g. Tobler and Powell 2013). Then, in the absence of spatial recaptures across clusters, σ might be underestimated and density overestimated, even if there were many spatial recaptures at short distances within clusters. I was therefore interested in whether representative samples of movements and superior estimates of σ and density could be obtained in situations where there is uncertainty regarding home range size, or some individuals (e.g. of different age or sex classes) have much larger ranges than others, by manipulating cluster shape and orientation, and the distance between adjacent clusters, to increase the variety and maximum of distances between

detectors within clusters, and to reduce the minimum distance between detectors in different clusters.

To address this question, I simulated (following the above-described methods) sampling of mothers occupying relatively large home ranges (8 km^2, expected $\sigma = 651$) at relatively small cross- and line-shaped clusters (345 m detector spacing within clusters, corresponding with an expected home range size of 1.5 km^2), such that the maximum liner distance across clusters (690 m and 1380 m for crosses and lines, respectively) was smaller than the expected home range radius (1596 m). Linear clusters were all oriented in the same direction, and cluster centroids were a minimum of either 2 or 4 km apart. Simulated activity centers were clustered within 25 km^2 territories, such that mothers still used only a fraction of the territory. In addition to simple numbers of animals, recaptures, and spatial recaptures, I recorded distances moved between spatial recaptures, and fit a single SECR model with a half-normal encounter rate function to each simulated data set, recording estimates of σ and density and associated measures of uncertainty obtained from the inverse of the information matrix. I conducted 100 replicates with each cluster shape.

6.2.3 Survey design and implementation in Kibale National Park (KNP)

KNP was too large to space the 60 available CTs evenly throughout the study area and still detect mothers at more than one location (Fig 6.4a). Habitat and habitat quality for chimpanzees varies considerably within KNP (Fig. 6.4b, Potts et al. 2009), so I preferred to sample throughout the park rather relying on data from one or a few intensive arrays covering a small spatial subset of KNP, and opted for a clustered design with many small clusters.

Ideally, locations for cluster centroids would have been selected according to a randomized design to ensure representativity (Efford and Fewster 2013, Efford and Boulanger 2019), and a grid of points with random origin superimposed over the entire park did indeed form the starting point for the design, however, the actual design was constrained by limited resources and other considerations. For example, only 60 CTs were available, allowing for only twelve clusters of at least five CTs each. Because CTs would need to be closely spaced within clusters to inform σ of mothers, I wanted the design to provide opportunities to detect individuals of other social classes at more than one cluster to inform σ of those more wide-ranging animals. I therefore chose linear clusters which maximized the distance between CTs within clusters, and minimized the distance between CTs in different adjacent clusters (when oriented in the same direction).

Territory size information (Table 6.1) indicated that CTs approximately 4 km apart should provide some opportunities to detect members of communities with large territories at more than one cluster, so I initially generated a grid with randomized origin at 4 km spacing as potential locations of cluster centroids. This yielded 52 potential centroids, a random subset of twelve of which might not have included any adjacent points (Fig. 6.4a). I therefore opted to sample northern and southern portions of the park (separated by a road that approximately bisects it; Fig. 6.4a) at different times, to increase spatial sampling intensity achievable with the same number of cameras deployed at fixed locations.

In addition to providing an abundance estimate for KNP, the design needed to accommodate two secondary objectives. Investigators wished to estimate the size of the habituated Ngogo community which occupied a large territory near the center of the

northern portion of KNP (to compare with the known size) and compare the frequency of snare injuries in core and peripheral areas of the park.

Field logistics also needed to be taken into consideration. Much of the park was difficult to access. There were few roads and few established trails beyond the Ngogo territory. A single field crew needed to be able to visit all trap locations biweekly, travelling on foot over difficult terrain (another reason to divide KNP into smaller portions to be sampled at different times). Furthermore, not all habitats could be feasibly sampled using CTs. The low-lying southwestern portion of the park is marshy with many rivers to cross and no road access from the west (Fig. 6.4b), and the density of vegetation at camera height precluded sampling in bushlands or grasslands (Fig. 6.5).

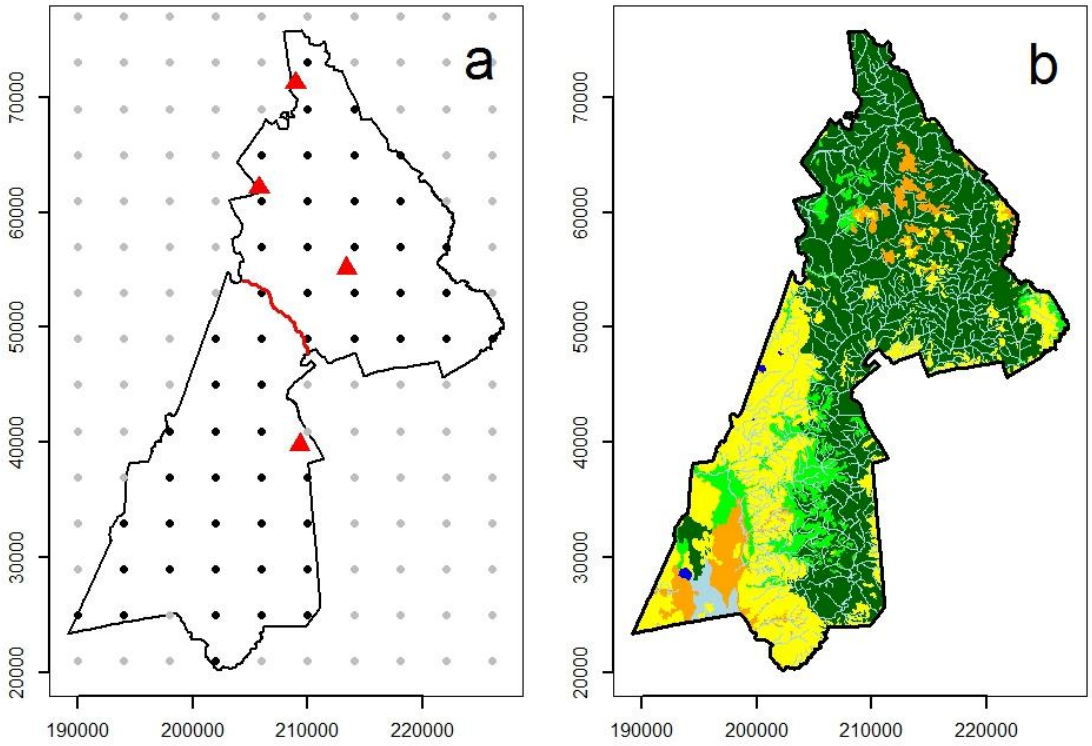

Figure 6.4. Maps of Kibale National Park (KNP), Uganda (boundary as heavy black lines, axes show Universal Transverse Mercators for longitude zone 36), showing (a) potential centroids of clusters of detectors as black dots at 4 km spacing, research stations or camps at which researchers could begin and end fieldwork when visiting different detectors (red triangles), and the road we used to divide the park into northern and southern portions, which would be sampled in sequence, and (b) rivers as light blue lines, and habitat types as described by Drichi (2003). High tropical forests appear in dark green, planted and degraded or encroached high tropical forests in light green, sparsely-treed woodland and bushland in orange, grasslands in yellow, open (sedge-dominated) wetlands in light blue, and open water in dark blue. Some of the degraded forest and open bushland and grassland habitat depicted here have been restored to more closely resemble native forests since these data were collected (Omeja et al. 2011).

Figure 6.5. Photographs of bushland and grassland habitat in Kibale National Park, Uganda (2016), where we were not able to sample chimpanzees using camera traps.

Locations for the twelve centroids in the northern portion of the park were therefore selected in collaboration with SA. We first excluded points that fell in grassland or bushland habitats where we could not feasibly sample. We excluded two additional points in the southeast because they were far from research facilities, roads, and trails. We excluded three points that fell very close to the northeastern boundary, but retained two points near the western boundary to facilitate the comparison of the frequency of snare injuries (Fig 6.6a, b). Three points randomly fell near the periphery of the territory of the Ngogo community (numbers 6, 12, and 13; Fig. 6.6a). We wished to sample this community effectively so that we could estimate community-specific abundance, but not more intensively than other areas, so that the comparison would inform the effectiveness of the design. We left point 12 in the design-specified random

location near the southern territory boundary, but shifted point 6 south and east to ensure that entire cluster fell within the Ngogo territory, and shifted 13 east, just outside the Ngogo territory (Fig. 6.6c, d). Cluster orientations were selected to ensure that entire clusters fell within forested habitat, and that some adjacent clusters were oriented in the same direction.

The sixty Bushnell Trophy Cam™ trail cameras (www.bushnell.com; specific models varied) were deployed over two weeks in January of 2016 by one crew of three or four people, always including myself and led by SA. We travelled to the locations of centroids and searched the vicinity for chimpanzee sign (dung, wadges, nests, drumming trees, and trails), which was found at or near all of the centroids. One CT was placed close to the centroid; peripheral CTs were set approximately 400 meters apart (mean 440, range 239 – 781) in approximately linear configurations (Fig 6.6d). SA had abundant prior experience sampling chimpanzees with CTs and recommended placing most cameras on trails rather than targeting attractants like fruiting trees, as trail sets more frequently yield clear images of chimpanzee faces, facilitating individual identification. CTs were set 0.75 – 1.0 m above the ground, set to high sensitivity, programmed to record video, and left at the same locations for twelve months. CTs were visited every two weeks or as needed to change memory cards and batteries.

After twelve months of sampling, 645 videos of chimpanzees had been recorded, yielding approximately 1800 images of chimpanzee faces, and SA began removing cameras to the southern portion of the park. Although we discussed which centroids in the southern portion should be sampled, this choice was largely constrained by limited access and the distribution of forested habitat, so my contributions to these decisions

were minimal. Therefore, implementation in the southern portion of KNP will not be described here.

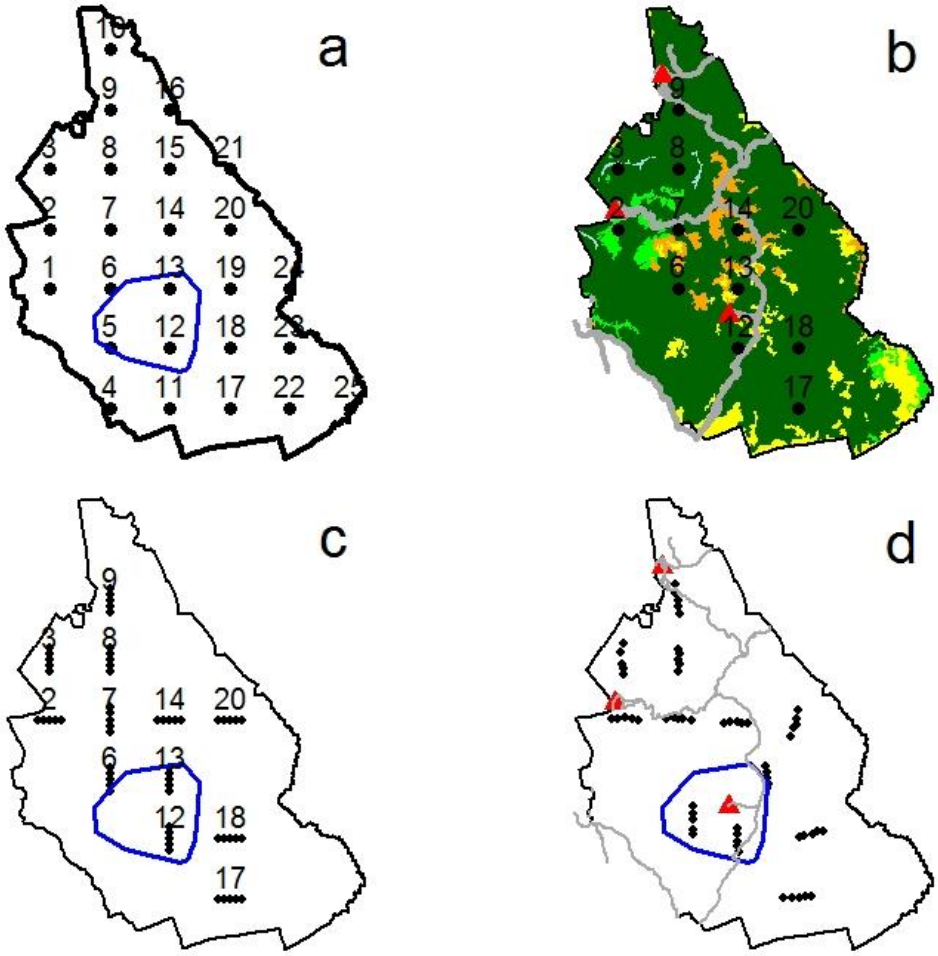

Figure 6.6. From a theoretical to a realized survey design for chimpanzees in the northern portion of Kibale National Park, Uganda, 2015–2016. The approximate boundary of the Ngogo community's territory appears as a blue polygon in panels a, b, and d. Panel a shows the twenty-five randomized locations of potential centroids of clusters of camera traps, panel b shows the twelve points selected, habitat (see Figure 6.2 caption), roads and established trails as grey lines, and research stations and camps as red triangles, panel c shows the design-specified locations for camera traps (at 400 m spacing; orientation of clusters largely arbitrary) and panel d shows the actual locations where cameras were deployed.

6.2.4 SECR analysis of data from the Ngogo community

Identification of individual, non-infant (aged ≥ 5 years) chimpanzees detected at CTs, performed by SA and other experienced observers under his supervision, was still ongoing in summer of 2019, but was complete for individuals detected at the ten CTs deployed within the territory of the Ngogo community. A maximum of one detection per individual, per location, per day, was included in the SECR data to ensure recaptures at the same location were independent events (conditional on activity center location). The resulting data set included a total of 658 detections of 122 different weaned individuals; there were 563 recaptures, 185 spatial recaptures, and mean DPA was 5.4.

I estimated density and population size using SECR models fit by maximum likelihood (Borchers and Efford 2008, Efford and Fewster 2013). I treated the data as having arisen from a single, continuous survey rather than from discrete temporal occasions, and estimated the intercept (λ_0) and spatial scale (σ) of the encounter rate function by maximizing the conditional SECR likelihood for count detectors; variances were obtained from the inverse of the information matix (Borchers and Efford 2008). I assumed the encounter rate decreased with increasing distance between animals' activity centers and CTs according to a half-normal function, and that the number of detections of an individual at a location over the duration of the survey followed a binomial distribution with size equal to the number of days CTs operated at each location. Sampling effort was also defined explicitly in the model as the number of camera-days at each location (Efford et al. 2013). I restricted the possible locations of activity centers of detected animals (the "state space", "region of integration", "integration mesh", or "habitat mask") to forested portions (habitat data from Drichi

[2003]) of the expanded territory of the Ngogo community as depicted in Figure 1B of Mitani et al. (2010; Fig. 6.7).

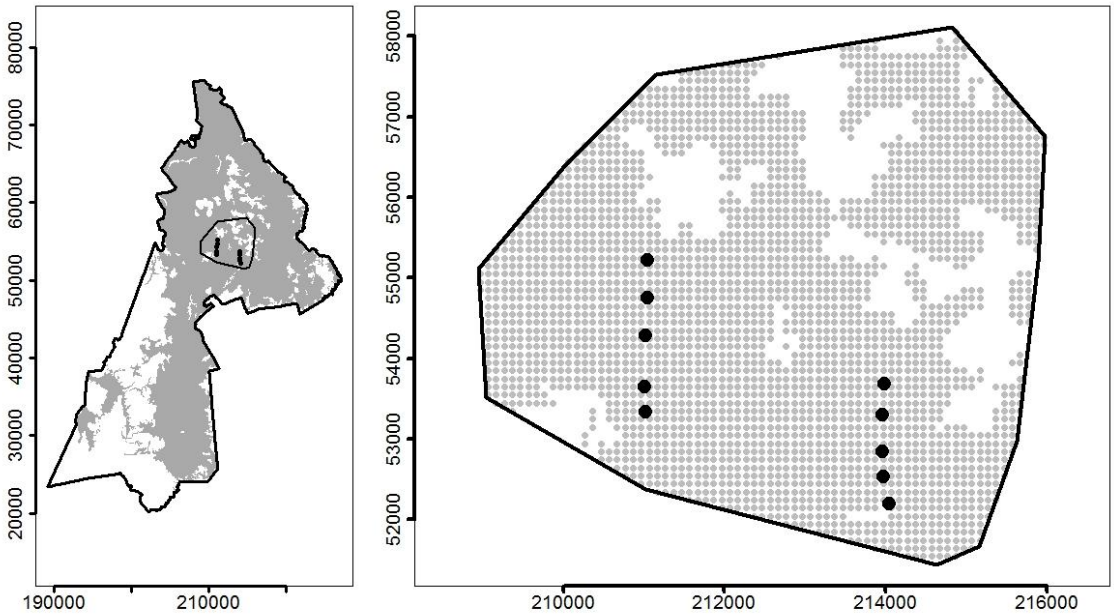

Figure 6.7. Location of the territory of the Ngogo community within Kibale National Park, Uganda (black lines), CTs deployed to sample Ngogo chimpanzees (2016; black dots), and forested (grey) vs. non-forested (grassland or bushland; white) habitats. Axis labels show UTM coordinates. Right: grey dots depict the habitat mask used when fitting SECR models and estimating population sizes.

In consultation with SA, I considered multiple models of the encounter rate function representing different hypotheses about patterns of variation in encounter rates of animals with CTs placed at their activity center (λ_0) and the scale of movements during sampling (σ). Specifically, we investigated whether either or both parameters differed between sexes, or among age classes (adult, subadult, or juvenile), including potential interactions between these effects. Although we expected home range size of adult females to be a function of reproductive status and the status of most adult female community members was known, it was not known for all of them for the entire duration of the survey, and it will not always be identifiable (especially pregnancy) in

photographic surveys of unhabituated chimpanzees, so we did not consider reproductive status as a covariate. We did consider the possibility that the presence of snare injuries would affect encounter rates (λ_0), e.g. by improving observers' ability to confidently identify animals. I fit a total of 50 models, including a model with constant λ_0 and σ, and models with single effects and all additive combinations of injuries, age class, and sex, and interactions between age class and sex affecting λ_0, crossed with single, additive, and interactive effects of age class and sex affecting σ.

I evaluated support for the different models using AIC_c and associated ΔAIC_c values and AIC_c weights (Burnham and Anderson 2002). I estimated total and sex- and age class-specific densities as derived parameters from high-ranking models using a Horvitz-Thompson-like estimator. I assumed population size was Poisson distributed when estimating the variance of $\widehat{D}$ to include process variation in abundance in the sampling variance (Efford and Fewster 2013). I estimated total and sex- and age class-specific population sizes by multiplying density estimates and associated measures of uncertatinty by the area of the habitat mask, i.e., by the area of forested habitat within the Ngogo territory boundary.

All simulations and analyses were performed using R software (version 3.5.3; R Core Team [2019]) using functions implemented in the 'secr' (Efford 2019b) and 'secrdesign' (Efford 2019c) packages.

6.3 Results

6.3.1 Simulations

Generally, simulations reinforced concerns that if mothers used small home ranges, few of them might be detected, and they would seldom be recaptured at different locations. Where the expected home range size was 1.5 or 4.0 km^2, all designs yielded means of < 10 and < 30 recaptures, respectively, ≤ 5 and between 6 and 20 spatial recaptures, respectively, and mean DPA was < 1.50 and < 1.70, respectively (Table 6.3). Where expected home range size was 8 km^2, all designs yielded means of > 35 recaptures, > 20 spatial recaptures, and mean DPA ranged from 1.39 to 1.75. Sample sizes of recaptures and spatial recaptures improved with closer within-cluster detector spacing, but at the simulated values of density and λ_0, samples remained small after 12 months even where detector spacing was only slightly greater than σ, corresponding with half the expected home range radius from the same size of territory (Table 6.3). Less than 6% of the population sampled was detected by any design, and this fell to < 2% where mothers used small home ranges (Table 6.3). Crosses detected lower, more variable *n*, but more spatial recaptures and therefore total recaptures and DPA, relative to lines (Table 6.3). Results were similar when cluster centroids were 1 and 4 km apart (Table 6.3).

Table 6.3. Means and coefficient of variation (CV) of the number of animals detected (*n*) as a percentage of the total population size, recaptures (R), spatial recaptures (SR), and detections per animal (DPA) from simulated surveys of different types of populations (Poisson-distributed [P], and in large, medium, or small territories [LT, MT, ST]), from designs with different cluster shapes, and spacings between adjacent traps within clusters (W), and between cluster centroids (B). The table spans five pages, and is organized into sets of 10 rows with the same survey design, and 20 rows with the same design except shape (separated by horizontal lines).

Design			Population		Summary of data collected							
Shape	W	B	Type	σ	*n* (%)	R	SR	DPA	CV(*n*)	CV(R)	CV(SR)	CV(DPA)
+	345	1000	LT	282	1.1	8.1	5.3	1.47	0.29	0.51	0.59	0.14
+	345	1000	MT	282	1.1	8.2	5.4	1.48	0.28	0.51	0.58	0.14
+	345	1000	S T	282	1.1	8.0	5.4	1.48	0.26	0.50	0.57	0.14
+	345	1000	LT	461	2.6	26.4	19.9	1.65	0.21	0.32	0.34	0.10
+	345	1000	MT	461	2.5	25.2	19.0	1.64	0.20	0.32	0.36	0.10
+	345	1000	P	461	2.5	25.4	19.1	1.65	0.16	0.30	0.32	0.10
+	345	1000	S T	461	2.4	24.2	18.4	1.64	0.19	0.34	0.36	0.10
+	345	1000	LT	651	4.9	56.7	44.4	1.75	0.17	0.24	0.25	0.08
+	345	1000	MT	651	4.9	55.5	43.3	1.74	0.15	0.24	0.26	0.08
+	345	1000	S T	651	5.0	56.2	44.0	1.73	0.13	0.24	0.25	0.08
—	345	1000	LT	282	1.2	6.9	4.1	1.38	0.27	0.51	0.62	0.13
—	345	1000	MT	282	1.2	6.7	3.9	1.37	0.27	0.49	0.59	0.12
—	345	1000	S T	282	1.1	6.9	4.0	1.39	0.26	0.50	0.60	0.13
—	345	1000	LT	461	2.8	23.5	16.6	1.55	0.20	0.32	0.36	0.09
—	345	1000	MT	461	2.7	23.1	16.2	1.55	0.19	0.32	0.36	0.09
—	345	1000	P	461	2.7	22.6	15.9	1.54	0.16	0.29	0.32	0.09
—	345	1000	S T	461	2.6	21.8	15.4	1.54	0.18	0.32	0.36	0.09
—	345	1000	LT	651	5.2	52.3	39.5	1.65	0.17	0.25	0.27	0.07
—	345	1000	MT	651	5.1	51.4	38.8	1.65	0.15	0.24	0.26	0.07
—	345	1000	S T	651	5.2	52.2	39.3	1.65	0.12	0.22	0.24	0.07

Design			Population			Summary of data collected						
Shape	W	B	Type	σ	*n* (%)	R	SR	DPA	CV(*n*)	CV(R)	CV(SR)	CV(DPA)
+	345	4000	LT	282	1.0	7.6	5.0	1.47	0.28	0.50	0.58	0.14
+	345	4000	MT	282	1.1	7.8	5.1	1.48	0.28	0.51	0.60	0.15
+	345	4000	S T	282	1.1	8.0	5.3	1.49	0.27	0.49	0.57	0.14
+	345	4000	LT	461	2.5	24.8	18.6	1.63	0.20	0.33	0.35	0.10
+	345	4000	MT	461	2.5	24.8	18.7	1.63	0.20	0.32	0.35	0.10
+	345	4000	P	461	2.5	24.8	18.5	1.63	0.16	0.29	0.31	0.10
+	345	4000	S T	461	2.6	25.0	18.5	1.63	0.17	0.31	0.34	0.10
+	345	4000	LT	651	4.8	51.9	40.3	1.69	0.16	0.26	0.27	0.08
+	345	4000	MT	651	4.9	53.0	41.0	1.70	0.15	0.24	0.25	0.07
+	345	4000	S T	651	4.9	53.1	41.0	1.70	0.13	0.23	0.25	0.08
—	345	4000	LT	282	1.1	5.6	3.8	1.38	0.28	0.63	0.62	0.13
—	345	4000	MT	282	1.1	6.5	3.7	1.37	0.28	0.53	0.65	0.13
—	345	4000	S T	282	1.1	6.7	3.9	1.38	0.26	0.51	0.61	0.13
—	345	4000	LT	461	2.7	22.2	15.4	1.53	0.20	0.31	0.35	0.09
—	345	4000	MT	461	2.7	21.8	15.1	1.52	0.19	0.32	0.35	0.09
—	345	4000	P	461	2.7	22.2	15.5	1.52	0.15	0.29	0.33	0.09
—	345	4000	S T	461	2.7	22.3	15.4	1.53	0.17	0.30	0.34	0.09
—	345	4000	LT	651	5.1	49.7	37.0	1.62	0.15	0.24	0.25	0.07
—	345	4000	MT	651	5.1	48.4	36.0	1.61	0.14	0.23	0.25	0.07
—	345	4000	S T	651	5.1	49.2	36.5	1.62	0.12	0.22	0.24	0.07
+	564	1000	LT	282	1.2	5.6	2.6	1.29	0.27	0.54	0.75	0.11
+	564	1000	MT	282	1.2	5.7	2.5	1.30	0.26	0.53	0.71	0.11
+	564	1000	S T	282	1.2	5.6	2.5	1.30	0.26	0.53	0.74	0.11
+	564	1000	LT	461	2.9	22.1	14.8	1.50	0.20	0.32	0.36	0.08
+	564	1000	MT	461	2.8	21.8	14.8	1.50	0.19	0.33	0.37	0.09
+	564	1000	P	461	2.8	20.6	13.8	1.48	0.15	0.31	0.35	0.09

Design			Population		Summary of data collected							
Shape	W	B	Type	σ	*n* (%)	R	SR	DPA	CV(*n*)	CV(R)	CV(SR)	CV(DPA)
+	564	1000	S T	461	2.7	20.6	13.8	1.49	0.18	0.32	0.37	0.09
+	564	1000	LT	651	5.2	51.5	38.3	1.64	0.16	0.25	0.26	0.07
+	564	1000	MT	651	5.2	51.3	38.3	1.64	0.14	0.24	0.25	0.07
+	564	1000	S T	651	5.3	51.7	38.6	1.63	0.12	0.23	0.25	0.07
—	564	1000	LT	282	1.3	5.1	2.0	1.26	0.26	0.55	0.82	0.10
—	564	1000	MT	282	1.3	4.9	1.9	1.25	0.26	0.54	0.82	0.10
—	564	1000	S T	282	1.2	5.0	1.9	1.27	0.24	0.54	0.84	0.11
—	564	1000	LT	461	3.1	18.9	11.2	1.40	0.19	0.33	0.40	0.08
—	564	1000	MT	461	3.0	18.5	11.1	1.40	0.18	0.34	0.41	0.08
—	564	1000	P	461	3.0	18.0	10.8	1.39	0.15	0.31	0.37	0.08
—	564	1000	S T	461	2.9	17.8	10.8	1.40	0.16	0.34	0.41	0.08
—	564	1000	LT	651	5.6	44.7	30.8	1.52	0.15	0.25	0.28	0.06
—	564	1000	MT	651	5.5	45.2	31.1	1.53	0.14	0.24	0.27	0.07
—	564	1000	S T	651	5.7	45.9	31.5	1.52	0.12	0.22	0.25	0.06
+	564	4000	LT	282	1.2	5.3	2.4	1.28	0.27	0.56	0.78	0.11
+	564	4000	MT	282	1.2	5.3	2.2	1.29	0.26	0.55	0.77	0.11
+	564	4000	S T	282	1.2	5.4	2.4	1.29	0.26	0.54	0.75	0.11
+	564	4000	LT	461	2.8	20.9	13.8	1.47	0.19	0.33	0.38	0.08
+	564	4000	MT	461	2.8	20.7	13.6	1.47	0.19	0.33	0.37	0.09
+	564	4000	P	461	2.8	20.4	13.4	1.47	0.15	0.29	0.35	0.08
+	564	4000	S T	461	2.8	20.7	13.7	1.48	0.16	0.31	0.36	0.08
+	564	4000	LT	651	5.1	47.5	34.7	1.59	0.15	0.25	0.26	0.07
+	564	4000	MT	651	5.1	47.6	34.6	1.60	0.14	0.24	0.25	0.07
+	564	4000	S T	651	5.2	47.9	35.0	1.60	0.12	0.23	0.25	0.07
—	564	4000	LT	282	1.2	4.8	1.8	1.25	0.25	0.56	0.82	0.10
—	564	4000	MT	282	1.2	4.7	1.8	1.25	0.26	0.58	0.85	0.10

Design			Population		Summary of data collected							
Shape	W	B	Type	σ	*n* (%)	R	SR	DPA	CV(*n*)	CV(R)	CV(SR)	CV(DPA)
—	564	4000	S T	282	1.3	4.9	1.9	1.26	0.24	0.55	0.81	0.10
—	564	4000	LT	461	3.0	17.7	10.2	1.38	0.18	0.33	0.40	0.07
—	564	4000	MT	461	3.0	17.4	10.0	1.38	0.18	0.33	0.39	0.08
—	564	4000	P	461	3.0	17.6	10.2	1.38	0.15	0.31	0.37	0.07
—	564	4000	S T	461	3.0	17.4	10.1	1.38	0.16	0.33	0.39	0.07
—	564	4000	LT	651	5.6	41.9	28.0	1.48	0.15	0.24	0.27	0.06
—	564	4000	MT	651	5.5	41.5	27.8	1.49	0.13	0.23	0.26	0.06
—	564	4000	S T	651	5.6	42.0	28.0	1.49	0.11	0.21	0.25	0.06
+	798	1000	LT	282	1.3	4.1	0.9	1.20	0.27	0.61	1.10	0.09
+	798	1000	MT	282	1.3	4.0	0.9	1.20	0.24	0.59	1.21	0.09
+	798	1000	S T	282	1.3	4.2	1.0	1.20	0.23	0.59	1.15	0.09
+	798	1000	LT	461	3.2	17.6	9.7	1.36	0.19	0.33	0.40	0.07
+	798	1000	MT	461	3.1	17.5	9.5	1.36	0.18	0.33	0.41	0.07
+	798	1000	P	461	3.1	16.8	9.2	1.35	0.14	0.32	0.41	0.07
+	798	1000	S T	461	3.0	16.7	9.2	1.36	0.16	0.33	0.42	0.07
+	798	1000	LT	651	5.6	45.2	31.0	1.52	0.15	0.24	0.28	0.06
+	798	1000	MT	651	5.5	44.3	30.5	1.51	0.14	0.25	0.27	0.07
+	798	1000	S T	651	5.7	45.2	30.8	1.51	0.12	0.23	0.27	0.07
—	798	1000	LT	282	1.3	4.1	0.8	1.20	0.25	0.57	1.22	0.09
—	798	1000	MT	282	1.3	4.0	0.9	1.19	0.24	0.55	1.21	0.08
—	798	1000	S T	282	1.3	3.9	0.8	1.19	0.23	0.56	1.19	0.09
—	798	1000	LT	461	3.3	15.2	7.3	1.30	0.18	0.35	0.46	0.07
—	798	1000	MT	461	3.2	15.2	7.3	1.30	0.16	0.32	0.44	0.07
—	798	1000	P	461	3.2	14.9	7.0	1.30	0.14	0.31	0.45	0.07
—	798	1000	S T	461	3.1	14.7	7.0	1.31	0.15	0.34	0.44	0.07
—	798	1000	LT	651	6.0	39.1	24.0	1.42	0.14	0.25	0.30	0.06

Design			Population		Summary of data collected							
Shape	W	B	Type	σ	*n* (%)	R	SR	DPA	CV(*n*)	CV(R)	CV(SR)	CV(DPA)
—	798	1000	MT	651	5.9	37.5	23.0	1.41	0.12	0.23	0.29	0.06
—	798	1000	S T	651	6.0	39.0	23.9	1.42	0.11	0.21	0.26	0.06
+	798	4000	LT	282	1.3	3.9	0.8	1.20	0.26	0.57	1.17	0.09
+	798	4000	MT	282	1.3	3.9	0.8	1.20	0.24	0.58	1.18	0.09
+	798	4000	S T	282	1.3	3.9	0.8	1.20	0.25	0.58	1.18	0.09
+	798	4000	LT	461	3.1	16.2	8.4	1.34	0.19	0.34	0.44	0.07
+	798	4000	MT	461	3.1	15.7	8.2	1.33	0.17	0.33	0.43	0.07
+	798	4000	P	461	3.1	16.3	8.7	1.34	0.14	0.29	0.39	0.07
+	798	4000	S T	461	3.1	16.1	8.5	1.34	0.15	0.32	0.43	0.07
+	798	4000	LT	651	5.6	41.4	27.3	1.48	0.15	0.24	0.27	0.06
+	798	4000	MT	651	5.6	41.1	27.1	1.47	0.13	0.24	0.27	0.06
+	798	4000	S T	651	5.6	41.5	27.3	1.48	0.12	0.22	0.25	0.06
—	798	4000	LT	282	1.3	3.9	0.7	1.20	0.26	0.57	1.27	0.09
—	798	4000	MT	282	1.3	3.9	0.7	1.19	0.24	0.58	1.28	0.09
—	798	4000	S T	282	1.3	3.8	0.7	1.19	0.23	0.58	1.27	0.09
—	798	4000	LT	461	3.2	14.4	6.6	1.29	0.18	0.33	0.45	0.07
—	798	4000	MT	461	3.2	14.5	6.6	1.29	0.16	0.32	0.44	0.06
—	798	4000	P	461	3.2	14.4	6.5	1.29	0.15	0.32	0.44	0.06
—	798	4000	S T	461	3.2	14.4	6.7	1.29	0.15	0.31	0.44	0.06
—	798	4000	LT	651	5.9	35.7	21.1	1.39	0.13	0.23	0.28	0.05
—	798	4000	MT	651	5.9	35.6	21.1	1.39	0.12	0.23	0.28	0.05
—	798	4000	S T	651	5.9	36.1	21.3	1.39	0.11	0.22	0.27	0.05

Poisson-distributed populations versus group territoriality

Mean sample sizes of animals, recaptures, movements, and DPA were similar when Poisson-distributed and clustered populations were sampled, but there was consistently greater variability among iterations of the same simulation scenario when activity centers were clustered, and as the size of territories increased (i.e., where activity centers were clustered at a larger spatial scale; Table 6.4). Therefore, there was greater potential for a survey of group-living territorial species with spatially clustered activity centers to yield sparse or inadequate data than would be expected if activity centers were distributed randomly.

Table 6.4. Means of coefficients of variation (CVs) of numbers of animals detected (*n*), total recaptures, spatial recaptures, and mean detections per animal (DPA), across six simulation scenarios for each type of simulated population. Each value is the mean across six CVs, where each CVs was calculated as the standard deviation divided by the mean across 1000 replicates with the same cluster geometry and within-cluster trap spacing. The minimum distance between cluster centroids and σ were fixed at 4 km and 461 meters, respectively. See Table 6.3 for scenario-specific means and CVs.

Population type	*n*	Recaptures	Spatial recaptures	DPA
Large territories	0.19	0.33	0.39	0.080
Medium territories	0.18	0.32	0.39	0.080
Small territories	0.16	0.31	0.38	0.080
Homogeneous Poisson	0.15	0.30	0.37	0.078

Detailed simulations with small clusters

In scenarios where clusters of detectors were small relative to home range size, mean sample sizes of animals detected, recaptures, spatial recaptures, and DPA always exceeded 74, 48, 35, and 1.60, respectively; lines yielded slightly larger samples of animals detected, slightly smaller samples of recaptures, spatial recaptures, and fewer DPA than crosses.

Linear clusters detected a more vaired sample of distances moved (Fig. 6.8). Where centroids were ≥ 2 km apart, animals were occasionally detected at different clusters (but more frequently between linear clusters; Fig. 6.8). Where centroids were ≥ 4 km apart, there was only one spatial recapture between crosses and only four between lines, across all 100 replicates, but linear clusters still provided a more representative sample of the scale of animal movements (Fig. 6.8).

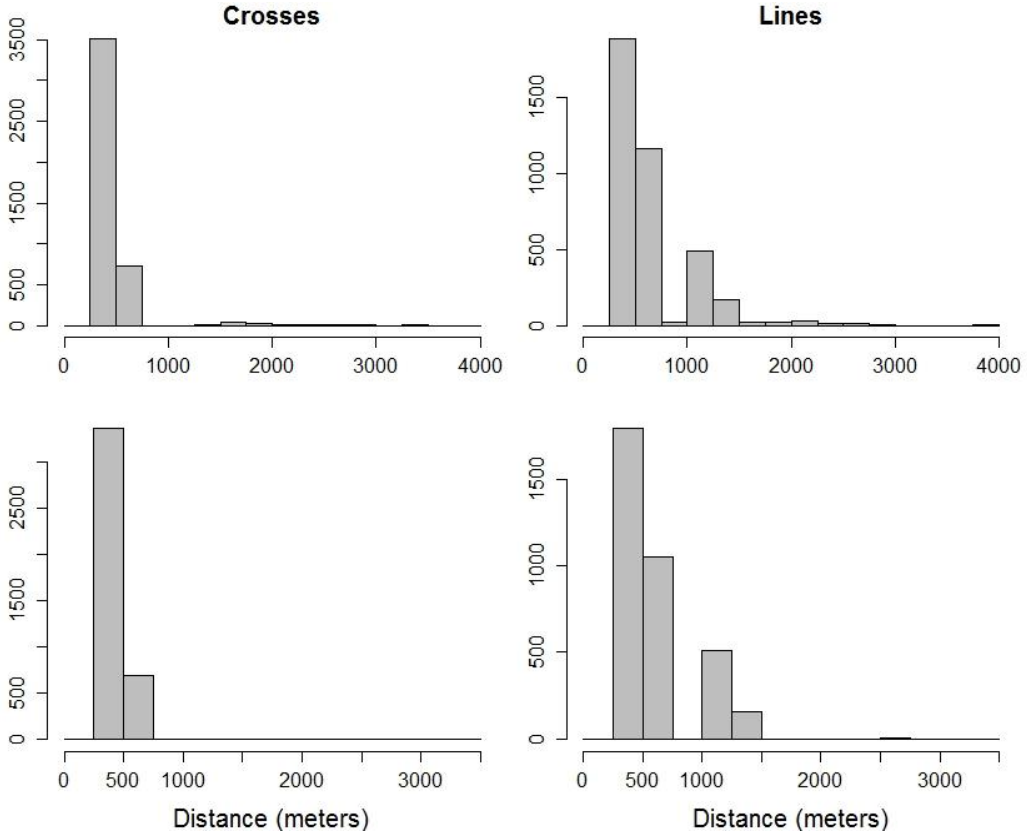

Figure 6.8. Distances moved between spatial recaptures in simulated SECR surveys of eastern chimpanzee mothers employing clusters of detectors of different shapes (crosses and lines). The top row shows results with centroids ≥ 2 km apart, the bottom row results with centroids ≥ 4 km apart. Histograms show all movements from 100 replicates with each cluster shape and distance between centroids. A single spatial recapture at a distance of 3310 m between crosses 4 km apart occurred but is not apparent on the plot.

Both σ and density were estimated with greater accuracy and precion from designs employing linear clusters (Figs. 6.9 and 6.10, Table 6.5). Where centroids were ≥ 2 km apart, σ was slightly overestimated (Fig. 6.9); mean densities across replicates were unbiased, but the distribution of densities estimated from cross-shaped clusters was skewed, with more frequent negatively biased estimates, such that median density across replicates underestimated the true density (Fig. 6.10). Where centroids were ≥ 4 km apart such that animals were recaptured only within clusters in the majority of replicates, designs with cross-shaped clusters yielded slightly negatively biased estimates of σ, and slightly positively biased estimates of density, but estimates from designs with linear clusters were accurate (Figs. 6.9 and 6.10).

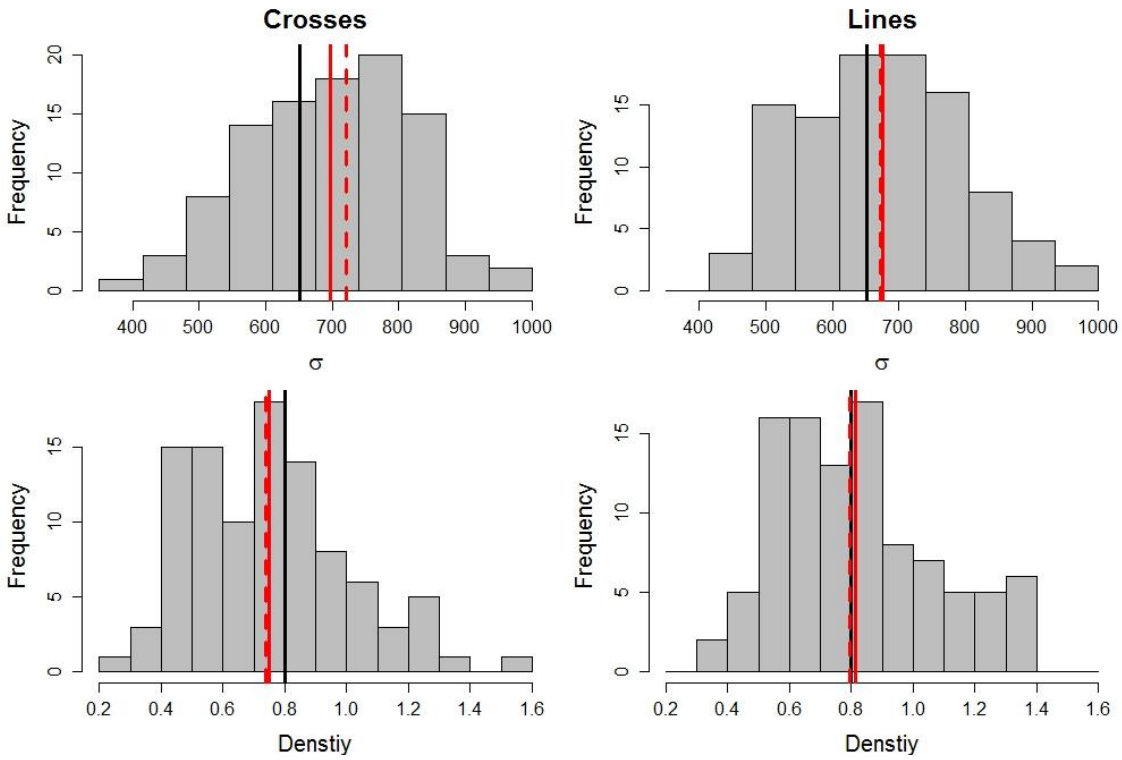

Figure 6.9. Estimates of the scale parameter of the encounter rate function (σ, meters) from SECR models fit to simulated data from eastern chimpanzee mothers from simulated surveys employing clusters of detectors of different shapes (crosses [left] and lines [right]). The top row shows results with centroids ≥ 2 km apart, the bottom row results with centroids ≥ 4 km apart. Histograms show 100 estimates from 100 replicates with each cluster shape and distance between cluster centroids. True values are shown as heavy black lines, means across replicates as solid red lines, and medians across replicates as dashed red lines.

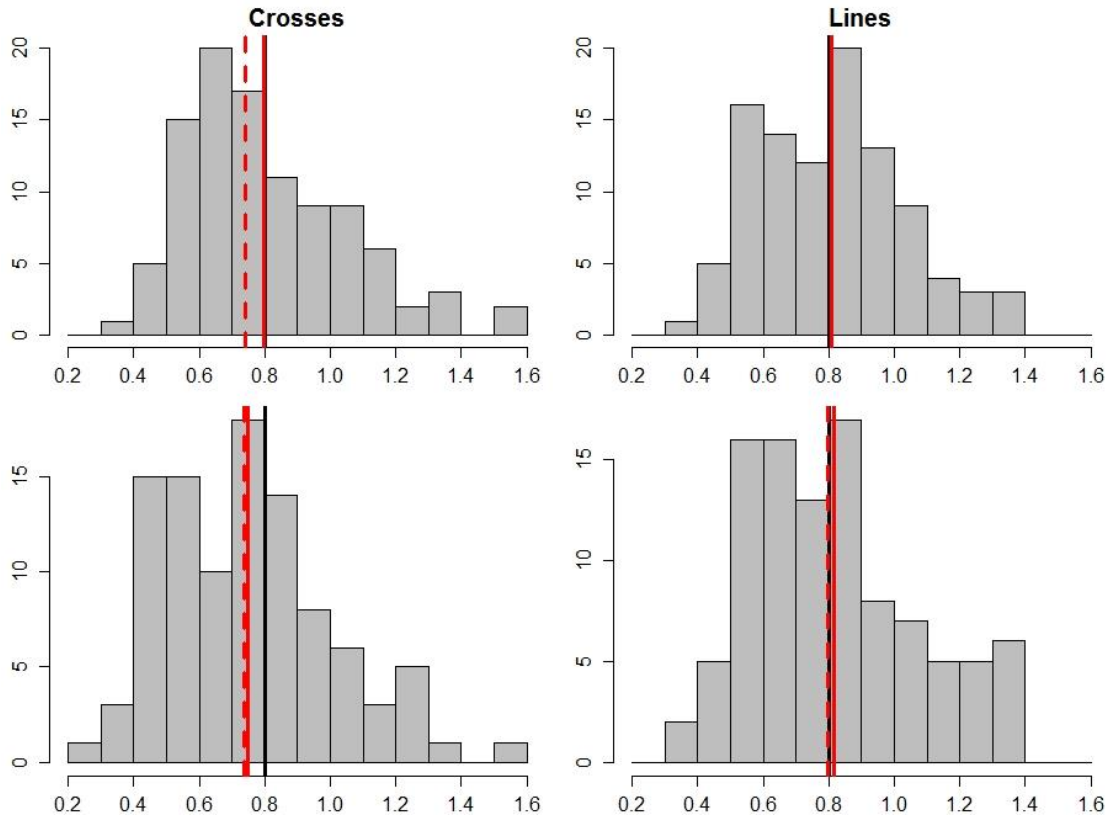

Figure 6.10. Estimates of density (animals / km^2) from SECR models fit to simulated data from eastern chimpanzee mothers from simulated surveys employing clusters of detectors of different shapes (crosses [left] and lines [right]). The top row shows results with centroids ≥ 2 km apart, the bottom row results with centroids ≥ 4 km apart. Histograms show 100 estimates from 100 replicates with each cluster shape and distance between cluster centroids. True values are shown as heavy black lines, means across replicates as solid red lines, and medians across replicates as dashed red lines.

Table 6.5. Means of coefficients of variation (CVs) of estimates of σ and density from SECR models fit to data from simulated surveys of eastern chimpanzee mothers employing different shapes for clusters of detectors (crosses and lines), and different minimum distances between cluster centroids.

Minimum distance	Crosses		Lines	
between centroids (km)	σ	Density	σ	Density
2	0.17	0.31	0.15	0.27
4	0.22	0.39	0.18	0.31

6.3.3 SECR analysis of data from the Ngogo community

All high AIC_c-ranked SECR models fit to data from the ten CTs deployed in the territory of the Ngogo community included effects of sex and visible injuries on λ_0, and the top four models also included differences in σ among age classes (Table 6.6). Only three models had $\Delta AIC_c < 2.0$ and AIC_c weight > 0.10; they accounted for 62.4% of the total AIC_c weight across the candidate set (Table 6.6). All other models had $\Delta AIC_c > 3$, and all but the top five models had AIC_c weights < 0.05. The top five models yielded similar estimates of density of similar precision (Table 6.6). Model selection uncertainty was therefore not a major concern, so we estimated abundance from the top-ranked model.

Table 6.6. Estimates of the density of weaned chimpanzees from the top five AIC_c-ranked SECR models fit to data from Ngogo territory, Kibale National Park, Uganda, 2016. "CV" denotes the coefficient of variation of the density estimates, and "ac" denotes an effect of age class.

Model	AIC_c weight	Density (per km^2)	CV
λ_0 ~ injury + sex; σ ~ ac	0.313	6.09	0.094
λ_0 ~ injury + sex; σ ~ ac + sex	0.178	6.15	0.094
λ_0 ~ injury + ac + sex; σ ~ ac	0.133	6.10	0.094
λ_0 ~ injury + ac + sex; σ ~ ac + sex	0.064	6.15	0.095
λ_0 ~ injury + ac + sex; σ ~ 1	0.062	5.98	0.093

Males had higher encounter rates than females, and encounter rates of animals with visible injuries were nearly double those of uninjured animals of the same sex (Table 6.7). Older animals used larger ranges than younger animals (Table 6.7). Estimates of σ from the 2nd-ranked model, which included differences in σ between sexes as well as age classes, indicated that males used slightly larger ranges than females of the same age class (Table 6.7).

Table 6.7. Point estimates of the parameters of the encounter rate function function for different categories of weaned eastern chimpanzees in Ngogo territory, Kibale National Park, Uganda, 2016. Estimates of λ_0 are per day, and of σ are over the duration of the survey, in meters.

Covariates			Parameter estimates			
			Top model		2^{nd}-ranked model	
Age class	Sex	Injury	λ_0	σ	λ_0	σ
Adult	F	0	0.0050	999	0.0054	944
Adolescent	F	0	0.0050	945	0.0054	896
Juvenile	F	0	0.0050	737	0.0054	696
Adult	M	0	0.0086	999	0.0083	1027
Adolescent	M	0	0.0086	945	0.0083	974
Juvenile	M	0	0.0086	737	0.0083	757
Adult	F	1	0.0092	999	0.0096	944
Adolescent	F	1	0.0092	945	0.0096	896
Juvenile	F	1	0.0092	737	0.0096	696
Adult	M	1	0.0157	999	0.0147	1027
Adolescent	M	1	0.0157	945	0.0147	974
Juvenile	M	1	0.0157	737	0.0147	757

Chimpanzee density within forested habitat estimated from the top AIC_c-ranked model was 6.09 / km^2 (SE = 0.57, CV = 0.094, 95% confidence interval 5.1 – 7.3). The associated estimate of population size of weaned individuals was 170.8, nearly identical to the size of the Ngogo community in 2016 as determined from daily direct observations (Table 6.8). Most age and sex class-specific estimates were also accurate, and all included the known or approximately known value within their 95% confidence interval (Table 6.8).

Table 6.8. Age and sex class-specific abundance estimates with associated standard errors (SE) and 95% confidence intervals (CI) from the top AIC_c-ranked SECR model, and known or approximately known abundances from daily direct observations (provided by Samuel Angedakin).

Age and sex class	SECR estimate	SE	95% CI	Approximately known value from direct observations
Adult females	50	8.3	36 – 69	61
Adolescent females	13	4.3	7 – 24	13
Juvenile females	23	6.4	13 – 39	22
Adult males	40	7.2	28 – 57	34
Adolescent males	12	3.9	6 – 22	12
Juvenile males	34	7.4	22 – 52	28
All weaned individuals	171	16.0	142 – 205	170

6.4 Discussion

6.4.1 Simulations

Generally, simulation results were consistent with prior work showing that unless animal densities or encounter rates are high, designs with wide detector spacing relative to the scale of movements during samping (e.g. detectors spaced more than half the expected home range radius, or more than 2σ, apart) yield few spatial recaptures and therefore insufficient information to estimate σ or density reliably (Sollmann et al. 2012, Sun et al. 2014, Wilton et al. 2014). Efford and Boulanger (2019) recommended rejecting designs that yield fewer than six spatial recaptures in simulations, and we obtained five or fewer whenever we assumed home ranges of mothers averaged only 1.5 km^2 in size. Nearly all designs yielded samples of animals, recaptures, spatial recaptures, and DPA I deemed sufficient to model heterogeneity in detection and yet estimate density with reasonable precision when we assumed mothers used larger ranges. This seems consistent with the idea that designs adequate for mothers would also be adequate for social classes with larger σ than mothers.

As might be expected, sample sizes were more variable across iterations of the same scenario when activity centers were clustered near territory centers, because of the potential for different numbers of detectors to fall within areas of locally high or low density. Clark (2019) simulated SECR sampling of populations with variable density within a region of interest using clustered designs with varying numbers of detectors per cluster, and found that designs with many clusters of few traps yielded more consistent results across iterations than designs with few clusters of many traps. Sampling designs with more clusters of detectors are likely to outperform designs with fewer clusters whenever the total number of detectors is limited and activity centers are distributed neither uniformly nor randomly at a constant expected denstiy across the region of interest.

If spatial recaptures occur only within clusters, the distance between cluster centroids has little or no effect on sample sizes or the performance of SECR models (Clark 2019, this study). It has been recommended that in these situations, the extent of each cluster should at least equal that of one home range (Tobler and Powell 2013, Efford and Boulanger 2019), but this could require a large number of detectors if other design recommendations (traps spaced σ to 2σ apart, and many clusters throughout the region of interest) are also followed. I attempted to increase the scale of movements detectable within clusters and circumvent the need for cluster extents as large as home ranges by using linear clusters, and spacing them close enough together that some animals might be detected at more than one cluster. In my simulations with close within-cluster detector spacing and small cluster extent relative to the scale of movements, linear clusters improved representativity of samples of movements, and estimates of σ and density, especially where the closer distance between linear clusters

aligned in the same direction allowed for more frequent spatial recaptures across clusters. However, if home ranges are elongated (elliptical rather than circular) and aligned in a consistent direction (e.g. perpendicular or parallel) with respect to linear arrays of detectors, SECR models yield biased estimates (Ivan et al. 2013, Efford 2019d), so researchers should consider whether territories or home ranges might be elongated in a consistent direction before designing a survey with a linear arrary or linear clusters. For example, chimpanzees on McCarthy et al.'s (2015) study area relied heavily on riparian fragments of forested habitat along creeks and rivers. Surveys employing linear arrays of detectors, or linear searchers for fecal DNA (i.e., along transects), would not be expected to perform well if transects were aligned in a consistent direction with respect to these riparian fragments.

To my knowledge, the survey design for chimpanzees in KNP was the first attempt to cope with uncertainty or variation in home range size by manipulating cluster geometry and spacing to provide more representative samples of movements both within and between clusters. However, Clark (2019) suggested that "cross-cluster sampling" could improve estimates from designs with small clusters of detectors, and conducted post hoc simulations which demonstrated that when detector spacing and cluster extent were defined with female black bears in mind, densities of males, whose ranges are larger than and usually encompass those of several females, were estimated with greater accuracy and precision when clusters were spaced close enough together to allow males to be detected at more than one cluster.

Based on my review of territory and home range sizes of eastern chimpanzees in forested habitats, I expected mothers at Ngogo to use smaller home ranges than other social classes, and therefore for adult females to have smaller ranges on average, and

lower σ, than other classes. I also hoped and expected to detect many members of these other social classes at both of the clusters of detectors deployed within the Ngogo territory, but we did not. Of the 185 movements detected, only two were across clusters, and one was made by a female. Furtheremore, estimates of σ were similar between sexes; the top-ranked model did not include a sex effect on σ, and estimates from the 2nd-ranked model which included a difference in σ between sexes yielded similar sex-specific estimates. However, chimpanzee community structure and membership are not always stable. The Ngogo community, after previously expanding its territory at the expense of a neighbouring community (Mitani et al. 2010), was dividing itself into "sub-communities" during sampling, and most community members, including adult males, spent most of their time within smaller "neighbourhoods" within the (former) Ngogo territory (SA, Personal communication). Since then, the community has fissioned into at least two distinct communities with their own territories. This may explain the smaller-than-expected differences in σ between sexes, and the lack of spatial recaptures across clusters.

Prior SECR CT surveys of chimpanzees achieved large samples and accurate and relatively precise estimates of density from spatially intensive surveys of small study areas (Head et al. 2013, Despres-Einspenner et al. 2017). Despite deploying fewer CTs per area and per habituated community, we obtained large samples of recaptures, spatial recaptures, and many detections per individual from Ngogo chimpanzees, and hence accurate estimates of abundance, because (1) encounter rates at Ngogo were much higher than either the value assumed in simulations, or those achieved during two prior photographic surveys of chimpanzees, and (2) contrary to expectations, adult females moved as far or nearly as far as other social classes between

CTs. Monthly encounter rates of female chimpanzees on other forested study areas (converted from estimates of monthly or weekly probabilities of detection from the SECR models they fitted) were approximately 0.020 and 0.083 for two latent groups of individuals (Head et al. 2013), and 0.001 to 0.04 depending on a variety of factors including prior detection (Després-Einspenner et al. 2017). At Ngogo, the estimated daily encounter rate of uninjured females converts to an expected 1.5 encounters per 30 days – almost two orders of magnitude higher than the prior surveys. The difference cannot be attributed to observers' ability to confidently identify the Ngogo chimpanzees, because prior surveys also targeted habituated communities, and researchers or staff identifying individuals from videos were already familiar with individuals sampled at CTs (Head et al. 2013, Després-Einspenner et al. 2017). Head et al. (2013) targeted multiple species including chimpanzees, but one of Després-Einspenner et al.'s (2017) arrays targeted chimpanzees specifically, and both researchers set many CTs on trails, so I cannot explain the large differences in encounter rates between surveys, unless the commonality of snare injuries at Ngogo made it easier for observers to discriminate among all individuals. That the abundance of adult females was slightly underestimated may indicate that this class of animals was not sampled as effectively as other social classes, but this was not apparent in the estimates of detection parameters from the adult females we did detect. Granjon et al. (2017) conducted genetic SECR surveys of the Ngogo community and estimated abundance using spatial and nonspatial estimators. Their SECR analysis underestimated abundance, but I suspect this was attributable to an inappropriately large region of integration considering that chimpanzees recognize the boundaries of their territories, such that members of one community are unlikely to be detected within the

territory of another, regardless of the distance between their activity centers and those detectors (see Chapter 2 and Després-Einspenner et al. [2017]).

6.4.2 Synthesis and recommendations for survey design

SECR models can yield accurate estimates of animal abundance from a wide range of designs, provided minimum requirements with respect to detector spacing and array extent are met (Efford 2011, Marques et al. 2011, Sollmann et al. 2012, Sun et al. 2014, Wilton et al. 2014, Clark 2019). Even though my simulations indicated that SECR surveys employing clusters of only five CTs could fail to yield sufficient data from some social classes to reliably estimate their abundance, the combination of (1) results from simulations where mothers used relatively large home ranges, (2) the analysis of data from Ngogo which suggests that adult females used larger-than-expected home ranges on average, and (3) the accurate and reasonably precise estimates of abundance obtained from three CT surveys of habituated communities, indicate that it is feasible to efficiently and reliably enumerate chimpanzees over larger areas by photographic SECR, even in the presence of uncertainty regarding animal densities, encounter rates, and home range sizes.

Where encounter rates were low and CT placement did not specifically target chimpanzees, detections still accumulated over time (Head et al. 2013, Després-Einspenner et al. 2017), possibly because chimpanzees focused their activity within different portions of their territory at different times to take advantage of resources available only temporarily (e.g. seasonally). Therefore, if the spatial survey design provides opportunities for spatial recaptures at a representative sample of distances, survey duration can be increased until sufficient detections are obtained. For example,

we had considered sampling northern and southern portions of KNP for only six months each, but later opted to leave CTs in place for twelve months to increase sample sizes. Increasing survey duration increases the expected number of violations of the assumption of demographic closure, but the consequences of closure violation are minor unless the sampled population is in severe decline (Dupont et al. 2019, Chapter 5).

Neither the simulations nor the field survey allowed me to identify optimal design specifications or minimum sample sizes for photographic SECR surveys of chimpanzees. Optimal numbers and spacings of detectors, and of clusters of detectors, and survey duration will vary with animal density, encounter rates, and home range sizes, and variation in these parameters (Clark 2019); pilot surveys are therefore likely to be invaluable when surveying previously unstudied populations. Furthermore, neither this nor prior simulation studies provided specific recommendations regarding minimum numbers of animals, recaptures, spatial recaptures, or DPA for reliable inference (the criteria for adequate sample sizes that I defined in the methods section were intended to help interpret simulation results rather than as guidelines for real surveys). Després-Einspenner et al. (2017) anlyzed spatial and temporal subsets of their data and argued that as few as five CTs deployed within a chimpanzee community for ten months could detect a large fraction of the community, and provide sufficient data to estimate abundance reliably even if CTs were deployed at random locations, but especially if they target habitat features known to be used by chimpanzees. This result was reassuring as the survey of KNP had already been carried out with clusters of five detectors spaced far enough apart that most sampled communities would be exposed to a risk of detection at only one or two clusters.

Efford and Boulanger (2019) approximated the precision of SECR estimates of density from sample size information. Approximating equations predicted that precision was maximized where the number of animals detected equalled the number of recaptures and animals were detected twice each on average (optimal DPA = 2); however, this assumed no variation in detection parameters or animal density (Efford and Boulanger 2019), and all three analyses of data from chimpanzees detected at CTs revealed that detection parameters do vary, including among individuals (Head et al. 2013, Després-Einspenner et al. 2017, this study). Head et al. (2013) obtained accurate and reasonably precise (CV = 0.12) density estimates in the presence of heterogeneity between sexes and latent groups of individuals from their data set with DPA = 3.5, but Després-Einspenner et al. (2017) showed that it could be problematic to model effects of prior detection even where mean DPA was ≈ 5.

Prior simulation studies, published photographic SECR surveys of chimpanzees, and this study do lead to some specific general recommendations regarding the design of surveys over large spatial scales. For example, the above paragraph leads me to recommend designing surveys with expected DPA of at least three, or continuing to sample at CTs already deployed until mean DPA exceeds three. We achieved a mean DPA of 5.4 with 10 CTs deployed within Ngogo territory for twelve months. At Taï, mean DPA was 26.1 after 1720 trap-weeks of sampling a single community at targeted locations, and 7.5 after 760 trap-weeks at randomly-selected locations (Després-Einspenner et al. 2017).

Clustered designs are more efficient than designs with fixed spacing between all adjacent detectors and are recommended for surveys over large areas. Furthermore, because chimpanzee density varies locally with habitat quality (Potts et al. 2009), and

activity centers may be clustered near the center of territories, designs with many small clusters are preferred over designs with few large clusters, and the locations for (centroids of) clusters should be selected according to a randomized design to provide representative samples over the region of interest. Available data suggests five CTs could yield adequate data from entire communities, and it is not necessary to expose all individuals or even all communities to a risk of detection, so there is great potential to survey large areas efficiently with relatively few CTs.

If clusters are small relative to the scale of movements during sampling (i.e. smaller than the expected or true home range or territory size), superior estimates can be obtained by altering cluster geometry to increase the maximum linear distance between CTs within clusters, or by spacing some clusters close enough together to provide opportunities for recaptures across clusters. When designing surveys, especially in the presence of uncertainty regarding territory or home range sizes, researchers should consider not only the extent and spacing of adjacent detectors within clusters as a function of expected mean home range size or σ, but the total opportunities for recaptures at different distances provided by interdetector distances within and between clusters to allow for uncertainty and variation in home range size and σ. Such designs need not employ clusters with common shapes, numbers of detectors, or within-cluster detector spacing, so could deviate from previous descriptions of clustered designs, most of which used constant cluster geometry and assumed clusters yielded independent samples. Data from Ngogo suggest detector spacing within clusters was unnecessarily close, because even the least mobile members of the community had larger-than-expected σ and were frequently detected at CTs up to 1 km apart. Future surveys of forested habitats could employ wider spacing (e.g. $\approx$ 1 km) of most adjacent detectors to

improve spatial coverage and therefore representativity, but I recommed that surveys include some detectors spaced e.g. ≤ 0.5 km apart because some social classes (or other groupings) of individuals may use smaller ranges than others, and surveys should be designed to detect the scale of their movements, as well as those of more mobile animals.

Chapter 7: Conclusions and Directions for Future Research

7.1 Distance sampling with camera traps

The extension of the familiar, well-described, and well-supported distance sampling framework for designing surveys and analyzing data to estimate animal abundance to accommodate data from camera traps represents an important development. The need for novel methods for estimating abundance of African great apes motivated the development of CTDS, and the method was successfully applied to estimate chimpanzee densities (Cappelle et al. 2019), but it is applicable to a wide range of species, including many that are among the most difficult to enumerate (e.g. because they inhabit dense forests, or are cryptic, elusive, or nocturnal), and many that are of social or economic importance or conservation concern. CTs detect a wide variety of animals of various taxa and thousands of them are already in use (Chapter 2), so methods that can take advantage of this wealth of data to provide information critical to assessements of population status are almost certain to be useful. Cappelle et al. (in review) estimated densities of four species that occur at a range of densities from CTDS data collected during a single survey, and obtained plausible estimates for all of them, though estimates for the rarest of them were imprecise. They estimated that they obtained sufficient data to estimate densities of an additional 17 species, including species listed as vulnerable to critically endangered by the IUCN.

That animals are not available for detection by CTs when stationary or outside the vertical range of sensors was potentially problematic because it complicates the quantification of the effective survey duration or temporal sampling effort during CTDS

surveys (Howe et al. 2017a). In Chapter 3 and Howe et al. (2017a) we demonstrated how overestimation of temporal sampling effort and underestimation of density could be avoided by including data only from times when all animals are active at ground level and hence available for detection, or by correcting naïve density estimates using an independent estimate of the proportion of time captive animals of the same species were active. However, local, concurrent estimates of availability would be preferred over independent estimates from the same species at a different time or location, and ideally availability would be estimable without collecting additional data. Cappelle et al. (2019) estimated chimpanzee density by CTDS after correcting for availability for detection by CTs as estimated from relative numbers of videos obtained per hour over the course of a day. We obtained an estimate of availability that was reasonably consistent with estimates of the proportion of time directly observed, habituated chimpanzees spent active on the ground, and an accurate estimate of density. Cappelle et al.'s (2019) estimate of availability did not have an associated estimate of variance, but Rowcliffe et al.'s (2014) maximum likelihood estimators of animals' daily proportion of time active and availability for detection at CTs do. Rowcliffe et al.'s (2014) methods could be used to estimate availability for detection from the same CT data that are used to estimate abundance by CTDS, and the associated variance could be incorporated into the total variance of estimated densities via the delta method. Both methods for estimating availability rely on the assumption that 100% of the population is available during the daily peak of activity. This may be reasonable for many species, especially those that are always on the ground when active and have predictable daily schedules. In the case of, for example, semi-arboreal or fossorial species, ancillary data might be needed to either support this assumption, or estimate the average proportion of

the population that is active during the daily peak of activity. Overall, it seems that the need to estimate availability should not prevent successful application of CTDS.

Animals' reactions to CTs may be more problematic than limited availability for detection. Effects of CTs on animal locations at any scale violates the assumption, common to most distance sampling methods, that locations of points (or lines) are independent of the locations of objects to which distances are measured. Avoidance of or attraction to the sites where CTs are deployed could affect the encounter rate, causing potentially severe under- or overestimation of density, respectively. Estimates of availability for detection might also be biased. Attraction may be apparent in images or videos, but animals that avoid the entire site provide no evidence of having done so, so it will be difficult to estimate or quantify the magnitude of this potential source of bias. Furthermore, even within the zone of potential detection by a CT, any reaction to the device or the site could affect the distances between CTs and animals at snapshot moments. Deploying CTs one to several weeks in advance of the actual survey could allow resident animals to become accustomed to them and so reduce reactions during the survey. Censoring observations of animals obviously reacting to the camera could reduce positive bias in the encounter rate caused by attraction and bias in the observed distances, but is clearly only a partial solution.

Censoring observations of animals reacting to CTs, and even truncating data to avoid bias associated with e.g. reduced detectability at very short distances (e.g., because small animals may pass beneath the field of view, and large animals might not be identifiable to species if they obscure the entire field of view) reduces the total number of observations of distance included in the data. However, currently, there is no associated correction to our estimate of temporal effort – the number of opportunities to

detect animals at a point (T_k / t; Chapter 3). Therefore, censoring and truncation cause underestimation of the encounter rate (observations per opportunity in CTDS). The total number of opportunities is typically very large (e.g., the number of 2-second intervals over weeks, months, or years), so bias might be slight, but it would still be preferable to explicitly account for the lost opportunities, as well as the lost observations, when data are censored or truncated.

Trends in abundance may be of equal or greater interest than absolute abundance, but precise estimates are required to detect all but dramatic differences in abundance between replicate surveys. Animals' non-random movements and habitat use combined with the small area monitored by individual CTs will almost inevitably lead to high variation in the encounter rate among locations, and hence imprecise density estimates, especially for animals that are rare or patchily-distributed. Great apes and many other species of conservation concern exist at relatively low densities and interact with their habitat in complex ways, so estimated densities of these species may have the greatest associated uncertainty. However, densities of more common, ubiquitous or generalist species can be estimated more precisely from surveys of shorter duration, and many species, common or rare, are subject to the same risk factors, for example hunting or poaching. Therefore, CTDS can provide information relevant to the conservation of, and potentially informative regarding trends in mortality and abundance of, great apes and other species of conservation concern, even if surveys do not yield precise estimates of their mortality rates or abundances, by identifying any sudden changes in the abundance of other species. CTDS monitoring of common species can therefore serve as an early warning system for potential declines in sympatric species that are more difficult and take longer to enumerate.

CTDS severely violates the assumption that observations are independent, which causes model selection criteria unadjusted for overdispersion (such as AIC) to favour overparameterized models. The new methods for selecting among candidate models of the detection function presented in Chapter 4 and Howe et al. (2019) can improve our ability to identify parsimonious models when observations lack independence, so could be useful when selecting among models fitted to data collected at CTs, and possibly in other contexts, such as cue counting surveys or surveys of social animals. However, our adjusted criteria and procedures improved inferences from simulated data only slightly, and their performance was not consistently superior to AIC with real data. More applications and comparisons to other approaches to model selection are needed before these methods can be recommended for general use.

In my opinion, CTDS and time-lapse photography, where images are recorded at regular intervals regardless of whether or not an animal triggers a sensor, provides potentially the best marriage of technology and statistical methods currently available for estimating animal abundance from CT data. Time-lapse photography avoids many of the potential shortcomings of CTDS as currently described. Failure to detect animals close to the camera and heterogeneity in detectability with angle relative to the center of the field of view associated with the performance of the sensor would be of no concern. Cameras could be programmed to record images at exactly the predetermined snapshot moments without any missed detections due to slow trigger speeds or delays between the time when the camera stops recording images or videos and the time it can be triggered again, and images could be recorded more frequently at times when the target species (or more of the target species) are expected to be active to improve efficiency. The effective detection distance would be limited only by intervening vegetation,

undulating terrain, and image quality, so the area effectively monitored by each CT would be larger (especially in more open habitats), and the detection function would have a broad plateau with almost certain detection out to a longer distance than sensors could provide, increasing sample sizes and facilitating reliable estimation of detectability. Some CTs can be programmed to record images on a time lapse as well as when the sensor is triggered, and improved CTs are being developed and marketed to researchers, so other benefits of CTs (detecting very rare species, observing animal behaviour, etc.) could still be realized. Whether an image resulted from a time-lapse photograph or an animal triggering the sensor could be included as a covariate of the detection function. A major disadvantage of time-lapse photography is that it is expected to yield a large number of images with no animals, and processing them could become very time consuming, but as described in Chapter 2 and below, this is becoming less problematic.

7.2 Spatially explicit capture–recapture

Spatially explicit capture–recapture (SECR) is an increasingly popular framework for estimating abundance of individually identifiable animals, and provides many advantages. SECR models do not assume perfect detection of any animals, regardless of their location relative to the CT, so partial avoidance of or imperfect detection by CTs are not as problematic as in the CTDS context. Furthermore, CT placement need not be completely random; researchers can target habitat features known to be preferred or used by the targeted species to increase encounter rates and therefore sample sizes (though care should still be taken to ensure representative samples are obtained). Reactions to CTs also pose less of a problem. Reactions that

affect distances between CTs and animals but do not prevent animals from being detected and identified have no adverse effect (in fact apes that show interest in CTs may present their faces, facilitating identification) and various types of reactions that affect the encounter rate (e.g. trap-specific or general, permanent or Markovian) can be modelled to avoid or minimize bias.

When I started researching great apes in 2014, primatologists had only recently recognized the potential of SECR (Head et al. 2013, Moore and Vigilant 2014). This collaboratively-funded PhD provided opportunities to analyze existing data sets and design new surveys to evaluate and rigorously apply SECR methods to chimpanzees. Analyses of photographic data (1) demonstrated that spatially intensive photographic sampling of small study areas can yield accurate estimates of chimpanzee density, of superior precision to those obtained from either line transect surveys to nests or CTDS (Després-Einspenner et al. 2017, Capelle et al. 2019), (2) identified several sources of heterogeneity in the parameters of the detection function that had not previously been considered (Després-Einspenner et al. 2017, Chapter 6), (3) demonstrated how the group territoriality chimpanzees exhibit can adversely affect inferences from small study areas (Després-Einspenner et al. 2017), (4) informed survey design for larger study areas spanning the territories of multiple stable social groups ("communities") of chimpanzees, including in the presence of variation and uncertainty in the sizes of communities' territories and individuals' home ranges (Chapter 6), and (5) demonstrated the potential of photographic SECR for efficiently enumerating chimpanzees at landscape scales (Després-Einspenner et al. 2017, Chapter 6).

In addition, until recently, concerns about the consequences of violation of the assumption of demographic closure required by many CR and SECR estimators of

abundance had been raised, but inadequately addressed. Here, analyses of real data sets and simulations demonstrated that when demographically open but approximately stable chimpanzee populations are sampled over long durations (e.g. 1 year), densities estimated from SECR models that assume demographic closure yield estimates with little or no bias (Després-Einspenner et al. 2017, Chapter 5, also see Dupont et al. 2019). Simulations further demonstrated that if declining populations are sampled, there is potential for closure violation to cause overestimation of abundance at the end of the survey, and hence to mask those declines (Chapter 5).

Successful implementation of SECR would require that rates of misidentification error (incorrect identifications of individuals from genetic profiles or images) are minimized, certainly below 5%, and preferably below 1%. When errors are more frequent, models that assume animals are identified without error yield biased estimates, and estimates from models that allow for errors are likely to be too imprecise to be useful (Chapter 2). Negligible error rates are likely being achieved in fecal genetic surveys, but accuracy of individual identification from CT data is more difficult to quantify (Chapter 2). When identifying individuals from images, low-quality images in which distinctive features are not clearly visible should be discarded. Ideally, multiple observers would independently identify individuals from the same images, and only identifications upon which all observers agreed would be included in the data to minimize errors. Manually identifying and matching individuals from CT data is time consuming (Capelle et al. 2019, Chapter 6), but this situation could soon improve as described in Chapter 2 and below.

7.3 Synthesis

The most appropriate combination of sampling and analytical methods for monitoring great apes will depend on several study-specific factors, including study objectives and their relative importance, how much is already known about the population of interest, the size of the area it occupies, and the level of precision required. The combination of fecal genetic sampling and SECR is likely to be efficient and effective where neither the area to be searched nor the total number of samples to be analyzed need be very large, to reduce the time and resources required to search for and analyze the samples. Genetic sampling may therefore be most efficient for small populations that are limited in distribution (Guschanski et al. 2009, Chancellor et al. 2012, Roy et al. 2014), and where chimpanzees occupying fragmented habitat are sampled (McCarthy et al. 2015). Genetic samples can also be used to address a wide range of other questions (Arandjelovic and Vigilant 2018). Photographic SECR avoids costs associated with molecular analyses, can be effective on small study areas, and clustered or creative designs could facilitate efficient monitoring over large spatial scales (Head et al. 2013, Després-Einspenner et al. 2017, Chapter 6). Photographic SECR analyses are informative regarding sociodemographic structure (Head et al. 2013, Chapter 6), and the images and videos obtained can also be used to address other questions (Chapter 2). Regardless of the sampling method, SECR often yields more precise estimates of great ape abundance than indirect methods and methods that do not require individual identification (Chapter 2, Cappelle et al. 2019), so might be preferred where precise estimates are required.

CTDS does not require that CTs be spaced close enough together to detect the same animals at more than one location, but requires a randomized design. These

characteristics make it well-suited for surveys of great apes over large areas where little is previously known about the population of interest, because even surveys that yield sparse data can provide estimates of occupancy and abundance, and even imprecise estimates of abundance have value where other estimates are unavailable or out of date. CTDS shows great promise as a multispecies biomonitoring tool; limited data available at this time suggests densities of a wide range of species, including chimpanzees, could be estimated from a single survey, and that densities of common animals could be estimated with reasonable precision (Chapter 3, Howe et al. 2017a, Cappelle et al. 2019, in review).

The research described in this thesis is immediately applicable using technology, field methods, and software already available and familiar to many ecologists, and could help inform urgent conservation decisions. Furthermore, positive feedback is being generated by the increasing implementation of CT surveys and the rapid development of methods for processing and analyzing the resulting images and data. As more CTs have been purchased for research purposes, CT technology has improved and become more affordable (Glover-Kapfer et al. 2019), providing more of the high-quality images or videos in which animals and individuals are easier to identify. As photographic data sets became increasingly large and time-consuming to process manually, automated methods for managing data and processing images, including to identify animals to species or even to individual, were developed to ensure the data could be utilized (Niedballa et al. 2016, Cruchant et al. 2017, Tabak et al. 2019). As more animals are captured in videos or rapid bursts of photographs and confidently identified, galleries of known individuals grow, further improving the performance of automated methods for recognizing individuals, including new individuals (Freytag et al. 2016). And finally, as

CT and computer vision technology improve and become more affordable and accessible, CT surveys become more efficient and feasible. For these reasons, and because both CTDS and photographic SECR fall within larger frameworks and so can accommodate ongoing developments in those frameworks, I suggest that the usefulness of the methods described here for estimating abundance of great apes and other species from CT data will only increase in the near future.

Bibliography

Ahumada JA, Hurtado J, Lizcano D. 2013. Monitoring the status and trends of tropical forest terrestrial vertebrate communities from camera trap data: a tool for conservation. PLoS One 8:e73707

Ahumada JA, Silva CEF, Gjapersad K, Hallam C, Hurtado J, Martin E, McWilliam A, Mugerwa B, O'Brien T, Rovero F, Sheil D, Spironello WR, Winarni N, Andelman SJ. 2011. Community structure and diversity of tropical forest mammals: data from a global camera trap network. Philosophical Transactions of the Royal Society B: Biological Sciences 366:2703–2711

Akaike H. 1973. Information theory as an extension of the maximum likelihood principle. Pp. 267-281 *in* BN Petrov and F Csaki (eds). Second international symposium on information theory. Akademiai Kiado, Budapest, Hungary

Anderson DR, Burnham KP, White GC. 1994. AIC model selection in over dispersed capture-recapture data. Ecology 75:1780–93

Anile S, Ragni B, Randi E, Mattucci F, Rovero F. 2014 Wildcat population density on the Etna volcano, Italy: a comparison of density estimation methods. Journal of Zoology 293:252-261

Apps P, McNutt JW. 2018. Are camera traps fit for purpose? A rigorous, reproducible and realistic test of camera trap performance. African Journal of Ecology 56:710–720

Arandjelovic M, Bergl RA, Ikfuingei R, Jameson C, Parker M, Vigilant L. 2015. Detection dog efficacy for collecting faecal samples from the critically endangered Cross River gorilla (*Gorilla gorilla diehli*) for genetic censusing. Royal Society Open Science 2:140423

Arandjelovic M, Guschanski K, Schubert G, Harris TR, Thalmann O, Siedel H, Vigilant L. 2009. Two-step multiplex polymerase chain reaction improves the speed and accuracy of genotyping using DNA from noninvasive and museum samples. Molecular Ecology Resources 9:28–36

Arandjelovic M, Head J, Kühl H, Boesch C, Robbins MM, Maisels F, Vigilant L. 2010. Effective non-invasive genetic monitoring of multiple wild western gorilla groups. Biological Conservation 143:1780–1791

Arandjelovic M, Head J, Rabanal LI, Schubert G, Mettke E, Boesch C, Robbins MM, Vigilant L. 2011. Non-invasive genetic monitoring of wild central chimpanzee PLoS One 6:e14761

Arandjelovic M, Vigilant L. 2018. Non-invasive genetic censusing and monitoring of primate populations. American Journal of Primatology 80:e22743

Arcus Foundation. 2014. State of the apes: extractive industries and ape conservation. Arcus Foundation. New York, USA and Cambridge, UK

Ardovini A, Cinque L, Della Rocca F, Sangineto E. 2007. A semi-automatic approach to photo identification of wild elephants. pp 225–232 *in* Pattern Recognition and Image Analysis. Springer, Berlin Heidelberg, Germany

Arnason AN, Mills KH. 1981. Bias and loss of precision due to tag loss in Jolly-Seber estimates for mark–recapture experiments. Canadian Journal of Fisheries and Aquatic Sciences 38:1077–1095

Augustine B. 2019. OpenPopSCR. R package. https://github.com/benaug/OpenPopSCR

Augustine BC, Royle JA, Murphy SM, Chandler RB, Cox JJ, Kelly MJ. 2018. Spatial capture–recapture for categorically marked populations with an application to genetic capture–recapture. Ecosphere 10:e02627

Balestrieri A, Ruiz-González A, Vergara M, Capelli E, Tirozzi P, Alfino S, Minuti G, Prigioni C, Saino N. 2016. Pine marten density in lowland riparian woods: a test of the Random Encounter Model based on genetic data. Mammalian Biology 81:439-446

Banks SC, Piggott MP, Hansen BD, Robinson NA, Taylor AC. 2002. Wombat coprogenetics: enumerating a common wombat population by microsatellite analysis of fecal DNA. Australian Journal of Zoology 50:193–204

Basabose AK, Inoue E, Kamungu S, Murhabale B, Akomo-Okoue EF, Yamagiwa J. 2015. Estimation of chimpanzee community size and genetic diversity in Kahuzi-Biega National Park, Democratic Republic of Congo. American Journal of Primatology 77:1015–1025

Bateson PPG. 1977. Testing an observer's ability to identify individual animals. Animal Behaviour 25:247–248

Bednar–Friedl B, Behrens DA, Getzner M. 2012. Optimal dynamic control of visitors and endangered species in a national park. Environmental & Resource Economics 52:1–22

Beja-Pereira A, Oliveira R, Alves PC, Schwartz MK, Luikart G. 2009. Advancing ecological understandings through technological transformations in noninvasive genetics. Molecular Ecology Resources 9:1279–1301

Boesch C, Boesch-Achermann H. 2000. The Chimpanzees of the Taï Forest: Behavioural Ecology and Evolution. Oxford University Press, Oxford, UK

Boesch C, Kohou G, Néné H, Vigilant L. 2006. Male competition and paternity in wild chimpanzees of the Taï forest. American Journal of Physical Anthropology 130:103–115

Bonin A, Bellemain E, Eidesen PB, Pompanon F, Brochmann C, Taberlet P. 2004. How to track and assess genotyping errors in population genetics studies. Molecular Ecology 13:3261–3273

Bonner JS, Holmberg J. 2013. Mark-recapture with multiple, non-invasive marks. Biometrics 69:766–775

Borchers D. 2012. A non-technical overview of spatially explicit capture–recapture models. Journal of Ornithology 152:435-444

Borchers DL, Buckland ST, Zucchini W. 2002. Estimating Animal Abundance: Closed Populations. Springer Science and Business Media, New York, USA

Borchers D, Distiller G, Foster R, Harmsen B, Milazzo L. 2014. Continuous-time spatially explicit capture–recapture models, with an application to a jaguar camera-trap survey. Methods in Ecology and Evolution 5:656–665

Borchers DL, Efford MG. 2008. Spatially explicit maximum likelihood methods for capture–recapture studies. Biometrics. 64:377-85

Boulanger J, McLellan B. 2001. Closure violation in DNA-based mark-recapture estimation of grizzly bear populations. Canadian Journal of Zoology 79:642–651

Boulanger J, Nielsen SE, Stenhouse GB. 2018. Using spatial mark-recapture for conservation monitoring of grizzly bear populations in Alberta. Scientific Reports 8:5204

Bowkett AE, Plowman AB, Stevens JR, Davenport TR, van Vuuren BJ. 2009. Genetic testing of dung identification for antelope surveys in the Udzungwa Mountains, Tanzania. Conservation Genetics 10:251-255

Bradley BJ, Chambers K and Vigilant L. 2001. Accurate DNA-based sex identification of apes using non-invasive samples. Conservation Genetics 2:179-181

Bradley BJ, Doran-Sheehy DM, Vigilant L. 2008. Genetic identification of elusive animals: re-evaluating tracking and nesting data for wild western gorillas. Journal of Zoology 275:333–340

Bretagnolle V, Thibault J, Dominici J. 1994. Field identification of individual ospreys using head marking pattern. Journal of Wildlife Management 58:175–178

Brust CA, Burghardt T, Groenenberg M, Kading C, Kuhl HS, Manguette ML, Denzler J. Towards automated visual monitoring of individual gorillas in the wild. 2017. pp 2820–2830 *in* Proceedings of the IEEE International Conference on Computer Vision

Buckland ST. 1984. Monte Carlo confidence intervals. Biometrics 40:811–817

Buckland ST. 2006. Point transect surveys for songbirds: robust methodologies. The Auk 123:345–357

Buckland ST, Anderson DR, Burnham KP, Laake JL, Borchers DL, Thomas L. 2001. Introduction to Distance Sampling: Estimating Abundance of Biological Populations. Oxford University Press, Oxford, UK

Buckland ST, Anderson DR, Burnham KP, Laake JL, Borchers DL, Thomas L. 2004. Advanced Distance Sampling: Estimating Abundance of Biological Populations. Oxford University Press, Oxford, UK

Buckland ST, Goudie IBJ, Borchers DL. 2000. Wildlife population assessment: past developments and future directions. Biometrics 56:1–12

Buckland ST, Plumptre AJ, Thomas L, Rexstad EA. 2010. Design and analysis of line transect surveys for primates. International Journal of Primatology 31:833–47

Buckland ST, Rexstad EA, Marques TA, Oedekoven CS. 2015. Distance Sampling: Methods and Applications. Springer, Heidelberg, Germany

Buckland ST, Summers RW, Borchers DL, Thomas LE. 2006. Point transect sampling with traps or lures. Journal of Applied Ecology 43:377–384

Burnham KP, Anderson DR. 2001. Kullback-Leibler information as a basis for strong inference in ecological studies. Wildlife research 28:111–119

Burnham KP, Anderson DR. 2002. Model Selection and Inference: A Practical Information Theoretic Approach. Second Edition. Springer Science and Business Media, New York, USA

Burnham KP, Anderson DR, Laake JL. 1980. Estimating density from line-transect sampling of biological populations. Wildlife Monographs 72:1–102

Burnham PK, Buckland ST, Laake JL, Borchers DL, Marques TA, Bishop JRB, Thomas L. 2004. Further topics in distance sampling. Chapter 11, pages 307–392 i*n* Buckland ST, Anderson DR, Burnham KP, Laake JL, Borchers DL, and Thomas L. (eds). Advanced Distance Sampling: Estimating Abundance of Biological Populations. Oxford University Press, Oxford, UK

Burton AC, Neilson E, Moreira D, Ladle A, Steenweg R, Fisher JT, Bayne E, Boutin S. 2015. Review: wildlife camera trapping: a review and recommendations for linking surveys to ecological processes. Journal of Applied Ecology 52:675–685

Campbell G, Kuehl H, Diarrassouba A, N'Goran PK, Boesch C. 2011. Long-term research sites as refugia for threatened and over-harvested species. Biology Letters 7:723–726

Campbell G, Kuehl H, Kouamé PNG, Boesch C. 2008. Alarming decline of West African chimpanzees in Côte d'Ivoire. Current Biology 18:R903–R904

Cappelle N, Boesch C, Howe EJ, Kühl H. In review. Estimating animal abundance and effort-precision relationship with camera trap distance sampling. Ecosphere

Cappelle N, Després-Einspenner ML, Howe EJ, Boesch C, Kühl HS. 2019. Validating camera trap distance sampling for chimpanzees. American Journal of Primatology 81:e22962

Caravaggi A, Zaccaroni M, Riga F, Schai-Braun SC, Dick JT, Montgomery WI, Reid N. 2016. An invasive-native mammalian species replacement process captured by camera trap survey random encounter models. Remote Sensing in Ecology and Conservation 2:45–58

Carvalho JS, Marques TA, Vicente L. 2013. Population status of *Pan troglodytes verus* in Lagoas de Cufada Natural Park, Guinea-Bissau. PLoS One 8:e71527

Caughlan L, Oakley KL. 2001. Cost considerations for long-term ecological monitoring. Ecological Indicators 1:123–134

Chancellor RL, Langergraber K, Ramirez S, Rundus AS, Vigilant L. 2012. Genetic sampling of unhabituated chimpanzees (*Pan troglodytes schweinfurthii*) in Gishwati Forest Reserve, an isolated forest fragment in western Rwanda. International Journal of Primatology 33:479–488

Chandler RB, Royle JA. 2013. Spatially explicit models for inference about density in unmarked or partially marked populations. The Annals of Applies Statistics 7:936–954

Chandler RB, Royle JA, King DI. 2011. Inference about density and temporary emigration in unmarked populations. Ecology 92:1429–1435

Chapman CA, Wrangham RW. 1993. Range use of the forest chimpanzees of Kibale: implications for the understanding of chimpanzee social organization. American Journal of Primatology 31:263–273

Clark JD. 2019. Comparing clustered sampling designs for spatially explicit estimation of population density. Population Ecology 61:93–101

Clark CJ, Poulsen JR, Malonga R, Elkan, PW Jr. 2009. Logging concessions can extend the conservation estate for Central African tropical forests. Conservation Biology 23:1281–1293

Cohen J. 1960. A coefficient of agreement for nominal scales. Educational and psychological measurement 20:37–46

Cormack RM. 1964. Estimates of survival from the sighting of marked animals. Biometrika 51:429–438

Cox DR, Snell EJ. 1989. Analysis of Binary Data. Second edition. Chapman and Hall, New York, USA

Creel S, Spong G, Sands JL, Rotella J, Zeigle J, Joe L, Murphy KM, Smith D. 2003. Population size estimation in Yellowstone wolves with error-prone non-invasive microsatellite genotypes. Molecular Ecology 12:2003–2009

Crunchant AS, Egerer M, Loos A, Burghardt T, Zuberbühler K, Corogenes K, Leinert V, Kulik L, Kühl HS. 2017. Automated face detection for occurrence and occupancy estimation in chimpanzees. American Journal of Primatology 79:e22627

Cruz P, Paviolo A, Bó RF, Thompson JJ, Di Bitetti MS. 2014. Daily activity patterns and habitat use of the lowland tapir (*Tapirus terrestris*) in the Atlantic Forest. Mammalian Biology-Zeitschrift für Säugetierkunde 79:376-83

Cusack JJ, Dickman AJ, Rowcliffe JM, Carbone C, Macdonald DW, Coulson T. 2015b. Random versus game trail-based camera trap placement strategy for monitoring terrestrial mammal communities. PLoS One 10:e0126373

Cusack JJ, Swanson A, Coulson T, Packer C, Carbone C, Dickman AJ, Kosmala M, Lintott C, Rowcliffe JM. 2015a. Applying a random encounter model to estimate lion density from camera traps in Serengeti National Park, Tanzania. The Journal of Wildlife Management 79:1014-1021

Darroch JN. 1958. The multiple-recapture census: I. Estimation of a closed population. Biometrika 45:343–359

Denes FV, Silveira LF, Beissinger SR. 2015. Estimating abundance of unmarked animal populations: accounting for imperfect detection and other sources of zero inflation. Methods in Ecology and Evolution 6:543–556

Després-Einspenner M-L, Howe EJ, Drapeau P, Kühl HS. 2017. An empirical evaluation of camera trapping and spatially explicit capture-recapture models for estimating chimpanzee density. American Journal of Primatology 79:e22647

Devos C, Sanz C, Morgan D, Onononga J-R, Laporte N, Huynen M-C. 2008b. Comparing ape densities and habitats in Northern Congo: surveys of sympatric gorillas and chimpanzees in the Odzala and Ndoki regions. American Journal of Primatology 70:1–13

Devos C, Walsh PD, Arnhem E, Huynen M-C. 2008a. Monitoring population decline: can transect surveys detect the impact of the Ebola virus on apes. Oryx 42:367–374

DeYoung RW, Honeycutt RL. 2005. The molecular toolbox: genetic techniques in wildlife ecology and management. Journal of Wildlife Management 69:1362–1384

Dice LR. 1938. Some census methods for mammals. Journal of Wildlife Management 2:119–130

Dillon A. Kelly MJ. 2008. Ocelot home range, overlap and density: comparing radio telemetry with camera trapping. Journal of Zoology 275:391–398

Dorazio RM, Royle JA. 2003. Mixture models for estimating the size of a closed population when capture rates vary among individuals. Biometrics 59:351–364

Drichi P. 2003. National Biomass Study Technical Report of 1996–2002. Forest Department, Ministry of Water Lands and Environment, P.O. Box 1613, Kampala, Uganda.

Driessen MM, Jarman PJ, Troy S, Callander S. 2017. Animal detections vary among commonly used camera trap models. Wildlife Research 44:291–297

Dudley JP, Ginsberg JR, Plumptre AJ, Hart JA, Campos LC. 2002. Effects of war and civil strife on wildlife and wildlife habitats. Conservation Biology 16:319–329

Dupont P, Milleret C, Gimenez O, Bischof R. 2019. Population closure and the bias-precision trade-off in spatial capture–recapture. Methods in Ecology and Evolution 10:661–672

Efford MG. 2004. Density estimation in live-trapping studies. Oikos 106:598-610

Efford MG. 2011. Estimation of population density by spatially explicit capture–recapture analysis of data from area searches. Ecology 92:2202–2207

Efford MG. 2014. Bias from heterogeneous usage of space in spatially explicit capture–recapture analyses. Methods in Ecology and Evolution 5:599–602

Efford MG. 2017. SECR: Spatially explicit capture-recapture models. R package version 3.1.3. https://CRAN.R-project.org/package=secr

Efford MG. 2019d. Non-circular home ranges and the estimation of population density. Ecology 100:e02580

Efford MG. 2019a. openCR: Open population capture–recapture. R package version 1.4.1 https://cran.r-project.org/package=openCR

Efford MG. 2019b. secr: Spatially explicit capture-recapture models. R package version 3.2.0. https://CRAN.R-project.org/package=secr

Efford MG. 2019c. secrdesign: Sampling Design for Spatially Explicit Capture-Recapture. R package version 2.5.7. https://CRAN.R-project.org/package=secrdesign

Efford MG, Borchers DL, Byrom AE. 2009b. Density estimation by spatially explicit capture–recapture: likelihood-based methods. pp 255–269 *in* Thompson DL, Cooch EG, Conroy MJ (eds). Modeling Demographic Processes in Marked Populations. Springer, New York, USA

Efford MG, Borchers DL Mowat G. 2013. Varying effort in capture–recapture studies. Methods in Ecology and Evolution 4:629–636

Efford MG, Boulanger J. 2019. Fast evaluation of study designs for spatially explicit capture-recapture. Methods in Ecology and Evolution 10:1529–1535

Efford MG, Dawson DK, Borchers DL. 2009a. Population density estimated from locations of individuals on a passive detector array. Ecology 90:2676–2682

Efford MG, Fewster RM. 2013. Estimating population size by spatially explicit capture–recapture. Oikos 122:918–928

Efford MG, Hunter CM. 2018. Spatial capture–mark–resight estimation of animal population density. Biometrics 74:411–420

Efford MG, Warburton B, Coleman MC, Barker RJ. 2005. A field test of two methods for density estimation. Wildlife Society Bulletin 33:731–738

Ely JJ, Frels WI, Howell S, Izard MK, Keeling ME, Lee DR. 2006. Twinning and heterpaternity in chimpanzees (*Pan troglodytes*). American Journal of Physical Anthropology 130:96-102.

Ennis S, Gallagher TF. 1994. A PCR-based sex-determination assay in cattle based on the bovine amelogenin locus. Animal Genetics 25:425–427

FAO (Food and Agriculture Organization of the United Nations). 2010. Global forest resources assessment 2010. Rome, Italy

Ferraro PJ, Pattanayak SK. 2006. Money for nothing? A call for empirical evaluation of biodiversity conservation investments. PLoS biology 4:e105

Fewster RM, Buckland ST, Burnham KP, Borchers DL, Jupp PE, Laake JL, Thomas L. 2009. Estimating the encounter rate variance in distance sampling. Biometrics 65:225–236

Fiske I, Chandler R. 2011. unmarked: An R package for fitting hierarchical models of wildlife occurrence and abundance. Journal of Statistical Software 43:1–23

Flagstad Ø, Røed K, Stacy JE, Jakobsen KS. 1999. Reliable noninvasive genotyping based on excremental PCR of nuclear DNA purified with a magnetic bead protocol. Molecular Ecology 8:879–883

Forcada J, Aguilar A. 2000. Use of photographic identification in capture–recapture studies of Mediterranean monk seals. Marine Mammal Science 16:767–793

Foster RJ, Harmsen BJ. 2012. A critique of density estimation from camera-trap data. Journal of Wildlife Management 76:224–236

Foster VC, Sarmento P, Sollmann R, Tôrres N, Jácomo ATA, Negrões N, Fonseca C, Silveira L. 2013. Jaguar and puma activity patterns and predator-prey interactions in four Brazilian biomes. Biotropica 45:373–379

Frantzen MAJ, Silk JB, Ferguson JWH, Wayne RK, Kohn MH. 1998. Empirical evaluation of preservation methods for faecal DNA. Molecular Ecology 7:1423–1428

Freytag A, Rodner E, Simon M, Loos A, Kühl HS, Denzler J. 2016. Chimpanzee faces in the wild: Log-euclidean cnns for predicting identities and attributes of primates. pp 51–63 *in* German Conference on Pattern Recognition. Springer, Cham, Switzerland

Friday N, Smith TD, Stevick PT, Allen J. 2000. Measurement of photographic quality and animal distinctiveness for the photographic identification of humpback whales. Marine Mammal Science 16:355–374

Gagneux P, Boesch C, Woodruff DS. 1997. Microsatellite scoring errors associated with non-invasive genotyping based on nuclear DNA amplified from shed hair. Molecular Ecology 6:861–868

Gardner B, Reppucci J, Lucherini M, Royle JA. 2010. Spatially explicit inference for open populations: estimating demographic parameters from camera-trap studies. Ecology 91:3376-3383

Gardner B, Sollmann R, Kumar NS, Jathanna D, Karanth KU. 2018. State space and movement specification in open population spatial capture–recapture models. Ecology and Evolution 8:10336-10344

Garner KJ, Ryder OA. 1996. Mitochondrial DNA diversity in gorillas. Molecular Phylogenetics and Evolution 6:39–48

Gerloff U, Schlötterer C, Rassmann K, Rambold I, Hohmann G, Fruth B, Tautz D. 1995. Amplification of hypervariable simple sequence repeats (microsatellites) from excremental DNA of wild living bonobos (*Pan paniscus*). Molecular Ecology 4:515–518

Glennie R, Borchers DL. 2019. openpopscr: Open population spatial capture–recapture. R package version 1.0.0. https://github.com/r-glennie/openpopscr/

Glennie R, Borchers DL, Murchie M, Harmsen BJ, Foster RJ. 2019. Open population maximum likelihood spatial capture–recapture. Biometrics 75:1–11

Glennie R, Buckland ST, Thomas L. 2015. The effect of animal movement on line transect estimates of abundance. PLoS One 10:e0121333

Glover-Kapfer P, Soto-Navarro CA, Wearn OR. 2019. Camera-trapping version 3.0: current constraints and future priorities for development. Remote Sensing in Ecology and Conservation.

Goossens B, Waits LP, Taberlet P. 1998. Plucked hair samples as a source of DNA: reliability of dinucleotide microsatellite genotyping. Molecular Ecology 7:1237–1241

Granjon AC, Rowney C, Vigilant L, Langergraber KE. 2017. Evaluating genetic capture-recapture using a chimpanzee population of known size. The Journal of Wildlife Management 81:279-288

Griffiths M, van Schaik CP. 1993. Camera-trapping: a new tool to study elusive rain forest animals. Tropical Biodiversity 1:11–13

Gruen L, Fultz A, Pruetz J. 2013. Ethical issues in African great ape field studies. ILAR Journal 54:24–32

Guschanski K, Vigilant L, McNeilage A, Gray M, Kagoda E, Robbins M. 2009. Counting elusive animals: comparing field and genetic census of the entire mountain gorilla population of Bwindi Impenetrable National Park, Uganda. Biological Conservation 142:290–300

Hamel S, Killengreen ST, Henden JA, Eide NE, Roed-Eriksen L, Ims RA, Yoccoz NG. 2013. Towards good practice guidance in using camera-traps in ecology: influence of sampling design on validity of ecological inferences. Methods in Ecology and Evolution 4:105–113

Harcourt AH, Parks SA. 2003. Threatened primates experience high human densities: adding an index of threat to the IUCN Red List criteria. Biological Conservation 109:137–149

Harmsen BJ, Foster RJ, Silver S, Ostro L, Doncaster CP. 2010. Differential use of trails by forest mammals and the implications for camera-trap studies: a case study from Belize. Biotropica 42:126–133

Hashimoto C. 1995. Population census of the chimpanzees in the Kalinzu forest, Uganda: comparison between methods with nest counts. Primates 36:477–488

Head JS, Boesch C, Robbins MM, Rabanal LI, Makaga L, Kühl HS. 2013. Effective sociodemographic population assessment of elusive species in ecology and conservation management. Ecology and Evolution 3:2903–2916

Hedmark E, Ellegren H. 2006. A test of the multiplex pre-amplification approach in microsatellite genotyping of wolverine faecal DNA. Conservation Genetics 7:289–293

Hicks TC, Darby L, Hart J, Swinkels J, January N, Menken S. 2010. Trade in orphans and bushmeat threatens one of the Democratic Republic of the Congo's most important populations of Eastern Chimpanzees (*Pan troglodytes schweinfurthii*). African Primates 7:1-8

Hill K, Boesch C, Goodall J, Pusey A, Williams J, Wrangham R. 2001. Mortality rates among wild chimpanzees. Journal of Human Evolution 40:437-450

Hockings M, Stolton S, Leverington F, Dudley N, Courrau J. 2006. Evaluating Effectiveness: A Framework for Assessing Management Effectiveness of Protected Areas, Second Edition. IUCN, Gland, Switzerland and Cambridge, UK

Hofmeester TR, Rowcliffe JM, Jansen PA. 2017. A simple method for estimating the effective detection distance of camera traps. Remote Sensing in Ecology and Conservation 3:81–89

Hoppe-Dominik B, Kühl HS, Radl G, Fischer F. 2011. Long term monitoring of large rainforest mammals in the Biosphere Reserve of Taï National Park, Cote d'Ivoire. African Journal of Ecology 49:450–458

Howe EJ, Buckland ST, Després-Einspenner ML, Kühl HS. 2017a. Distance sampling with camera traps. Methods in Ecology and Evolution 8:1558–1565

Howe EJ, Buckland ST, Després-Einspenner ML, Kühl HS. 2017b. Data from: Distance sampling with camera traps. Dryad Digital Repository, https://doi.org/10.5061/dryad.b4c70

Howe EJ, Buckland ST, Després-Einspenner ML, Kühl HS. 2018. Data from: Model selection with overdispersed distance sampling data. Dryad Digital Repository, https://doi.org/10.5061/dryad.j2p2h3s

Howe EJ, Buckland ST, Després-Einspenner ML, Kühl HS. 2019. Model selection with overdispersed distance sampling data. Methods in Ecology and Evolution 10:38–47

Howe EJ, Obbard ME, Kyle CJ. 2013. Combining data from 43 standardized surveys to estimate densities of female American black bears by spatially explicit capture–recapture. Population Ecology 55:595–607

Huijbregts B, De Wachter P, Ndong Obiang LS, Akou ME. 2003. Ebola and the decline of gorilla (*Gorilla gorilla*) and chimpanzee (*Pan troglodytes*) populations in Minkebe Forest, north-eastern Gabon. Oryx 37:437–443

Humle T, Maisels F, Oates JF, Plumptre A, Williamson EA. 2016. *Pan troglodytes*. The IUCN Red List of Threatened Species 2016: e.T15933A129038584

Hutchinson JM, Waser PM. 2007. Use, misuse and extensions of "ideal gas" models of animal encounter. Biological Reviews 82:335–359

IUCN. 2014. The IUCN red List of threatened species. Version 2014.3. www.iucnredlist.org.

IUCN. 2017. The IUCN red list of threatened species. Version 2017-3. www.iucnredlist.org.

Ivan JS, White GC, Shenk TM. 2013. Using simulation to compare methods for estimating density from capture–recapture data. Ecology 94:817–826

Iwata Y, Ando C. 2007. Bed and bed-site reuse by western lowland gorillas (*Gorilla g. gorilla*) in Moukalaba-Doudou National Park, Gabon. Primates 48:77–80

Jacobs CE, Ausband DE. 2018. An evaluation of camera trap performance–What are we missing and does deployment height matter? Remote Sensing in Ecology and Conservation 4:352–360

Jathanna D, Karanth KU, Johnsingh AJT. 2003. Estimation of large herbivore densities in the tropical forests of southern India using distance sampling. Journal of Zoology 261:285-290

Jędrzejewski W, Puerto MF, Goldberg JF, Hebblewhite M, Abarca M, Gamarra G, Calderón LE, Romero JF, Viloria ÁL, Carreño R, Robinson HS. 2017. Density and population structure of the jaguar (*Panthera onca*) in a protected area of Los Llanos, Venezuela, from 1 year of camera trap monitoring. Mammal Research 62:9–19

Johnson DS, Laake JL, Ver Hoef JM. 2010. A model-based approach for making ecological inference from distance sampling data. Biometrics 66:310–318

Johnson JB, Omland KS. 2004. Model selection in ecology and evolution. Trends in Ecology and Evolution 19:101–108

Junker J, Blake S, Boesch C, Campbell G, Toit LD, Duvall C, Ekobo A, Etoga G, Galat-Luong A, Gamys J, Ganas-Swaray J, Gatti S, Ghiurghi A, Granier N, Hart J, Head J, Herbinger I, Hicks TC, Huijbregts B, Imong IS, Kuempel N, Lahm S, Lindsell J, Maisels F, McLennan M, Martinez L, Morgan B, Morgan D, Mulindahabi F, Mundry R, N'Goran KP, Normand E, Ntongho A, Okon DT, Petre C-A, Plumptre A, Rainey H, Regnaut S, Sanz C, Stokes E, Tondossama A, Tranquilli S, Sunderland-Groves J, Walsh P, Warren Y, Williamson EA, Kuehl HS. 2012. Recent decline in suitable environmental conditions for African great apes. Diversity and Distributions 18:1077–1091

Kahlenberg SM, Emery Thompson M, Wrangham RW. 2008. Female competition over core areas in *Pan troglodytes schweinfurthii*, Kibale National Park, Uganda. International Journal of Primatology 29:931–947

Kamgang SA, Bobo KS, Maisels F, Ambahe RD, Ongono DE, Gonder MK, Johnson P, Marino J, Sinsin B. 2018. The relationship between the abundance of the Nigeria-

Cameroon chimpanzee (*Pan troglodytes ellioti*) and its habitat: a conservation concern in Mbam-Djerem National Park, Cameroon. BMC Ecology 18:40

Karanth KU. 1995. Estimating tiger *Panthera tigris* populations from camera-trap data using capture–recapture models. Biological conservation 71:333-338

Karanth KU, Nichols JD. 1998. Estimation of tiger densities in India using photographic captures and recaptures. Ecology 79:2852–2862

Karanth KU, Nichols JD, Kumar NS, Hines JE. 2006. Assessing tiger population dynamics using photographic capture–recapture sampling. Ecology 87:2925–2937

Keim JL, Lle SR, DeWitt PD, Fitzpatrick JJ, Jenni NS. 2019. Estimating the intensity of use by interacting predators and prey using camera traps. Journal of Animal Ecology 88:690–701

Kelly MJ. 2008. Design, evaluate, refine: camera trap studies for elusive species. Animal Conservation 11:182–184

Kendall WL. 1999. Robustness of closed capture-recapture methods to violations of the closure assumption. Ecology 80:2517-2525

Kendall WL, Pollock KH, Brownie C. 1995. A likelihood-based approach to capture–recapture estimation of demographic parameters under the robust design. Biometrics 51:293–308

Klailova M, Casanova C, Henschel P, Lee P, Rovero F, Todd A. 2012. Non-human predator interactions with wild great apes in Africa and the use of camera traps to study their dynamics. Folia Primatologica 83:312–328

Köndgen S, Kühl H, N'Goran PK, Walsh PD, Schenk S, Ernst N, Biek R, Formenty P, Mätz-Rensing K, Schweiger B, Junglen S. 2008. Pandemic human viruses cause decline of endangered great apes. Current Biology 18:260-264

Koster SH, Hart JA. 1988. Methods of estimating ungulate populations in tropical forests. African Journal of Ecology 26:117-126

Kouakou CY, Boesch C, Kuehl H. 2009. Estimating chimpanzee population size with nest counts: validating methods in Taï National Park. American Journal of Primatology 71:447–457

Kuehl HS, Todd A, Boesch C, Walsh PD. 2007. Manipulating decay time for efficient large-mammal density estimation: gorillas and dung height. Ecological Applications 17:2403-2414

Kühl HS, Burghardt T. 2013. Animal biometrics: quantifying and detecting phenotypic appearance. Trends in Ecology and Evolution 28:432–441

Kühl H, Maisels H, Ancrenaz M, Williamson EA. 2008. Best practice guidelines for surveys and monitoring of great ape populations. IUCN/SSC Primate Specialist Group, Gland, Switzerland

Kühl HS, Sop T, Williamson EA, Mundry R, Brugière D, Campbell G, Cohen H, Danquah E, Ginn L, Herbinger I, Jones S. 2017. The critically endangered western chimpanzee declines by 80%. American Journal of Primatology 79:e22681.

Kukielka E, Barasona JA, Cowie CE, Drewe JA, Gortazar C, Cotarelo I, Vicente J. 2013. Spatial and temporal interactions between livestock and wildlife in South Central Spain assessed by camera traps. Preventive Veterinary Medicine 112:213–221

Kumar S, Singh SK. 2016. Visual animal biometrics: survey. IET Biometrics 6:139–156

Laake J, Borchers D, Thomas L, Miller D, J Bishop. 2016. mrds: Mark recapture distance sampling. R package version 2.1.5. https://CRAN.R-project.org/package=mrds

Laake J, Borchers D, Thomas L, Miller D, J Bishop. 2017. mrds: Mark recapture distance sampling. R package version 2.1.17. https://CRAN.R-project.org/package=mrds

Laake, J, Borchers D, Thomas L, Miller D, Bishop J. 2018. mrds: Mark-Recapture Distance Sampling. R package version 2.2.0. https://CRAN.R-project.org/package=mrds

Laake JL, Collier BA, Morrison ML, Wilkins RN. 2011. Point-based mark-recapture distance sampling. Journal of Agricultural, Biological, and Environmental Statistics 16:389–408

Laing SE, Buckland ST, Burn RW, Lambie D, Amphlett A. 2003. Dung and nest surveys: estimating decay rates. Journal of Applied Ecology 40:1102–1111

Landis JR, Koch GG. 1977. The measurement of observer agreement for categorical data. Biometrics 33:159–l74

Laporte NT, Stabach JA, Grosch R, Lin TS, Goetz SJ. 2007. Expansion of industrial logging in Central Africa. Science 316:1451

Lashey MA, Cove MV, Chitwood MC, Penido G, Gardner B, DePerno CS, Moorman CE. 2018. Estimating wildlife activity curves: comparison of methods and sample size. Scientific Reports 8:4173

Lebreton J-D, Burnham KP, Clobert J, Anderson DR 1992. Modeling survival and testing biological hypotheses using marked animals: a unified approach with case studies. Ecological Monographs 62:67–118

Le Saout S, Chollet S, Chamaillé-Jammes S, Blanc L, Padié S, Verchere T, Gaston AJ, Gillingham MP, Gimenez O, Parker KL, Picot D. 2014. Understanding the paradox of deer persisting at high abundance in heavily browsed habitats. Wildlife Biology 20:122–136

Leuchtenberger C, Zucco CA, Ribas C, Magnusson W, Mourão G. 2014. Activity patterns of giant otters recorded by telemetry and camera traps. Ethology Ecology & Evolution 26:19–28

Liang K-Y, McCullagh P. 1993. Case studies in binary dispersion. Biometrics 49:623–630

Link WA. 2004. Individual heterogeneity and identifiability in capture–recapture models. Animal Biodiversity and Conservation 27:87–91

Link WA, Yoshizaki J, Bailey LL, Pollock KH. 2010. Uncovering a latent multinomial: analysis of mark–recapture data with misidentification. Biometrics 66:178–185

Linkie M, Dinata Y, Nugroho A, Haidir IA. 2007. Estimating occupancy of a data deficient mammalian species living in tropical rainforests: sun bears in the Kerinci Seblat region, Sumatra. Biological Conservation 137:20–27

Loos A, Ernst A. 2013. An automated chimpanzee identification system using face detection and recognition. EURASIP Journal on Image and Video Processing 1:49

Lucas TCD, Moorcroft EA, Freeman R, Rowcliffe JM, Jones KE. 2015. A generalised random encounter model for estimating animal density with remote sensor data. Methods in Ecology and Evolution 6:500–509

Lukacs PM, Burnham KP. 2005. Estimating population size from DNA-based closed capture-recapture data incorporating genotyping error. Journal of Wildlife Management 69:396–403

Lynam AJ, Jenks KE, Tantipisanuh N, Chutipong W, Ngoprasert D, Gale GA, Steinmetz R, Sukmasuang R, Bhumpakphan N, Grassman Jr LI, Cutter P. 2013. Terrestrial activity patterns of wild cats from camera-trapping. Raffles Bulletin of Zoology 61:407–415

MacKenzie DI, Nichols JD, Lachman GB, Droege S, Royle JA, Langtimm CA. 2002. Estimating site occupancy rates when detection probabilities are less than one. Ecology 83:2248–2255

MacKenzie DI, Royle JA. 2005. Designing occupancy studies: general advice and allocating survey effort. Journal of Applied Ecology 42:1105–1114

Manzo E, Bartolommei P, Rowcliffe JM, Cozzolino R. 2012. Estimation of population density of European pine marten in central Italy using camera trapping. Acta Theriologica 57:165–172

Marini F, Franzetti B, Calabrese A, Cappellini S, Focardi S. 2009. Response to human presence during nocturnal line transect surveys in fallow deer (*Dama dama*) and wild boar (*Sus scrofa*). European Journal of Wildlife Research 55:107–115

Marques FFC and Buckland ST. 2003. Incorporating covariates into standard line transect analyses. Biometrics 59:924–935

Marques TA, Buckland ST, Borchers DL, Tosh D, McDonald RA. 2010 Point transect sampling along linear features. Biometrics 66:1247-1255

Marques TA, Buckland ST, Bispo R, Howland B. 2013. Accounting for animal density gradients using independent information in distance sampling surveys. Statistical Methods & Applications 22:67–80

Marques TA, Thomas L, Fancy SG, Buckland ST. 2007. Improving estimates of bird density using multiple-covariate distance sampling. The Auk 124:1229–1243

Marques TA, Thomas L, Royle JA. 2011. A hierarchical model for spatial capture–recapture data: comment. Ecology 92:526–528

Marshall AR, Lovett JC, White PCL. 2008. Selection of line-transect methods for estimating the density of group-living animals: lessons from the primates. American Journal of Primatology 70:452–462

Mathews A, Mathews A. 2004. Survey of gorillas (*Gorilla gorilla gorilla*) and chimpanzees (*Pan troglodytes troglodytes*) in southwestern Cameroon. Primates 45:15–24

Mathewson PD, Spehar SN, Meijaard E, Sasmirul A, Marshall AJ. 2008. Evaluating orangutan census techniques using nest decay rates: implications for population estimates. Ecological Applications 18:208–221

McCarthy MS, Lester JD, Howe EJ, Arandjelovic M, Stanford CB, Vigilant L. 2015. Genetic censusing identifies an unexpectedly sizeable population of an endangered large mammal in a fragmented forest landscape. BMC Evolutionary Biology 15:21

McCullagh P, Nelder JA. 1989. Generalized Linear Models. Second Edition. Chapman and Hall, New York, USA

McKelvey KS, Schwartz MK. 2004. Genetic errors associated with population estimation using non-invasive molecular tagging: problems and new solutions. Journal of Wildlife Management 68:439–448

Meek PD, Ballard GA, Fleming PJ. 2015. The pitfalls of wildlife camera trapping as a survey tool in Australia. Australian Mammalogy 37:13–22

Meek P, Fleming P, Ballard G, Banks P, Claridge A, Sanderson J, Swann D. (eds). 2014. Camera Trapping: Wildlife Management and Research. CSIRO Publishing, Collingwood, Australia

Mehlman PT, Doran DM. 2002. Influencing western gorilla nest construction at Mondika Research Center. International Journal of Primatology 23:1257–1285

Miller CR, Joyce P, Waits LP. 2005. A new method for estimating the size of small populations from genetic mark-recapture data. Molecular Ecology 14:1991–2005

Miller DL. 2015. Distance: distance sampling detection function and abundance estimation. R package version 0.9.4. https://CRAN.R-project.org/package=Distance

Miller DL. 2017. Distance: distance sampling detection function and abundance estimation. R package version 0.9.7. https://CRAN.R-project.org/package=Distance

Miller DL, Burt ML, Rexstad EA, Thomas L. 2013. Spatial models for distance sampling data: recent developments and future directions. Methods in Ecology and Evolution 4:1001–1010

Mills LS, Citta JJ, Lair KP, Schwartz MK, Tallmon DA. 2000. Estimating animal abundance using noninvasive DNA sampling: promise and pitfalls. Ecological Applications 10:283–294

Mitani JC, Call J, Kappeler PM, Palombit RA, Silk JB (eds). 2012. The Evolution of Primate Societies. University of Chicago Press, Chicago, USA and London, UK

Mitani JC, Watts DP, Amsler SJ. 2010. Lethal intergroup aggression leads to territorial expansion in wild chimpanzees. Current Biology 20:R507-R508

Moeller AK, Lukacs PM, Horne JS. 2018. Three novel methods to estimate abundance of unmarked animals using remote cameras. Ecosphere 9:e02331

Monteiro L, Bonnemaison D, Vekris A, Petry KG, Bonnet J, Vidal R, Cabrita J, Mégraud F. 1997. Complex polysaccharides as PCR inhibitors in feces: Helicobacter pylori model. Journal of Clinical Microbiology 35:995–998

Montgomery S. 2009. Walking With the Great Apes, Jane Goodall, Dian Fossey, Biruté Galdikas. Chelsea Green Publishing, White River Junction, VT, USA

Moore DL, Vigilant L. 2014. A population estimate of chimpanzees (*Pan troglodytes schweinfurthii*) in the Ugalla region using standard and spatially explicit genetic capture–recapture methods. American Journal of Primatology 76:335–346

Morgan B, Adeleke A, Bassey T, Bergl R, Dunn A, Gonder K, Greengrass E, Koulagna DK, Mbah G, Nicholas A, Oates J, Omeni F, Saidu Y, Sommer V, Sunderland-Groves J, Tiebou J, Williamson L. 2011. Regional action plan for the conservation of the Nigeria-Cameroon chimpanzee (*Pan troglodytes ellioti*). IUCN/SSC Primate Specialist

Group and Zoological Society of San Diego, CA, USA. http://www.primate-sg.org/PDF/Nigeria_Cameroon_Chimpanzee_Action_Plan_2011_English.pdf

Morgan D, Sanz S, Onononga JR, Strindberg S. 2006. Ape abundance and habitat use in the Goualougo Triangle, Republic of Congo. International Journal of Primatology 27:147–179

Morin PA, Chambers KE, Boesch C, Vigilant L. 2001. Quantitative polymerase chain reaction analysis of DNA from noninvasive samples for accurate microsatellite genotyping of wild chimpanzees (*Pan troglodytes verus*). Molecular Ecology 10:1835–1844

Morin PA, Moore JJ, Chakraborty R, Jin L, Goodall J, Woodruff DS. 1994a. Kin selection, social structure, gene flow, and the evolution of chimpanzees. Science 265:1193–1201

Morin PA, Wallis J, Moore JJ, Woodruff DS. 1994b. Paternity exclusion in a community of wild chimpanzees. Molecular Ecology 3:469–478

Morrison TA, Yoshizaki J, Nichols JD, Bolger DT. 2011. Estimating survival in photographic capture–recapture studies: overcoming misidentification error. Methods in Ecology and Evolution 2:454–463

Muller MN, Wrangham RW. 2014. Mortality rates among Kanyawara chimpanzees. Journal of Human Evolution 66:107–114

Nakashima Y, Fukasawa K, Samejima H. 2018. Estimating animal density without individual recognition using information derivable exclusively from camera traps. Journal of Applied Ecology 55:735–744

Nakashima Y, Iwata Y, Ando C, Nze Nkoguee C, Inoue E, Akomo EF, Nguema PM, Bineni TD, Banak LN, Takenoshita Y, Ngomanda A. 2013. Assessment of landscape-scale distribution of sympatric great apes in African rainforests: Concurrent use of nest and camera-trap surveys. American Journal of Primatology 75:1220–1230

Navidi W, Arnheim N, Waterman MS. 1992. A multiple-tubes approach for accurate genotyping of very small DNA samples by using PCR: statistical considerations. American Journal of Human Genetics 50:347–359

Negrões N, Sarmento P, Cruz J, Eira C, Revilla E, Fonseca C, Sollmann R, Tôrres NM, Furtado MM, Jácomo AT, Silveira L. 2010. Use of camera-trapping to estimate puma density and influencing factors in central Brazil. Journal of Wildlife Management 74:1195–1203

Newey S, Davidson P, Nazir S, Fairhurst G, Verdicchio F, Irvine RJ, van der Wal R. 2015. Limitations of recreational camera traps for wildlife management and conservation research: A practitioner's perspective. Ambio 44:624–635

Newing HS. 1994. Behavioural ecology of duikers (*Cephalophus* spp.) in forest and secondary growth, Taï, Côte d'Ivoire. Ph.D. thesis, University of Stirling, Scotland

Newing HS. 2001. Bushmeat hunting and management: implications of duiker ecology and interspecific competition. Biodiversity and Conservation 10:99–118

Niedballa J, Sollmann R, Courtiol A, Wilting A. 2016. camtrapR: an R package for efficient camera trap data management. Methods in Ecology and Evolution 7:1457–1462

N'Goran PK. 2006. Quelques résultats de la première phase du biomonitoring au Parc National de Taï (août 2005 – mars 2006). Ministere de l'Environnement et des Eaux et Forets, Ministere de l'Enseignement Superieur et de la Recherce Scientifique, Abidjan, Côte d'Ivoire.

N'Goran Kouamé P, Boesch C, Mundry R, N'Goran EK, Herbinger I, Yapi FA, Kühl HS. 2012. Hunting, law enforcement, and African primate conservation. Conservation Biology 26:565–571

Nishida T, Corp N, Hamai M, Hasegawa T, Hiraiwa-Hasegawa M, Hosaka K, Hunt KD, Itoh N, Kawanaka K, Matsumoto-Oda A, Mitani JC. 2003. Demography, female life history, and reproductive profiles among the chimpanzees of Mahale. American Journal of Primatology 59:99-121

Noss AJ, Gardner B, Maffei L, Cuéllar E, Montaño R, Romero-Muñoz A, Sollman R, O'Connell AF. 2012. Comparison of density estimation methods for mammal populations with camera traps in the Kaa-Iya del Gran Chaco landscape. Animal Conservation 15:527–535

Nsubuga AM, Robbins MM, Roeder AD, Morin PA, Boesch C, Vigilant L. 2004. Factors affecting the amount of genomic DNA extracted from ape faeces and the identification of an improved sample storage method. Molecular Ecology 13:2089–2094

Obbard ME, Howe EJ, Kyle CJ. 2010. Empirical comparison of density estimators for large carnivores. Journal of Applied Ecology 47:76–84

Obbard ME, Stapleton S, Middel KR, Thibault I, Brodeur V, Jutras C. 2015. Estimating the abundance of the Southern Hudson Bay polar bear subpopulation with aerial surveys. Polar Biology 38:1713–1725

Ogawa H, Idani G, Moore JJ, Pintea L, Hernandez A. 2007. Sleeping parties and bed distribution of chimpanzees in the savanna woodland, Ugalla, Tanzania. International Journal of Primatology 28:1397–1412

Omeja PA, Chapman CA, Obua J, Lwanga JS, Jacob AL, Wanyama F, Mugenyi R. 2011. Intensive tree planting facilitates tropical forest biodiversity and biomass accumulation in Kibale National Park, Uganda. Forest Ecology and Management 261:703–709

Otis DL, Burnham KP, White GC, Anderson DR. 1978. Statistical inference from capture data on closed animal populations. Wildlife Monographs 62:3–135

Paetkau D. 2003. An empirical exploration of data quality in DNA-based population inventories. Molecular Ecology 6:1375–1387

Paetkau D. 2004. The optimal number of markers in genetic capture-mark–recapture studies. The Journal of Wildlife Management 68:449–452

Palsbøll PJ, Allen J, Bérubé M, Clapham PJ, Feddersen TP, Hammond PS, Hudson H, Jorgensen S. Katona AH, Larsen F, Larsen J, Lien DK, Mattila J, Sigurjónsson RR, Sears R, Smith T, Sponer R, Stevick P, Øien N. 1997. Genetic tagging of humpback whales. Nature (London) 388:767–769

Pebsworth PA, LaFleur M. 2014. Advancing primate research and conservation through the use of camera traps: introduction to the special issue. International Journal of Primatology 35:825–840

Petit E, Valiere N. 2006. Estimating population size with non-invasive capture-mark-recapture data. Conservation Biology 20:1062–1073

Pettorelli N, Lobora AL, Msuha MJ, Foley C, Durant SM. 2010. Carnivore biodiversity in Tanzania: revealing the distribution patterns of secretive mammals using camera traps. Animal Conservation 13:131–139

Piel AK, Cohen N, Kamenya S, Ndimuligo SA, Pintea L, Stewart FA. 2015. Population status of chimpanzees in the Masito-Ugalla Ecosystem, Tanzania. American Journal of Primatology 77:1027–1035

Pledger S. 2000. Unified maximum likelihood estimates for closed capture–recapture models using mixtures. Biometrics 56:434–442

Plumptre AJ. 2000. Monitoring mammal populations with line transect techniques in African forests. Journal of Applied Ecology 37:356-368

Plumptre AJ, Cox D. 2006. Counting primates for conservation: primate surveys in Uganda. Primates 47:65–73

Plumptre AJ, Reynolds V. 1994. The effect of selective logging on the primate populations in the Budongo Forest Reserve, Uganda. Journal of Applied Ecology 31:631–641

Plumptre AJ, Reynolds V. 1996. Censusing chimpanzees in the Budongo forest, Uganda. International Journal of Primatology 17:85–99

Plumptre AJ, Reynolds V. 1997. Nesting behavior of chimpanzees: implications for censuses. International Journal of Primatology 18:475–485

Plumptre AJ, Rose R, Nangendo G, Williamson EA, Didier K, Hart J, Mulindahabi F, Hicks C, Griffin B, Ogawa H, Nixon S, Pintea L, Vosper A, McLennan M, Amsini F, McNeilage A, Makana JR, Kanamori M, Hernandez A, Piel A, Stewart F, Moore J, Zamma K, Nakamura M, Kamenya S, Idani G, Sakamaki T, Yoshikawa M, Greer D, Tranquilli S, Beyers R, Hashimoto C, Furuichi T, Bennett E. 2010. Eastern chimpanzee (*Pan troglodytes schweinfurthii*): status survey and conservation action plan 2010-2020. IUCN, Gland, Switzerland

Pollock KH, Nichols JD, Brownie C, and Hines JE. 1990. Statistical inference for capture–recapture experiments. Wildlife Monographs 107:3–97

Potts KB, Chapman CA, Lwanga JS. 2009. Floristic heterogeneity between forested sites in Kibale National Park, Uganda: insights into the fine-scale determinants of density in a large-bodied frugivorous primate. Journal of Animal Ecology 78:1269–1277

Poulsen JR, Clark CJ, Bolker BM. 2011. Decoupling the effects of logging and hunting on an Afrotropical animal community. Ecological Applications 21:1819–1836

Pradel R, Hines JE, Lebreton JD, Nichols JD. 1997. Capture–recapture survival models taking account of transients. Biometrics 53:60–72

R Core Team. 2015. R: A language and environment for statistical computing, version 3.2.1. R Foundation for Statistical Computing, Vienna, Austria. http://www.R-project.org/

R Core Team. 2016. R: A language and environment for statistical computing, version 3.3.2. R Foundation for Statistical Computing, Vienna, Austria. http://www.R-project.org/

R Core Team. 2017. R: A language and environment for statistical computing, version 3.4.2. R Foundation for Statistical Computing, Vienna, Austria. https://www.R-project.org

R Core Team. 2019. R: A language and environment for statistical computing, version 3.5.3. R Foundation for Statistical Computing, Vienna, Austria. http://www.R-project.org/

Reich BJ, Gardner B. 2014. A spatial capture–recapture model for territorial species. Environmetrics 25:630–637

Richards SA. 2008. Dealing with overdispersed count data in applied ecology. Journal of Applied Ecology 45:218–227

Roon DA, Waits LP, Kendall KC. 2005. A simulation test of the effectiveness of several methods for error-checking non-invasive genetic data. pp 203–215 *in* Animal Conservation Forum (Vol. 8, No. 2,). Cambridge University Press.

Rovero F, Marshall AR 2004. Estimating the abundance of forest antelopes by line transect techniques: a case from the Udzungwa Mountains of Tanzania. Tropical Zoology 17:267-277

Rovero F, Marshall AR. 2009. Camera trapping photographic rate as an index of density in forest ungulates. Journal of Applied Ecology 46:1011–1017

Rovero F, Zimmermann F (eds). 2016. Camera Trapping for Wildlife Research. Pelagic Publishing Ltd. Exeter, UK

Rovero F, Zimmermann F, Berzi D, Meek P. 2013. "Which camera trap type and how many do I need?" A review of camera features and study designs for a range of wildlife research applications. Hystrix, the Italian Journal of Mammalogy 24:148–156

Rowcliffe JM, Carbone C, Jansen PA, Kays R, Kranstauber B. 2011. Quantifying the sensitivity of camera traps: an adapted distance sampling approach. Methods in Ecology and Evolution 2:464–476

Rowcliffe JM, Carbone C, Kays R, Kranstauber B, Jansen PA. 2012. Bias in estimating animal travel distance: the effect of sampling frequency. Methods in Ecology and Evolution 3:653–662

Rowcliffe, JM, Field J, Turvey ST, Carbone C. 2008. Estimating animal density using camera traps without the need for individual recognition. Journal of Applied Ecology 45:1228–1236

Rowcliffe JM, Jansen PA, Kays R, Kranstauber B, Carbone C. 2016. Wildlife speed cameras: measuring animal travel speed and day range using camera traps. Remote Sensing in Ecology and Conservation 2:84–94

Rowcliffe JM, Kays R, Carbone C, Jansen PA. 2013. Clarifying assumptions behind the estimation of animal density from camera trap rates. Journal of Wildlife Management 77:876

Rowcliffe JM, Kays R, Kranstauber B, Carbone C, Jansen PA. 2014. Quantifying levels of animal activity using camera trap data. Methods in Ecology and Evolution 5:1170–1179

Roy J, Vigilant L, Gray M, Wright E, Kato R, Kabano P, Basabose A, Tibenda E, Kühl HS, Robbins MM. 2014. Challenges in the use of genetic mark-recapture to estimate the population size of Bwindi mountain gorillas (*Gorilla beringei beringei*). Biological Conservation 180:249–261

Royle JA, Chandler RB, Sollmann R, Gardner B. 2013c. Spatial Capture-Recapture. Academic Press

Royle, JA, Chandler RB, Gazenski KD, Graves TA. 2013a. Spatial capture-recapture models for jointly estimating population density and landscape connectivity. Ecology 94:287–294

Royle JA, Chandler RB, Sun CC, Fuller AK. 2013b. Integrating resource selection information with spatial capture–recapture. Methods in Ecology and Evolution 4:520–530

Royle JA, Karanth KU, Gopalaswamy AM, Kumar NS. 2009a. Bayesian inference in camera-trapping studies for a class of spatial capture–recapture models. Ecology 90:3233–3244

Royle JA, Nichols JD, Karanth KU, Gopalaswamy AM 2009b. A hierarchical model for estimating density in camera-trap studies. Journal of Applied Ecology 46:118–127

Royle JA, Young KV. 2008. A hierarchical model for spatial capture–recapture data. Ecology 89:2281–2289

Schneider S, Taylor GW, Linquist S, Kremer SC. 2019. Past, present and future approaches using computer vision for animal re-identification from camera trap data. Methods in Ecology and Evolution 10:461–470

Schwarz CJ, Seber GA. 1999. Estimating animal abundance: review III. Statistical Science 1:427–456

Schwartz CJ, Stobo WT. 1999. Estimation and effects of tag-misread rates in capture–recapture studies. Canadian Journal of Fisheries and Aquatic Sciences 56:551–559

Schwartz MK, Luikart G, Waples RS. 2007. Genetic monitoring as a promising tool for conservation and management. Trends in Ecology & Evolution 22:25–33

Seber GAF. 1965. A note on the multiple–recapture census. Biometrika 52:249–259

Séquin ES, Jaeger MM, Brussard PF, Barrett RH. 2003. Wariness of coyotes to camera traps relative to social status and territory boundaries. Canadian Journal of Zoology 81:2015–2025

Silver SC, Ostro LE, Marsh LK, Maffei L, Noss AJ, Kelly MJ, Wallace RB, Gomez H, Ayala G. 2004. The use of camera traps for estimating jaguar *Panthera onca* abundance and density using capture/recapture analysis. Oryx 38:148–154

Soisalo MK, Cavalcanti SMC. 2006. Estimating the density of a jaguar population in the Brazilian Pantanal using camera-traps and capture–recapture sampling in combination with GPS radio-telemetry. Biological Conservation 129:487–496

Sollmann R, Furtado MM, Gardner B, Hofer H, Jácomo AT, Tôrres NM, Silveira L. 2011. Improving density estimates for elusive carnivores: accounting for sex-specific

detection and movements using spatial capture–recapture models for jaguars in central Brazil. Biological Conservation 144:1017–1024

Sollmann R, Gardner B, Belant JL. 2012. How does spatial study design influence density estimates from spatial capture–recapture models? PLoS One 7:e34575

Sollmann R, Mohamed A, Kelly MJ. 2013a. Camera trapping for the study and conservation of tropical carnivores. The Raffles Bulletin of Zoology 28:21–42

Sollmann R, Mohamed A, Samejima H, Wilting A. 2013b. Risky business or simple solution – relative abundance indices from camera trapping. Biological Conservation 159:405–412

Stanley TR, Burnham KP. 1999. A closure test for time-specific capture–recapture data. Environmental and Ecological Statistics 6:197–209

Stevens DL Jr, and Olsen AR. 2004. Spatially-balanced sampling of natural resources. Journal of the American Statistical Association 99:262–278

Stevick PT, Palsbøll PJ, Smith TD, Bravington MV, Hammond PS. 2001. Errors in identification using natural markings: rates, sources, and effects on capture recapture estimates of abundance. Canadian Journal of Fisheries and Aquatic Sciences, 58:1861–1870

Stokes EJ, Strindberg S, Bakabana PC, Elkan PW, Iyenguet FC, Madzoké B, Malanda GA, Mowawa BS, Moukoumbou C, Ouakabadio FK, Rainey HJ. 2010. Monitoring great ape and elephant abundance at large spatial scales: measuring effectiveness of a conservation landscape. PLoS One 5:e10294

Sun CC, Fuller AK, Royle JA. 2014. Trap configuration and spacing influences parameter estimates in spatial capture-recapture models. PLoS One 9:e88025

Sunderland-Groves JL, Ekinde A, Mboh H. 2009. Nesting behavior of Gorilla *gorilla diehli* at Kagwene Mountain, Cameroon: implications for assessing group size and density. International Journal of Primatology 30:253–266

Sutherland C, Fuller AK, Royle JA. 2015. Modelling non-Euclidean movement and landscape connectivity in highly structured ecological networks. Methods in Ecology and Evolution 6: 169–177

Tabak MA, Norouzzadeh MS, Wolfson DW, Sweeney SJ, VerCauteren KC, Snow NP, Halseth JM, Di Salvo PA, Lewis JS, White MD, Teton B. 2019. Machine learning to classify animal species in camera trap images: applications in ecology. Methods in Ecology and Evolution 10:585–590

Taberlet P, Griffin S, Goossens B, Questiau S, Manceau V, Escaravage N, Waits LP, Bouvet J. 1996. Reliable genotyping of samples with very low DNA quantities using PCR. Nucleic Acids Research 24:3189–3194

Taberlet P, Waits LP, Luikart G. 1999. Noninvasive genetic sampling: look before you leap. Trends in Ecology & Evolution 14:323–327

Tagg N, Willie J. 2013. The influence of transect use by local people and reuse of transects for repeated surveys on nesting in Western Lowland Gorillas (*Gorilla gorilla gorilla*) and Central Chimpanzees (*Pan troglodytes troglodytes*) in Southeast Cameroon. International Journal of Primatology 34:554–570

Thomas L, Buckland ST, Rexstad EA, Laake JL, Strindberg S, Hedley SL, Bishop JR, Marques TA, Burnham KP. 2010. Distance software: design and analysis of distance sampling surveys for estimating population size. Journal of Applied Ecology 47:5–14

Thompson ME, Kahlenberg SM, Gilby IC, Wrangham RW. 2007. Core area quality is associated with variance in reproductive success among female chimpanzees at Kibale National Park. Animal Behaviour 73:501–512

Thompson ME, Wrangham RW. 2008. Diet and reproductive function in wild female chimpanzees (*Pan troglodytes schweinfurthii*) at Kibale National Park, Uganda. American Journal of Physical Anthropology 135:171–181

Thorn M, Scott DM, Green M, Bateman PW, Cameron EZ. 2009. Estimating brown hyaena occupancy using baited camera traps. South African Journal of Wildlife Research 39:1–10

Tobler MW, Powell GVN. 2013. Estimating jaguar densities with camera traps: Problems with current designs and recommendations for future studies. Biological Conservation 159:109–118

Todd AF, Kuehl HS, Cipolletta C, Walsh PD. 2008. Using dung to estimate gorilla density: Modeling dung production rate. International Journal of Primatology 29:549–563

Trailcampro.com. Accessed Aug, 2015. http://www.trailcampro.com/

Tredick CA, Vaughan MR, Stauffer DF, Simek SL, Eason T. 2007. Sub-sampling genetic data to estimate black bear population size: a case study. Ursus 18:179–188

Treves A, Mwima P, Plumptre AJ, Isoke S. 2010. Camera-trapping forest–woodland wildlife of western Uganda reveals how gregariousness biases estimates of relative abundance and distribution. Biological Conservation 143:521–528

Trolle M, Kéry M. 2003. Estimation of ocelot density in the Pantanal using capture–recapture analysis of camera-trapping data. Journal of Mammalogy 84:607–614

Trolliet F, Vermeulen C, Huynen MC, Hambuckers A. 2014. Use of camera traps for wildlife studies: a review. Biotechnologie, Agronomie, Société et Environnement 18:446–454

Tutin CEG, Parnell RJ, White LJT, Fernandez M. 1995. Nest building by lowland gorillas in the Lopé Reserve, Gabon: environmental influences and implications for censusing. International Journal of Primatology 16:53–76

Tweh CG, Kouakou CY, Chira R, Freeman B, Githaiga JM, Kerwillain S, Molokwu-Odozi M, Varney M, Junker J. 2018. Nest counts reveal a stable chimpanzee population in Sapo National Park, Liberia. Primate Conservation 32:12

Tweh CG, Lormie MM, Kouakou CY, Hillers A, Kühl HS, Junker J. 2015. Conservation status of chimpanzees *Pan troglodytes verus* and other large mammals in Liberia: a nationwide survey. Oryx 49:710–708

Vale RTR, Fewster RM, Carroll EL, Patenaude NJ. 2014. Maximum likelihood estimation for model $M_{t,\alpha}$ for capture–recapture data with misidentification. Biometrics 70:962–971

Van Schaik CP, Priatna A, Priatna D. 1995. Population estimates and habitat preferences of orangutans based on line transects of nests. pp 129–147 *in* The Neglected Ape. Springer, Boston, MA

Van Schaik CP, Wich S, Utami S, Odom K. 2005. A simple alternative to line transects of nests for estimating orangutan densities. Primates 46:249–254

Vigilant L. 2002. Technical challenges in the microsatellite genotyping of a wild chimpanzee population using feces. Evolutionary Anthropology S1:162–165

Vincent C, Meynier L, Ridoux V. 2001. Photo-identification in grey seals: legibility and stability of natural markings. Mammalia 65:363–372

Waits JL, Leberg PL. 2000. Biases associated with population estimation using molecular tagging. pp 191–199 *in* Animal Conservation Forum (Vol. 3, No. 3) Cambridge University Press

Waits LP, Luikart G, Taberlet P. 2001. Estimating the probability of identity among genotypes in natural populations: cautions and guidelines. Molecular Ecology 10:249–256

Waits LP, Paetkau D. 2005. Noninvasive genetic sampling tools for wildlife biologists: a review of applications and recommendations for accurate data collection. Journal of Wildlife Management 69:1419–1433

Wallis J. 1995. Seasonal influence on reproduction in chimpanzees of Gombe National Park. International Journal of Primatology 16:435–451

Walsh PD, Abernethy KA, Bermejo M, Beyers R, De Wachter P, Akou ME, Huijbregts B, Mambounga, DI, Toham AK, Kilbourn AM, Lahm SA, Latour S, Maisels F, Mbina C, Mihindou Y, Ndong Obiang S, Effa EN, Starkey MP, Telfer P, Thibault M, Tutin

CEG, White LJT, Wilkie DS. 2003. Catastrophic ape decline in western equatorial Africa. Nature 422:611–614

Walsh PD, Tutin CEG, Oates JF, Baillie JEM, Maisels F, Stokes EJ, Gatti S, Bergl RA, Sunderland-Groves J, Dunn A. 2008. Gorilla gorilla. The IUCN Red List of Threatened Species. Version 2014.3. www.iucnredlist.org

Walsh PD, White LJT. 2005. Evaluation the steady state assumption: simulations of gorilla nest decay. Ecological Applications 15:1342–1350

Warren VE, Marques TA, Harris D, Thomas L, Tyack PL, Aguilar de Soto N, Hickmott LS, Johnson MP. 2017. Spatio-temporal variation in click production rates of beaked whales: Implications for passive acoustic density estimation. The Journal of the Acoustical Society of America 141:1962–74

Wearn O, Glover-Kapfer P. 2017. Camera-trapping for conservation: a guide to best-practices. WWF Conservation Technology Series 1. WWF-UK, Woking, United Kingdom.

Wearn OR, Rowcliffe JM, Carbone C, Bernard H, Ewers RM. 2013. Assessing the status of wild felids in a highly-disturbed commercial forest reserve in Borneo and the implications for camera trap survey design. PLoS One 8:e77598

Wellington K, Bottom C, Merrill C, Litvaitis JA. 2014. Identifying performance differences among trail cameras used to monitor forest mammals. Wildlife Society Bulletin 38:634–638

White GC, Anderson DR, Burnham KP, Otis DL. 1982. Capture-recapture and removal methods for sampling closed populations. Los Alamos National Laboratory LA-8787-NERP

White GC, Shenk TM. 2001. Population estimation with radio marked animals. pp 329–350 *in* JJ Millspaugh and JM Marzluff (eds). Design and Analysis of Radio Telemetry Studies. Academic Press, San Diego, California, USA

Williams JM, Lonsdorf EV, Wilson ML, Schumacher-Stankey J, Goodall J, Pusey AE. 2008. Causes of death in the Kasekela chimpanzees of Gombe National Park, Tanzania. American Journal of Primatology 70:766-777

Wilson KR, Anderson DR. 1985. Evaluation of two density estimators of small mammal population size. Journal of Mammalogy 66:13–21

Wilton CM, Puckett EE, Beringer J, Gardner B, Eggert LS, Belant JL. 2014. Trap array configuration influences estimates and precision of black bear density and abundance. PLoS One 9:e111257

Woodruff DS. 1993. Non-invasive genotyping of primates. Primates 34:333–346

Wood BM, Watts DP, Mitani JC, Langergraber KE. 2017. Favorable ecological circumstances promote life expectancy in chimpanzees similar to that of human hunter-gatherers. Journal of Human Evolution 105:41–56

Woods JG, Paetkau D, Lewis D, McLellan BN, Proctor M, Strobeck C. 1999. Genetic tagging of free-ranging black and brown bears. Wildlife Society Bulletin 27:616–627

Wright JA, Barker RJ, Schofield MR, Frantz AC, Byrom AE, Gleeson DM. 2009. Incorporating genotype uncertainty into mark–recapture-type models for estimating abundance using DNA samples. Biometrics 65:833–840

Yanggen D, Angu K, Tchamou N (eds). 2010. Lanscape-scale conservation in the Congo Basin: lessons learned from the Central African Regional Program for the Environment (CARPE). IUCN, Gland, Switzerland

Yoshizaki J, Brownie C, Pollock KH, Link WA. 2011. Modeling misidentification errors that result from use of genetic tags in capture–recapture studies. Environmental and Ecological Statistics 18:27–55

Yoshizaki J, Pollock KH, Brownie C, Webster RA. 2009. Modeling misidentification errors in capture–recapture studies using photographic identification of evolving marks. Ecology 90:3–9

Zero VH, Sundaresan SR, O'Brien TG, Kinnaird MF. 2013. Monitoring an endangered savannah ungulate, Grevy's zebra *Equus grevyi*: choosing a method for estimating population densities. Oryx 47:410–419